

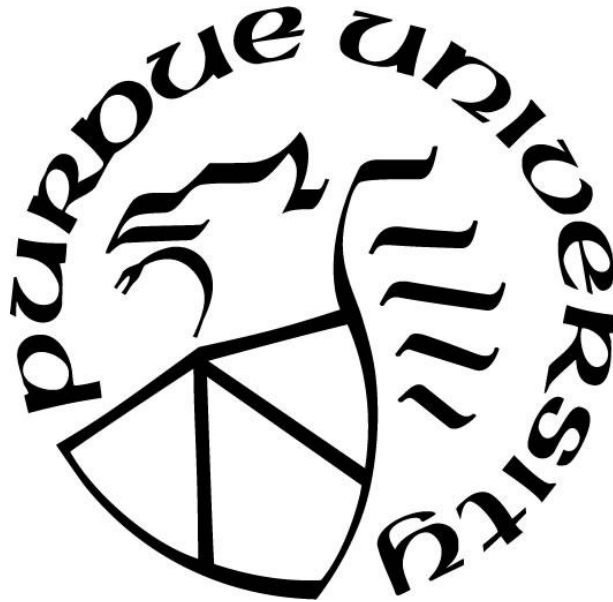
**AN INTERDISCIPLINARY STUDY OF SUSTAINABLE ELECTRONICS
IN RELIABILITY, RECYCLING, AND STEM EDUCATION**

by
Congying Wang

A Dissertation

*Submitted to the Faculty of Purdue University
In Partial Fulfillment of the Requirements for the degree of*

Doctor of Philosophy



School of Materials Engineering

West Lafayette, Indiana

December 2021

**THE PURDUE UNIVERSITY GRADUATE SCHOOL
STATEMENT OF COMMITTEE APPROVAL**

Dr. Carol A. Handwerker, Co-Chair

School of Materials Engineering

Dr. John E. Blendell, Co-Chair

School of Materials Engineering

Dr. David Johnson

School of Materials Engineering

Dr. Marisol Koslowski

School of Mechanical Engineering

Approved by:

Dr. David Bahr

*To those who suffer from
unregulated recycling of e-waste*

ACKNOWLEDGMENTS

I would like to thank my parents for their endless support, even when oceans apart. I am grateful for my advisors, Carol Handwerker, who expanded my boundary with her knowledge, beliefs, passion, patience, and care; John Blendell, who tolerated many “the last question(s)” during the hours hijacked by my visits and brought countless laughter into our discussions. I would not be able to be where I am without the support. I would like to thank my committee members Marisol Koslowski and David Johnson for their ongoing advice and guidance. I would like to thank Fu Zhao, Melissa Reeves, Kory Cooper, and Monica Cardella, whose intellectual support made this interdisciplinary work possible. I would like to thank Ruth Strevener, Brent Jesiek, and Tamara Moore for their mentorship on engineering education. I am grateful for my colleges, Xi Chen and Xiaorong Cai, with whom I had fruitful discussions and tackled many tasks together. I would like to thank my best friends, Alyssa Yaeger, Xianyi Hu, and Matthew Korey, who entertained me and kept me going through this journey.

I appreciate the support through the National Science Foundation (NSF) Grant Number 1610420 (Controlling Heterogeneous Stress Relaxation in Tin Films: Whiskers, Grain boundary sliding, and beyond) and Grant Number 1144843 (Integrative Graduate Education and Research Traineeship: Sustainable Electronics).

TABLE OF CONTENTS

LIST OF TABLES	10
LIST OF FIGURES	11
ABSTRACT	16
1. INTRODUCTION	18
1.1 Introduction to sustainable electronics	18
1.2 Reliability of Pb-free materials in electronics: Sn whiskers	20
1.2.1 Spontaneous growth of Sn whiskers in Pb-free coatings	20
1.2.2 Growth mechanisms of Sn whiskers	21
1.2.3 Anisotropic properties of β -tin	22
1.2.4 Sources of global stresses in Sn films	23
1.2.4.1 Residual stresses during electrodeposition.....	23
1.2.4.2 Intermetallic Compounds (IMC) formation	24
1.2.4.3 Externally applied mechanical or thermomechanical stresses	25
1.2.5 Sources of local stresses in Sn films	25
1.2.5.1 Oxidation.....	25
1.2.5.2 Inhomogeneous IMC formation.....	25
1.2.5.3 Orientation.....	26
1.2.5.4 GB geometry (inclined GBs).....	26
1.2.5.5 Yielding and slip behavior	26
1.2.6 Nucleation of shallow grains.....	27
1.2.6.1 Pre-existing shallow grains	28
1.2.6.2 Newly nucleated grains	28
1.2.7 Orientation effects on whisker nucleation.....	31
1.2.8 Scope of the project.....	32
1.3 End-of-life treatment of electronics.....	34
1.3.1 Scope of the project.....	35
1.4 Sustainability education in STEM.....	38
1.4.1 Misconceptions.....	38
1.4.2 Ritual knowledge.....	39

1.4.3	Foreign Knowledge	39
1.4.4	Scope of the project.....	40
1.5	References	41
2.	RELATING TEMPERATURE AND THERMAL STRAINS TO FATIGUE BEHAVIOR OF THERMALLY CYCLED TIN FILMS	46
2.1	Introduction	46
2.2	Experiments and Methods	47
2.3	Results and Discussion	48
2.4	Conclusion	53
2.5	References	53
3.	LOCAL VARIATIONS IN GRAIN FORMATION, GRAIN BOUNDARY SLIDING, AND WHISKER GROWTH ALONG GRAIN BOUNDARIES IN LARGE-GRAIN SN FILMS	56
3.1	Introduction	56
3.2	Experiments	57
3.3	Results and Discussion	59
3.4	Conclusions	67
3.5	References	68
4.	WHISKER NUCLEATION BY SLIP-ASSISTED GRAIN ROTATION DURING THERMAL CYCLING	71
4.1	Introduction	71
4.2	Experiments	73
4.2.1	Large-grain film preparation	73
4.2.2	Thermal cycling.....	74
4.2.3	Characterization	75
4.3	Results	76
4.3.1	Grain boundary sliding and whisker nucleation.....	76
4.3.2	Grain formation by rotation.....	79
4.3.3	Grain boundary migration	81
4.4	Discussion.....	82
4.4.1	Individual deformation mechanisms and their contribution to whisker grain nucleation.....	82

4.4.1.1	GB sliding	82
4.4.1.2	GB rotation	83
4.4.1.3	Local yielding: slip behavior	84
4.4.1.4	Short-distance diffusion	88
4.4.2	Nucleation mechanism for whisker grains	89
4.4.3	GB migration	91
4.5	Conclusions	92
4.6	References	93
5.	NUCLEATION DUE TO LOCALIZED ROTATION AND YIELDING AND THE CONDITIONS FOR WHISKER GROWTH IN SN FILMS	97
5.1	Introduction	97
5.2	Experiments	99
5.2.1	Sample preparation	99
5.2.2	Rapid thermal cycling	99
5.2.3	Time-dependent characterization	100
5.2.4	CTE analysis along the GB	100
5.3	Results and Discussion	102
5.3.1	Evolution of local microstructure	102
5.3.2	Evolution of local orientation	104
5.3.3	Grain geometry in rotated regions	108
5.3.4	Crystal plasticity simulations	110
5.4	Conclusions	113
5.5	References	114
6.	THE TRANSITION FROM INFORMAL TO FORMAL ELECTRONICS RECYCLING IN GUIYU: A REVIEW OF THE GUIYU CIRCULAR ECONOMY INDUSTRIAL PARK	117
6.1	Introduction	117
6.2	Informal Recycling in Guiyu: An overview	120
6.2.1	Historical development of the recycling industry	120
6.2.2	Emergence of the e-waste recycling industry	120
6.2.3	Environmental pollution and societal consequences	121
6.3	Planning of GCEIP	122

6.3.1	Initiatives	122
6.3.2	Barriers	123
6.3.3	Policy design of GCEIP	124
6.4	Implementation of GCEIP	128
6.4.1	Projects and timeline	128
6.4.2	Companies in residence.....	129
6.4.3	Source control of e-waste	130
6.4.4	Recycling technologies and waste treatment.....	130
6.4.4.1	Dismantling	132
6.4.4.2	Hydrometallurgy: Gold recovery	133
6.4.4.3	Pyrometallurgy: Cu recovery	134
6.4.4.4	Physical separation.....	135
6.5	Contextualized Analysis: The Transformation of Informal Recycling to Formal Recycling in Guiyu	135
6.5.1	Changes in the local recycling industry	135
6.5.2	Synergy of the solution	137
6.5.2.1	Reconstruction of backyard workshops	138
6.5.2.2	End Markets of Recycled Products	139
6.5.3	Comparisons between GCEIP and similar efforts.....	140
6.5.3.1	National level	140
6.5.3.2	Global level	141
6.5.4	Limitations	141
6.6	Conclusion.....	142
6.7	References	144
7.	MOTIVATING STUDENTS BY CONTEXTUALIZING SUSTAINABILITY IN INTERDISCIPLINARY GRADUATE PROGRAM OR K-12 CLASSROOM.....	150
7.1	Introduction to sustainability education and challenges.....	150
7.2	Case study 1: Cultivating student motivation in Interdisciplinary Graduate Education and Research Traineeship (IGERT) on Sustainable Electronics	151
7.2.1	Overview of the NSF IGERT program in sustainable electronics	151
7.2.1.1	Class structure	151

7.2.1.2	Domestic workshops	152
7.2.1.3	International workshops	152
7.2.1.4	Examples of student-driven programming.....	152
7.2.2	Research questions	153
7.2.3	Conceptual framework	154
7.2.3.1	Self-determination Theory	154
7.2.3.2	Expectancy-Value Model.....	155
7.2.4	Methodology	156
7.2.5	Internalization of student motivation	156
7.2.6	Contextualization of sustainability education via problem-based learning (PBL).....	163
7.2.7	Integration of societal and cultural sectors.....	167
7.2.8	Conclusions	170
7.3	Case study 2: Revealing hidden societal factors in sustainability education in a K-12 classroom for underrepresented middle-school youth.....	171
7.3.1	Purpose of study	171
7.3.2	Project design	172
7.3.3	Preliminary findings	173
7.3.3.1	Student motivation	173
7.3.3.2	Societal and economic awareness	174
7.3.4	Conclusions	174
7.4	References	175
8.	CONCLUSIONS	179
	PUBLICATIONS.....	182

LIST OF TABLES

Table 1.1. Families of potential slip systems in Sn.....	27
Table 1.2. Hard concepts in sustainability education summarized from literature. Categorization is based on the theory of difficulty [46].	38
Table 2.1. Sample types, properties, and cycling conditions.....	47
Table 3.1. Characterization techniques employed in this study.....	59
Table 4.1. Rotated slip trace vectors (All references are Cartesian coordinates)	85
Table 4.2. Families of potential slip systems in Sn and the corresponding slip plane families....	86
Table 4.3. Angles between rotated slip traces and non-equivalent slip plane normal (°).....	87
Table 4.4. Selected angles between rotated slip traces and the normal of potential slip planes... 88	
Table 5.1. The mismatch of CTE along different GB segments shown in Fig. 5.7.....	109
Table 5.2. The Euler angles (Bunge) used the crystal plasticity simulation in Fig. 5.8.	110
Table 6.1. Timeline of the development of GCEIP regarding policies, major projects, and investment prior to the construction of GCEIP.....	123
Table 6.2. An overview of e-waste and circular economy-related policies in China after 2009. (Compiled from various sources).....	126
Table 6.3. The functions and capacities of major plants and projects constructed in GCEIP after 2014. (Source: compiled from various sources)	128

LIST OF FIGURES

Figure 1.1. The traditional life cycles of electronics	18
Figure 1.2. The structure and the content of the dissertation.....	19
Figure 1.3. Sn whiskers grew from the coatings on electronics components. Reprinted from [8], copyright 2013, with permission from Elsevier.....	20
Figure 1.4. SEM Top-view and FIB cross-section showing a whisker growing from a grain with oblique grain boundaries. Reprinted from [15], copyright 2006, with permission from Elsevier.	21
Figure 1.5. Whiskers grow from shallow grains via grain boundary sliding-limited diffusional creep. Reprinted from [9], copyright 2006, with permission from Elsevier.....	22
Figure 1.6. Elastic modulus (red) and the CTEs (black) of Sn along different orientations. Reprinted from [19], copyright 2006, with permission from IEEE.....	23
Figure 1.7. Schematics showing whisker nucleation via Dynamic Recrystallization (DRX). Reprinted from [30], copyright 2009, with permission from Springer Nature.....	29
Figure 1.8. (a) the SEM image showing a whisker formed at one grain boundary; (b) the orientation map with IPF colors. Grain 1 is the surface defect grain in (a); (c) calculated average peak width showing the grain 1 has a relatively lower elastic energy density than the matrix grains. Reprinted from [32], copyright 2013, with permission from Elsevier.....	30
Figure 1.9. Four different grain boundaries (GBs) responses have been observed in thermally cycled Sn-alloy films: (a) no obvious microstructural changes; (b) surface defects formation; (c) grain boundary sliding; (4) surface defects formation and grain boundary sliding. Reprinted from [33], copyright 2016, with permission from Springer Nature.....	31
Figure 1.10. (a) a schematic skeleton of designed microstructure; (b-e) IPF colored orientation map showing four different orientation texture assigned to the polycrystalline structure in (a); (f-i) calculated ESED (elastic energy density) distribution maps for elastic energy with respect to orientations; (i-m) calculated ESED maps for thermoelastic energy with respect to orientations. Reprinted from [35], copyright 2014, with permission from Springer Nature.....	32
Figure 1.11. Stress-strain curves for 1.5- μm -thick and 7.5- μm -thick Sn films. Reprinted from [8], copyright 2013, with permission from Elsevier.....	33
Figure 1.12. The scope of the first part of the study. Large-grained Sn films are utilized to simplify the local stress states near GBs. The research questions include (1) what mechanisms contribute to the nucleation of shallow grains and (2) how post-nucleation microstructure determines whether a surface grain becomes a whisker or not.....	34
Figure 1.13. The transboundary flow of global e-waste. Reprinted from [40], copyright 2016, with permission from Springer Nature.....	37
Figure 2.1. SEM images of Sn films illustrating the accumulation of fatigue damage at different cycles under (a-d) cold cycling, (e-h) hot cycling, and (i-l) full cycling.....	49

Figure 2.2. The development of cracks and subsided grains with an increasing number of cycles in Sample F.	50
Figure 2.3. Densities of (a-b) whiskers and (c) cracks of three different conditions were illustrated as a function of the increasing thermal cycles.	52
Figure 3.1. Optical images of (a) a typical as-received SAC305 solder film without noticeable grain boundaries and (b) the thermally cycled film with apparent grain boundaries presented in this study. Films in (a) and (b) are not the same sample.....	58
Figure 3.2. Local surface morphology, orientation, and associated distributions of dislocation density as indicated by the full-width at half-max (FWHM) of the diffracted beams and elastic strain energy density (ESED) at GB-I before (a-d) and after (e-h) 1000 thermal cycles. Evolution of surface morphology [(a) and (e)] and orientation [(b) and (f)] shows the growth of whiskers from the pre-existing grain 1 and newly formed grains 2-5 circled by high-angle GBs (black lines). Grains 6-12 nucleated with the formation of low-angle GBs (red lines). The changes of dislocation density [(c) and (g)] and ESED [(d) and (h)] indicate that stress level of the characterized region significantly decreased after new grains formed	61
Figure 3.3. (a-b) Side-view SEM images of selected whiskers and sub-grains taken at a tilt of 52° of the same region characterized in Fig. 1. Cross-sections were made in the direction (c) perpendicular for grains 6-2-7 and (d) parallel for grains 4-1-11 to GB-I as marked by black dashed lines in (a-b) to show the subsurface microstructure. GBs distinguished based on ion-beam grain contrast are indicated by black dotted lines.	62
Figure 3.4. Local surface morphology, orientation, and associated distributions of dislocation density as indicated by FWHM of the diffracted beams and elastic strain energy density (ESED) at GB-II before (a-d) and after (e-h) 1000 thermal cycles. Evolution of surface morphology [(a) and (e)] and orientation [(b) and (f)] shows GB sliding and migration occurred. A low-angle GB formed, indicated by the white arrow in (f). The changes of dislocation density [(c) and (g)] and ESED [(d) and (h)] indicate that the majority of the relaxation from GB sliding took place close to GB-II.	64
Figure 3.5. (a) Top-view and (b) tilted-view SEM images show two sets of slip traces (marked by blue and red dashed lines) near the nucleated shallow grain at GB-II in the region marked by the white dashed square in Fig. 3(e). (c) Potential slip planes identified via the trace directions and grain orientations. (d-g) Ion-beam images of the cross-sections Cut 1, 2, and 3 marked by black dashed lines in (b). (f) An enlarged view of the area enveloped by the dashed square in (e) indicates a shallow surface grain nucleated at the GB near the surface. The location of the shallow grain agrees with the location of the newly-formed low-angle GB indicated by the white arrow in Fig. 3(f).....	65
Figure 3.6. (a) Microstructural variations along the GB revealed by cross-sections from a region showing both whisker formation and GB sliding. (b-c) FIB cross-sections along the dashed lines in (a) showed changes in surface normal near the original GB, changes in GB inclination through the film thickness, and shallow grain formation (b only). Reproduced from [14], copyright 2016, with permission from Springer Nature.	65
Figure 4.1. Surface of as-solidified (large-grain) Sn film on Cu substrate in optical microscopy (a) and SEM (b) showed a pseudo-bicrystal microstructure.	74

Figure 4.2. Real-time measured profile of the rapid thermal cycling technique.	75
Figure 4.3. (a-c) SEM images of one monitored region's surface morphology at 10, 40, and 160 cycles. The dashed line in (a) marked the initial GB. (d-f) Enlarged images of three regions along the GB that demonstrated the most local deformation. A1-A9 noted 9 points analyzed with Electron Backscatter Diffraction (EBSD). The unit cell figures represented the local orientation at each corresponding position.	77
Figure 4.4. Ridge-like deformation region at (a) 160 cycles and (b) 230 cycles; (c) Three height profiles along the green, red, and blue lines marked in (b), obtained from Atomic Force Microscopy measurement.	78
Figure 4.5. The microstructural changes in (a-b) Region-4, (c-d) Region-5 (at 70 and 160 cycles) and (e-f) Region-6 at 0 and 160 cycles. B1-B6 represented the orientations of six selected locations in these regions at 160 cycles. (g) Point-to-origin misorientation angle profile along the line marked by the yellow arrow in (f).	80
Figure 4.6. (a) Top-view of the Region-4 from the AFM measurement. (b) Three height profiles along the green, red, and blue lines marked in (a).	81
Figure 4.7. (a-c) Morphological evolution of a monitored region, Region-7, at 0, 40, and 160 cycles. B7-B10 represented the orientations of four selected locations at 160 cycles. (d-e) Morphological evolution of another monitored region along the same GB at 0 and 160 cycles. (f) Point-to-origin misorientation angle profile along the line marked by the yellow arrow in (e).	82
Figure 4.8. (a) Initial geometry of the bicrystal simulation. 10% compressive strain was applied. (b) Simulated dislocation density map of the deformed bicrystal where dislocation density peaked within the upper left corner of Grain B close to the GB. (c-e) Schematic diagrams of the nucleation mechanism for whisker grains (shallow grains) in thermally cycled large-grained Sn films.	90
Figure 5.1. The geometry of the sample reference and crystal reference. θ is the inclination angle between the GB direction and normal direction.	100
Figure 5.2. (a) Low-magnification SEM image of a selected region before cycling. (b) Orientation map of the area marked by the black square in (a) after 7 cycles. (c-e) SEM images of the monitored area at 65, 120, and 250 cycles. (f) and (g) are high-magnification images of area A and area B shown in (e) at 350 cycles.	103
Figure 5.3. (a-d) SEM image of another monitored region after 7, 120, 250, and 350 cycles. New GB traces were observed between Grain 1 and Grain 4 in (b) at 120 cycles where a sinking grain later developed in (c-d). The three different GBs of the Grain 3 slid in sequence between 120 cycles and 350 cycles.	103
Figure 5.4. (a-b) SEM top-view of the region is shown in Fig. 2 and 3. (c-d) Misorientation angles between each pair of points in (a-b) with the increased number of thermal cycles.	105
Figure 5.5. Pole figures of the pairs of points (1 and 2, 3 and 4) in Figure 7(a) at 120 and 350 cycles.	106
Figure 5.6. Pole figures of the pairs of points (5 and 6, 7 and 8) in Figure 8(a) at 120 and 350 cycles.	107

Figure 5.7. (a) SEM image of one monitored region at 350 cycles. (b) and (c) show the cross-sections at the positions marked by Line 1 and Line 2 in (a). (d) SEM top-view of another monitored region at 350 cycles. (e) and (f) show the cross-sections at the positions marked by Line 3 and Line 4 in (d).....	108
Figure 5.8. (a) The bicrystal geometry used by the crystal plasticity simulation. (b-e) Rotation maps and pole figures after deformation of four pairs of orientations listed in Tab. 5.2. Simulation credit: Xiaorong Cai. Reproduced with permission. Unpublished.	111
Figure 5.9. (a) The bicrystal geometry and orientation used by the 3D crystal plasticity simulation. (b) The evolution of normal displacement during deformation. (c) The misorientation map during deformation. (d) The nucleation of a subgrain near the free surface in the left grain. Simulation credit: Xiaorong Cai. Reproduced with permission. Unpublished.	112
Figure 6.1. Geographic location of (a) Guiyu town, Guangdong Province, China, and (b) Guiyu Circular Economy Industrial Park (GCEIP).	118
Figure 6.2. An overview of the mixed technologies employed in pre-processing and treatments in Guiyu Circular Economy Industrial Park.	131
Figure 6.3. The end products of a cellphone dismantling procedure carried out in GCEIP. (a) dismantling the housing and large-size electronic components; (b) dismantling integrated circuits and PCBs; (c) dismantling and sorting different types of small electronic components such as cameras and memories. Photo credits: Congying Wang.	132
Figure 6.4. The recycling and treatment processes for gold recovery. (a) The stocks of dismantled and sorted integrated circuits (ICs). (b) The inlet of ICs. (c) Physical separation equipment. (d) Hydrometallurgy facilities and (e) waste gas tower on the roof of one of the plants. (f) Waste solution processing by mechanical vapor compression (MVP) equipment. Photo credits: Congying Wang.	134
Figure 6.5. The recycling scheme of (a) informal sectors in Guiyu before the construction of GCEIP, and (b) integrated informal sectors and formal sectors in Guiyu after GCEIP	137
Figure 7.1. Overview of the changes in students' motivation for major self-organized projects throughout the IGERT program.....	157
Figure 7.2. (a) The values of IGERT in sustainable electronics were well-perceived by the participants. (b) Students understood the three core values of IGERT in sustainable electronics deeper throughout the program.	158
Figure 7.3. (a) Values that between students and faculty and between faculty and program are in great alignment, creating a benign environment to grow relatedness within the program. (b) The majority of the students started to see the shared value among the cohort after the international learning experience in India or the collaborative projects required in an interdisciplinary course.	159
Figure 7.4. Near the end of the IGERT program, students were more confident and qualified to participate in various activities including the planning and preparation of optional projects beyond the original programming. Students reported a higher level of confidence in dealing with projects at a later stage due to previous collaborative experiences.	160

Figure 7.5. (a) All students believed that they were involved in the design of the IGERT program. (b-c) A large portion of the students identified the self-designed seminar course as the starting point. 165

Figure 7.6. (a) Students were more involved in later learning experiences than earlier ones. (b) Students actively participated in the preparation and planning of the self-organized seminar course and self-organized Puerto Rico field trip. 166

Figure 7.7. International field trips were highlighted by the rating on the most valuable aspects of the IGERT in sustainable electronics program that were perceived by the students. 168

ABSTRACT

Our next-generation engineers must be able to design technologies and create partnerships for broad applications that sustain the environment and protect human health. This dissertation reports on technologies and partnerships that support sustainable electronics by (1) improving the reliability of Sn-alloys in electronics by understanding the formation of whiskers in Sn thin films under thermomechanical stresses, (2) assessing the social, political, and economic determinants of a town's transition to cleaner recycling of e-waste, and (3) establishing a framework highlighting the contextualization and shared value to integrate sustainability in STEM education.

Tin whiskers grow spontaneously from shallow surface grains with oblique grain boundaries (GBs) to relax the stresses in Sn films via GB-sliding-limited creep due to local compressive stress gradients. Understanding how shallow grains nucleate relative to local stress states and microstructure is a prerequisite for suppressing Sn whiskers and improving system reliability because the nucleation of shallow grains determines the distribution of Sn whiskers in films. In polycrystalline films, Sn whiskers were observed to nucleate and grow during thermal cycling below temperature, indicating that whisker formation is highly sensitive to local stress states. To simplify the identification of heterogeneous stress localization resulting from β -Sn's anisotropic elasticity and thermal expansion, large-grained Sn films were prepared and employed to quantify the evolution of stress relaxation responses observed near GBs on free surfaces during thermal cycling. The observed responses include (1) nucleation of new grains accompanied by local yielding as evidenced from slip bands and grain misorientation changes, (2) GB sliding and diffusion with local surface uplift, (3) localized GB migration, and (4) whisker formation. Different combinations of processes occurred at different GBs, with GB sliding and near-GB rotation occurring at fewer thermal cycles than other phenomena. The significantly different nucleation, whisker growth, and GB sliding phenomena observed are discussed in light of surface and sub-surface changes in orientation and morphology and the occurrence of slip traces along the GBs displaying GB sliding. These results suggest that local yielding and surface rotation are essential in determining whether whisker growth or GB sliding occurs along a given grain boundary. Secondly, incremental characterization of local microstructure and orientation as a function of the increased number of thermal cycles together with crystal plasticity simulations suggest that the local crystallographic and morphological changes are due to subgrain formation

near some GBs, leading to recrystallization and whisker formation. Furthermore, slip bands were commonly observed, demonstrating that dislocations are active in Sn under these conditions, even at low strains. Lastly, we have shown the interplay between mechanisms that simultaneously affect whisker nucleation, such as slip, GB sliding, rotation, diffusion, and GB migration. For these contributions, the results of this work have important implications for understanding whisker nucleation and growth phenomena resulting from multiple stress relaxation mechanisms.

For the end-of-life treatment of e-waste, recent studies have examined the formal and informal sectors and suggested that the two sectors might merge. However, few studies provide any quantitative analysis of the components of the informal sector and the implications of the reformation of e-waste recycling. This study fills this gap by investigating the political, technological, and economic solutions that reformulated the local recycling industry in Guiyu China. This study focuses on the implementation of Guiyu Circular Economy Industrial Park (GCEIP) from a historical perspective because the development of a sustainable recycling scheme for e-waste must be understood in that context. Comparing the organizing format of the local recycling sectors before and after the GCEIP highlighted practical improvements driving the upgrade to an economically viable, greener industry. The results suggest that centralizing waste treatment in high-tech facilities while maintaining the advantage of manual dismantling is critical, and can occur with collaboration among local government, companies, and research institutes through subsidies, investment, and patents. Screening transboundary e-wastes and maintaining original networks of sources and markets contribute to a stable and manageable recycling business. The results of this work have valuable implications for developing countries.

In developing principles of sustainability education, one challenge is the misconception that sustainability can be achieved by technological advances alone. A graduate-level curriculum and an educational module in a junior-high classroom demonstrated that having an authentic context introduced by interdisciplinary curricula with a global perspective highlighted the societal and economic factors so that students established a holistic understanding of sustainable electronics and their possible roles in creating them. The contextualization of sustainable electronics also fortified the shared goals and values among the learning community, promoting students' motivations to make more sustainable decisions.

1. INTRODUCTION

1.1 Introduction to sustainable electronics

There is perhaps no telling of how many electronics are generated every year in modern society. A glimpse at waste electronics revealed that about 52 million tons of e-waste are generated in 2021, and the number will soon excel 120 million tons annually by 2050 [1]. In a linear economy, the production and the consumption model relied on continuous and increasing input of resources and assumed an infinite capacity of the environment regarding absorbing waste and pollution—we “take, make and dispose” [2], leaving a planet with less life-sustaining resources and a polluted environment. A traditional linear product life cycle of electronics is shown in Fig. 1.1.

Product life cycles of electronics:

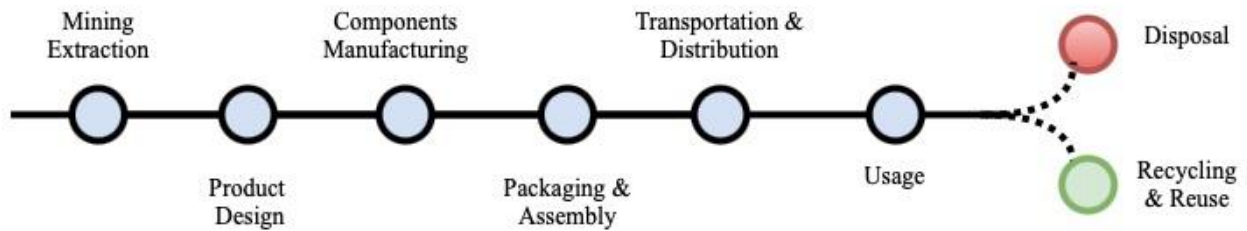


Figure 1.1. The traditional life cycles of electronics

A sustainable system needs inputs from industrial, economic, and societal sectors to fulfill the prosperity for the planet and human beings [3]. However, only recently did the electronics industry consider environmental functions and goals other than economic costs. A circular economy is one of the frameworks that has been employed to guide the design, manufacturing, and end-of-life treatment of electronics [4]. The circular economy of electronics considers [5]:

1. The green manufacturing of components or green assembly of electronics;
2. The supply chains and the corresponding energy cost;
3. The use or restrictions of hazardous materials in electronics, of which the restrictions are often associated with the legislation;
4. The behaviors of how people consume and dispose electronics;
5. The end-of-life management of the e-waste;

Additionally, putting sustainability in perspective of higher education, the topics include pollution control and prevention, resource minimization, green manufacturing, eco-design, economics, and social topics [6]. However, the eco-design and social topics were seldom covered in environmental engineering, where sustainability is widely taught.

Thus, this dissertation approaches sustainable electronics through multiple sectors, including green assembly, end-of-life management, and education, as shown in Fig. 1.2. The rest of the chapter introduces the Sn whiskers in Pb-free materials, the recycling techniques of electronics, and the difficult concepts in current sustainability education. Lastly, a synthesis of each chapter concerning sustainable electronics is provided.

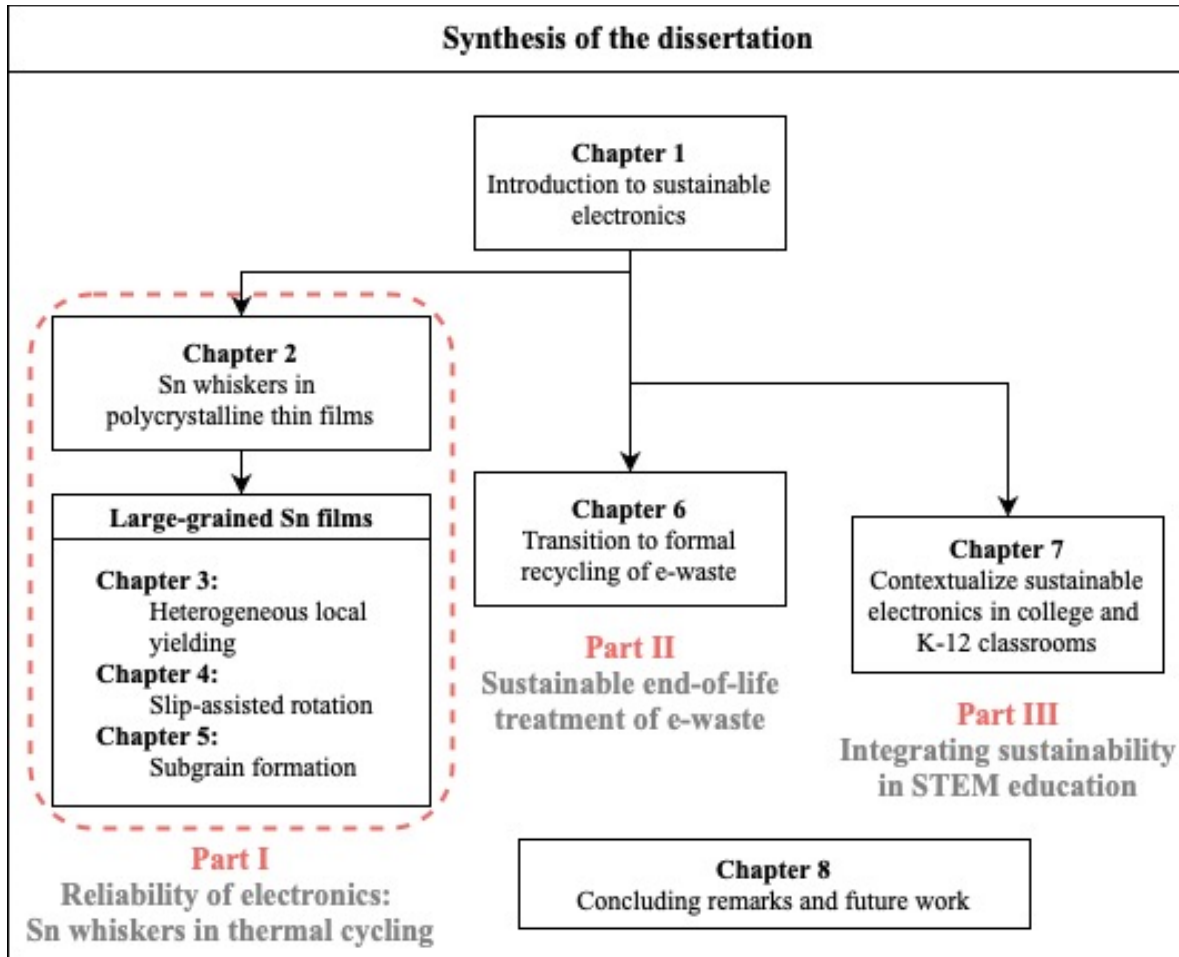


Figure 1.2. The structure and the content of the dissertation.

1.2 Reliability of Pb-free materials in electronics: Sn whiskers

1.2.1 Spontaneous growth of Sn whiskers in Pb-free coatings

β -Sn is widely used in electronics because of its great physical properties such as solderability and conductivity, as well as its relatively wide availability. In printed circuit boards (PCBs) manufacturing, Sn is deposited on copper leads to prevent oxidation, and to improve the wettability. One issue is the formation and growth of tin whiskers, known as a stress relaxation response in Sn films [7]. Those whiskers are able to grow to a millimeter scale [8], leading to potential short-circuits in electronics and undermining the reliability of electronic devices, as shown in Figure 1.3. For example, Sn whiskers caused catastrophic failures in the power industry, commercial electronics, and even military missiles and satellites [9].

The addition of Pb was the standard solution because alloying tin with lead would largely reduce the propensity of forming tin whiskers [10]. However, lead in electronics negatively affects the environment or human health in every phase of the electronic life cycles: the material processing operation becomes dangerous; workers in the factories may face severe health risks; other recyclable materials used in electronics may be polluted by lead and thus become unrecoverable. With increasing environmental concerns, the European Union has banned the use of Pb in the electrical industry since 2003 [11]. Therefore, understanding and suppressing Sn whiskers in Pb-free coatings reemerged as a critical research topic for the reliability of electronics.

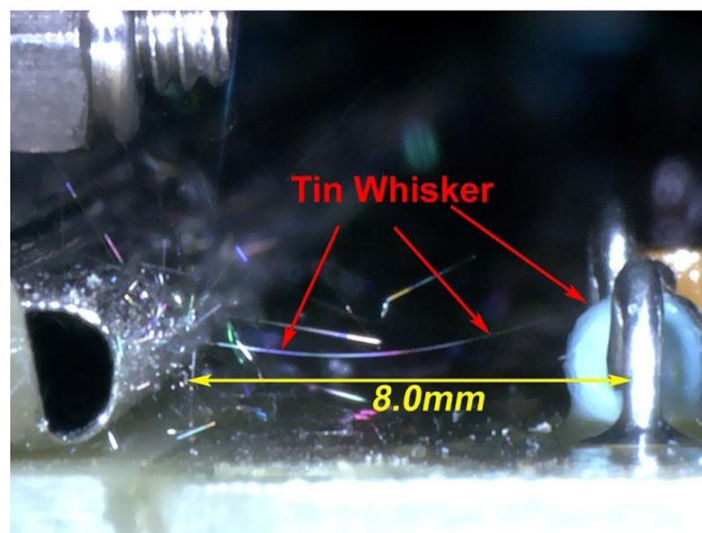


Figure 1.3. Sn whiskers grew from the coatings on electronics components. Reprinted from [8], copyright 2013, with permission from Elsevier.

1.2.2 Growth mechanisms of Sn whiskers

Whiskers grow from the roots to relax the compressive stresses in Sn films [12]. Recent studies pointed out that oblique grain boundaries (GBs) near the surface are the deposit sites of the mass necessary for whisker growth [12-14], as shown in Figure 1.4.

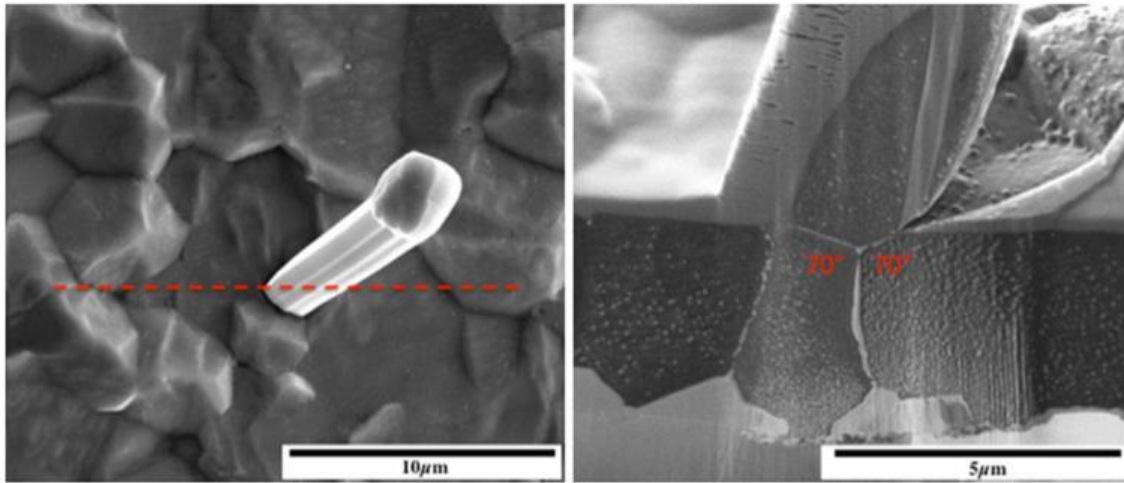


Figure 1.4. SEM Top-view and FIB cross-section showing a whisker growing from a grain with oblique grain boundaries. Reprinted from [15], copyright 2006, with permission from Elsevier.

Sarobol et al. [15] further proposed a whisker growth model based on GB-sliding-limited creep in which atoms deposited under the oblique GBs of the shallow surface grain via long-distance diffusion, creating an out-of-plane shear. When the out-of-plane shear is greater than the sliding friction, the shallow surface grain then grows out as a whisker, as illustrated in Fig. 1.5. Shallow grains, i.e., surface grains not rooted to the substrate with a large θ , as marked in Fig. 1.5, were also related to the 3-D strain gradients generated at the whisker roots [16].

However, in electrodeposited tin films, most grains are columnar grains that grow from the substrate up to the surface. Therefore, how surface grains formed before whisker growth remains to be a question. In fact, only 1 of 10,000 grains would grow as a whisker in Sn thin films [17], indicating that, apart from global stress states, local stress states are vital to the formation or distribution of the shallow grains. Before answering the question of how local stress states affect the formation of shallow grains, the reasons for the heterogeneous stress localization should be visited and are explained in the following section.

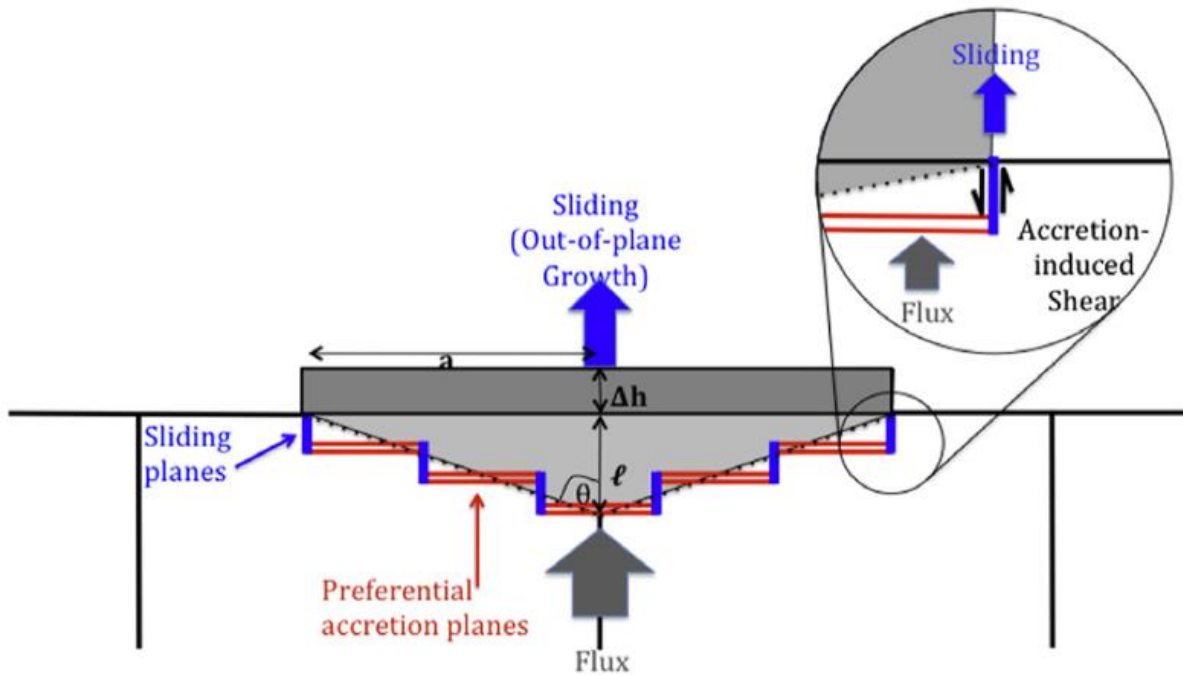


Figure 1.5. Whiskers grow from shallow grains via grain boundary sliding-limited diffusional creep. Reprinted from [9], copyright 2006, with permission from Elsevier.

1.2.3 Anisotropic properties of β -tin

β -tin is a body-centered tetragonal (BCT) crystalline structure in which the lattice parameters $c = 0.318$ nm, $a = b = 0.583$ nm, and the ratio of c/a is equal to 0.546 [18], as shown in the upper right corner of Fig. 1.6. There are 4 atoms per unit cell, and each atom has 4 nearest neighbors, 2 second-nearest neighbors, and 8 third-nearest atoms.

This lattice structure results in anisotropic elasticity and thermal expansion of β -tin, as illustrated in Fig.1.6. The elasticity of $\langle 001 \rangle$ directions is greater by a factor of 3 than that of $\langle 100 \rangle$ directions. Besides, the coefficient of thermal expansion (CTE) along $\langle 001 \rangle$ ($16.4 \times 10^{-6}/\text{K}$ at 298K) is about two times of those along $\langle 100 \rangle$ axis ($32 \times 10^{-6}/\text{K}$ at 298K) [19].

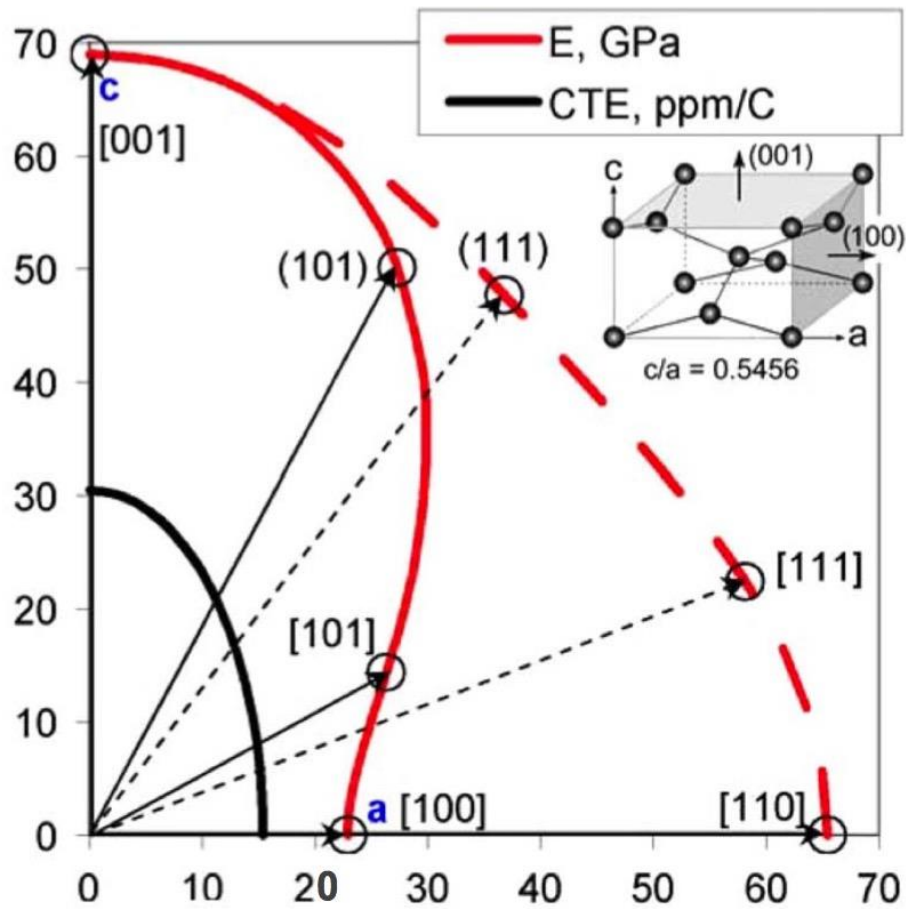


Figure 1.6. Elastic modulus (red) and the CTEs (black) of Sn along different orientations. Reprinted from [19], copyright 2006, with permission from IEEE.

1.2.4 Sources of global stresses in Sn films

The following section provides a review of the common sources of the global stresses in Sn films based on the assumption that the stress gradients in the entire film are uniform.

1.2.4.1 Residual stresses during electrodeposition

For films prepared by electrodeposition, the residual stress needs to be considered. The residual stress usually originates from the different thermal strains between the substrate and deposited film; for example, during the cooling process from deposition temperature, the compressive stress occurs in the film if the substrate has a smaller coefficient of thermal expansion.

However, in the case of tin, the electroplating operation is under room temperature, where the differences of thermal strains cannot generate adequate, if any, residual stress. Still, the effects of residual stress were previously studied. Boettinger et al. [12] calculated the residual stress in pure tin films of 15-minute electroplating using cantilever beam detection. The results proved the existence of a small residual stress but failed to solve the problem of continuous growth of surface defects after the residual stress has been relieved.

1.2.4.2 Intermetallic Compounds (IMC) formation

Residual stress of electrodeposition only stands for a small part of compressive stress developing in Sn films within a short time. For Sn films on Cu substrates, a layer of Cu-Sn intermetallic compound (IMC) will grow at the interface rapidly even at room temperature (298K), which is nearly 60 percent of the melting point (505K) of Sn. In this case, the interdiffusion between Cu substrates and Sn thin films is relatively fast. According to Tu [20], in the diffusivity measurement, Cu diffuses more rapidly across the interface into the Sn layer than that Sn does into Cu substrate. As a result, the IMC nucleates on the Sn side and preferentially grows along the Sn-Sn grain boundary.

The first study on the IMC formation as a major source of the driving force was conducted by Lee and Lee [21], where the stress evolution was measured via wafer curvature. In this paper, the compressive stress was introduced by the formation of Cu_6Sn_5 during electrodeposition, and then relieved by the growth of tin whiskers. However, the focus has been set only on the IMC formed in the electroplating process as a residual stress, thereby the effect of IMC formed during room temperature aging was ignored with an unrealistic assumption that the pre-formed IMC layer would act as a diffusion barrier for further interdiffusion to occur and no external stress is needed. Later, Tu and Li [7] proposed that creep is the mechanism behind the whisker growth where stress has been generated and relieved at the same time. In this model, the IMC formed via diffusion and chemical reaction would result in an increase of the volume on the Sn side, thus introducing the compressive stress within the Sn film; the general diffusion between atoms and vacancies is limited by the oxide layer and only happens at the whisker roots.

1.2.4.3 Externally applied mechanical or thermomechanical stresses

Many studies have been conducted on whisker formation with applied mechanical stresses [22-24], such as static bending or cyclic bending and thermomechanical stresses during thermal cycling [25, 26]. The mismatch of the coefficients of thermal expansion (CTE) between substrates and Sn films induces the thermomechanical stresses. For example, for commonly used Cu substrates, Sn films prefer to extend more than copper substrate during heating, thereby leading to the presence of compressive stresses in films; in contrast, tensile stresses are imposed in Sn films during cooling.

1.2.5 Sources of local stresses in Sn films

The following section provides a review of the common sources of the local stresses in Sn films.

1.2.5.1 Oxidation

Tu [24] stated a relatively weak spot on the oxide layer is a necessary condition for tin surface defects to form. Jadhav et al. [27c] ion-polished selected part of the film surface and removed the oxide layer, and observed whiskers formation with in-situ SEM. The study found that whiskers did not form from oxide-free regions but rather grow at the neighboring area, indicating a weak spot on the oxide layer is not the dominating factor in stress localization in Sn films.

1.2.5.2 Inhomogeneous IMC formation

Although IMC formation plays a key role in generating global stress, it is not the dominant factor determining the preferred whisker formation spots. Sobiech correlated the IMC morphology to the location of the whiskers because the irregular shape of the IMC induces inhomogeneous compressive stress among the Sn layer [28]. The assumption is that large IMC would result in higher compressive stress locally and thereby providing the preferred sites of whiskers. However, the anisotropic properties of Sn were not taken into consideration. Later, through etching the Sn film away from the Cu substrate, comparison between the underlying IMC morphology and the

observed whisker sites was reported by Pei et al. [29], where no obvious correlation between the location of whiskers and IMC can be interpreted.

1.2.5.3 Orientation

Because of the anisotropic properties of beta-Sn, when films experience temperature change, isothermal aging (with IMC growth), or external loading, there will be asymmetrically elastic and thermal stress responses, resulting in a complicated and anisotropic local stress state. Therefore, the film orientation becomes another critical factor of the selection mechanism of tin whisker formation, where only a small number of specific grains grow as surface defects and relax most of the stress imposed.

1.2.5.4 GB geometry (inclined GBs)

Boettinger et al. [12] claimed that while the columnar microstructure in pure Sn and Sn- Cu alloy leading to the formation and growth of whiskers and hillocks, the Pb-Sn film remains original surface geometry, indicating its ability to uniformly release the stress. The reason that accounts for the different relaxation behaviors refers to the absence of horizontal grain boundaries in Sn and Sn-Cu films. The fig below illustrated different types of stress state resulted from different geometry, leading to different stress relaxation responses. When diffusional creep occurs, without oblique interfaces, the diffusion fluxes are forced toward the free surface or the interface between the IMC and film in the same direction as vertical grain boundaries. As mentioned before, diffusion among film surfaces is limited because of the oxide layer; hence the rarely existed oblique or parallel interfaces in columnar microstructure become preferred sites for Sn diffusion, which is followed by the accumulation of atoms underneath the oblique grain boundaries.

1.2.5.5 Yielding and slip behavior

In FCC structures, active slip systems are on planes with the highest planar atomic density and along the directions with the highest linear atomic density. Theoretically, there are many other combinations of slip systems, but only one nonequivalent slip system, $\{111\}\langle 110 \rangle$, can be activated. This can be explained either via crystallography (shortest unit slip distance) or critical resolved shear stress (CRSS). However, when analyzing slip behaviors in β -Sn, 12 nonequivalent

slip systems have already been reported in the past 70 years; and there is no guideline or dominant parameter, unlike FCC structure, capable of predicting or identifying what types of slip systems will be activated in different experimental conditions. To put the complex slip behavior of β -Sn in perspective, families of 10 nonequivalent slip systems observed in single crystals β -Sn is shown in Tab. 1.1.

Table 1.1. Families of potential slip systems in Sn

Slip system family	Number of slip systems in family
$\{100\}\langle 001\rangle$	2
$\{100\}\langle 010\rangle$	2
$\{100\}\langle 011\rangle$	4
$\{110\}\langle 001\rangle$	2
$\{110\}\langle 1\bar{1}1\rangle/2$	4
$\{110\}\langle 1\bar{1}0\rangle$	2
$\{001\}\langle 010\rangle$	2
$\{001\}\langle 110\rangle$	2
$\{011\}\langle 01\bar{1}\rangle$	4
$\{211\}\langle 01\bar{1}\rangle$	8

1.2.6 Nucleation of shallow grains

As most grains are columnar in electrodeposited films, the origin of these shallow grains remains unclear. These grains could be formed before or during thermal cycling:

1.2.6.1 Pre-existing shallow grains

“Pre-existing grains” refers to the grains nucleated prior to any room temperature aging or external loadings and, in this study, before the thermal cycling. Previous studies provide multiple answers to the origin of the pre-existing shallow grains, such as (1) the formation of the shallow grains during electroplating or vapor deposition [12]; (2) stress-induced GB migration underneath the surface as a mechanism to form a shallow surface grain [14]; and (3) the high elastic strain energy density (ESED) of misorientated grains (relative to their neighbors) as the determining factor of the whisker roots [14].

1.2.6.2 Newly nucleated grains

“Nucleated grains” refer to the shallow grains formed during thermal cycling. Vianco et al. [30,31] stated that dynamic recrystallization acts as the driving force for whisker grains (i.e., shallow grains) nucleation under cyclic stress states, as illustrated in Fig. 1.7. Dislocations created by the external stress formed a low-angle grain boundary, thus generating a new DRX grain. The recrystallized grain would continue growing at the expense of previously localized strain energy, and then grow as a whisker because a stress gradient would be created between the areas of higher stress and those of lower stress. This stress gradient could lead to the mass transport from matrix grains to nucleated grain. Though this model provides a theoretical framework, it fails to explicitly answer what happened under the film surface, e.g., how dislocations generate and interact to cause nucleation and GB migration.

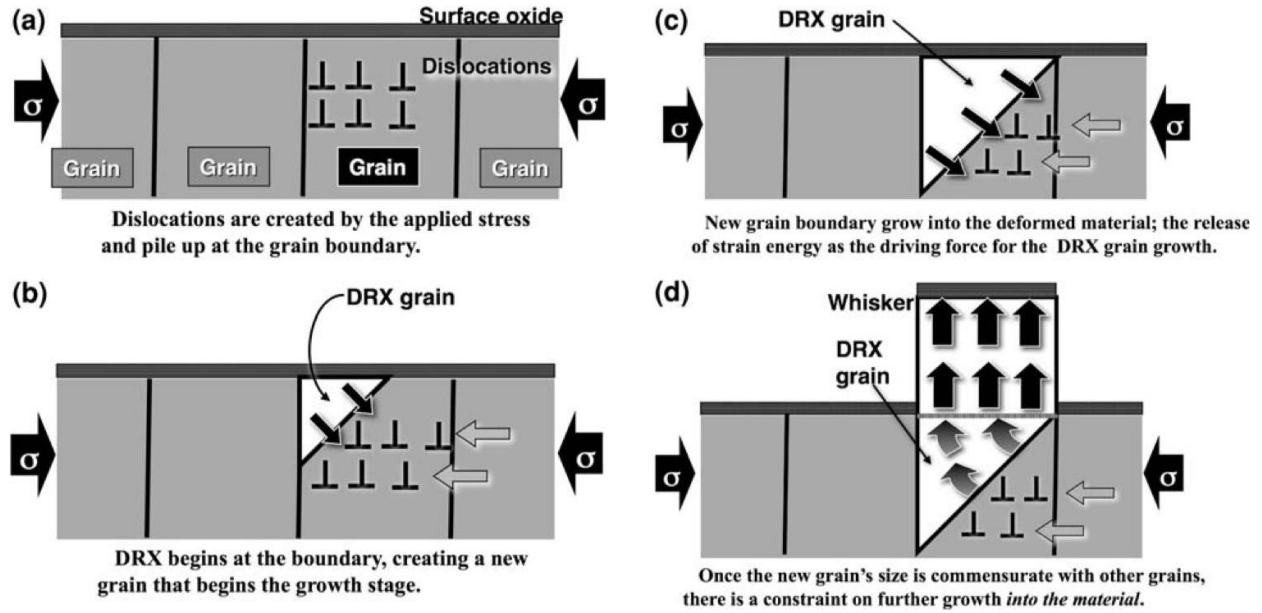


Figure 1.7. Schematics showing whisker nucleation via Dynamic Recrystallization (DRX). Reprinted from [30], copyright 2009, with permission from Springer Nature.

Sarobel et al. observed surface defects (whiskers and hillocks) grew from small grains with relatively lower ESED and dislocation density near GBs in large-grain Sn-alloy films after thermal cycling [32]. This experiment suggested that grains nucleated from large parent grains via recrystallization and become growth sites of surface defects, as seen in Fig. 1.8. Sarobol et al. [32] also reported an orientational relationship—usually a greater-than- 15° misorientation angle between matrix grains and a smaller-than- 15° misorientation angle around surface defects, which implies that the grain boundaries of surface defects originated from dislocation motions. Although small grains with lower stress energy have been directly observed at the grain boundary, the orientation of the selected region was not reported, leading to difficulties in the direct comparison of the crystallographic change before and after thermal cycling.

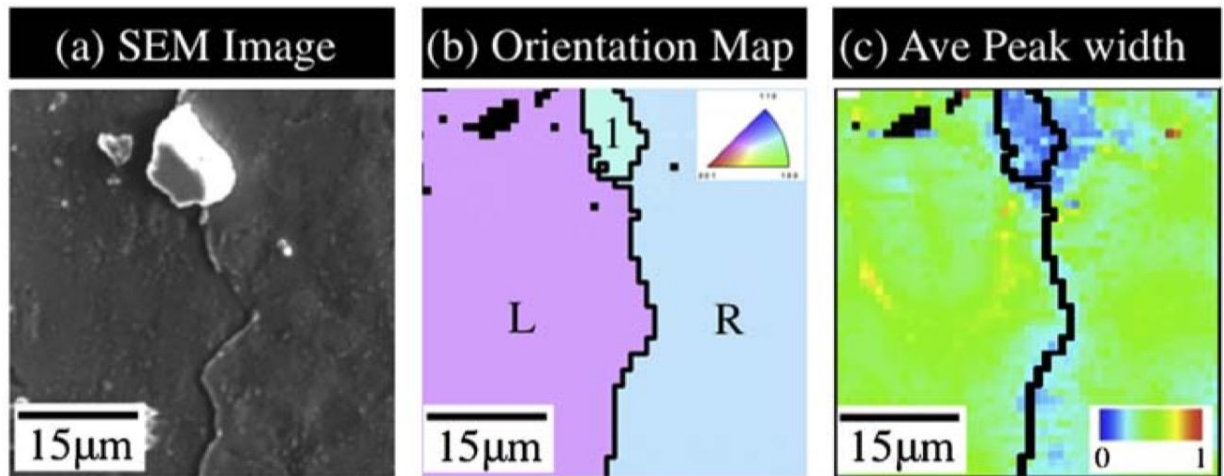


Figure 1.8. (a) the SEM image showing a whisker formed at one grain boundary; (b) the orientation map with IPF colors. Grain 1 is the surface defect grain in (a); (c) calculated average peak width showing the grain 1 has a relatively lower elastic energy density than the matrix grains. Reprinted from [32], copyright 2013, with permission from Elsevier.

As a continuum effort, Chen et al. [33] labeled the deformation type of 108 GBs in a large-grain film and categorized those GBs into four groups: surface defects, GB sliding, surface defects, and GB sliding, and non-deformation, as shown in Fig. 1.9. Based on quantified macroscopic deformation and corresponding microscopic orientation, Chen et al. [33] summarized the grain-grain misorientation and grain boundary plane angle dependence of defect formation versus GB sliding. These findings shed light on the effects of grain geometry on the stress relaxation behavior. According to their results, GBs sliding events were observed more frequently in highly inclined GBs than in vertical GBs. More characterization on the geometry of boundaries exhibiting different stress relaxation responses is required to draw a preliminary conclusion on the correlation between geometry and local stress states.

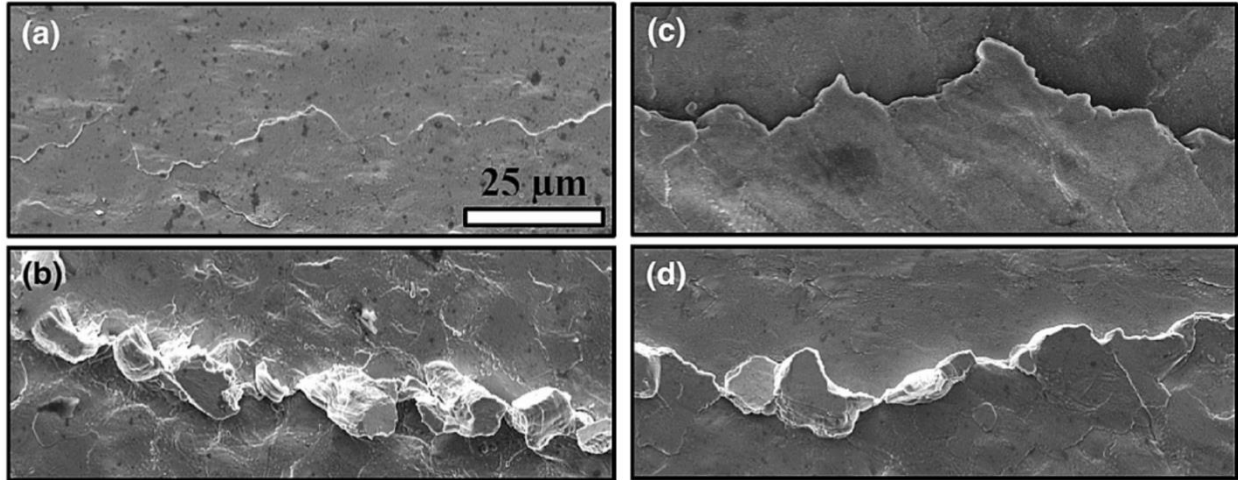


Figure 1.9. Four different grain boundaries (GBs) responses have been observed in thermally cycled Sn-alloy films: (a) no obvious microstructural changes; (b) surface defects formation; (c) grain boundary sliding; (4) surface defects formation and grain boundary sliding. Reprinted from [33], copyright 2016, with permission from Springer Nature.

1.2.7 Orientation effects on whisker nucleation

The anisotropy of β -tin could explain these observations. Koppes et al. [34] postulated that if the c-axis directions of two neighboring grains are located in the plane and normal to the interface, a higher local thermoelastic stress would be introduced at the grain boundary in thermal cycling tests. Chen et al. [35] simulated both the elastic energy density and the thermoelastic energy density for four different orientation textures in the same microstructure skeleton, where thermoelastic energy density reflected the stress localization during thermal cycling experiments. Computed energy density maps (Fig. 1.10) revealed that the stress localization varies with respect to different orientation textures. In other words, the orientation plays an essential role in whisker formation because which grains grow as whiskers rely on the local stress state instead of the global stress state. However, as the formation and growth of whiskers is a plastic deformation process, this simulation cannot be related to the experimental results directly because it only considered elastic energy density. An effective analysis of the orientation dependence in surface defects formation is absent.

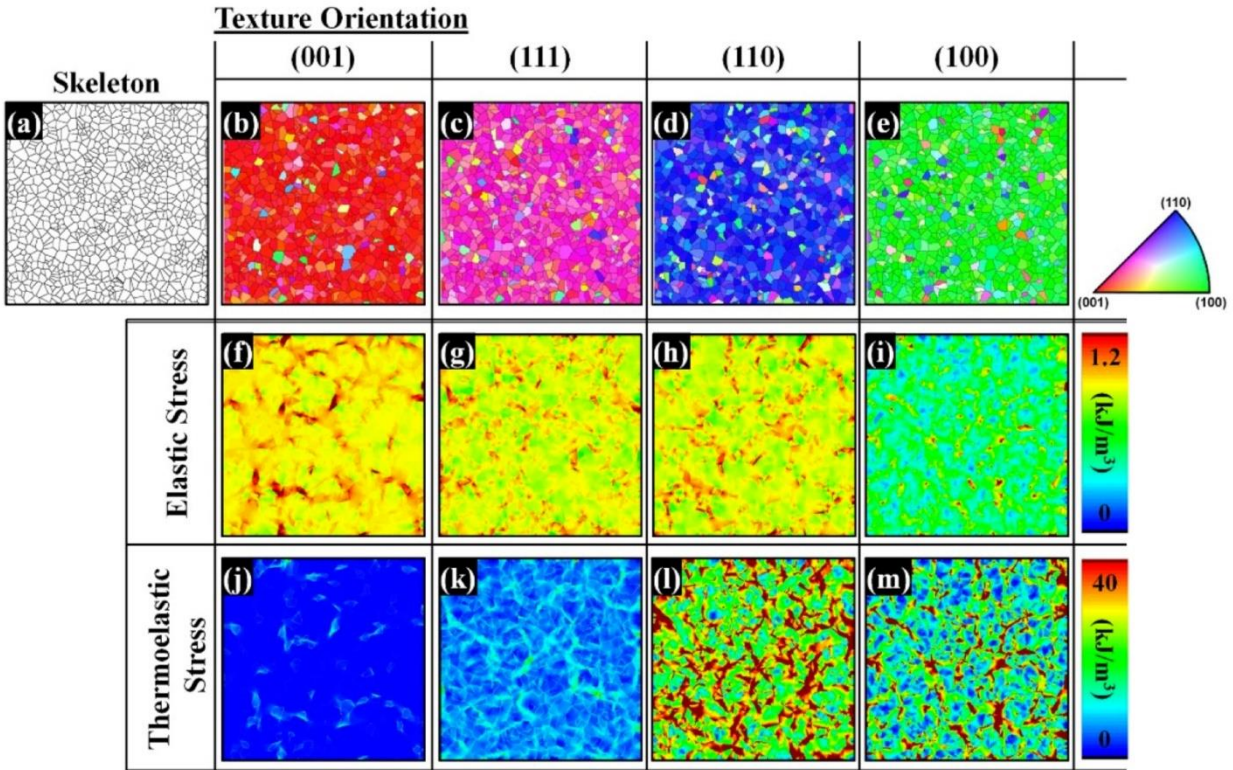


Figure 1.10. (a) a schematic skeleton of designed microstructure; (b-e) IPF colored orientation map showing four different orientation texture assigned to the polycrystalline structure in (a); (f- i) calculated ESED (elastic energy density) distribution maps for elastic energy with respect to orientations; (i-m) calculated ESED maps for thermoelastic energy with respect to orientations.

Reprinted from [35], copyright 2014, with permission from Springer Nature.

1.2.8 Scope of the project

In summary, whiskers grow to relax stresses in Sn films. A fair collection of studies has examined the variables in β -Sn films associated with the global stress states, such as intermetallic compounds (IMCs) growth, mechanical loading, and thermal cyclic loading. Besides global stress states, the fact that only one grain out of thousands becomes a whisker indicates strong local effects, i.e., heterogeneous distribution of stresses in films. In polycrystalline β -Sn films, the properties from grain to grain varies; therefore, local orientation plays a critical role in both stress accumulation and relaxation when Sn films experience any mechanical or thermomechanical stresses. To simplify the identification of heterogeneous stress localization resulting from β -Sn's anisotropic elasticity and thermal expansion, large-grained Sn films were prepared and employed

to quantify the evolution of stress relaxation responses observed near GBs on free surfaces during thermal cycling. Apart from the simple pseudo-bicrystal geometry between each pair of grains, large-grained Sn films also exhibit a greater extent of stress relaxation under thermomechanical stresses, as measured in Fig. 1.11. Therefore, large-grained Sn films are ideal samples for accelerating experiments on whisker formation during thermal cycling.

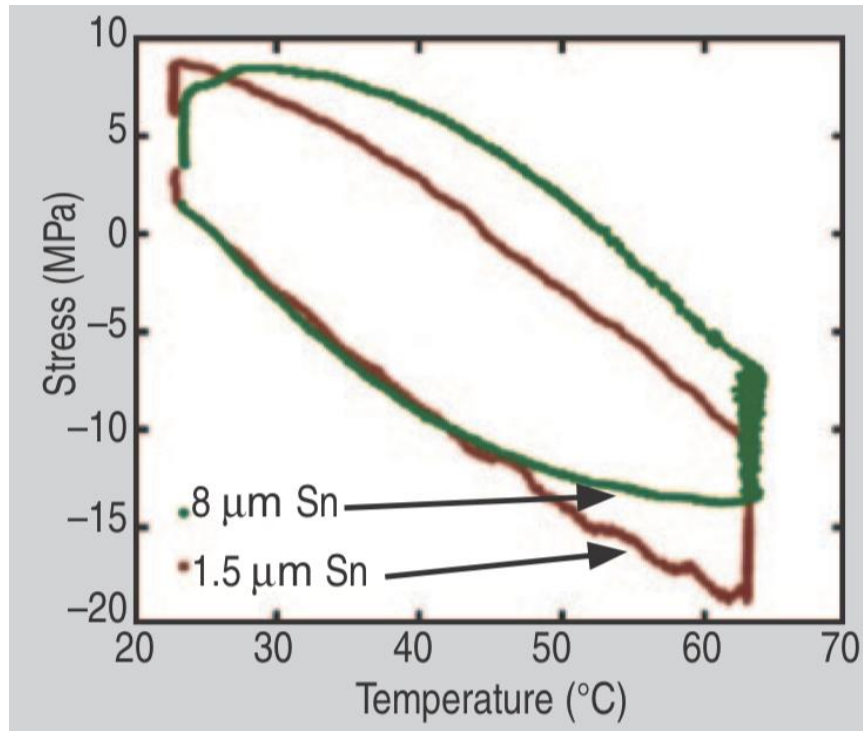


Figure 1.11. Stress-strain curves for 1.5- μm -thick and 7.5- μm -thick Sn films. Reprinted from [8], copyright 2013, with permission from Elsevier.

The growth and formation of surface defects are due to plastic deformation, in which dislocation movement often is the fundamental mechanism. Therefore, it is reasonable to break down the plastic deformation problems into dislocation motions. In order to fill the gap between observed deformation and the underlying dislocation mechanism, two key questions involving slip behaviors need to be solved, i.e., (1) what plastic deformation mechanisms contribute to the nucleation of shallow surface grains and how, i.e., their sequences and interplays, and (2) what factors determine whether the nucleated shallow grains will become whiskers or not, with a special focus on the GB microstructure.

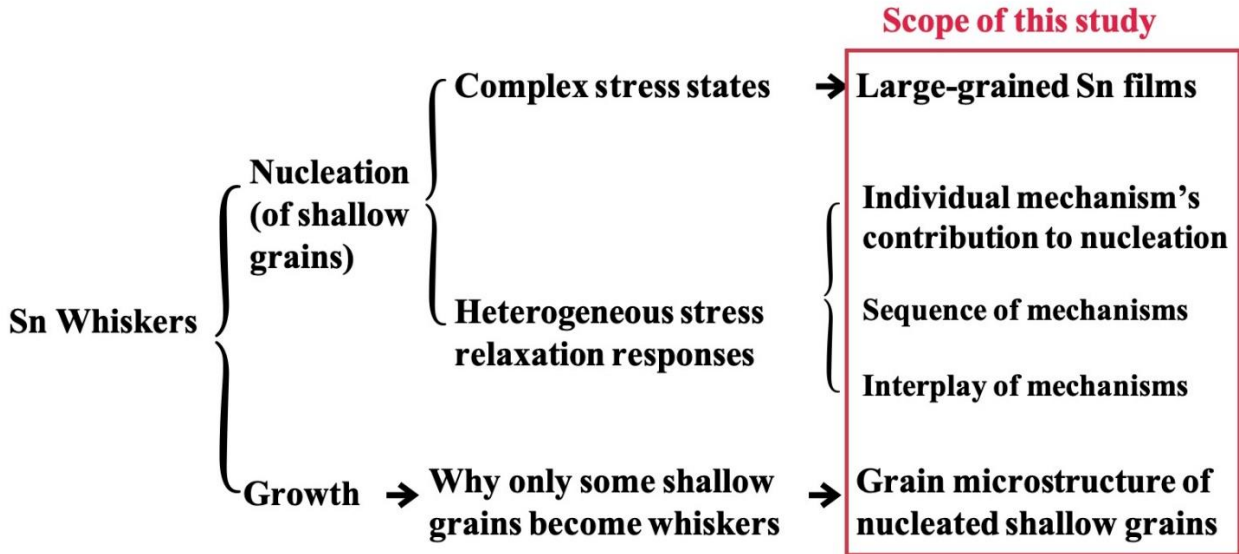


Figure 1.12. The scope of the first part of the study. Large-grained Sn films are utilized to simplify the local stress states near GBs. The research questions include (1) what mechanisms contribute to the nucleation of shallow grains and (2) how post-nucleation microstructure determines whether a surface grain becomes a whisker or not.

1.3 End-of-life treatment of electronics

With the soaring manufacturing of electronics, e-waste has become a global concern. In 2019, the world generated over 50 million tons of e-waste, i.e., 7.3 kg per capita [36]. The end-of-life treatment of electronics is associated with many Sustainable Development Goals (SDGs) such as good health and well-being, economic growth, clean waste, material footprint, and hazardous waste [3, 36]. The end-of-life market of electronics was estimated to reach \$62.5 billion annually [1] and a large portion of the value originates from waste printed circuit boards (WPCBs) that contain valuable metals such as gold, copper, and silver.

The challenges in recycling e-waste include (1) environmental pollution and human health risks due to informal recycling, (2) low recycling rate, and (3) lack of sustainability in product design.

Two recycling routes exist for e-waste, i.e., formal recycling and informal recycling. Formal recycling refers to a recycling enterprise that has collection and dismantling equipment, standardized processing procedures, and waste management that meets the national standards and

is authorized by the government [37]. In contrast, informal recycling refers to workshops and "backyard" recycling systems utilizing primitive technologies such as open-air combustion and acid leaching without the proper disposal of the hazardous residues [38]. Additionally, most informal recycling belongs to nonfunctional recycling (discarded products are collected and recycled only for several specific metals, and other metals are not recovered in the original form), leading to undesirable materials losses. Regarding the recycling rate, only less than 20% of e-waste was recycled, and only 15% of which was formally recycled [1,36,39]. Insufficient e-waste feedstock, in turn, negatively impacts the profitability of the formal recycling enterprises. Concerning product design, the current focus of the electronics industry is on performances and appearances, instead of sustainability. For example, within the past 10 years, many nanomaterials have been used in electronics, which means the recycling procedures such as sorting need much more input (e.g., energy, labor) than before to produce the same output. In this case, functional recycling becomes less profitable and more difficult to operate. Another example is the non-removable batteries in laptops and cell phones that will cause plenty of trouble during recycling.

An even more pressing issue is the unfair distribution of e-waste recycling activities that caused severe impacts in developing countries, as illustrated in Fig. 1.13 [40]. E-waste has been continuously exported from Europe, North America, and part of eastern Asia (Japan and Korea) to the poor countries in the rest of Asia and, South America, and Africa. A study traced the e-waste in the US via GPS devices and reported that more than 45% was exported and over 95% of which ended up in developing countries through illegal channels [41]. For example, in the past 40 years, China became the largest e-waste dumping site in the world and has absorbed 350 million tons of e-waste from the global market [42]. Without sufficient funds to establish formal recycling enterprises, those developing countries processed the majority of e-waste in the informal sector, blinded by the so-called economic gains. The intense and unregulated informal recycling of transboundary e-waste has adversely affected the environment and human health in those regions.

1.3.1 Scope of the project

Minimizing informal recycling activities is critical for the sustainable end-of-life treatment of electronics. Recent studies have started to revisit the concept of informality in recycling and reported empirical examples where informal sectors coordinate with formal sectors, jointly contributing to a greener recycling solution. Guiyu, a town in China known for its large-scale

informal e-waste recycling industry, has created the Guiyu Circular Economy Industrial Park (GCEIP) as a systematic effort to integrate the informal sector into the formal recycling industry under the circular economy framework. This case study provides a detailed examination of GCEIP regarding policy design, using publicly available reports and data collected during a field trip. The objective of GCEIP is to offer advanced e-waste treatment while maintaining competitive characteristics of the old informal businesses, including manual dismantling and private e-waste collection networks. Those characteristics sustain the successful implementation of GCEIP with increased reuse value as well as sufficient e-waste sources. Meanwhile, Guiyu's struggles during this transition reflect that societal and historical contexts are often overlooked factors that profoundly shaped the local recycling industry. Contextualized in the historical development and societal consequences of Guiyu's informal sectors, the second part of the study analyzes the policy design, facility construction, technology development, and market establishment that enabled the transition and alignment of the local informal recycling industry to the formal sector.

UNFAIR FLOW

Most electronic waste from developed countries ends up in poor nations that lack regulation. China processed around 70% of the world's e-waste in 2012; the rest goes to India and other countries in eastern Asia and Africa, including Nigeria.

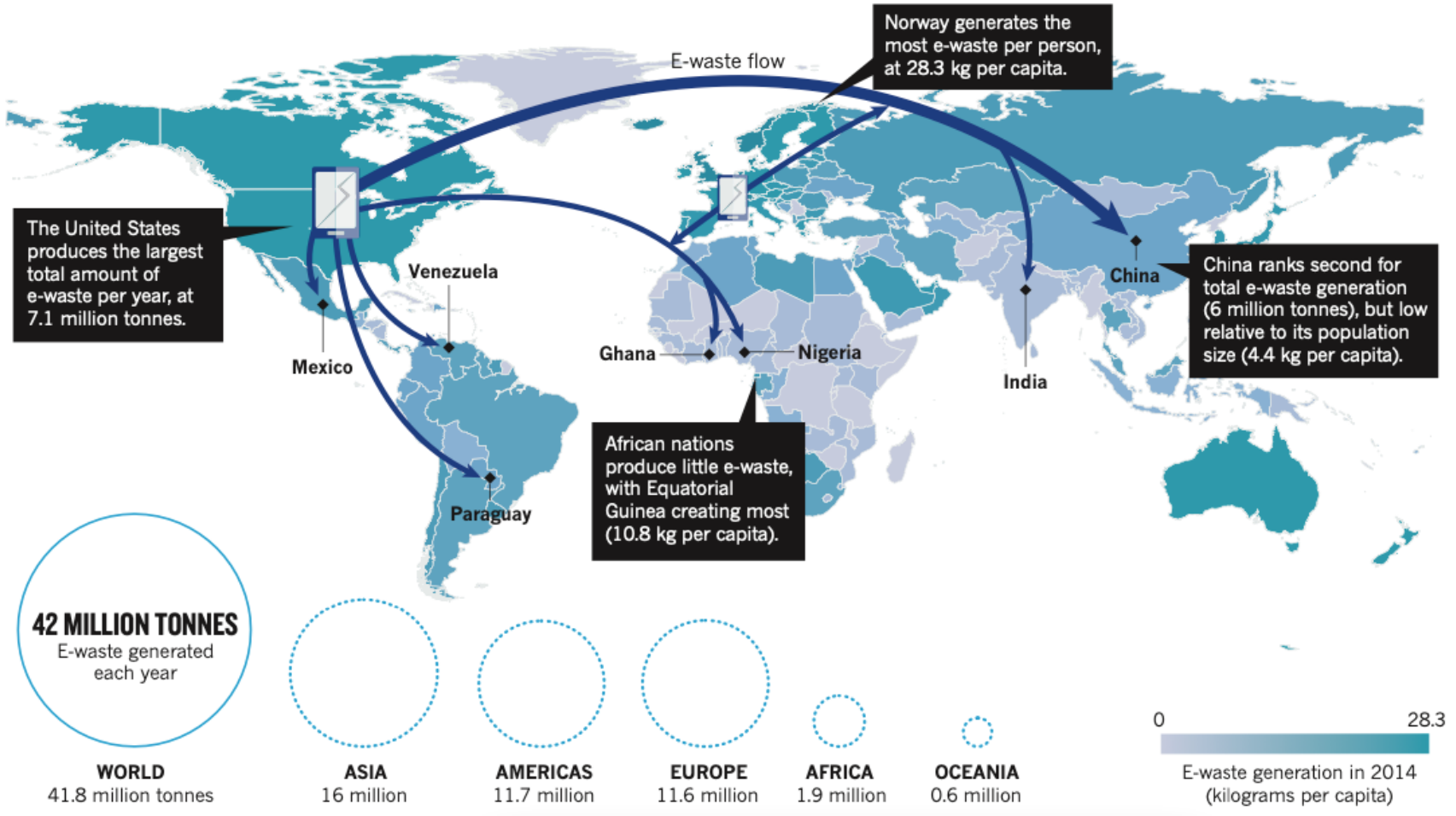


Figure 1.13. The transboundary flow of global e-waste. Reprinted from [40], copyright 2016, with permission from Springer Nature.

1.4 Sustainability education in STEM

Our next-generation engineers must be able to develop technologies with restricted natural resources with the purpose of sustaining the environment and protecting human health. Scholars have identified the three pillars of sustainability as environmental, economic, and societal, making sustainability an inherently interdisciplinary subject [43]. Though universities around the world (especially in the U.S.) have established a substantial amount of interdisciplinary programs, some concepts, including sustainability, still lack cultural and societal considerations [44, 45]. For example, in the context of sustainable electronics, as detailed in section 1.3, the complexity of e-waste lies not only in the recycling technology but also in the unfair distribution of e-waste among developed countries and developing countries. Tab. 1.2 summarized the current difficult concepts in sustainability education and categorized those concepts into misconceptions, ritual knowledge, and foreign knowledge based on the theory of difficulty [46].

Table 1.2. Hard concepts in sustainability education are summarized in the literature. Categorization is based on the theory of difficulty [46].

Categories	Concepts
Misconceptions	(1) Believe that technology can offer complete solutions to sustainability and ignore the societal and economic aspects [47, 48] (2) Believe that only environmental science studies sustainability [49]
Ritual Knowledge	(3) Think of sustainability as a concept [50]
Foreign knowledge	(4) Students need to evaluate and critique electronics-related environmental policies or organizational activities all around the world with contextual awareness [52] (5) Students need to predict the responses of all stakeholders involved in the sustainable electronics given a scenario and offer relevant suggestions [52]

1.4.1 Misconceptions

Engineers today consider how to advance technologies with limited natural resources to achieve a sustainable future that holds our planet paramount. Sustainability has been integrated

into a variety of engineering curriculum where educators face the challenge of the misconception perceived by students that technology can offer complete solutions to sustainability. This is a misconception that resulted from the ignorance of societal and economic effects [47, 48]. Another common misconception is that only environmental scientists should teach or study sustainability in higher education. So far, sustainability is still mostly covered in traditional "environment-related" departments such as civil engineering and environmental engineering in the format of a mono-discipline curriculum [49]. In addition, as the main body of the students' majors in engineering, the environmental part may be unconsciously weighted over the society and economy.

1.4.2 Ritual knowledge

Sustainability can readily fall into the categories of ritual knowledge (recognizing problems as ritualized knowledge). Students can memorize the definition with few efforts, i.e., "to achieve sustainability, we need to consider societal, economic, and environmental factors altogether." But what does this sentence really mean? Sustainability is never merely a concept: it contains professional values, partnership mindsets, and strategic thinking skills [50]. If the sustainability education aims for students to obtain the "true" understanding, it means the students will be able to break down the sustainability into the essential elements, group that knowledge into different categories, and carefully examine and evaluate the roles of each element and each group as well as their interactions. Here, understanding the "concept of sustainability" equals the comprehensive background knowledge and analyzing skills in all sub-fields plus the complex reasoning thinking methods. This belongs to expert problem solving (compared to novices) described in teaching and learning STEM [51], i.e., "classifying problem types based on their underlying principles and key attributes; place new problems into appropriate categories and quickly select corresponding solution strategies."

1.4.3 Foreign Knowledge

Emerging with the most advanced technologies, the electronics industry is never a "local" business, and the global context of electronics inevitably brings in foreign knowledge in the topic (knowledge too foreign for learners to engage it readily). For example, the concepts of informal cycling and formal cycling. Informal recycling refers to those recycling processes that are low-

technology, low-cost but high-pollution. Within informal recycling, valuable metals such as gold, silver, lead, and copper can be recovered from e-wastes without skilled-labor or much technology. These concepts are active research fields in sustainability. The generation and development of either informal recycling, formal recycling, or both in one region are associated with complex societal, economic, and environmental reasons in that local area, with potential historical and cultural impacts involved as well [38]. For sustainability education in the U.S., where formal recycling seems just like the “right thing to do,” it is hard for domestic students to understand the context of the informal recycling in many emerging economies, which is the opposite option to their experiences [52]. This pair of concepts asks students to make non-judgmental observations, to analyze without cultural filters, and to compare and contrast the two ideas without “our current beliefs, prejudices, and routines,” [53] to avoid the learning experiences as Perkin wrote in [54]:

“The way those people on the other side of the ocean do things just does not make sense, and indeed often seems simply wrong... viewing what is strange and uncomfortable as also mistaken or evil.”

The expected learning outcome for the concepts of formal recycling and informal recycling is not to differentiate the “right” from “wrong” but to allow students to obtain a systematic and inclusive background in terms of e-waste recycling and bear this core knowledge in their minds when making decisions in future careers.

1.4.4 Scope of the project

The objective of this program is to nurture sustainability thinking for the future engineers so that the misconceptions or difficult concepts could be addressed prior to or at an earlier stage of the college education. Two case studies in higher education and K-12 classrooms are discussed in Chapter 7 by integrating authentic contexts, global perspective, and culture awareness into current sustainability education.

1.5 References

- [1] World Economic Forum. (2019). *A new circular vision for electronics: Time for a global reboot*. http://www3.weforum.org/docs/WEF_A_New_Circular_Vision_for_Electronics.pdf
- [2] Ghisellini, P., Cialani, C., & Ulgiati, S. (2016). A review on circular economy: the expected transition to a balanced interplay of environmental and economic systems. *Journal of Cleaner Production*, 114, 11-32. <https://doi.org/10.1016/j.jclepro.2015.09.007>
- [3] United Nations. (2015). *Sustainable development goals*. <https://sdgs.un.org/goals>
- [4] Philips. (n.d.). *Decoupling growth from resource consumption*. Circular Economy. Retrieved June 27, 2021, from <https://www.philips.com/a-w/about/sustainability/circular-economy.html>
- [5] Gama, M., Herrmann, C., & Fisher, T. (2016). *Circular economy in the electronics sector: A holistic perspective*. In. IEEE. <http://dx.doi.org/10.1109/egg.2016.7829848>
- [6] Glavič, P. (2006). Sustainability engineering education. *Clean Technologies and Environmental Policy*, 8(1), 24-30. <https://doi.org/10.1007/s10098-005-0025-4>
- [7] Tu, K. N., & Li, J. C. M. (2005). Spontaneous whisker growth on lead-free solder finishes. *Materials Science and Engineering: A*, 409(1-2), 131-139. <https://doi.org/10.1016/j.msea.2005.06.074>
- [8] Chason, E., Jadhav, N., Pei, F., Buchovecky, E., & Bower, A. (2013). Growth of whiskers from Sn surfaces: Driving forces and growth mechanisms. *Progress in Surface Science*, 88(2), 103-131. <https://doi.org/10.1016/j.progsurf.2013.02.002>
- [9] NASA. *Whisker Failures*. <https://nepp.nasa.gov/whisker/failures/index.htm>
- [10] Smetana, J. (2007). Theory of Tin Whisker Growth: “The End Game”. *IEEE Transactions on Electronics Packaging Manufacturing*, 30(1), 11-22. <https://doi.org/10.1109/tepm.2006.890645>
- [11] RoHS. (2003). *Restriction of Hazardous Substances in Electrical and Electronic Equipment*. https://ec.europa.eu/environment/topics/waste-and-recycling/rohs-directive_en
- [12] Boettinger, W. J., Johnson, C. E., Bendersky, L. A., Moon, K.-W., Williams, M. E., & Stafford, G. R. (2005). Whisker and Hillock formation on Sn, Sn–Cu and Sn–Pb electrodeposits. *Acta Materialia*, 53(19), 5033-5050. <https://doi.org/10.1016/j.actamat.2005.07.016>
- [13] Frolov, T., Boettinger, W. J., & Mishin, Y. (2010). Atomistic simulation of hillock growth. *Acta Materialia*, 58(16), 5471-5480. <https://doi.org/10.1016/j.actamat.2010.06.023>

- [14] Sarobol, P., Wang, Y., Chen, W. H., Pedigo, A. E., Koppes, J. P., Blendell, J. E., & Handwerker, C. A. (2013). A Predictive Model for Whisker Formation Based on Local Microstructure and Grain Boundary Properties. *JOM*, 65(10), 1350-1361. <https://doi.org/10.1007/s11837-013-0717-x>
- [15] Sarobol, P., Blendell, J. E., & Handwerker, C. A. (2013). Whisker and hillock growth via coupled localized Coble creep, grain boundary sliding, and shear induced grain boundary migration. *Acta Materialia*, 61(6), 1991-2003. <https://doi.org/10.1016/j.actamat.2012.12.019>
- [16] Hektor, J., Marijon, J.-B., Ristinmaa, M., Hall, S. A., Hallberg, H., Iyengar, S., Micha, J.-S., Robach, O., Grennerat, F., & Castelnau, O. (2018). Evidence of 3D strain gradients associated with tin whisker growth. *Scripta Materialia*, 144, 1-4. <https://doi.org/10.1016/j.scriptamat.2017.09.030>
- [17] Chen, W.-H. (2014). *Evaluation of local anisotropic elasticity and thermal expansion on whisker formation sites in beta-tin thin films*. Purdue University.
- [18] Qiu, S. L., & Marcus, P. M. (2012). Equilibrium lines and barriers to phase transitions: the cubic diamond to beta-tin transition in Si from first principles. *J Phys Condens Matter*, 24(22), 225501. <https://doi.org/10.1088/0953-8984/24/22/225501>
- [19] Bieler, T. R., Jiang, H., Lehman, L. P., Kirkpatrick, T., & Cotts, E. J. (2006). *Influence of Sn Grain Size and Orientation on the Thermomechanical Response and Reliability of Pb-free Solder Joints*. In: IEEE. <http://dx.doi.org/10.1109/ectc.2006.1645849>
- [20] Tu, K. N. (1973). Interdiffusion and reaction in bimetallic Cu-Sn thin films. *Acta Metallurgica*, 21(4), 347-354. [https://doi.org/10.1016/0001-6160\(73\)90190-9](https://doi.org/10.1016/0001-6160(73)90190-9)
- [21] Lee, B.-Z., & Lee, D. N. (1998). Spontaneous growth mechanism of tin whiskers. *Acta Materialia*, 46(10), 3701-3714. [https://doi.org/10.1016/s1359-6454\(98\)00045-7](https://doi.org/10.1016/s1359-6454(98)00045-7)
- [22] Fisher, R. M., Darken, L. S., & Carroll, K. G. (1954). Accelerated growth of tin whiskers. *Acta Metallurgica*, 2(3), 368-373. [https://doi.org/10.1016/0001-6160\(54\)90053-x](https://doi.org/10.1016/0001-6160(54)90053-x)
- [23] Shibutani, T., Wu, J., Yu, Q., & Pecht, M. (2008). Key reliability concerns with lead-free connectors. *Microelectronics Reliability*, 48(10), 1613-1627. <https://doi.org/10.1016/j.microrel.2008.06.004>
- [24] Tu. (1994). Irreversible processes of spontaneous whisker growth in bimetallic Cu-Sn thin-film reactions. *Physical Review B: Condensed Matter*, 49(3), 2030-2034. <https://doi.org/10.1103/physrevb.49.2030>
- [25] Wang, Y. (2014). *Microstructure evolution and surface defect formation in tin films*. Purdue University.

- [26] Chen, W.-H., Wang, C., Sarobol, P., Blendell, J., & Handwerker, C. (2020). Local variations in grain formation, grain boundary sliding, and whisker growth along grain boundaries in large-grain Sn films. *Scripta Materialia*, 187, 458-463. <https://doi.org/10.1016/j.scriptamat.2020.06.033>
- [27] Jadhav, N., Buchovecky, E., Chason, E., & Bower, A. (2010). Real-time SEM/FIB studies of whisker growth and surface modification. *JOM*, 62(7), 30-37. <https://doi.org/10.1007/s11837-010-0105-8>
- [28] Sobiech, M. L. (2010). *Whisker formation on Sn thin films*. Universität Stuttgart. <http://elib.uni-stuttgart.de/handle/11682/1335>
- [29] Pei, F., Jadhav, N., & Chason, E. (2012). Correlation Between Surface Morphology Evolution and Grain Structure: Whisker/Hillock Formation in Sn-Cu. *JOM*, 64(10), 1176-1183. <https://doi.org/10.1007/s11837-012-0442-x>
- [30] Vianco, P. T., & Rejent, J. A. (2009). Dynamic Recrystallization (DRX) as the Mechanism for Sn Whisker Development. Part I: A Model. *Journal of Electronic Materials*, 38(9), 1815-1825. <https://doi.org/10.1007/s11664-009-0879-z>
- [31] Vianco, P. T., Neilsen, M. K., Rejent, J. A., & Grant, R. P. (2015). Validation of the Dynamic Recrystallization (DRX) Mechanism for Whisker and Hillock Growth on Sn Thin Films. *Journal of Electronic Materials*, 44(10), 4012-4034. <https://doi.org/10.1007/s11664-015-3779-4>
- [32] Sarobol, P., Koppes, J. P., Chen, W. H., Su, P., Blendell, J. E., & Handwerker, C. A. (2013). Recrystallization as a nucleation mechanism for whiskers and hillocks on thermally cycled Sn-alloy solder films. *Materials Letters*, 99, 76-80. <https://doi.org/10.1016/j.matlet.2013.02.066>
- [33] Chen, W.-H., Sarobol, P., Handwerker, C. A., & Blendell, J. E. (2016). Heterogeneous Stress Relaxation Processes at Grain Boundaries in High-Sn Solder Films: Effects of Sn Anisotropy and Grain Geometry During Thermal Cycling. *JOM*, 68(11), 2888-2899. <https://doi.org/10.1007/s11837-016-2070-3>
- [34] Koppes, J. P. (2012). *Effect of crystallographic orientation on hillock formation in thermally cycled large grain tin films*. Purdue University.
- [35] Chen, W.-H., Sarobol, P., Holaday, J. R., Handwerker, C. A., & Blendell, J. E. (2014). Effect of crystallographic texture, anisotropic elasticity, and thermal expansion on whisker formation in β -Sn thin films. *Journal of Materials Research*, 29(2), 197-206. <https://doi.org/10.1557/jmr.2013.378>
- [36] Balde, C. P., Forti, V., Gray, V., Kuehr, R., & Stegmann, P. (2017). *The global e-waste monitor 2017: Quantities, flows and resources*. United Nations University, International Telecommunication Union, and International Solid Waste Association. <https://www.itu.int/en/ITU-D/Climate-Change/Documents/GEM%202017/Global-E-waste%20Monitor%202017%20.pdf>

- [37] Cao, J., Lu, B., Chen, Y., Zhang, X., Zhai, G., Zhou, G., Jiang, B., & Schnoor, J. L. (2016). Extended producer responsibility system in China improves e-waste recycling: Government policies, enterprise, and public awareness. *Renewable and Sustainable Energy Reviews*, 62, 882-894. <https://doi.org/10.1016/j.rser.2016.04.078>
- [38] Chi, X., Streicher-Porte, M., Wang, M. Y., & Reuter, M. A. (2011). Informal electronic waste recycling: a sector review with special focus on China. *Waste Management*, 31(4), 731-742. <https://doi.org/10.1016/j.wasman.2010.11.006>
- [39] Yang, C., Tan, Q., Liu, L., Dong, Q., & Li, J. (2017). Recycling Tin from Electronic Waste: A Problem That Needs More Attention. *ACS Sustainable Chemistry & Engineering*, 5(11), 9586-9598. <https://doi.org/10.1021/acssuschemeng.7b02903>
- [40] Wang, Z., Zhang, B., & Guan, D. (2016). Take responsibility for electronic-waste disposal. *Nature*, 536(7614), 23-25. <https://doi.org/10.1038/536023a>
- [41] Hopson, E., & Puckett, J. (2016). *Scam recycling: e-Dumping on Asia by US recyclers*. Basel Action Network. <https://wiki.ban.org/images/1/12/ScamRecyclingReport-web.pdf>
- [42] Wong, N. W. M. (2018). Electronic waste governance under “one country, two systems”: Hong Kong and mainland China. *International Journal of Environmental Research and Public Health*. <https://www.mdpi.com/1660-4601/15/11/2347/pdf>
- [43] Mihelcic, J. R., Phillips, L. D., & Watkins, D. W. (2006). Integrating a Global Perspective into Education and Research: Engineering International Sustainable Development. *Environmental Engineering Science*, 23(3), 426-438. <https://doi.org/10.1089/ees.2006.23.426>
- [44] Wan Alwi, S. R., Manan, Z. A., Klemeš, J. J., & Huisinigh, D. (2014). Sustainability engineering for the future. *Journal of Cleaner Production*, 71, 1-10. <https://doi.org/10.1016/j.jclepro.2014.03.013>
- [45] De Graaff, E., & Ravesteijn, W. (2001). Training complete engineers: Global enterprise and engineering education. *European Journal of Engineering Education*, 26(4), 419-427. <https://doi.org/10.1080/03043790110068701>
- [46] Hansen, E. (2011). *Idea-based Learning*. Stylus Publishing Llc.
- [47] Guerra, A. (2017). Integration of sustainability in engineering education. *International Journal of Sustainability in Higher Education*, 18(3), 436-454. <https://doi.org/10.1108/ijsh-02-2016-0022>
- [48] Segalàs, J., Ferrer-Balas, D., & Mulder, K. F. (2010). What do engineering students learn in sustainability courses? The effect of the pedagogical approach. *Journal of Cleaner Production*, 18(3), 275-284. <https://doi.org/10.1016/j.jclepro.2009.09.012>

- [49] Mesa, J., Esparragoza, I., & Maury, H. (2017). *Sustainability in Engineering Education: A Literature Review of Case Studies and Projects*. In. Latin American and Caribbean Consortium of Engineering Institutions. <http://dx.doi.org/10.18687/laccei2017.1.1.241>
- [50] Sibbel, A. (2009). Pathways towards sustainability through higher education. *International Journal of Sustainability in Higher Education*, 10(1), 68-82.
<https://doi.org/10.1108/14676370910925262>
- [51] Felder, R. M., & Brent, R. (2016). *Teaching and Learning STEM*. John Wiley & Sons.
- [52] Wong, M. H., Wu, S. C., Deng, W. J., Yu, X. Z., Luo, Q., Leung, A. O., Wong, C. S., Luksemburg, W. J., & Wong, A. S. (2007). Export of toxic chemicals - a review of the case of uncontrolled electronic-waste recycling. *Environmental Pollution*, 149(2), 131-140.
<https://doi.org/10.1016/j.envpol.2007.01.044>
- [53] Stephens, J. C., Hernandez, M. E., Román, M., Graham, A. C., & Scholz, R. W. (2008). Higher education as a change agent for sustainability in different cultures and contexts. *International Journal of Sustainability in Higher Education*, 9(3), 317-338.
<https://doi.org/10.1108/14676370810885916>
- [54] Perkins, D. (2010). *Making learning whole: How seven principles of teaching can transform education*. John Wiley & Sons.

2. RELATING TEMPERATURE AND THERMAL STRAINS TO FATIGUE BEHAVIOR OF THERMALLY CYCLED TIN FILMS

The following chapter is a group effort. Ying Wang performed the experiments; Congying Wang collected and analyzed the data. Congying Wang, John Blendell, and Carol Handwerker all contributed to the manuscript.

2.1 Introduction

High-Sn component surface finishes can increase solderability and prevent oxidation of the Cu leads of various microelectronic components. However, when polycrystalline Sn thin films are stressed, film microstructures become unstable by multiple local responses, including cracking [1], grain boundary (GB) sliding [2], and whisker/hillock formation [1-4], resulting in issues regarding the reliability of electronics. Those stress relaxation responses are known to be sensitive to local stress states due to anisotropic thermal expansion and elasticity of β -Sn [5], i.e., when the temperature fluctuates, heterogeneous thermomechanical stress accumulated in Sn films due to the mismatch of coefficient of thermal expansion (CTE) between individual grains regardless of the substrates. Previous studies on thermomechanical fatigue of Sn films or solder joints [2, 6-10] reported multiple deformation behavior including surface roughening, cracking, GB sliding, and whiskers, many of which often occurred at the same time and space. However, varied experimental settings employed in studies on thermal fatigue of Sn films pose a challenge in relating specific responses to interventions. For example, cycling temperature influences both the introduced thermal strain and the temperature itself, which may trigger different stress relaxation mechanisms.

In this study, we examined the effects of temperature and applied thermal strains on local stress relaxation responses in β -Sn films through quantitative analysis of defects and cracks densities under three different cycling settings. We found that whisker densities increased not only with higher cycling temperature but also with higher global thermomechanical strains because hot cycling resulted in higher whisker densities relative to cold cycling and lower whisker densities relative to full cycling. Therefore, mechanisms other than diffusional creep can affect whisker nucleation, such as the GB sliding or grain rotation reported in the literature. In particular, the previously reported pinch-off mechanism of whiskers was prominently controlled by the macro strains. Fatigue cracks were dominated by total strains compared to temperature because their

densities remained almost the same in hot or cold cycling ranges and were significantly lower than the full cycling sample. The early stage of cycling is critical because whisker density quickly reached during rapid thermal cycling.

2.2 Experiments and Methods

A PVD Cu layer (300 nm) was deposited on a Ti adhesion layer (10 nm) sputtered on the Si substrate. A pure Sn layer (5 μm) was then electrodeposited on the Cu. We assume: (1) the limited formation of Cu₆Sn₅ had a negligible impact on local stress states inside individual grains, especially the regions near the film surface, as evidenced in the previous simulation [cite Chason]; (2) the CTE misfit between the film and the substrate was mainly controlled by the much thicker Si layer (0.6 mm) than the Ti and Cu adhesion layers. Rapid thermal cycling was employed as the accelerating testing technique with details reported in earlier studies [7, 11]. Three samples (Sample C, H, and F) were thermally cycled with different temperature ranges annotated as cold, hot, and full, respectively, as shown in Tab. 2.1.

Table 2.1. Sample types, properties, and cycling conditions

No.	Temperature (°C)	Time per cycle (<i>min</i>)	$\delta\alpha(\text{Sn-Si}) (10^{-6} K^{-1})$		$\delta\alpha(\text{Sn}) (10^{-6} K^{-1})$	
			[001]	[100]	[001]	[100]
C	-40 / +20	20				
H	+20 / +80	20	13.4	29.4	32	16
F	-40 / +80	20				

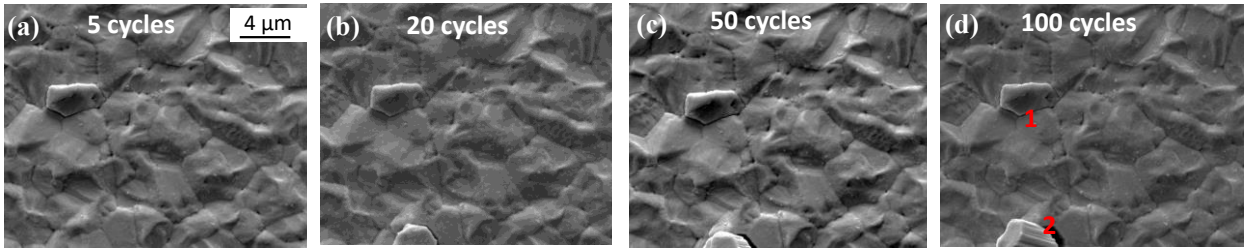
Although the CTEs of Sn and Si increase with the temperature, the fluctuation in the mismatch of the CTE between Sn and Si was small within the cycling temperature range. Therefore, the total global thermal strains introduced for the hot and the cold cycling were estimated to be equal and were half of the full cycling. We randomly chose 9 regions in each sample to trace the microstructure evolution and defects densities during thermal cycling at 1, 5, 20, 50, 100, and 165 cycles; Sample F was further cycled and examined at 150, 200, and 250 cycles.

2.3 Results and Discussion

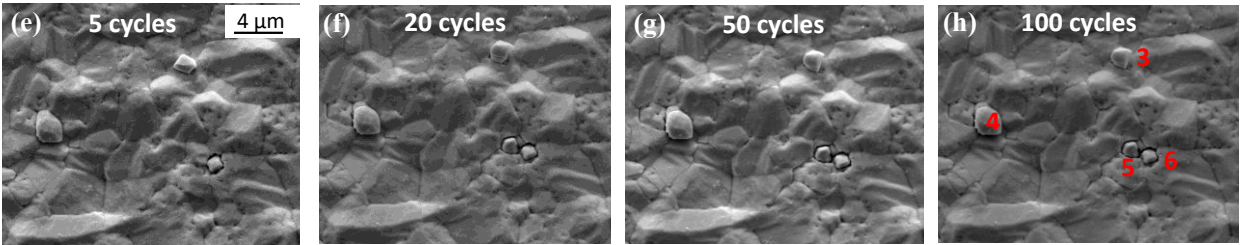
Fig. 2.1 showed an overview of the microstructural evolution of the three samples throughout the cycling process. Fatigue damage was noticeably more severe during full cycling than during cold and hot cycling. Whiskers started to nucleate in the early stage of cycling in all experimental conditions, as shown in Fig. 2.1(a), (e), and (i). Whiskers nucleated and grew in Sample C, indicating that local compressive stress gradients necessary for whisker formation could develop between individual grains even when under global tensile stress states, as seen in Fig. 2.1(a-d). Points 1-10 marked the whiskers in three different samples at the 100 cycles: the densities of whiskers of Sample H and F were approximately equal and were twice that of the cold cycling (Sample C). Sample F relaxed the most volume compared to Sample C and H, i.e., similar radius but longer whiskers. As seen in Fig. 2.1(l), a whisker disappeared at 200 cycles leaving a "root" as the radius of the whiskers in Sample F decreased during growth, similar to the previously reported pinch-off mechanism [7, 11].

Apart from whiskers, cracking and subsidence were commonly observed fatigue behavior. Fig. 2.2 demonstrated the initiation and propagation of fatigue cracks in Simple F. Both intergranular and transgranular types of cracks occurred. Microcracks or voids at GBs can form as the precursors of intergranular cracks, as circled in Fig. 2.2(c). Often, multiple microcracks formed at one GB and propagated as the number of cycles increased, merging as one long crack, see Fig. 2.2(d). This is because dislocations can emit from a crack tip and microvoids can form in those dislocation-free zones near the crack tips [12, 13]. The observation agreed with the traditional wedge-shaped cracks developed through the aggregation of discontinuous microcracks, and was evidenced by in-situ TEM characterization [14]. Those wedge-like intergranular cracks can also form to accommodate GB sliding [15] and the latter is a common fatigue damage in Sn or Sn-alloy films and joints. Fig 2.2(b-d) illustrates the development of slip bands on the free surface prior to transgranular cracking. Those parallel slip bands are common low-energy configurations in materials, so-called persistent slip bands (PSBs) [16]. With cyclic loading, strain accumulates in the form of dislocations. Each cycle, those dislocations multiply and arrange in a low-energy pattern to compensate for the energy increased because of the increased dislocation density. With accumulated cycles, PSBs continued to form and move to the free surface, leaving repeated extrusions and intrusions on the surface, which further act as the crack initiation sites [17].

Sample C: -40 / +20 °C (cold half cycling)



Sample H: +20 / +80 °C (hot half cycling)



Sample F: -40 / +80 °C (full cycling)

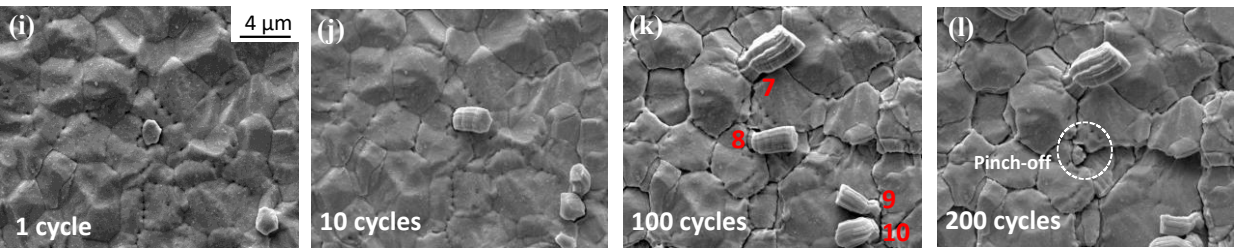


Figure 2.1. SEM images of Sn films illustrating the accumulation of fatigue damage at different cycles under (a-d) cold cycling, (e-h) hot cycling, and (i-l) full cycling.

Subsided grains were primarily observed in Sample F, as shown in Fig. 2.1 (k-l). Two exemplar subsided grains were observed at 50 cycles, as annotated in Fig. 2.2(d). This relaxation response, i.e., subsidence, was analyzed in a previous study that pointed out both a sinking grain and a whiskering grain depended on the inclined GBs at the root, but the stress states of the two were opposite [7]. In other words, grains grow as whiskers when atoms diffused from remote underneath their oblique GBs, while a grain could sink under tensile local stress states where atoms diffuse away from the root of the grain, leaving behind a subsided region.

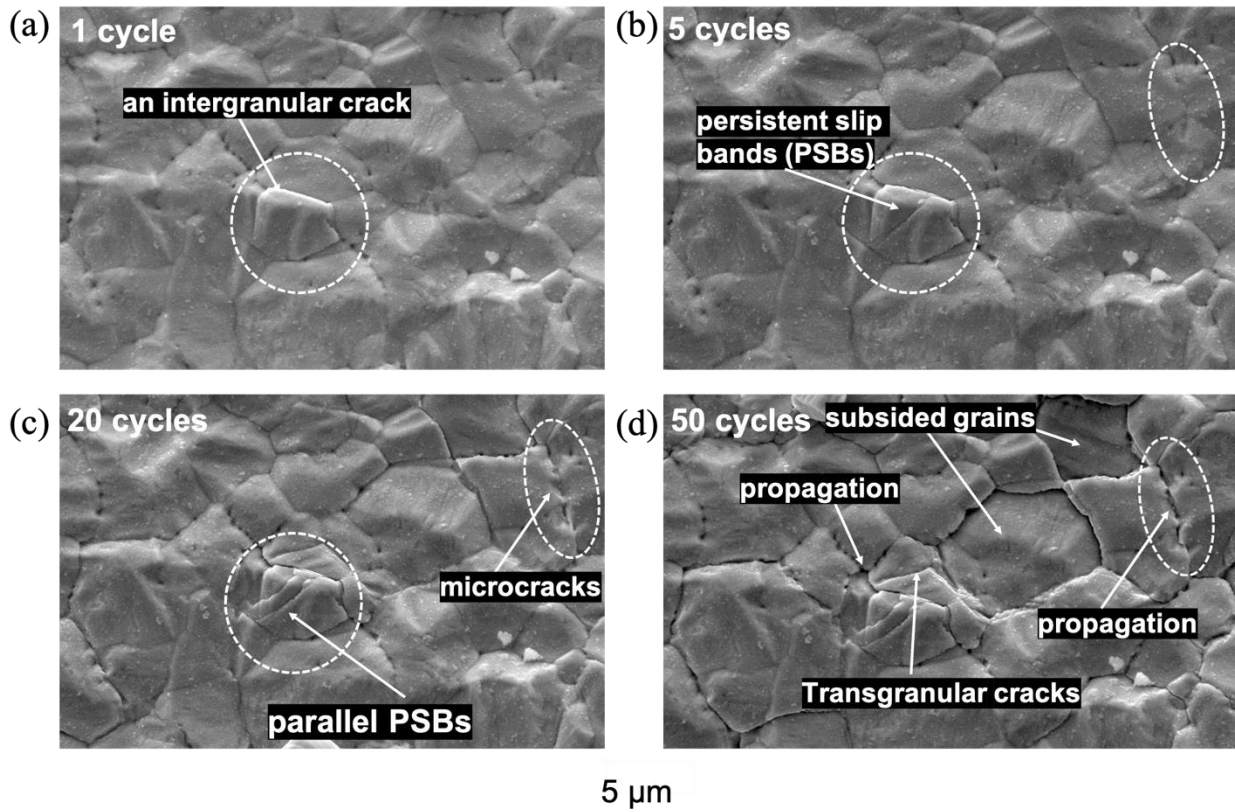


Figure 2.2. The development of cracks and subsided grains with an increasing number of cycles in Sample F.

Defects densities as a function of the number of cycles are shown in Fig. 2.3. In terms of whiskers, as shown in Fig. 2.3(a), Sample C exhibited the smallest whisker density, about half of Sample F. The whisker density of Sample H was higher than Sample C but still significantly lower than that of Sample F. If whisker nucleation is only controlled by diffusion, based on the integrated diffusion coefficient over the temperature cycles used, the hot cycle was predicted to have 60 times higher whisker density than the cold cycle. Therefore, while the temperature did influence the nucleation of whisker grains, it was far from a dominating factor. Other relaxation responses in addition to diffusional creep must contribute to a large portion of the nucleation of whisker grains. Previous studies claimed that local yielding, GB sliding, and grain rotation were other fundamental mechanisms influencing the nucleation of shallow grains. On the other hand, as seen in Fig. 2.3(b), the sum of whisker densities of Sample C and H was almost equal to the cumulative density of Sample F, indicating that the order of cycling (cold half, hot half, or full) had negligible impacts on stress localization in films. We can assume that one full cycle was equal to the one hot half

cycle plus one cold half cycle plus 20-minutes aging time at room temperature, and there were two explanations. First, the relaxed stresses were the same at -40°C , 20°C , and 80°C so the stress-strain hysteresis loops for the three conditions did not go up or down. Second, whisker formation was not sensitive to global stress states. Chason et al. [10] measured the stress-strain hysteresis loops of Sn films ($7.5\ \mu\text{m}$ thickness) during thermal cycling and demonstrated that significant amount of stresses relaxed at 23°C and 63°C and concluded that the degree of stress relaxation was greater at higher temperature, therefore the first explanation cannot be justified. Local stress states introduced by the mismatch of CTE between individual grains had greater influences on whisker formation.

In terms of cracks, Sample F again exhibited the highest density, whereas Sample C and H showed approximately the same density, as indicated in Fig. 2.3(c). The significant difference of cracks density between the full cycling sample and the half cycling ones suggested that introduced thermal strain was the predominant factor affecting the initiation and propagation of fatigue cracks. This is because once a microcrack occurred, the plasticity is no longer fully recovered. Cyclic slip irreversibility and the plastic strain accumulated in PSBs were deemed the primary source of fatigue damage, both of which increase with strain amplitudes [18-19]. The black curve in Fig. 2.3(a) represented the cumulative number of whiskers in sample F by summing up remaining whiskers and pinched-off whisker roots. Pinched-off whiskers were exclusively observed under full cycling conditions in Sample F as of 250 cycles. This is because the cracking of surface oxide is an inherently integrated process of the pinch-off mechanism [7] and was directly related to strain amplitudes [18-19] and, therefore, most active in Sample F.

Both density plots in Fig. 2.3(a) and (c) showed the saturation of defects after a certain number of cycles, although the saturation point of whiskers was earlier than that of cracks. For Sn films, in addition to the global thermal stress originated from the CTE misfit between the film and the substrate, the local thermal stress depends on the CTE misfit at grain boundaries. After 100 cycles, fatigue damage mainly accumulated via crack propagation where whiskers remained almost unchanged. An explanation is that, at the later stage, the heterogeneous thermal strain can be relaxed by the extra spacing and introduced little to no thermal stress into the films due to the development of many-site cracks. With decreasing local stress states, crack density saturated later than whisker density indicated that the stress required to initiate fatigue cracks is lower than that of whiskers. This is because once PSBs are formed, dislocations can slip along those low-energy

pathways and accumulate on the surface with little energy cost. Therefore, fatigue cracks keep nucleating at the roughened surface or GBs and propagating as long as there is global stress in the film.

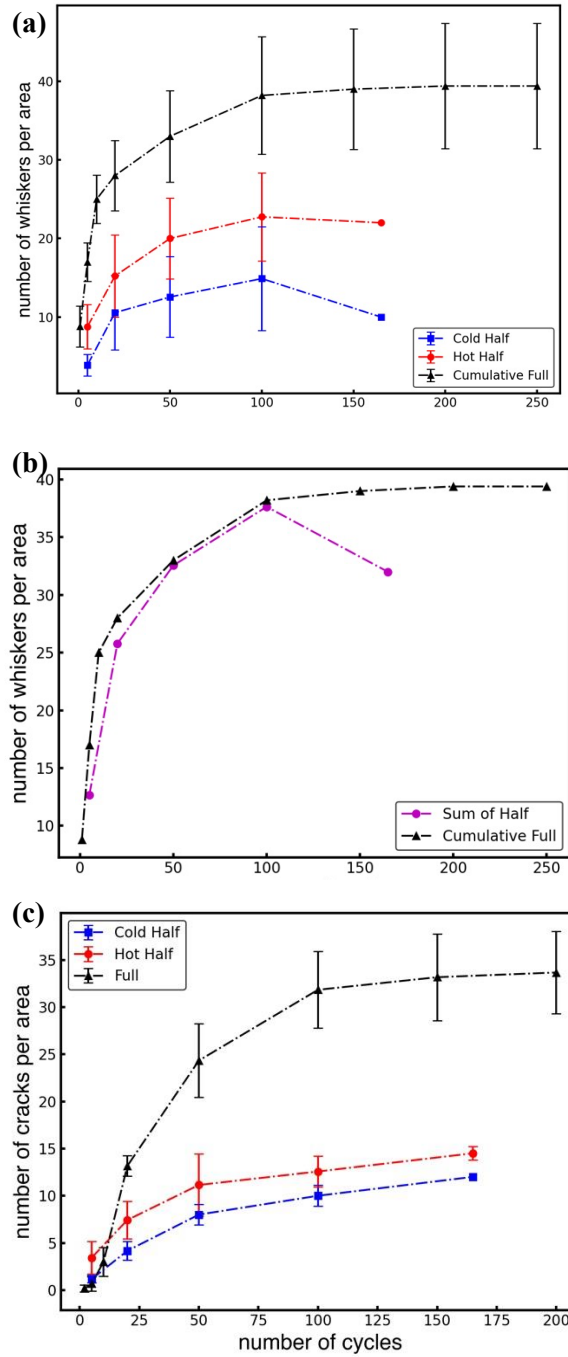


Figure 2.3. Densities of (a-b) whiskers and (c) cracks of three different conditions were illustrated as a function of the increasing thermal cycles.

2.4 Conclusion

In conclusion, the densities of fatigue defects in Sn thin films were measured concerning three thermal cycling settings. Whiskers nucleated and grew regardless of the global stress states, responding to localized compressive stresses developed between individual grains. By comparing the defects densities developed under different cycling conditions, we found whiskers were influenced by temperature and thermal strains while the cracks were prominently responsive to thermal strains. In rapid thermal cycling, relaxation of film stresses had negligible effects on stress localization compared to anisotropic thermal expansion of β -Sn. The crack density is responsive to the thermal strain as the introduced strain affects the dislocation motion. The dominant type of fatigue defects changed from whiskers to cracks with an increasing number of cycles until both reached the saturation points. Therefore, the early stage of cycling is critical if studying the nucleation of whiskers. Additionally, it can be concluded that dislocation motions facilitated whisker nucleation and crack initiation because the incremental characterization of film microstructure illustrated that slip bands often emerged and developed within regions where defects formed in later cycles.

2.5 References

- [1] Suganuma, K., Baated, A., Kim, K.-S., Hamasaki, K., Nemoto, N., Nakagawa, T., & Yamada, T. (2011). Sn whisker growth during thermal cycling. *Acta Materialia*, 59(19), 7255-7267. <https://doi.org/10.1016/j.actamat.2011.08.017>
- [2] Chen, W.-H., Wang, C., Sarobol, P., Blendell, J., & Handwerker, C. (2020). Local variations in grain formation, grain boundary sliding, and whisker growth along grain boundaries in large-grain Sn films. *Scripta Materialia*, 187, 458-463. <https://doi.org/10.1016/j.scriptamat.2020.06.033>
- [3] Sobiech, M. L. (2010). *Whisker formation on Sn thin films*. Universität Stuttgart. <http://elib.uni-stuttgart.de/handle/11682/1335>.
- [4] Tu. (1994). Irreversible processes of spontaneous whisker growth in bimetallic Cu-Sn thin-film reactions. *Phys Rev B Condens Matter*, 49(3), 2030-2034. <https://doi.org/10.1103/physrevb.49.2030>
- [5] Bieler, T. R., Hairong, J., Lehman, L. P., Kirkpatrick, T., Cotts, E. J., & Nandagopal, B. (2008). Influence of Sn Grain Size and Orientation on the Thermomechanical Response and Reliability of Pb-free Solder Joints. *IEEE Transactions on Components and Packaging Technologies*, 31(2), 370-381. <https://doi.org/10.1109/tcapt.2008.916835>

- [6] Telang, A. U., & Bieler, T. R. (2005). Characterization of microstructure and crystal orientation of the tin phase in single shear lap Sn–3.5Ag solder joint specimens. *Scripta Materialia*, 52(10), 1027-1031. <https://doi.org/10.1016/j.scriptamat.2005.01.043>
- [7] Wang, Y., Blendell, J. E., & Handwerker, C. A. (2014). Evolution of tin whiskers and subsiding grains in thermal cycling. *Journal of Materials Science*, 49(3), 1099-1113. <https://doi.org/https://doi.org/10.1007/s10853-013-7788-5>
- [8] Telang, A. U., & Bieler, T. R. (2005). The orientation imaging microscopy of lead-free Sn-Ag solder joints. *JOM*, 57(6), 44-49.
- [9] Chen, W.-H., Sarobol, P., Handwerker, C. A., & Blendell, J. E. (2016). Heterogeneous Stress Relaxation Processes at Grain Boundaries in High-Sn Solder Films: Effects of Sn Anisotropy and Grain Geometry During Thermal Cycling. *JOM*, 68(11), 2888-2899. <https://doi.org/10.1007/s11837-016-2070-3>
- [10] Chason, E., Jadhav, N., Pei, F., Buchovecky, E., & Bower, A. (2013). Growth of whiskers from Sn surfaces: Driving forces and growth mechanisms. *Progress in Surface Science*, 88(2), 103-131. <https://doi.org/10.1016/j.progsurf.2013.02.002>
- [11] Wang, Y. (2014). *Microstructure evolution and surface defect formation in Tin films*. Purdue University.
- [12] Thomson, R., Chuang, T.-J., & Lin, I.-H. (1986). The role of surface stress in fracture. *Acta Metallurgica*, 34(6), 1133-1143. [https://doi.org/10.1016/0001-6160\(86\)90223-3](https://doi.org/10.1016/0001-6160(86)90223-3)
- [13] Zhang, Y., Wang, Y.-B., Chu, W.-Y., & Hsiao, C.-M. (1994). The in-situ TEM observation of microcrack nucleation in titanium aluminide. *Scripta Metallurgica et Materialia*, 31(3), 279-283. [https://doi.org/10.1016/0956-716x\(94\)90283-6](https://doi.org/10.1016/0956-716x(94)90283-6)
- [14] Ding, Y., Wang, C., Li, M., & Wang, W. (2006). In situ TEM observation of microcrack nucleation and propagation in pure Tin solder. *Materials Science and Engineering: B*, 127(1), 62-69. <https://doi.org/10.1016/j.mseb.2005.09.050>
- [15] Langdon, T. G. (1993). The role of grain boundaries in high temperature deformation. *Materials Science and Engineering: A*, 166(1-2), 67-79. [https://doi.org/10.1016/0921-5093\(93\)90311-2](https://doi.org/10.1016/0921-5093(93)90311-2)
- [16] U. Essmann, U. Gösele, H. Mughrabi, *Philos. Mag. A Phys. Condens. Matter, Struct. Defects Mech. Prop.* 44 (1981) 405–426.
- [17] Sangid, M. D. (2013). The physics of fatigue crack initiation. *International Journal of Fatigue*, 57, 58-72. <https://doi.org/10.1016/j.ijfatigue.2012.10.009>
- [18] Mughrabi, H. (2015). Microstructural mechanisms of cyclic deformation, fatigue crack initiation and early crack growth. *Philos Trans A Math Phys Eng Sci*, 373(2038), 20140132. <https://doi.org/10.1098/rsta.2014.0132>

[19] Mughrabi, H. (2009). Cyclic slip irreversibilities and the evolution of fatigue damage. *Metallurgical and Materials Transactions B*, 40(4), 431-453.

3. LOCAL VARIATIONS IN GRAIN FORMATION, GRAIN BOUNDARY SLIDING, AND WHISKER GROWTH ALONG GRAIN BOUNDARIES IN LARGE-GRAIN SN FILMS

The following chapter was reprinted, with journal permission, from Chen, W.-H., Wang, C., Sarobol, P., Blendell, J., & Handwerker, C. (2020). Local variations in grain formation, grain boundary sliding, and whisker growth along grain boundaries in large-grain Sn films. *Scripta Materialia*, 187, 458-463. <https://doi.org/10.1016/j.scriptamat.2020.06.033>. The publication is a group effort. Chen, W. and Sarobel, P. performed sample synthesis, characterization, and data analysis. Wang, C. explained the stress relaxation mechanism based on experimental data and prepared the manuscript for this work.

3.1 Introduction

Begin a new chapter here. Each chapter must begin on a new page. If you are pasting in previously published articles, you will need to reformat the articles to match the guidelines that are set in this template. You will also want to use the heading styles above even though you may have previously applied styles in the original document. The styles above will ensure you meet the Graduate School requirements.

Whiskers can form spontaneously from β -Sn films and solder joints due to thermally-induced stresses [1], mechanical deformation, and stresses caused by intermetallic compound (IMC) growth [2] at Sn-Cu substrate interfaces. Whisker growth serves as a significant mechanism to locally relax compressive stresses in β -Sn [3,4] since the native oxide is effective at suppressing more generalized diffusional creep [5]. After the presence of the native oxide, the best understood condition for stress localization leading to a specific grain forming a whisker is film microstructure, i.e., shallow grains with oblique grain boundaries (GBs) preferentially form whiskers in predominantly columnar grained microstructures [see Fig. S-2(b) in Supplementary] [6–10]. The GBs of shallow grains, by the nature of the strain gradients between the root of the shallow grain (tensile) and the rest of the film (compressive) become the sinks and sources, respectively, for atomic diffusion [7–11]. The local driving force for whisker growth must be greater than the opposing GB sliding friction that depends on the area of the GB normal to the growth direction and the strength of the oxide that must fracture for growth to occur [9,12]. Quantifying what factors determine how and why specific grains form and grow as whiskers is necessary to move the understanding of whisker growth from the more general descriptions of localized Coble creep by GB diffusion of specific grains to a quantitative understanding of the interplay between various

stress relaxation mechanisms operating along individual boundaries. In previous studies, a pseudo-bicrystal Sn-based solder film with millimeter in-plane grain sizes was useful in demonstrating (1) nucleation of new grains that grew into whiskers along specific GBs during thermal cycling, (2) GB sliding along other GBs, and (3) a combination of GB sliding, grain nucleation and whisker growth along other grain boundaries [13,14].

In this study of similar pseudo-bicrystal Sn films, we have focused on the mechanism of how new grain boundaries formed and on relating the observed crystallographic changes and surface and sub-surface morphological changes to the extent of whisker growth and GB sliding. X-ray synchrotron analyses (XSA), scanning electron microscopy (SEM), electron backscatter diffraction (EBSD), and focused ion-beam (FIB) milling and imaging were used to quantify surface and sub-surface microstructure, including the presence of newly formed grains, crystallographic orientation changes, and evidence of dislocation formation along two specific GBs before and after thermal cycling.

3.2 Experiments

Films (~30 μm thick) with millimeter in-plane grains were solidified from SAC305 (96.5wt%Sn, 3.0wt%Ag, 0.5wt%Cu) solder paste on Cu substrates as previously reported [13,14]. The crystallographic orientations of grains in the as-fabricated film, the initial positions of the GBs, and whether small grains were present before thermal cycling were measured using EBSD. From EBSD results, two GBs (see Table S1 and Fig. S2 in Supplementary Materials) with high coefficients of thermal expansion in both grains normal to the GB traces at the free surface were characterized before and after thermal cycling by XSA measurements at the Advanced Light Source (ALS) beamline 12.3.2 (details in Tab 3.1) [15]. The method for locating the boundaries of interest in the synchrotron can be found in [14]. Before thermal cycling, the grains had flat surfaces, parallel to the overall film surface. Thermal cycling was performed for 1000 cycles in air ($-45\text{ }^{\circ}\text{C}$ to $85\text{ }^{\circ}\text{C}$ - three cycles per hour). Crystallographic grain orientations, elastic deviatoric strains, and peak-widths were determined from the diffraction data using the ALS-developed XMAS software [16] for single-grain reconstruction, i.e., only the strongest peak intensities in Laue diffraction patterns are indexed if the beam intersects multiple grains [17]. Maps of elastic strain energy density (ESED) were calculated from the diffraction data based on the deviatoric strain tensor [14, 17–19]. Maps of full-width at half-max (FWHM) of the diffracted beams,

proportional to the dislocation density [20], before and after thermal cycling were used to estimate local change in defect densities. Surface morphology and orientation changes identified by SEM, EBSD, and XSA were compared with sub-surface GB positions observed using FIB. As seen from the results comparing the microstructures between as-solidified and thermally-cycled films (see Fig 3.1), one of the boundaries exhibited wide-spread whisker formation (GB-I) and the other by GB sliding (GB-II). As described below, the dislocation densities in the regions around the GBs and the local ESED were lower after thermal cycling. From these combined measurements, similarities and differences in the responses of the two GBs to thermal cycling induced stresses are analyzed.

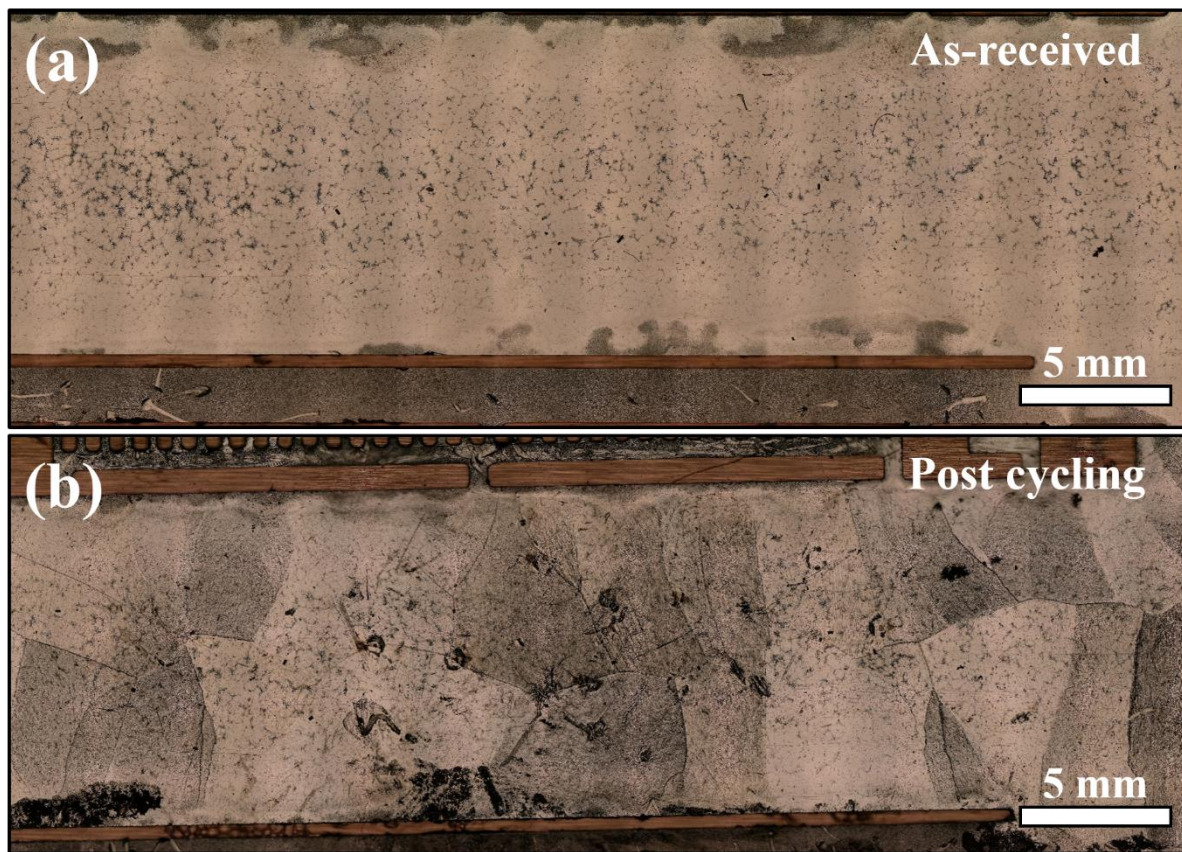


Figure 3.1. Optical images of (a) a typical as-received SAC305 solder film without noticeable grain boundaries and (b) the thermally cycled film with apparent grain boundaries presented in this study. Films in (a) and (b) are not the same sample.

Table 3.1. Characterization techniques employed in this study

Sample	Time	Characterization			
		EBSD	SEM	Synchrotron	FIB
Reported film	Before cycling	GB locations	Surface morphology	Crystallographic texture, FWHM, ESED (6 GBs, 2 μm step size)	/
	After 1000 cycles	/	Surface morphology	Crystallographic texture, FWHM, ESED (2 GBs, 1 μm step size)	GB geometry

3.3 Results and Discussion

Before thermal cycling, the shape of GB-I determined by EBSD [black lines in Fig. 3.2(a)] was also seen by SEM as small changes in surface roughness due to dendrite orientation differences and inter-dendritic shrinkage. The initial shapes of GB-I from EBSD and XSA [Fig. 3.2(b)] are in good agreement, suggesting that GB-I was approximately normal to the film surface. After thermal cycling, twelve grains had formed between the two parent grains, as seen by comparing Figs. 3.2(b) and (f). The grain orientation mapping in the surface normal direction shows that (a) grains 1 and 2 were pre-existing grains, (b) grains 3–5 formed with high-angle GBs (HAGBs, $>10^\circ$ misorientation) relative the original parent grains, and (c) grains 6-12 formed with low-angle GBs (LAGBs, 2° - 10° misorientation) relative to original parent grains. The whiskers mostly grew from grains with HAGBs (grains 1-5) except grain 8, which formed a LAGB with parent grain A as shown in Figs. 3.2(e) and (f). LAGBs have formed parallel to the original GB-I in grains A and B, located approximately 5-20 μm away from the original GB position. The decrease of FWHM [Figs. 3.2(c) and (g)] indicates that, after cycling, the dislocation density decreased near GB-I. The mean ESED of the entire mapping dropped from 151 kJ/m^3 to 44 kJ/m^3 after thermal cycling. The positions of the lowest local dislocation densities and the highest local ESEDs in Grain A coincide with sub-grain boundaries with misorientation angles less than 2° . These very low misorientation regions likely correspond to secondary dendrite arms from solidification and become more distinct during thermal cycling. After thermal cycling the ESED values are highest along the sub-grain boundaries of the grain-shaped regions and lowest in their

interiors. These results indicate that significant dislocation formation, motion, and reactions have led to the formation of multiple HAGBs and LAGBs, some of which form whiskers. Furthermore, ESED calculations and FWHM measurements show that the overall stresses/strains and dislocation densities are significantly lower after cycling than in the as-solidified state.

Surface and subsurface grain morphologies of GB-I were characterized using SEM and FIB in two regions near grains 6-2-7 and grains 4-1-11-5. Regarding crystallographic changes, multiple new GBs formed in these two regions along and near the original GBs during thermal cycling as indicated by ion-beam contrast in Figs. 3.3(c-d) and Fig. 3.2(f). Whiskers grew from shallow grains with oblique GBs. Grains 1 and 2 were pre-existing, but had rotated crystallographically from their original orientations by 7° and 35° , respectively. Relating the surface morphology [Fig. 3.2(e)] and cross-sectional geometries (Fig. 3.3) to the post-cycling orientation map [Fig. 3.2(f)], the twelve new grains can be categorized in the following three types.

1. Grain formation without surface morphological changes (grains 6, 7, 9, 10, 11, 12),
2. Shallow grain formation with asymmetrical whisker growth (grains 2, 4, and 5) showing non-uniform mass accumulation at the base of the new grains and changes in the angle between the normal of the top surface of the whisker and the original film surface normal),
3. Shallow grain boundary with symmetrical whisker growth (grains 1, 3, and 8) showing uniform mass accumulation from the surrounding of the base leading to the surface of the whisker grain remaining parallel to the film surface).

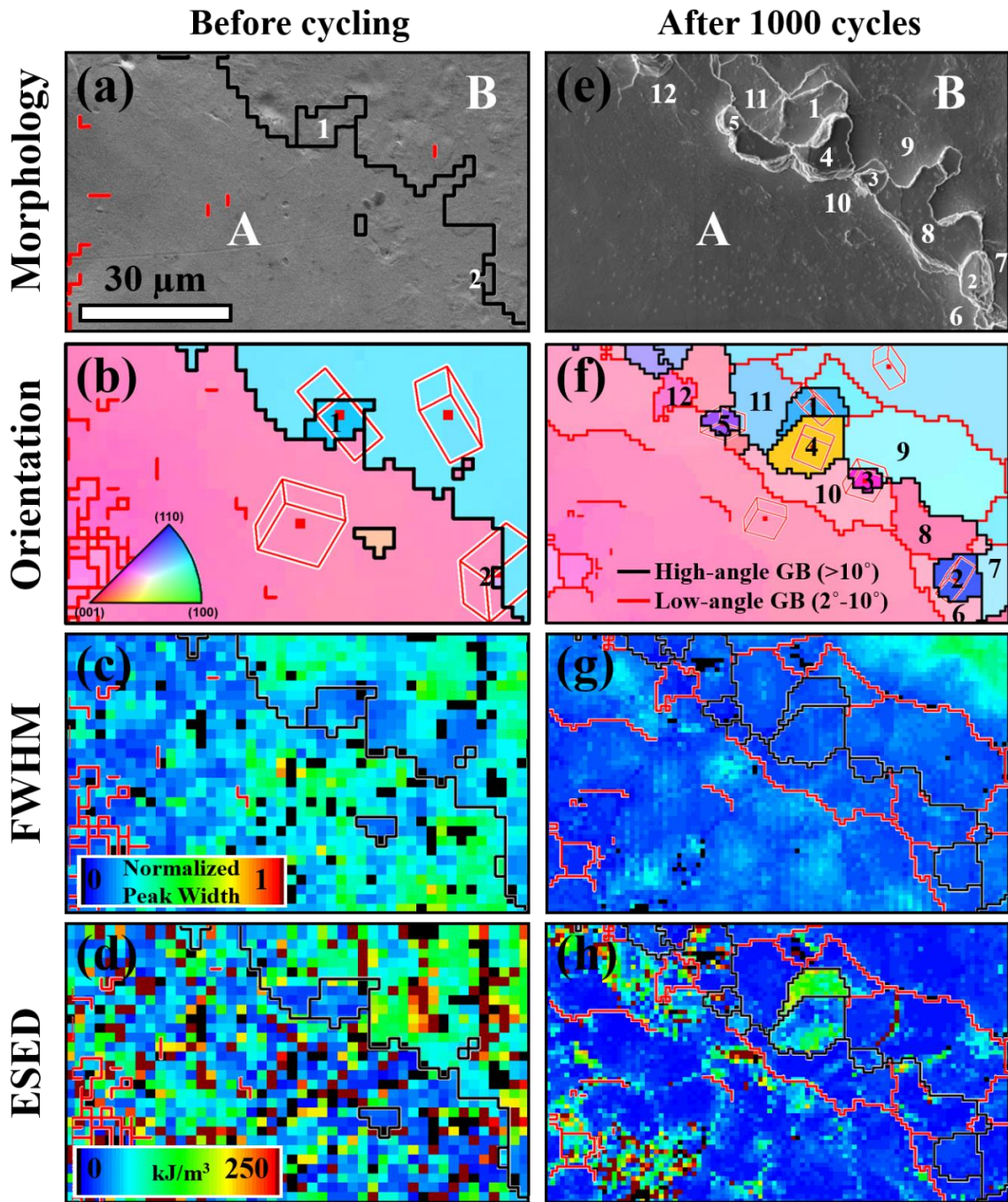


Figure 3.2. Local surface morphology, orientation, and associated distributions of dislocation density as indicated by the full-width at half-max (FWHM) of the diffracted beams and elastic strain energy density (ESED) at GB-I before (a-d) and after (e-h) 1000 thermal cycles. Evolution of surface morphology [(a) and (e)] and orientation [(b) and (f)] shows the growth of whiskers from the pre-existing grain 1 and newly formed grains 2-5 circled by high-angle GBs (black lines). Grains 6-12 nucleated with the formation of low-angle GBs (red lines). The changes of dislocation density [(c) and (g)] and ESED [(d) and (h)] indicate that stress level of the characterized region significantly decreased after new grains formed.

The top surfaces of whisker grains 2 and 4 in Figs. 3.3(a) and (b) did not remain parallel to the film surface [14, 21, 22], suggesting non-uniform mass transport to the base of the whisker. The side walls of the whiskers are rough, but with striations parallel and perpendicular to the growth direction, similar to whisker growth during thermal cycling in electrodeposited Sn films [1,12,23]. The observation that whisker grains with the greatest out-of-plane displacement along GB-I are shallow is consistent with the model of whisker growth based on GB sliding-limited diffusional creep [9].

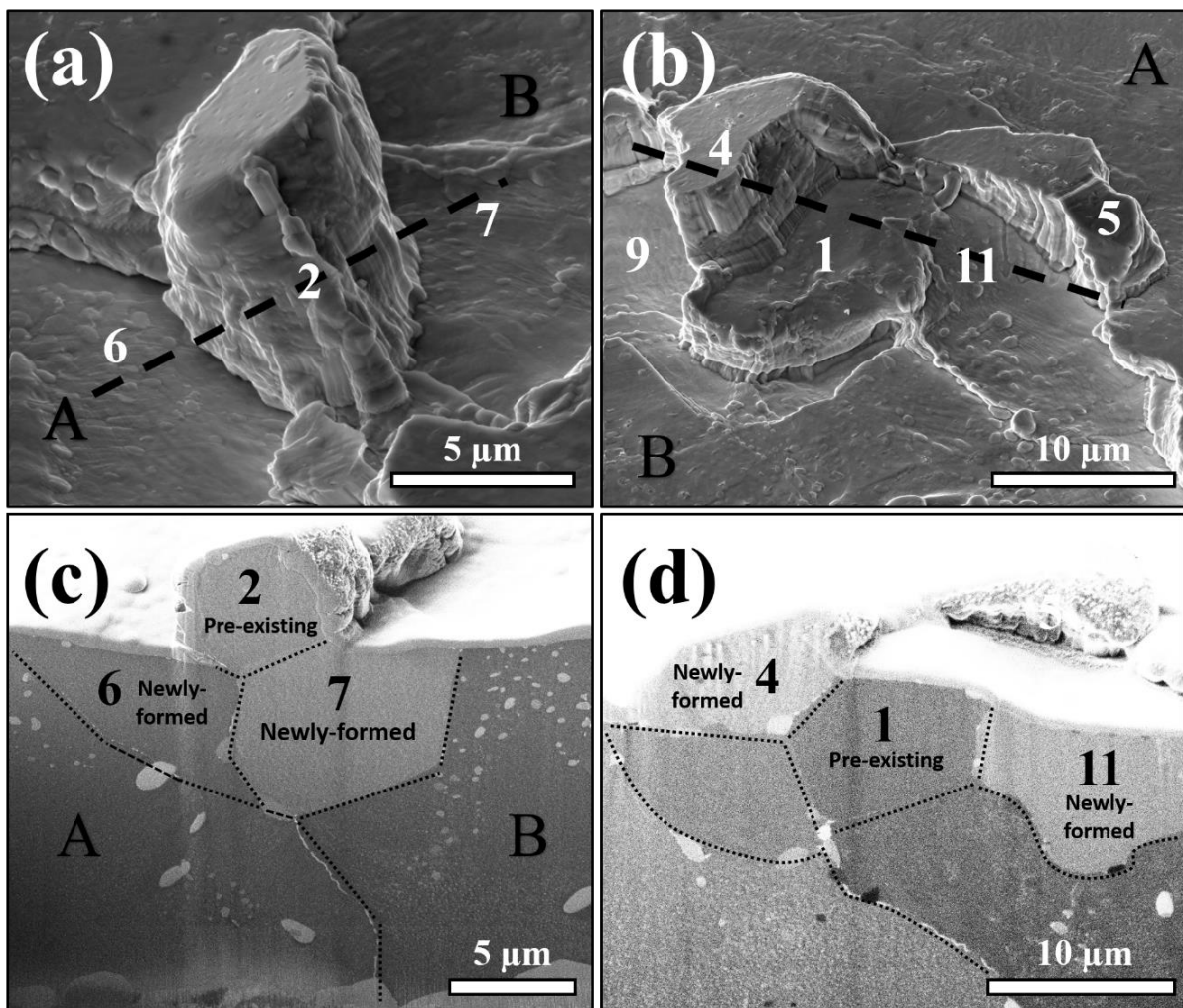


Figure 3.3. (a-b) Side-view SEM images of selected whiskers and sub-grains taken at a tilt of 52° of the same region characterized in Fig. 3.2. Cross-sections were made in the direction (c) perpendicular for grains 6-2-7 and (d) parallel for grains 4-1-11 to GB-I as marked by black dashed lines in (a-b) to show the subsurface microstructure. GBs distinguished based on ion-beam grain contrast are indicated by black dotted lines.

For GB-II, the difference between the shape of the HAGB before thermal cycling identified by EBSD in Fig. 3.4(a) and XSA in Fig. 3.4(b) indicates that GB-II is likely not normal to the film surface. During thermal cycling, the surfaces of grains C and D became displaced normal to the film surface, described previously as “GB sliding”. The local dislocation density near GB-II [Figs. 3.4(c) and (g)] was relatively low before thermal cycling and decreased during thermal cycling as compared to regions farther away. The mean ESED of grain D decreased from 75 kJ/m³ to 57 kJ/m³ after thermal cycling, whereas the mean ESED of grain C was very low before thermal cycling and increased slightly from 34 kJ/m³ to 41 kJ/m³. The finger-like region in grain D [indicated by the white arrow in Fig. 3.4(a)] was shallow before thermal cycling since it was detected by EBSD but only partially by XSA [Fig. 3.4(b)]. It is no longer present after thermal cycling as indicated by the boundary position in Figs. 3.4(e) and (f), likely disappearing during thermal cycling by curvature-driven GB migration before GB sliding occurred [15,24].

The displacement between grain C and grain D does not appear to be accompanied by a macroscopic rigid body rotation accompanied by a misorientation change between grain C and grain D. That is, grain D near the grain boundary did not slide over grain C thereby changing the surface normal of grain D. Formation of a single LAGB [inside the white dashed square in Fig. 3.4(e)] with a misorientation of 6° with respect to grain D was identified by a single pixel change in XSA [indicated by the arrow in Fig. 3.4(f)]. From XSA, the overall orientations of grain C and grain D before and after thermal cycling remain the same (different by less than 1°), except for the LAGB. Subsurface and surface microstructural changes in the region containing the LAGB were examined using FIB at three locations as shown in Fig. 3.5. All three cuts show that the displacement between grains C and D is caused by local mass accumulation at the surface of grain D and local rotation of the surface normal approximately 5-10 μm from the GB. In Cut 2 through the LAGB, the new GB is evident from grain contrast and changes in the GB inclination [Figs. 3.5(e) and (f)]. A non-180° dihedral angle is observed where the LAGB intersects the original GB to form a new triple junction. In the previous study, similar triple junctions were observed to form new shallow grains that became whiskers, as seen in Fig. 3.6 [14]. No distinct triple junction is seen in Figs. 3.5(d) and (g).

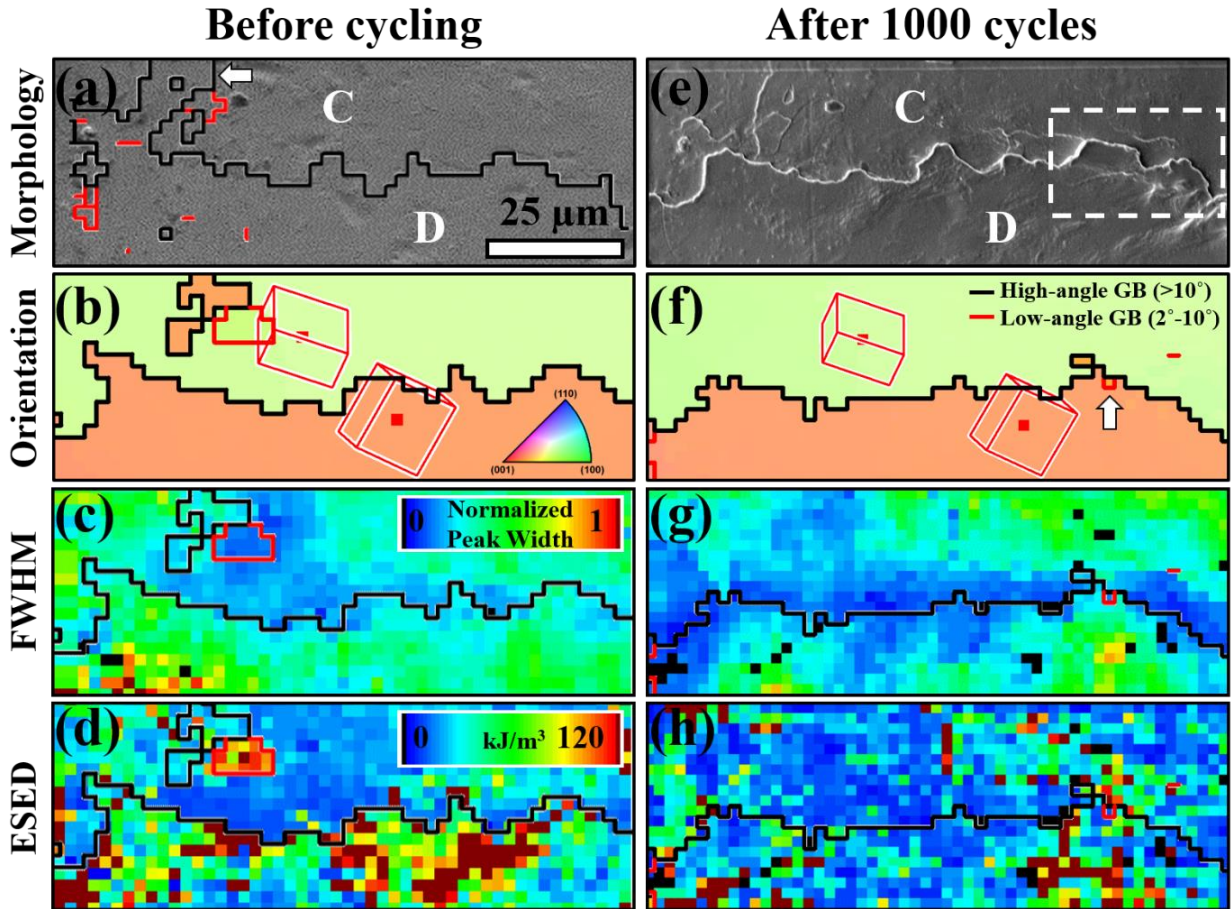


Figure 3.4. Local surface morphology, orientation, and associated distributions of dislocation density as indicated by FWHM of the diffracted beams and elastic strain energy density (ESED) at GB-II before (a-d) and after (e-h) 1000 thermal cycles. Evolution of surface morphology [(a) and (e)] and orientation [(b) and (f)] shows GB sliding and migration occurred. A low-angle GB formed, indicated by the white arrow in (f). The changes of dislocation density [(c) and (g)] and ESED [(d) and (h)] indicate that the majority of the relaxation from GB sliding took place close to GB-II.

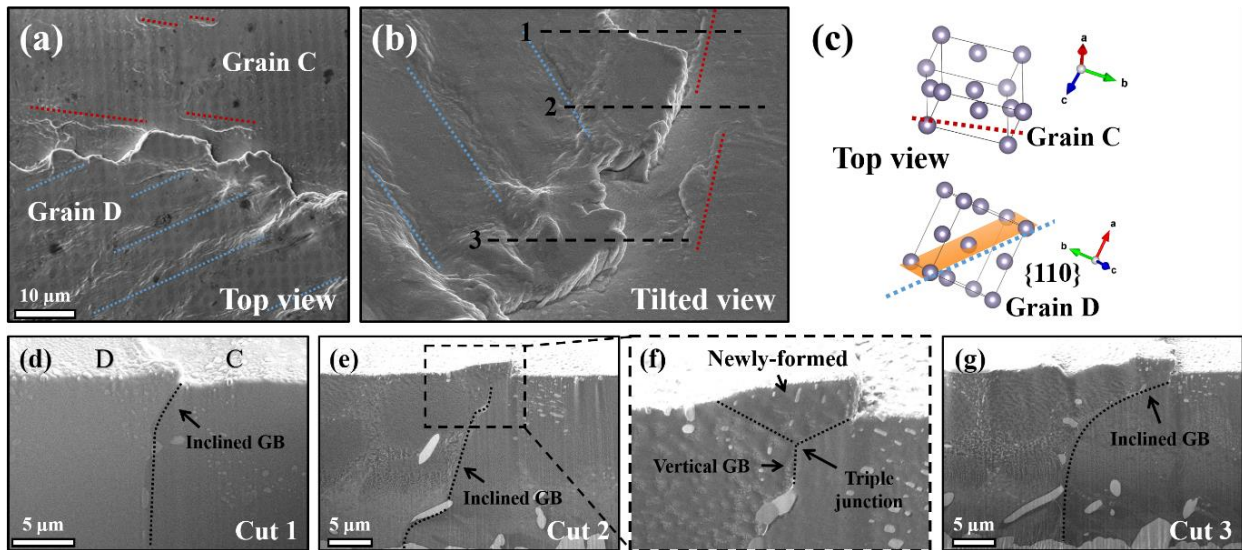


Figure 3.5. (a) Top-view and (b) tilted-view SEM images show two sets of slip traces (marked by blue and red dashed lines) near the nucleated shallow grain at GB-II in the region marked by the white dashed square in Fig. 3.4(e). (c) Potential slip planes identified via the trace directions and grain orientations. (d-g) Ion-beam images of the cross-sections Cut 1, 2, and 3 marked by black dashed lines in (b). (f) An enlarged view of the area enveloped by the dashed square in (e) indicates a shallow surface grain nucleated at the GB near the surface. The location of the shallow grain agrees with the location of the newly-formed low-angle GB indicated by the white arrow in Fig. 3.4(f).

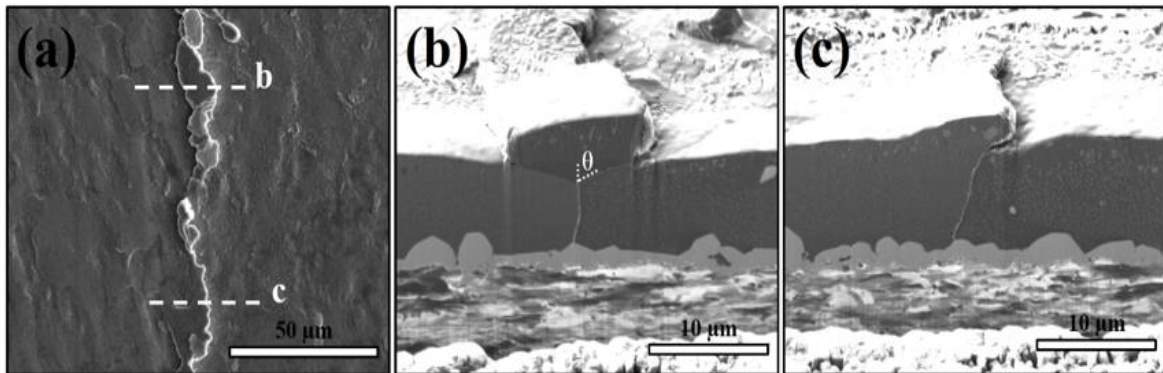


Figure 3.6. (a) Microstructural variations along the GB revealed by cross-sections from a region showing both whisker formation and GB sliding. (b-c) FIB cross-sections along the dashed lines in (a) showed changes in surface normal near the original GB, changes in GB inclination through the film thickness, and shallow grain formation (b only). Reproduced from [14], copyright 2016, with permission from Springer Nature.

The misorientation change for the new grain relative to grains C and D can be estimated by comparing the XSA orientation with the angle between the rotated surface of the new grain and the film surfaces of grain C and grain D away from the grain boundary [Fig. 3.4(e)]. The LAGB had a misorientation of 6° by XSA, whereas from FIB cross-sections, the rotation angle is 16° . Given that the XSA measurement was based only on a single pixel, additional experiments are necessary to determine whether this is generally seen with “GB sliding.” It is likely that there are changes in crystallographic misorientation for the regions with mass accumulation and changes in surface normal but were undetectable by XSA in this experiment. The implication of these results is that the phenomenon we refer to as “grain boundary sliding” will need two mechanisms for local mass accumulation: one component that causes lattice rotation and one that causes asymmetric out-of-plane displacement, as shown in Fig. 3.5. The combination of these two mechanisms leads to the change in the surface normal being observed in this case.

Parallel slip traces were also observed in grain C and grain D of GB-II after thermal cycling [red and blue in Fig. 3.5(a), respectively]. Based on the geometrical relationship between lattice orientations and slip traces, the activated slip plane of grain B was $\{110\}$ as illustrated in Fig. 3.5(c), based on the 5 families of slip systems of β -Sn [25–30], suggesting that yielding also occurred during thermal cycling as another stress relaxation mechanism. However, the directions of wavy slip traces for grain C did not match any of the 5 possible slip systems, indicating likely cross-slip of screw dislocations that may occur at higher temperature [31]. No slip traces were observed by SEM on the surfaces near GB-I.

A remaining question is what caused the differences in stress relaxation behavior observed for the two grain boundaries, particularly in the formation of new grain boundaries. Recent crystal plasticity simulations of yielding and dislocation accumulation at Sn GBs by Cai et al. suggest that different bi-crystal grain pairs show different patterns of stress localization [33]. High dislocation densities at the free surface for some grain boundaries were postulated to lead to sub-grain formation as a precursor to formation of new shallow GBs. The significant difference in the formation of new LAGBs and HAGBs between GB-I and GB-II observed here is likely related to the ability of the grain pairs to create high local dislocation densities at the free surface. When the LAGBs and HAGBs form shallow grains at the surface, they can grow into whiskers as observed here. Linking the phenomena reported here to differences in localized dislocation formation and

GB formation will require pairing interrupted cycling studies starting at low numbers of cycles with simulations of the specific grain boundaries being characterized.

3.4 Conclusions

In conclusion, dislocations and localized yielding appear to play an important role in stress relaxation in Sn films, with and without whisker formation.

For GB-I, widespread formation of HAGBs and LAGBs was observed through the thickness of the film, which requires the formation and interactions of dislocations. Of the newly formed grains, shallow grains formed whiskers consistent with the model of whisker growth based on GB sliding limited creep [8,10]. The high ESED in the original microstructure relaxed after thermal cycling, and the high dislocation density also decreased. The only indication of dislocation activity along GB-I was the formation of new grains and GBs during thermal cycling which requires the generation and reaction of dislocations.

For stress relaxation by GB sliding (GB-II), there was no change in crystallographic orientation between grains C and D detected by XSA, except for where a single LAGB formed. Although the new grain was shallow, it had not yet formed a whisker, as indicated in Fig. 3.4(f) and Fig. 3.5(f). The observed displacement between grains C and D was generally caused by highly localized, shallow mass accumulation in grain D at the interface, but changes in crystallographic orientation or new grain formation were not detected by XSA or FIB. The observation of slip traces along the free surfaces in GB-II indicates localized yielding but not sufficient dislocation content to form new grain boundaries, except for a single LAGB.

These results suggest that localized yielding is a critical factor in determining local stress responses such as the formation of new grains, GB sliding, and whisker growth. Future studies on the interplay between local orientation and yielding may help explain the role of local stress states and dislocation formation in grain rotation and grain nucleation. In particular, the results presented here for two GBs show stress relaxation by new grain formation, localized yielding, and mass accumulation in addition to whisker growth [6]. These dislocation-mediated processes may also be contributing to the more macroscopic phenomenon of power law creep reported previously for stressed tin films [32].

3.5 References

- [1] Suganuma, K., Baated, A., Kim, K.-S., Hamasaki, K., Nemoto, N., Nakagawa, T., & Yamada, T. (2011). Sn whisker growth during thermal cycling. *Acta Materialia*, 59(19), 7255-7267. <https://doi.org/10.1016/j.actamat.2011.08.017>
- [2] Tu. (1994). Irreversible processes of spontaneous whisker growth in bimetallic Cu-Sn thin-film reactions. *Phys Rev B Condens Matter*, 49(3), 2030-2034. <https://doi.org/10.1103/physrevb.49.2030>
- [3] Fisher, R. M., Darken, L. S., & Carroll, K. G. (1954). Accelerated growth of tin whiskers. *Acta Metallurgica*, 2(3), 368-373. [https://doi.org/10.1016/0001-6160\(54\)90053-x](https://doi.org/10.1016/0001-6160(54)90053-x)
- [4] Lee, B.-Z., & Lee, D. N. (1998). Spontaneous growth mechanism of tin whiskers. *Acta Materialia*, 46(10), 3701-3714. [https://doi.org/10.1016/s1359-6454\(98\)00045-7](https://doi.org/10.1016/s1359-6454(98)00045-7)
- [5] Jadhav, N., Buchovecky, E., Chason, E., & Bower, A. (2010). Real-time SEM/FIB studies of whisker growth and surface modification. *JOM*, 62(7), 30-37.
- [6] Boettinger, W. J., Johnson, C. E., Bendersky, L. A., Moon, K.-W., Williams, M. E., & Stafford, G. R. (2005). Whisker and Hillock formation on Sn, Sn-Cu and Sn-Pb electrodeposits. *Acta Materialia*, 53(19), 5033-5050. <https://doi.org/10.1016/j.actamat.2005.07.016>
- [7] Frolov, T., Boettinger, W. J., & Mishin, Y. (2010). Atomistic simulation of hillock growth. *Acta Materialia*, 58(16), 5471-5480. <https://doi.org/10.1016/j.actamat.2010.06.023>
- [8] Sarobol, P., Wang, Y., Chen, W. H., Pedigo, A. E., Koppes, J. P., Blendell, J. E., & Handwerker, C. A. (2013). A Predictive Model for Whisker Formation Based on Local Microstructure and Grain Boundary Properties. *JOM*, 65(10), 1350-1361. <https://doi.org/10.1007/s11837-013-0717-x>
- [9] Sarobol, P., Blendell, J. E., & Handwerker, C. A. (2013). Whisker and hillock growth via coupled localized Coble creep, grain boundary sliding, and shear induced grain boundary migration. *Acta Materialia*, 61(6), 1991-2003. <https://doi.org/10.1016/j.actamat.2012.12.019>
- [10] Smetana, J. (2007). Theory of Tin Whisker Growth: "The End Game". *IEEE Transactions on Electronics Packaging Manufacturing*, 30(1), 11-22. <https://doi.org/10.1109/tepm.2006.890645>
- [11] Hektor, J., Hall, S. A., Henningsson, N. A., Engqvist, J., Ristinmaa, M., Lenrick, F., & Wright, J. P. (2019). Scanning 3DXRD Measurement of Grain Growth, Stress, and Formation of Cu₆Sn₅ around a Tin Whisker during Heat Treatment. *Materials (Basel)*, 12(3), E446. <https://doi.org/10.3390/ma12030446>
- [12] Wang, Y. (2014). *Microstructure evolution and surface defect formation in tin films*. Purdue University.

- [13] Sarobol, P., Koppes, J. P., Chen, W. H., Su, P., Blendell, J. E., & Handwerker, C. A. (2013). Recrystallization as a nucleation mechanism for whiskers and hillocks on thermally cycled Sn-alloy solder films. *Materials Letters*, 99, 76-80.
<https://doi.org/10.1016/j.matlet.2013.02.066>
- [14] Chen, W.-H., Sarobol, P., Handwerker, C. A., & Blendell, J. E. (2016). Heterogeneous Stress Relaxation Processes at Grain Boundaries in High-Sn Solder Films: Effects of Sn Anisotropy and Grain Geometry During Thermal Cycling. *JOM*, 68(11), 2888-2899.
<https://doi.org/10.1007/s11837-016-2070-3>.
- [15] Kunz, M., Tamura, N., Chen, K., MacDowell, A. A., Celestre, R. S., Church, M. M., Fakra, S., Domning, E. E., Glossinger, J. M., Kirschman, J. L., Morrison, G. Y., Plate, D. W., Smith, B. V., Warwick, T., Yashchuk, V. V., Padmore, H. A., & Ustundag, E. (2009). A dedicated superbend x-ray microdiffraction beamline for materials, geo-, and environmental sciences at the advanced light source. *Rev Sci Instrum*, 80(3), 035108.
<https://doi.org/10.1063/1.3096295>
- [16] Tamura, N. (2014). XMAS: A Versatile Tool for Analyzing Synchrotron X-ray Microdiffraction Data. In *Strain and Dislocation Gradients from Diffraction* (pp. 125-155). Imperial College Press. https://doi.org/10.1142/9781908979636_0004
- [17] Tamura, N., MacDowell, A. A., Spolenak, R., Valek, B. C., Bravman, J. C., Brown, W. L., Celestre, R. S., Padmore, H. A., Batterman, B. W., & Patel, J. R. (2003). Scanning X-ray microdiffraction with submicrometer white beam for strain/stress and orientation mapping in thin films. *Journal of synchrotron radiation*, 10(2), 137-143.
- [18] Sarobol, P., Chen, W.-H., Pedigo, A. E., Su, P., Blendell, J. E., & Handwerker, C. A. (2013). Effects of local grain misorientation and β -Sn elastic anisotropy on whisker and hillock formation. *Journal of Materials Research*, 28(5), 747-756.
<https://doi.org/10.1557/jmr.2012.430>
- [19] Hektor, J., Micha, J.-S., Hall, S. A., Iyengar, S., & Ristinmaa, M. (2019). Long term evolution of microstructure and stress around tin whiskers investigated using scanning Laue microdiffraction. *Acta Materialia*, 168, 210-221.
<https://doi.org/10.1016/j.actamat.2019.02.021>
- [20] Ali, H. P. A., Kunz, M., Tamura, N., & Budiman, A. S. (2017). Probing Plasticity Mechanisms in Low Melting Temperature Metallic Nanostructures Using Synchrotron X-Ray Microdiffraction. *Procedia Engineering*, 215, 246-262.
<https://doi.org/10.1016/j.proeng.2017.12.146>
- [21] Pei, F., Jadhav, N., & Chason, E. (2012). Correlating whisker growth and grain structure on Sn-Cu samples by real-time scanning electron microscopy and backscattering diffraction characterization. *Applied Physics Letters*, 100(22), 221902.
<https://doi.org/10.1063/1.4721661>

- [22] Pei, F., Jadhav, N., & Chason, E. (2012). Correlation Between Surface Morphology Evolution and Grain Structure: Whisker/Hillock Formation in Sn-Cu. *JOM*, 64(10), 1176-1183. <https://doi.org/10.1007/s11837-012-0442-x>
- [23] Wang, Y., Blendell, J. E., & Handwerker, C. A. (2014). Evolution of tin whiskers and subsiding grains in thermal cycling. *Journal of Materials Science*, 49(3), 1099-1113. <https://doi.org/https://doi.org/10.1007/s10853-013-7788-5>
- [24] Goldstein, J. I., Newbury, D. E., Michael, J. R., Ritchie, N. W. M., Scott, J. H. J., & Joy, D. C. (2017). *Scanning Electron Microscopy and X-Ray Microanalysis*. Springer.
- [25] Bieler, T. R., & Telang, A. U. (2009). Analysis of Slip Behavior in a Single Shear Lap Lead-Free Solder Joint During Simple Shear at 25°C and 0.1/s. *Journal of Electronic Materials*, 38(12), 2694-2701. <https://doi.org/10.1007/s11664-009-0909-x>
- [26] Zhou, B., Bieler, T. R., Lee, T.-K., & Liu, K.-C. (2009). Methodology for Analyzing Slip Behavior in Ball Grid Array Lead-Free Solder Joints After Simple Shear. *Journal of Electronic Materials*, 38(12), 2702-2711. <https://doi.org/10.1007/s11664-009-0929-6>
- [27] Zhou, B., Muralidharan, G., Kurumadalli, K., Parish, C. M., Leslie, S., & Bieler, T. R. (2014). Microstructure and Sn Crystal Orientation Evolution in Sn-3.5Ag Lead-Free Solders in High-Temperature Packaging Applications. *Journal of Electronic Materials*, 43(1), 57-68. <https://doi.org/10.1007/s11664-013-2788-4>
- [38] Matin, M. A., Vellinga, W. P., & Geers, M. G. D. (2007). Thermomechanical fatigue damage evolution in SAC solder joints. *Materials Science and Engineering: A*, 445-446, 73-85. <https://doi.org/10.1016/j.msea.2006.09.037>
- [29] Kinoshita, Y., Matsushima, H., & Ohno, N. (2012). Predicting active slip systems in β -Sn from ideal shear resistance. *Modelling and Simulation in Materials Science and Engineering*, 20(3), 035003. <https://doi.org/10.1088/0965-0393/20/3/035003>
- [30] Zhou, B., Zhou, Q., Bieler, T. R., & Lee, T.-k. (2015). Slip, Crystal Orientation, and Damage Evolution During Thermal Cycling in High-Strain Wafer-Level Chip-Scale Packages. *Journal of Electronic Materials*, 44(3), 895-908. <https://doi.org/10.1007/s11664-014-3572-9>
- [31] Anderson, P. M., Hirth, J. P., & Lothe, J. (2017). *Theory of Dislocations*. Cambridge University Press.
- [32] Shin, J. W., & Chason, E. (2009). Stress behavior of electroplated Sn films during thermal cycling. *Journal of Materials Research*, 24(4), 1522-1528. <https://doi.org/10.1557/jmr.2009.0172>
- [33] Cai, X., Handwerker, C. A., Blendell, J. E., & Koslowski, M. (2020). Shallow grain formation in Sn thin films. *Acta Materialia*, 192, 1-10. <https://doi.org/10.1016/j.actamat.2020.03.014>

4. WHISKER NUCLEATION BY SLIP-ASSISTED GRAIN ROTATION DURING THERMAL CYCLING

The following chapter was submitted to *Acta Materialia* as Wang, C., Cai, X., Koslowski, M., Blendell, J., & Handwerker, C. (2021). Whisker nucleation by slip-assisted grain rotation during thermal cycling.

4.1 Introduction

Spontaneous whisker growth relieves high local stresses in metal films, particularly notable for columnar-grained Sn films in Pb-free electronics where the risk of whisker-induced short circuits is a continuing issue [1]. In columnar-grained, polycrystalline films, characteristic features of whisker formation and growth have been identified for compressive stresses generated by Cu₆Sn₅ intermetallic formation at room temperature at the Sn-Cu interface and thermal cycling of Sn films on a substrate with a different coefficient of thermal expansion (CTE). For example, under both conditions, whiskers are observed to form from shallow grains with "oblique" grain boundaries (GBs) [2-5]. As columnar-grained samples with vertical GBs are the predominant specimen type for whisker studies reported in the literature, the question is where those shallow grains originated. Previous studies suggested multiple possibilities, including pre-existing shallow grains formed during electrodeposition [5-6] and new shallow grains formed by grain boundary migration and pinch-off of columnar grains or by dislocation generation, recovery and recrystallization driven by compressive stresses [7-9]. Diffusional creep [10], GB sliding [2-3], GB migration [7], and grain nucleation [8-9] have all been reported to play significant roles in forming whisker grains in polycrystalline films.

However, columnar-grained polycrystalline films are not ideal for following how grains evolve and form active sites for whisker growth. Furthermore, the sheer number of grains interacting in a film and their 3D geometry and local responses are complicated by the anisotropic properties of β -Sn, including:

- (1) thermal expansion anisotropy, e.g., the CTE is 70 ppm/K in [001] and 23 ppm/K in [100];

- (2) elastic anisotropy, e.g., Young's modulus of β -Sn is 32 GPa in [001] and 16 GPa in [100];
- (3) temperature-dependent deformation behaviors, e.g., β -Sn films creep at room temperature (near the homologous temperature of 0.6) and deform rapidly [11];
- (4) the anisotropy of dislocation motion in β -Sn slip systems in which 32 independent slip systems have been identified [12-15].

An alternative film type, i.e., β -Sn films with large in-plane grain sizes (mm) relative to film thickness (10-30 μm), allows us to follow individual grain boundaries to relate specific stress relaxation responses to changes in local crystallography and morphology. Previous studies on such films reported different morphological and crystallographic changes along the entire lengths of different GBs which could be discriminated by the amount of local GB sliding, recrystallization, and whisker formation [16]. The observed range of microstructural changes indicated that crystallography of individual GBs has a profound influence on local stress states as well as on the resulting relaxation responses. In particular, in large-grained samples, the nucleation of new shallow grains that become whiskers as a result of thermal cycling has been reported [17]. Local high geometrically necessary dislocation densities (GNDs) [17], high elastic strain energy density (ESED) [17], and high out-of-plane thermal expansion differences between grain pairs [18] have been associated with the formation of shallow grains.

The sequence of processes and the specific mechanisms for how, when, and where shallow grains form are still being identified. In a recent synchrotron study of changes before and after thermal cycling, shallow grains nucleated by localized grain rotation, with slip traces occurring nearby on the free surface [18]. The work's main limitation is the lack of information about the time-dependent characterization, leaving questions such as (1) what the steps were to form the shallow grains and (2) what role slip took during the process. This limitation is partially addressed by a recent study employing a plasticity model to simulate the evolution of local stress states and associated deformation near GBs [19]. The study observed subgrains formation from regions that developed high dislocation density through gradual grain rotation [19]. Those newly nucleated subgrains resemble shallow grains, thereby capable of growing out as whiskers. The simulation considered slip behavior, echoing the previous observation of slip traces; however, the mechanism

of slip during grain rotation in whisker nucleation needs to be further examined, ideally under a condition where individual deformation mechanisms could be differentiated.

In the present study, we employed large-grained Sn films with a pseudo-bicrystal geometry to examine the local stress states between each grain pair. We focus on the individual stress relaxation mechanisms and their interplay, including grain rotation, GB sliding, slip, GB migration, and their effects on nucleation of potential whiskers (i.e., shallow grains). We examine the evolution of these time-dependent processes with increasing numbers of thermal cycles to fill the gap from previous studies that only examined the films before and after cycling when multiple whiskers had already nucleated and grown. In particular, we link the macroscopic plastic deformation to microscale dislocation activities by identifying the activated slip systems based on the geometrical relationships between slip traces and local orientation and slip. This sheds light on how dislocation motions lead to grain rotation and, thereby, the formation of shallow grains.

4.2 Experiments

4.2.1 Large-grain film preparation

Copper substrates (99.99% purity, ultrahigh conductivity, 6.35 mm thick, McMaster-Carr) were electropolished (50 mA/cm² current density) with a mixed polishing solution (700 ml phosphoric acid and 180 ml n-butyl alcohol) prior to electrodeposition to prepare scratch-free surfaces. The substrates were submerged in a methane sulfonic acid-based Sn plating electrolyte (SOLDERON, Dow Chemical) and electroplated [20] for approximately 4 minutes at room temperature with 30V applied voltage and a current density of 0.0133 A/cm² producing a polycrystalline film of 20 μm average thickness based on the increased mass, the density of Sn, and the area of deposition. The in-plane diameters of grains in the as-deposited columnar films ranged from 5 to 10 μm.

The large-grain films were prepared via melting and solidification. A thick layer (~5 mm) of flux (Kester TSF-6522) was applied to the entire film surface prior to melting, thus promoting wetting while inhibiting rapid dewetting. Melting was performed using a hot plate with a bulk aluminum plate to aid in heat transfer. The temperature of the aluminum plate was monitored by a thermocouple attached to its surface. When the Al plate's temperature uniformly reached 235°C, the as-deposited, fluxed film/substrate sample was placed on the aluminum plate. Samples were

removed from the hot plate as soon as the as-deposited film melted (when it became shinier), or the liquid Sn layer would start to dewet. The samples were then quenched on an Al cooling plate at room temperature. Quenching produces a large-grained film with millimeter in-plan grain sizes due to the difficulty of nucleating β -Sn during solidification, which has been well-documented in previous literature [21]. The microstructure of the as-melted film under optical microscopy and scanning electron microscopy is shown in Fig. 4.1. The particles on the free surface, decorating the GBs, were Cu_6Sn_5 . During solidification, Cu_6Sn_5 particles or plates were pushed forward by Sn dendrites until two grains meet to form a grain boundary.

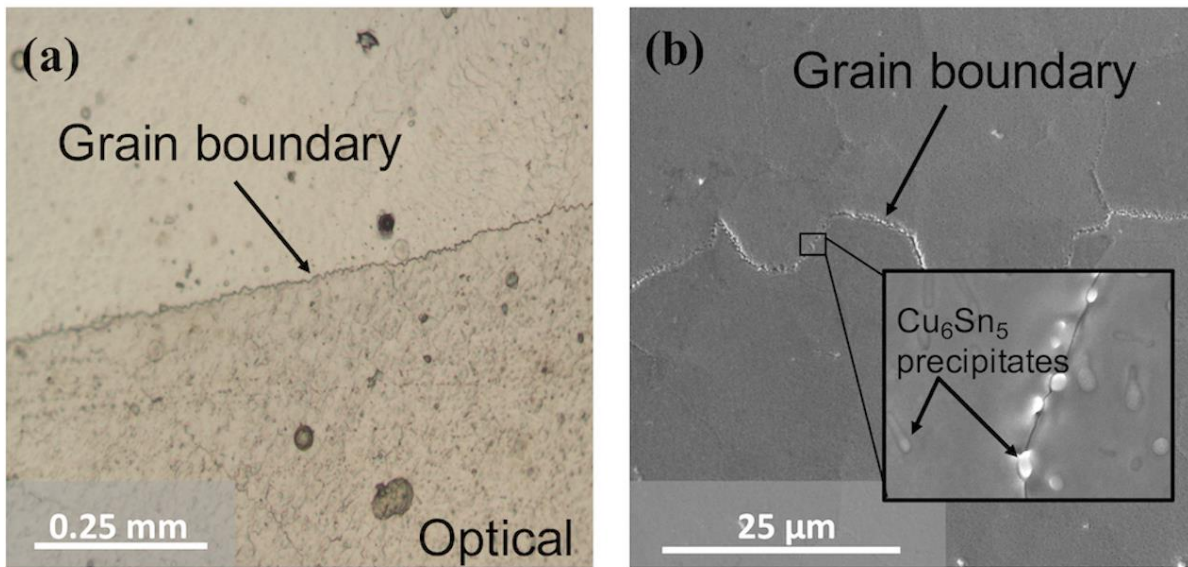


Figure 4.1. Surface of as-solidified (large-grain) Sn film on Cu substrate in optical microscopy (a) and SEM (b) showed a pseudo-bicrystal microstructure.

4.2.2 Thermal cycling

The films were thermally cycled by transferring them between two separate chambers set at 65°C and -25°C , with a hold time at each extreme of approximately 10 minutes, a technique described previously as "rapid thermal cycling" [20]. Due to the limitations of heat transfer, the actual cycling conditions deviated from the settings. A typical cycling profile of the film measured with a thermocouple on the sample is shown in Fig. 4.2.

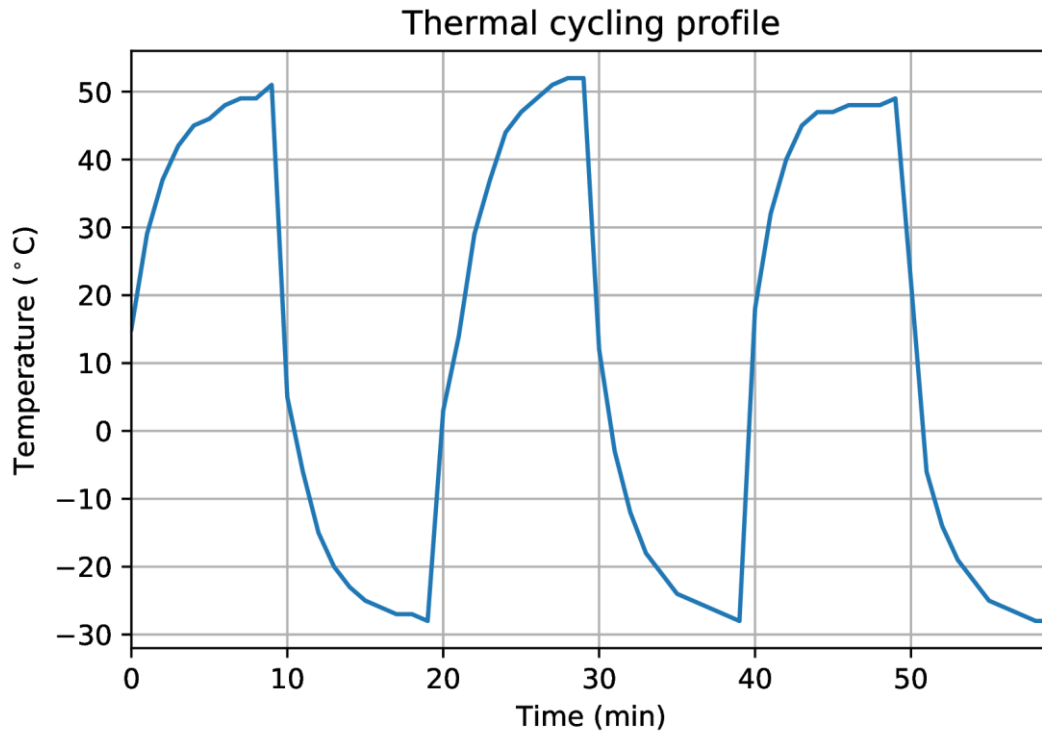


Figure 4.2. Real-time measured profile of the rapid thermal cycling technique.

4.2.3 Characterization

Before and at intervals during thermal cycling, the film was imaged by optical and scanning electron microscopy (Nova NanoSEM) to locate the grain boundaries, as shown in Fig. 4.1(a) featuring a grain boundary longer than one millimeter in the large-grain Sn films. As shown in Fig. 4.1(b), the GB structure after solidification showed substantial roughness at approximately a 15 μm length scale and Cu_6Sn_5 particles segregated to the GBs during solidification. The surface morphology was imaged after different numbers of cycles; only those with substantial morphological changes are presented in the results. This incremental cycling was limited to 230 cycles to focus on the early stage of the stress relaxation process. At the end of the cycling, Atomic Force Microscopy (AFM) analysis was performed on deformed regions to obtain the local height profile associated with the mass transport. Electron Backscattered Diffraction (EBSD) was performed near the monitored GBs that exhibited the most deformation.

4.3 Results

Only grain boundaries (GBs) that showed grain nucleation or substantial changes in surface morphology were analyzed. Often, features associated with different deformation mechanisms were observed at the same GB location and during the same cycling interval. Therefore, it is important to describe those features in detail and examine the links among deformation mechanisms. To guide the results and discussion, we used the following definitions from previous studies on GB phenomena [22–25]:

- Grain rotation: rotation of the crystal axes of a grain.
- GB sliding: rigid-body translation of one grain relative to the adjacent grain
- GB migration: grain boundary translation normal to the GB plane
- Local yielding: as manifested by slip traces on free surfaces.

4.3.1 Grain boundary sliding and whisker nucleation

GB sliding was commonly observed during thermal cycling; whiskers were also nucleated near GBs that showed sliding. For example, Fig. 4.3 shows the morphological changes on the surface near one GB between two large grains (Grain 1 and Grain 2) with increasing numbers of thermal cycles. Before cycling, the GB was detectable due to Cu_6Sn_5 particles decorating the GB. No noticeable microstructural changes were observed after 10 cycles [Fig. 4.3(a)]. After 40 cycles, some GB sliding had occurred along the entire GB, and a newly formed whisker was observed [Fig. 4.3(b)]. At 160 cycles, a larger whisker (arrow) formed with a flat top corresponding to the initial film surface near the first whisker. Meanwhile, noticeable GB sliding occurred along the entire GB. In our experiments, with an increasing number of cycles, it is not uncommon to observe "ridge-like" microstructures along GBs (resembling the topography where continental plates collide), as observed in previous studies of large-grain Sn-alloy films [16,18]. Though the formation of those "ridge-like" structures was denoted as GB sliding in this work, it is, in fact, a process in which sliding, rotation, migration, and diffusion occurred simultaneously. Three areas of interest, Region-1, Region-2, and Region-3 were characterized at higher magnification [Fig. 4.3(d-f)]. EBSD point analysis (annotated by A1-A9) was performed to examine the pre- and post-cycling orientation. A1 and A2 showed the orientation of Grain 1; A3 and A4 showed the orientation of Grain 2, as shown in Fig. 4.3(b). In contrast, A5-A9 showed the local orientations

near the GB. Parallel slip traces emerged on surfaces near A5, A7, and A8, as indicated in Fig. 4.3(d-f), and the directions of those parallel slip traces were similar. A6 showed the orientation of the nucleated whisker at 160 cycles. A9 showed the orientation of a subsided region at 160 cycles where loop slip traces developed.

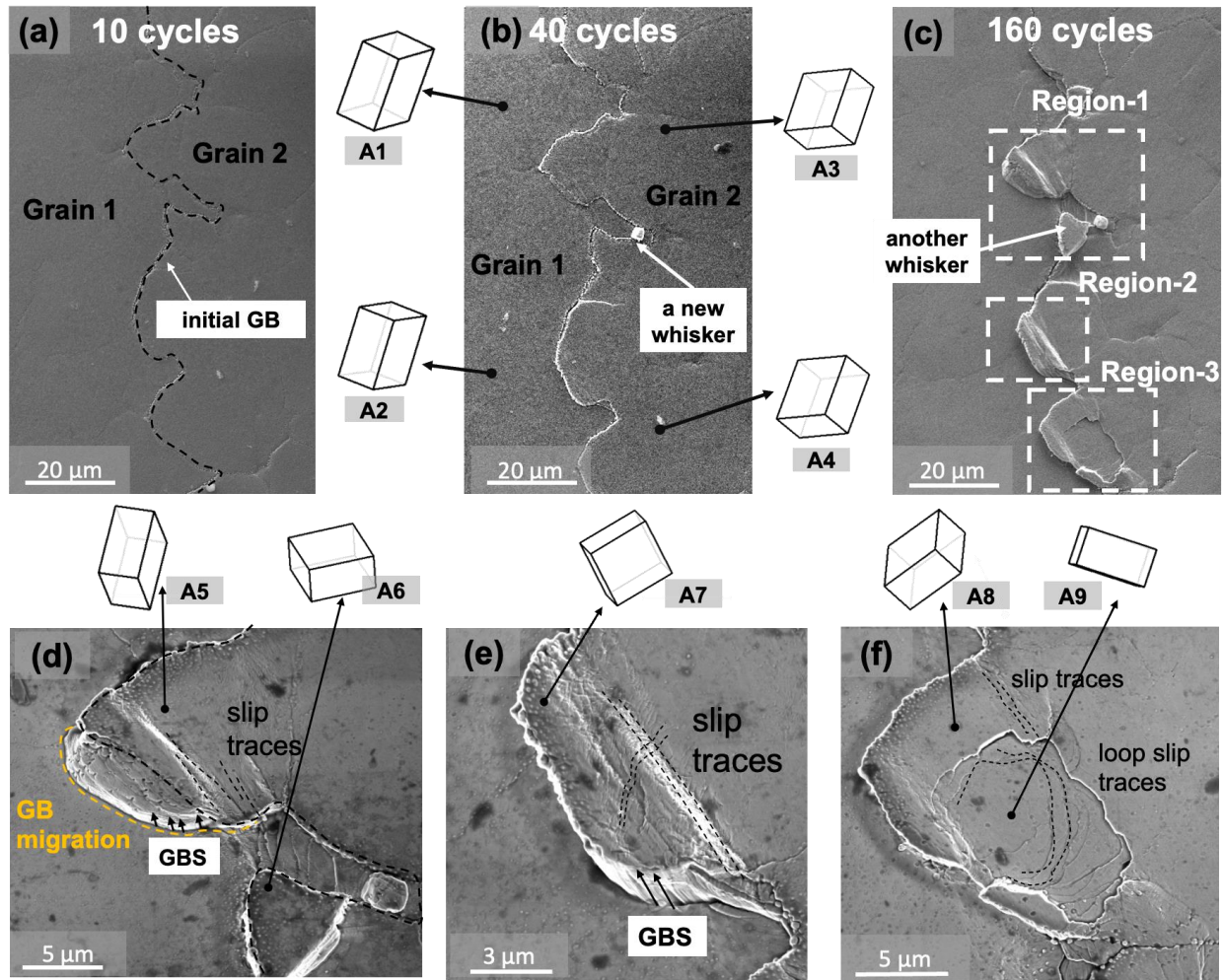


Figure 4.3. (a-c) SEM images of one monitored region's surface morphology at 10, 40, and 160 cycles. The dashed line in (a) marked the initial GB. (d-f) Enlarged images of three regions along the GB that demonstrated the most local deformation. A1-A9 noted 9 points analyzed with Electron Backscatter Diffraction (EBSD). The unit cell figures represented the local orientation at each corresponding position.

Fig. 4.4(a) and (b) showed the top-view and tilted-view of the Region-3 at 160 and 230 cycles, respectively. Three height profiles are plotted in Fig. 4.4(c) from the AFM that measured the surface morphology across the "ridge-like" microstructure at 230 cycles. This accretion or

“ridge-like” microstructural changes are referred as microstructural or morphological rotation in this study. The blue line crossed A8, and the red line crossed A9. Morphological rotation and subsidence in Region-3 were evident in those profiles.

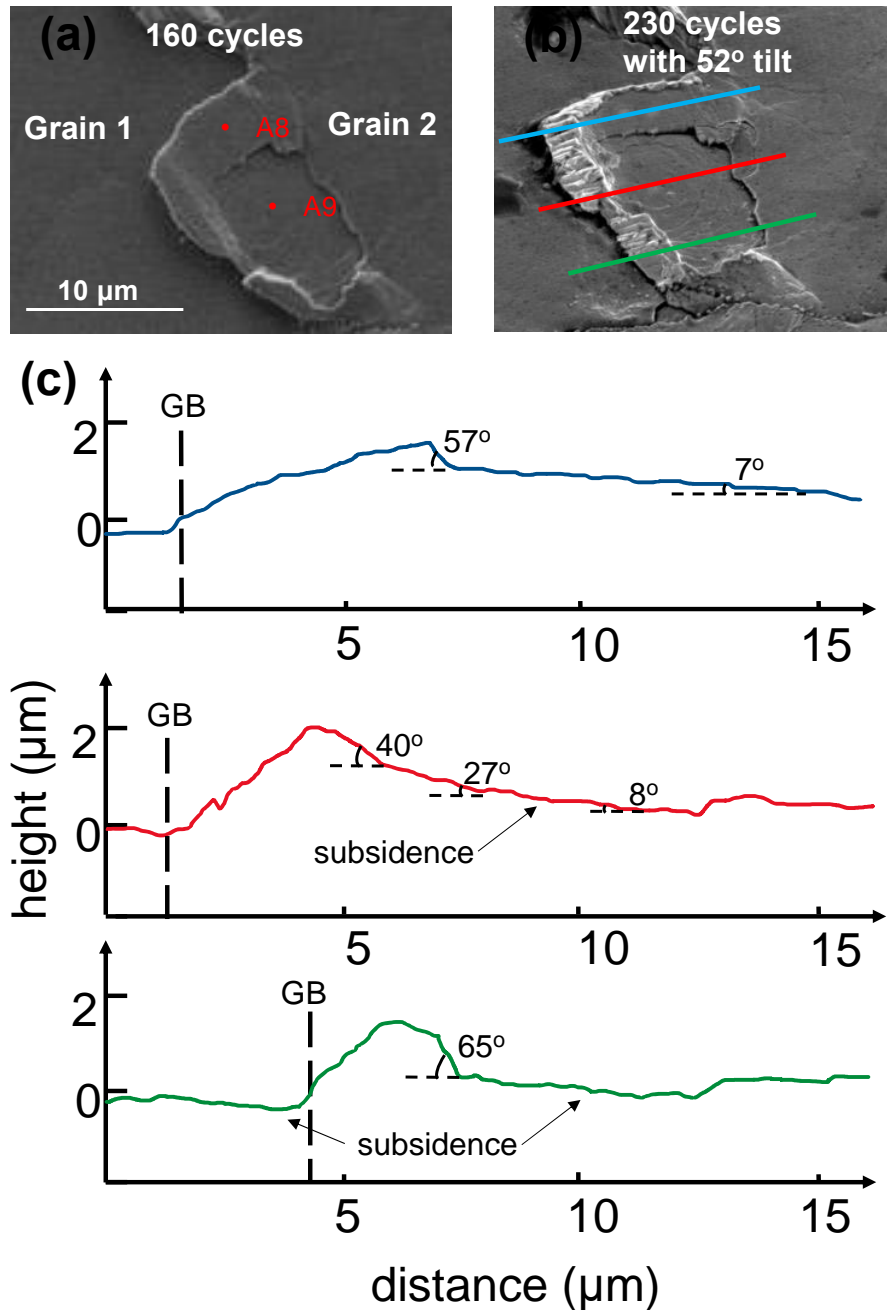


Figure 4.4. Ridge-like deformation region at (a) 160 cycles and (b) 230 cycles; (c) Three height profiles along the green, red, and blue lines marked in (b), obtained from Atomic Force Microscopy measurement.

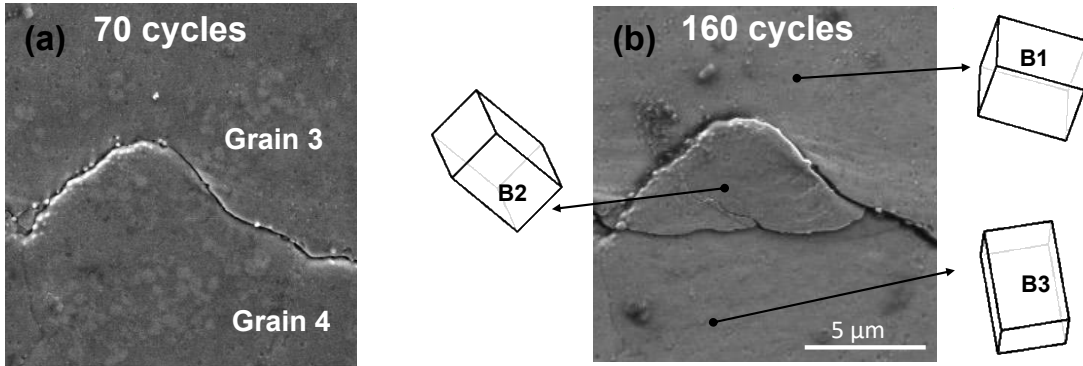
4.3.2 Grain formation by rotation

In regions where no whisker grew, crystallographic rotation occurred and resulted in the formation of new grains, such as the Region-4, Region-5, and Region-6 at different GBs as shown in Figure 4.5. In Region-4, the orientations of the three points near the GB were measured by EBSD and denoted as B1, B2, and B3. At 160 cycles, a surface step emerged between B2 and B3 whose orientations were significantly different. A new grain must have formed at B2 and the surface step indicated the location of the new grain's boundary. In Region-5, at 70 cycles, curved slip traces were observed on the surface near the GB, and a triangular surface step formed nearby. At 160 cycles, another surface step developed near the periphery of the curved slip traces. The lattice orientations of three points (B4, B5, and B6) were represented by tetragonal cells. Points B4 and B5 were originally in the same grain, i.e., Grain 3. In Region-6, similar morphological changes were observed. Comparing Fig. 4.5(e) and (f), at 160 cycles, the GB slid slightly. It is reasonable to assume no other grains existed along this GB because no other GB grooves were identified at 0 cycles. Additionally, a surface step formed on the surface did not develop from a pre-existing GB; if it had, Cu_6Sn_5 precipitates would have decorated the boundary there, as demonstrated in Fig. 4.1. The point-to-origin misorientation angles from the axis-angle pairs (Rodriguez vectors) across the GB along the direction of the yellow arrow [Fig. 4.5(f)] are shown in Fig. 4.5(g). They showed a 2° orientation jump at the location where the surface step emerged and a 15° orientational change at the original GB, suggesting a new subgrain has formed between two large parent grains.

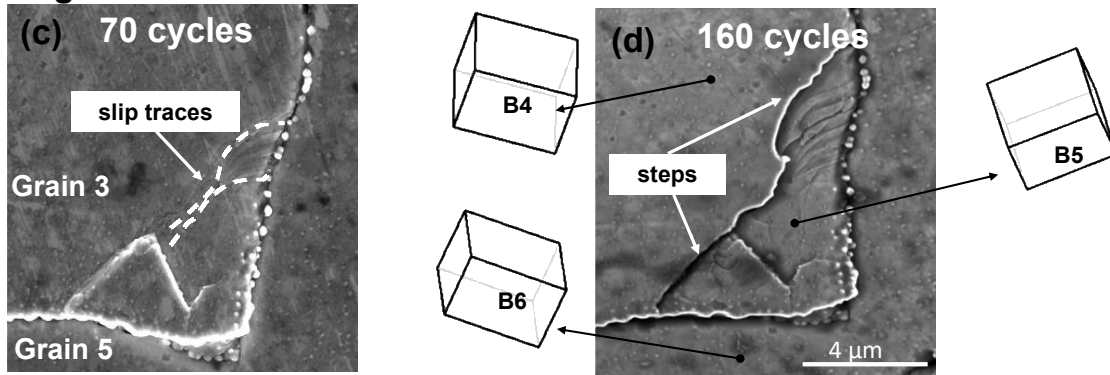
Fig. 4.6 showed the top-view and linear height analysis of the Region-4 at 160 cycles. Accretion near the GB on the side of Grain 4 was evident in B2 area where a new grain formed based on the orientational analysis illustrated in Fig. 4.6(b).

Grain formation by rotation

Region-4



Region-5



Region-6

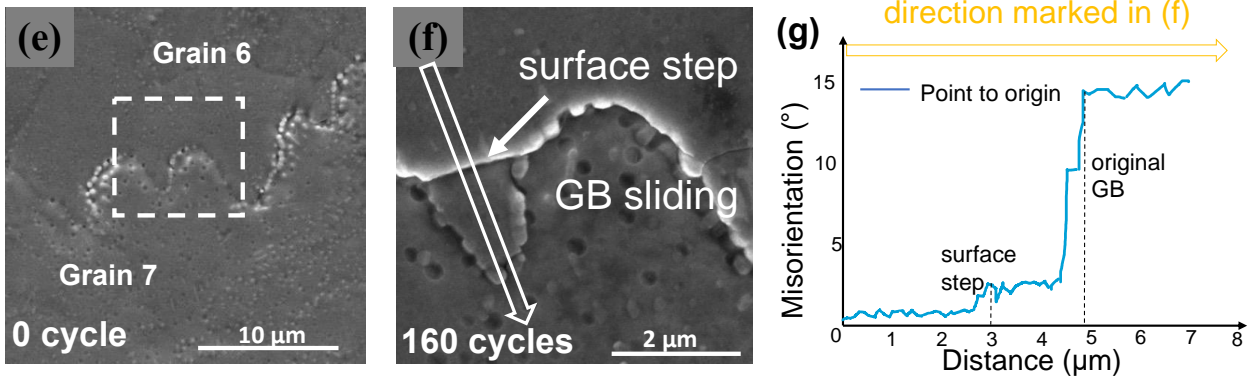


Figure 4.5. The microstructural changes in (a-b) Region-4, (c-d) Region-5 (at 70 and 160 cycles) and (e-f) Region-6 at 0 and 160 cycles. B1-B6 represented the orientations of six selected locations in these regions at 160 cycles. (g) Point-to-origin misorientation angle profile along the line marked by the yellow arrow in (f).

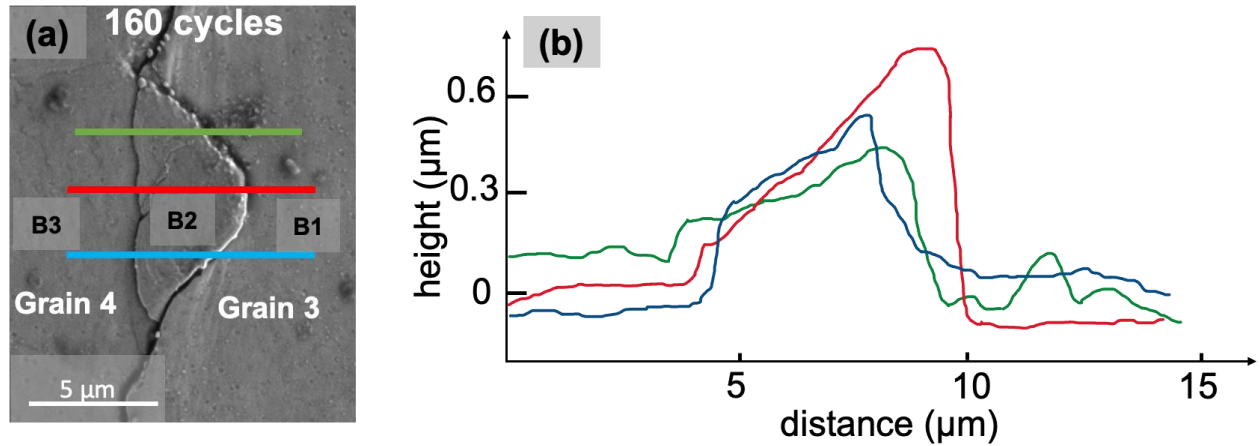


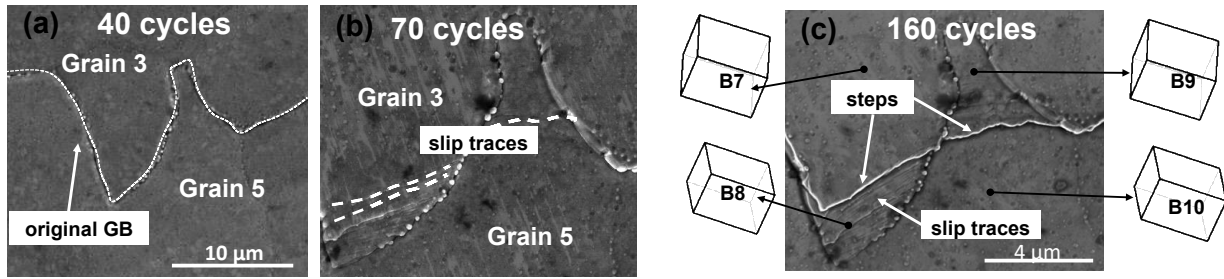
Figure 4.6. (a) Top-view of the Region-4 from the AFM measurement. (b) Three height profiles along the green, red, and blue lines marked in (a).

4.3.3 Grain boundary migration

Another type of response observed was sliding plus grain boundary migration in the absence of rotation. For instance, microstructures at 40, 70, and 160 cycles of Region-7 were analyzed in Fig. 4.7(a-c). A surface step formed near a highly curved segment of the original GB, and GB sliding occurred uniformly along the entire GB. As seen in Fig. 4.7(a), the locations noted as B7 and B8 were on the same side of the original GB; the same applied to B9 and B10. After 160 cycles, however, the orientations of B7 and B9 became the same, and the orientations of B8 and B10 became the same as well, as demonstrated in Fig. 4.7(c), indicating that the GB has migrated to locations with a smaller curvature. Region-8 exhibited similar changes comparing 0 and 160 cycles, as shown in Fig. 4.7(d-e). The point-to-origin misorientation profile along the direction of the yellow arrow [Fig. 4.7(e)] is shown in Fig. 4.7(f). A 45° orientational jump occurred at the location where the surface step emerged, and no obvious orientational change was detected at the original GB, indicating the segment of the GB in Region-8 has migrated to where the surface step was located.

Grain boundary migration

Region-7



Region-8

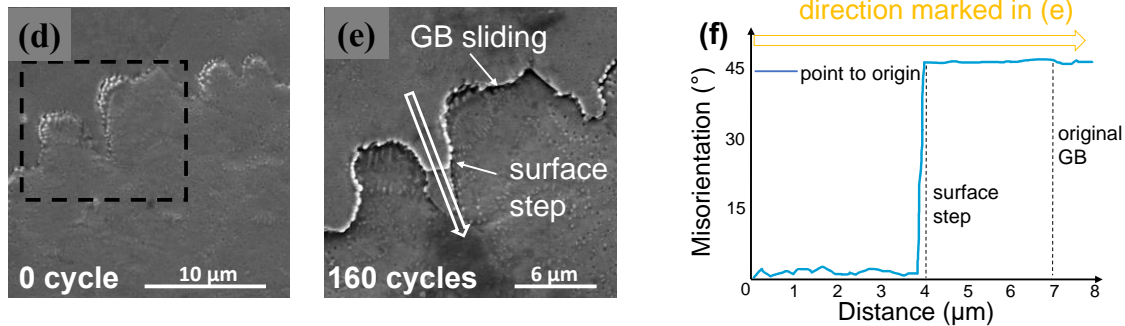


Figure 4.7. (a-c) Morphological evolution of a monitored region, Region-7, at 0, 40, and 160 cycles. B7-B10 represented the orientations of four selected locations at 160 cycles. (d-e) Morphological evolution of another monitored region along the same GB at 0 and 160 cycles. (f) Point-to-origin misorientation angle profile along the line marked by the yellow arrow in (e).

4.4 Discussion

4.4.1 Individual deformation mechanisms and their contribution to whisker grain nucleation

Nucleation of potential whisker grains occurred near GBs from the early stages of thermal cycling. In this section, we will discuss the contribution of each mechanism to nucleating whisker grains at different stages of thermal cycling and compare our analysis to previous studies based on Sn-alloy films with similar pseudo-bicrystal microstructure [16–18].

4.4.1.1 GB sliding

Almost every GB characterized in our study exhibited GB sliding, echoing previous observations that GB sliding contributed significantly to local deformation in large-grain solder films [16–18]. For example, as seen in Fig. 4.3, sliding striations were observed on the sidewalls

of A5 and A7, plus GB migration at A5. These observations reflected the complexity of the so-called "GB sliding" in the present study, i.e., grain rotation, sliding, migration, and diffusion occur simultaneously within a small region while an entire GB exhibited even more heterogeneous deformation. In particular, GB sliding seemed to take place prior to any other stress relaxation response, as seen in Fig. 4.3(b), Fig. 4.5(a) and (c), and Fig. 4.7(a) and (b), suggesting sliding could act as the pre-requisite for other relaxation mechanisms. "Stick-slip" behavior is a salient feature in GB sliding due to the existence of sliding friction. As illustrated in Fig. 4.3(d-e), the steps that emerged on the GB side walls likely reflected this behavior where local shear stresses accumulated along static GBs and then dropped as sliding happened. This "stick-slip" sliding phenomenon has been observed and integrated into previous whisker growth models [2,10]. We observed sliding at both original high-angle GBs and newly formed low-angle GBs, indicating that GB sliding was never entirely suppressed by other relaxation responses regardless of the local misorientation.

4.4.1.2 GB rotation

Grain rotation was common in the majority of deformed regions near GBs. Previous studies pointed out that grain rotation is critical for forming new grains in polycrystals since it allows subgrain formation near the original GB [26,27]. Low-angle and high-angle GBs can later develop from those subgrains, referred to as a "nucleation" process. Experiments in solder balls provided evidence of subgrain formation by rotation [28–30]. Notably, in the context of Sn whiskers, the formation of subgrain or low-angle GBs resulting from local lattice rotation was reported as the precursor of whisker nucleation in a synchrotron study of large grain-size films [18] and in plasticity simulation [19]. From post-cycling EBSD measurements, newly nucleated subgrains were detected by their differences in orientation from their parent grains, as shown in Fig. 4.3 and Fig. 4.5. For instance, after 160 cycles, the orientations of the deformed regions in Fig. 2(d-f) were significantly different from their parent grains (Grain 1 and Grain 2). Though the as-fabricated orientations differ slightly between regions close to or away from the GB due to the dendrite growth during solidification [21], the crystallography differences between dendrite arms are smaller than the changes observed in this experiment. Therefore, the orientational differences must result from rotation rather than due to the slightly misoriented dendrite arms formed during re-solidification.

In addition, the misorientation angles were also different from the AFM-measured angles. For example, as shown in Fig. 4.4, the angle between the surface of the "ridge" and the film surface (A8 and Grain2) was estimated to be approximately 7°, whereas the smallest crystallographic misorientation angle of A8 and A4 was approximately 33°. Similarly, in Region-4 (see Fig. 4.6), the angle between the top surface the ridge and the horizontal surface was approximately 5°, whereas the smallest crystallographic misorientation angle between B2 and B3 was approximately 58°. Those differences indicated that there is an additional crystallographic rotational component other than the rotation causing uplift, i.e., an in-plane crystallographic rotation. The importance of rotation during the early stage of subgrain formation is clear, as suggested in previous studies [18,19,26-30].

4.4.1.3 Local yielding: slip behavior

Local yielding is one of the mechanisms that coincided with grain rotation, shown by slip traces accumulating on the surface. Slip traces emerged on the surfaces of all monitored regions, indicating that the local deformation involved dislocation motion. For slip traces that were parallel it is reasonable to assume the active slip planes were the same. When two sets of slip traces accumulated on the rotating surface as shown in Fig. 4.3(e), more than one slip system must be active. Fig. 4.3(f) captured a subsided region enclosed by a circular surface step where multiple loop slip traces developed, resembling what was reported in small-grain Sn films [20,31]. Those loop traces may reflect the movement of screw dislocations. Using A4 as the parent grain's reference orientation, points A5-A8 (as shown in Fig. 4.3) were indexed by EBSD and compared with the parent grain (Grain 2) to quantify the plastic deformation during thermal cycling. Rotating the observed slip traces in the lab frame to the crystal frame of the parent grain orientation. Details of the rotation operation are provided below.

For the observed slip traces in the sample frame, their vectors were translated to the Beta-Sn frame using the Euler angles with Bunge notation. Considering the sample basis (x_1, y_1, z_1) and the grain basis (x_2, y_2, z_2) , the change of basis can be achieved by subsequent rotations:

$$(x_1, y_1, z_1) \xrightarrow{\psi_1} (x'_1, y'_1, z_1) \xrightarrow{\phi} (x'_1, y''_1, z_2) \xrightarrow{\psi_2} (x_2, y_2, z_2) \quad (\text{Equ 4.1})$$

where ψ_1 , Φ , and ψ_2 are Euler angles in Bunge convention. The rotation matrices for the three rotation steps are given by:

$$g_1(\psi_1) = \begin{bmatrix} \cos\psi_1 & \sin\psi_1 & 0 \\ -\sin\psi_1 & \cos\psi_1 & 0 \\ 0 & 0 & 1 \end{bmatrix} g_2(\Phi) = \begin{bmatrix} 1 & 0 & 0 \\ 0 & \cos\Phi & \sin\Phi \\ 0 & -\sin\Phi & \cos\Phi \end{bmatrix} g_3(\psi_2) = \begin{bmatrix} \cos\psi_2 & \sin\psi_2 & 0 \\ -\sin\psi_2 & \cos\psi_2 & 0 \\ 0 & 0 & 1 \end{bmatrix} \quad (\text{Equ 4.2})$$

And the rotation matrix in all is given by:

$$g(\psi_1, \Phi, \psi_2) = g_3(\psi_2)g_2(\Phi)g_1(\psi_1) \quad (\text{Equ 4.3})$$

Using above equations, the calculated vectors of slip traces in sample frame and crystal frame are tabulated in Tab. 4.1.

Table 4.1. Rotated slip trace vectors (All references are Cartesian coordinates)

Vectors	Observed (sample frame)	Rotated (crystal frame)
A5	[sin55°, cos55°, 0]	[0.35, 0.52, 0.78]
A6	[cos39°, -sin39°, 0]	[-0.51, 0.86, -0.01]
A7(1)	[cos28°, -sin28°, 0]	[-0.39, 0.91, 0.15]
A7(2)	[sin52°, cos52°, 0]	[0.39, 0.48, 0.79]
A8	[sin53°, cos53°, 0]	[0.37, 0.49, 0.78]

The angles between the observed slip traces and all potential slip planes (see Tab. 4.2 [12-15]) in the Cartesian coordinate systems were calculated using the equation below:

$$\Theta = \cos^{-1} \left(\frac{\vec{r}_c \cdot \vec{n}_c}{|\vec{r}_c| |\vec{n}_c|} \right) \quad (\text{Equ 4.4})$$

where \vec{r}_c is the vector of the rotation axis and \vec{n}_c is the slip plane normal. Both \vec{r}_c and \vec{n}_c were converted to Cartesian coordinates for the calculation. Therefore, the closer this angle is to

90°, the larger the possibility that dislocations moved along that slip plane to the surface for the observed traces. Angles between rotated slip trace vector and all possible slip plane normal calculated with Equ. (4) in Cartesian coordinates are shown in Tab. 4.3.

Table 4.2. Families of potential slip systems in Sn and the corresponding slip plane families

Slip system family	Number of slip systems in family	Slip plane family
$\{100\}\langle 001\rangle$	2	
$\{100\}\langle 010\rangle$	2	$\{100\}$
$\{100\}\langle 011\rangle$	4	
$\{110\}\langle 001\rangle$	2	
$\{110\}\langle 1\bar{1}1\rangle/2$	4	$\{110\}$
$\{110\}\langle 1\bar{1}0\rangle$	2	
$\{001\}\langle 010\rangle$	2	$\{001\}$
$\{001\}\langle 110\rangle$	2	
$\{011\}\langle 01\bar{1}\rangle$	4	$\{011\}$
$\{211\}\langle 01\bar{1}\rangle$	8	$\{211\}$

Table 4.3. Angles between rotated slip traces and non-equivalent slip plan normal (°)

slip planes	A5	A6	A7(1)	A7(2)	A8
(100)	69.4	59.4	60.0	66.9	68.1
($\bar{1}$ 00)	69.4	59.4	60.0	66.9	68.1
(010)	58.6	30.6	67.4	25.0	60.3
(0 $\bar{1}$ 0)	58.6	30.6	67.4	25.0	60.3
(1 $\bar{1}$ 0)	83.1	14.4	85.3	23.2	85.1
($\bar{1}$ 10)	83.1	14.4	85.3	23.2	85.1
(110)	51.9	75.6	51.2	68.8	52.2
($\bar{1}$ $\bar{1}$ 0)	51.9	75.6	51.2	68.8	52.2
(001)	39.0	89.2	39.2	81.1	38.3
(00 $\bar{1}$)	39.0	89.2	39.2	81.1	38.3
(101)	31.6	75.2	23.0	87.0	59.3
(10 $\bar{1}$)	59.0	76.6	63.9	71.1	59.3
(0 $\bar{1}$ 1)	64.3	64.9	60.3	72.6	63.1
(011)	21.2	66.4	30.2	55.3	22.2
(121)	12.8	65.8	21.4	54.0	14.3
(1 $\bar{2}$ 1)	75.3	38.7	66.5	48.3	73.5
(12 $\bar{1}$)	89.4	64.6	87.0	66.9	88.5
($\bar{1}$ 21)	42.5	40.3	54.3	30.6	44.7
(211)	23.6	86.4	13.8	82.0	22.1
(2 $\bar{1}$ 1)	56.2	48.8	45.2	60.1	54.2
(21 $\bar{1}$)	86.0	87.4	89.4	86.8	86.1
($\bar{2}$ 11)	64.5	50.2	73.9	46.9	65.7

The slip planes with angles larger than 85° were selected to represent the slip behavior, as shown in Table 4.4. The analyses indicated that a preferred slip plane, $(21\bar{1})$, was present in every analyzed location. More work is needed to identify the specific slip directions operating on $(21\bar{1})$.

Table 4.4. Selected angles between rotated slip traces and the normal of potential slip planes.

Trace locations	possible slip planes & corresponding angles (Θ)		
A5	$(12\bar{1})$, 89.4°	$(21\bar{1})$, 86.0°	/
A6	(001) , 89.2°	$(21\bar{1})$, 87.4°	(211) , 86.4°
A7(1)	$(21\bar{1})$, 89.4°	$(12\bar{1})$, 87.0°	$(1\bar{1}0)$, 85.3°
A7(2)	(101) , 87.0°	$(21\bar{1})$, 86.8°	/
A8	$(12\bar{1})$, 88.5°	$(21\bar{1})$, 86.1°	$(1\bar{1}0)$, 85.1°

4.4.1.4 Short-distance diffusion

Diffusion is critical for both whisker growth and whisker nucleation. In studies focusing on the growth stage of whiskers or hillocks, the diffusion mechanisms commonly operating are described as long-range lattice or GB diffusion along the stress gradients to the inclined grain boundaries of the shallow grains [2,6,32-35]. The accumulation of atoms at the base of the shallow grains creates a force along the GB normal to the film surface such that shallow grains with inclined boundaries slide out-of-plane. When near-GB whisker grains nucleate by rotation, shape accommodation must occur. Shape accommodation is necessary because the orientation of a non-round grain cannot change without mass redistribution, i.e., creep [22, 26]. The subsidence shown in Region-3 (Fig. 4.3 and 4.4) likely reflected active short-range diffusion that provided the necessary mass for the adjacent regions. Note there could be two types of subsidence: one was driven by mass conservation, and the other was driven by stress gradients. The former was represented by the subsidence near GBs, as shown in the left side of the green height profile in Fig. 4.4(c); the latter was represented by the sinking region around A9, as shown in the right side of the same green profile. The second type of subsidence was reported in previous studies that performed rapid thermal cycling on small-grain Sn films as a result of “reverse” whisker growth. This process occurred when the mass diffused under the shallow grains during compressive stress

states are less than mass diffused away from the shallow grains during tensile stress states [20]. Additional cross-sections are required to confirm whether the loop region near A9 sank as a reverse whisker.

4.4.2 Nucleation mechanism for whisker grains

A nucleation mechanism for shallow whisker grains is summarized in Fig. 4.8 based on the above examination of the roles of individual deformation mechanisms. First, for as-solidified large-grained films, the driving force of plastic deformation was the thermo-mechanical stresses resulting from the difference of thermal expansion between Sn films and Cu substrates. Under compressive stresses, power-law creep and GB sliding could occur and result in highly localized stress states at the GB. (Widespread lattice-diffusion-controlled and GB-diffusion-controlled creep are suppressed by the native Sn oxide [36]). We use here a two-dimensional finite element simulation of a bicrystal based on the previously reported plasticity model [19] to estimate the deformation of the grains in Fig. 4.8(a-b). The grain orientation was defined by the Bunge Euler angles $[\phi_1, \Phi, \phi_2]$, with the simulation frame (sample frame) for the reference x-y-z axes. The Euler angles of the left grain were $[57^\circ, 17^\circ, 64^\circ]$ and the right grain were $[79^\circ, 97^\circ, 54^\circ]$. In the simulation, plane strain conditions were used and a compressive displacement was applied to the right boundary. The left boundary was fixed in the horizontal direction and the bottom boundary was fixed in the vertical direction. Sliding of the GB was not allowed in the simulation to maintain the geometry of the GB. Due to the anisotropy of Sn, the mechanical responses, including stresses and strains, are different for grains of different orientations. During the compression, geometrically necessary dislocations are generated at the grain boundary near the top surface to maintain the compatibility of the lattice. The dislocation density map showed that the majority of those dislocations concentrated in a region with the shape of a shallow grain near the GB, as shown in Fig. 4.8(b). A schematic of all accumulated dislocations with different Burgers vectors is shown in Fig. 4.8(c). When one or more slip planes were activated by the local stress states, dislocations on those slip planes can slide or glide to rearrange into an edge GB, as shown in Fig. 4.8(d). During this stage, slip traces emerged on the surface near the GB; subsidence may also occur to supplement either diffusion or dislocation motions. In the end, the newly formed edge GB will form a shallow grain that may grow out as a whisker, as shown in Fig. 4.8(e-f). Vianco *et al.* proposed a qualitative dynamic recrystallization model for whisker grain nucleation in which small

grains nucleated near GBs from a pileup of dislocations and later grew into the deformed parent grains to form a larger shallow surface grains [8,9]. In contrast to this model based on a classic model of recrystallization, our results showed nucleation was driven by a combination of the movement and rearrangement of dislocations on certain slip planes and diffusion, causing the observed grain boundary sliding at the original interface, formation of a new grain boundary, and rotation grain. Using both experimental observations and simulations, we showed how dislocations accumulate near some GBs in response to the applied stresses as a result of crystallographic differences. Additionally, through the sequential measurements of local orientation and microstructure, we demonstrated the importance of grain rotation in whisker nucleation that was not in the previous model.

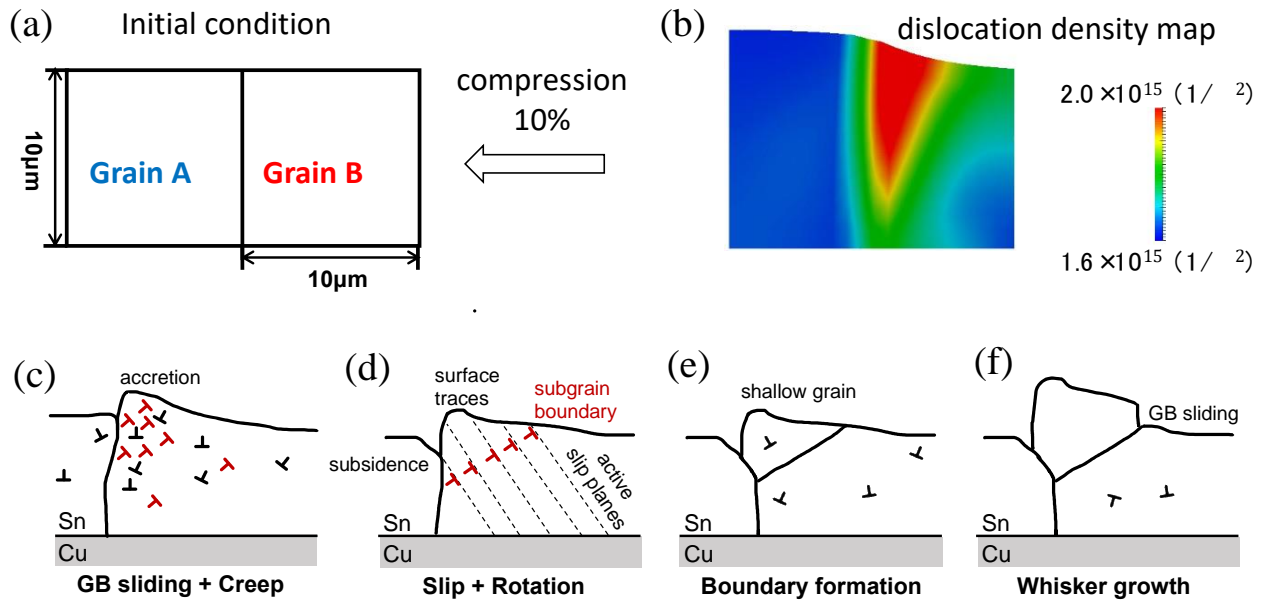


Figure 4.8. (a) Initial geometry of the bicrystal simulation. 10% compressive strain was applied. (b) Simulated dislocation density map of the deformed bicrystal where dislocation density peaked within the upper left corner of Grain B close to the GB. (c-e) Schematic diagrams of the nucleation mechanism for whisker grains (shallow grains) in thermally cycled large-grained Sn films.

4.4.3 GB migration

Apart from the nucleation of whisker grains, GB migration was occasionally observed throughout the cycling process. As illustrated in Fig. 4.7(b-c), two surface steps later formed at 160 cycles where slip traces had developed at 70 cycles. Orientation analysis revealed that B7 and B9 became the same orientation, while B8 and B10 changed to the same orientation as well. Yet prior to cycling, B7 and B8 belonged to the same parent grain, and B9 and B10 belong to the other neighboring one, see Fig. 4.7(a). It can be explained that, instead of nucleating grains, the GB simply migrated and stopped at the position where surface steps emerged. The same conclusion applied to Region-8, where a new grain seemed to form near the tip of the grain, yet there was no misorientation difference across the original GB, see Fig. 4.7(d-f). The observations suggested that GB in Region-8 migrated, and a surface step developed at the position where the migration stopped. No nucleation of whisker grains was involved in this type of deformation. Comparing Fig. 4.5 and Fig. 4.7, in both cases, surface steps appear to emerge on surfaces. However, the location of the surface step can indicate either newly formed GBs or migrated GBs. This finding suggested that future studies should rely on combined analysis of microstructure and crystallography to identify nucleated grains.

4.4.3.1 Driving forces

Shear-induced [37,38] and curvature-driven [39] GB migration have been studied with experimental observations and simulations using bicrystal or embedded-grain microstructure. If driven by curvature, the coupled GB motion (GB migration and GB sliding) is frequently accompanied by grain rotation with decreasing local curvature [23]. On the other hand, if driven by shear stress applied on a curved boundary, boundary migration can increase or decrease the original curvature. We observed both situations at different GBs (increased curvature in Fig. 4.3(d) and decreased curvature in Fig. 4.7) in the same Sn film. The results suggest two possibilities: first, both curvature and shear stress of the boundary drove the migration; or second, only shear stress played a role. Considering the zigzagged GBs formed from dendrite arms in an as-solidified sample, a reasonable conjecture is that those GBs with highest curvature tended to move towards the center of the curvature. Therefore, the GB migration characterized in this paper is likely driven by both mechanisms, although there was a small chance that the shear stress was the only variable influencing the local relaxation behavior.

4.4.3.2 The heterogeneity of grain rotation, GB sliding, and GB migration

Heterogeneous deformation processes appeared to lead to whisker grain nucleation, including grain rotation, local yielding, GB sliding, GB migration, and diffusion. Often, signatures of multiple deformation mechanisms were observed at the same time and location. Therefore, it is natural to consider the coupling effects of different stress relaxation mechanisms. For example, according to Taylor and Cahn, relative tangential displacement along a curved GB may give rise to grain rotation and vice versa [22,23]. Many of our experimental results showed both to be happening, as discussed in section 4.1, i.e., grains locally rotated to accommodate the height offset resulting from GB sliding and/or diffusion and eventually formed a new grain. Taylor and Cahn also suggested that grain rotation is necessary for GB migration. However, no orientation changes were observed near migrated regions in our results, as indicated in Fig. 4.7. An explanation is that the boundary can move by the motion of dislocation without change of orientation if more than one set of dislocations existed at the GB because the misfit angle can be preserved during the dislocation motion [40].

4.5 Conclusions

In our study, sequential characterization performed on individual GBs as a function of the number of thermal cycles made it possible to follow the evolution of heterogeneous deformation mechanisms. Heterogeneous plastic deformation behavior was observed for different GBs as well as along the same boundary. The phenomena observed include GB sliding, local yielding, grain rotation, diffusion, GB migration, and whisker formation.

At early stages (40 cycles), GB sliding was widely observed prior to any other responses and appears to be a prerequisite for whisker nucleation in large-grained Sn films. Localized grain rotation near the GBs was then observed which can result from local yielding and slip. Geometrically necessary dislocations were generated to accommodate shape changes near free surfaces, and then rearranged to form subgrain boundaries. We suggest that grain rotation is critical in nucleating shallow grains that may become whiskers. By analyzing the orientation changes between rotated regions and their parent grains and the geometric relationship of slip traces on the surface, $(21\bar{1})$ was identified as the most possible activated slip plane in the monitored regions at the early stage of thermal cycling. The presence of slip traces and the nucleation of shallow grains indicated the importance of local yielding in whisker nucleation. Though critical, grain rotation

must not be the sole mechanism contributing to the observed accretion that led to grain nucleation because the crystallographic rotation angles were significantly different than the microstructural rotation angles. Diffusion, especially short-range diffusion, and GB sliding can both provide the necessary mass for the localized accretion near GBs in addition to grain rotation. The types and extent of deformation that occurred along GBs examined in this study depended on the orientations of parent grains likely due to the anisotropic properties and complex slip behavior of β -Sn.

4.6 References

- [1] P. Zhang, Y. Zhang, Z. Sun, Spontaneous growth of metal whiskers on surfaces of solids: A review, *Journal of Materials Science & Technology*. 31 (2015) 675–698. <https://doi.org/10.1016/j.jmst.2015.04.001>.
- [2] P. Sarobol, J.E. Blendell, C.A. Handwerker, Whisker and hillock growth via coupled localized coble creep, grain boundary sliding, and shear induced grain boundary migration, *Acta Materialia*. 61 (2013) 1991–2003. <https://doi.org/10.1016/j.actamat.2012.12.019>.
- [3] P. Sarobol, Y. Wang, W.H. Chen, A.E. Pedigo, J.P. Koppes, J.E. Blendell, C.A. Handwerker, A predictive model for whisker formation based on local microstructure and grain boundary properties, *JOM*. 65 (2013) 1350–1361. <https://doi.org/10.1007/s11837-013-0717-x>.
- [4] W.J. Boettinger, C.E. Johnson, L.A. Bendersky, K.-W. Moon, M.E. Williams, G.R. Stafford, Whisker and hillock formation on Sn, Sn–Cu and Sn–Pb electrodeposits, *Acta Materialia*. 53 (2005) 5033–5050.
- [5] T. Frolov, W.J. Boettinger, Y. Mishin, Atomistic simulation of hillock growth, *Acta Materialia*. 58 (2010) 5471–5480. <https://doi.org/10.1016/j.actamat.2010.06.023>.
- [6] E. Chason, N. Jadhav, F. Pei, E. Buchovecky, A. Bower, Growth of whiskers from Sn surfaces: Driving forces and growth mechanisms, *Progress in Surface Science*. 88 (2013) 103–131.
- [7] E. Chason, F. Pei, C.L. Briant, H. Kesari, A.F. Bower, Significance of nucleation kinetics in Sn whisker formation, *Journal of Electronic Materials*. 43 (2014) 4435–4441. <https://doi.org/10.1007/s11664-014-3379-8>.
- [8] P.T. Vianco, J.A. Rejent, Dynamic recrystallization (DRX) as the mechanism for Sn whisker development. Part II: Experimental study, *Journal of Electronic Materials*. 38 (2009) 1826–1837.
- [9] P.T. Vianco, M.K. Neilsen, J.A. Rejent, R.P. Grant, Validation of the dynamic recrystallization (DRX) mechanism for whisker and hillock growth on Sn thin films, *Journal of Electronic Materials*. 44 (2015) 4012–4034.

- [10] J. Smetana, Theory of tin whisker growth: The end game, *IEEE Transactions on Electronics Packaging Manufacturing*. 30 (2007) 11–22. <https://doi.org/10.1109/tepm.2006.890645>.
- [11] J.W. Osenbach, Creep and its effect on Sn whisker growth, *Journal of Applied Physics*. 106 (2009) 094903.
- [12] A. Zamiri, T.R. Bieler, F. Pourboghra, Anisotropic crystal plasticity finite element modeling of the effect of crystal orientation and solder joint geometry on deformation after temperature change, *Journal of Electronic Materials* 38 (2) (2009) 231–240.
- [13] P. Darbandi, T.R. Bieler, F. Pourboghra, T.-k. Lee, Crystal plasticity finite-element analysis of deformation behavior in multiple-grained lead-free solder joints, *Journal of Electronic Materials* 42 (2) (2013) 201–214.
- [14] P. Darbandi, T.-k. Lee, T.R. Bieler, F. Pourboghra, Crystal plasticity finite element study of deformation behavior in commonly observed microstructures in lead free solder joints, *Computational Materials Science* 85 (C) (2014) 236–243.
- [15] Y. Kinoshita, H. Matsushim, N. Ohno, Predicting active slip systems in β -Sn from ideal shear resistance, *Modelling and Simulation in Materials Science and Engineering*. 20 (2012) 035003. <https://doi.org/10.1088/0965-0393/20/3/035003>
- [16] W.-H. Chen, P. Sarobol, C.A. Handwerker, J.E. Blendell, Heterogeneous stress relaxation processes at grain boundaries in high-Sn solder films: Effects of Sn anisotropy and grain geometry during thermal cycling, *JOM*. 68 (2016) 2888–2899. <https://doi.org/10.1007/s11837-016-2070-3>.
- [17] P. Sarobol, J.P. Koppes, W.H. Chen, P. Su, J.E. Blendell, C.A. Handwerker, Recrystallization as a nucleation mechanism for whiskers and hillocks on thermally cycled Sn-alloy solder films, *Materials Letter*. 99 (2013) 76–80.
- [18] W.-H. Chen, C. Wang, P. Sarobol, J. Blendell, C. Handwerker, Local variations in grain formation, grain boundary sliding, and whisker growth along grain boundaries in large-grain Sn films, *Scripta Materialia*. 187 (2020) 458–463. <https://doi.org/10.1016/j.scriptamat.2020.06.033>.
- [19] X. Cai, C.A. Handwerker, J.E. Blendell, M. Koslowski, Shallow grain formation in Sn thin films, *Acta Materialia*. 192 (2020) 1–10. <https://doi.org/10.1016/j.actamat.2020.03.014>.
- [20] Y. Wang, J.E. Blendell, C.A. Handwerker, Evolution of tin whiskers and subsiding grains in thermal cycling, *Journal of Materials Science*. 49 (2013) 1099–1113. <https://doi.org/10.1007/s10853-013-7788-5>.
- [21] D. Swenson, The effects of suppressed beta tin nucleation on the microstructural evolution of lead-free solder joints, *Journal of Materials Science: Materials in Electronics*. 18 (2006) 39–54. <https://doi.org/10.1007/s10854-006-9012-8>.

- [22] J. Taylor, J. Cahn, Shape accommodation of a rotating embedded crystal via a new variational formulation, *Interfaces and Free Boundaries*. 9 (2007) 493–512.
- [23] J.W. Cahn, J.E. Taylor, A unified approach to motion of grain boundaries, relative tangential translation along grain boundaries, and grain rotation, *Acta Materialia*. 52 (2004) 4887–4898. <https://doi.org/10.1016/j.actamat.2004.02.048>.
- [24] J.W. Cahn, Y. Mishin, A. Suzuki, Coupling grain boundary motion to shear deformation, *Acta Materialia*. 54 (2006) 4953–4975.
- [25] Z.T. Trautt, Y. Mishin, Grain boundary migration and grain rotation studied by molecular dynamics, *Acta Materialia*. 60 (2012) 2407–2424. <https://doi.org/10.1016/j.actamat.2012.01.008>.
- [26] R.D. Doherty, J.A. Szpunar, Kinetics of sub-grain coalescence—a reconsideration of the theory, *Acta Metallurgica*. 32 (1984) 1789–1798. [https://doi.org/10.1016/0001-6160\(84\)90235-9](https://doi.org/10.1016/0001-6160(84)90235-9).
- [27] J.C.M. Li, Possibility of subgrain rotation during recrystallization, *Journal of Applied Physics*. 33 (1962) 2958–2965. <https://doi.org/10.1063/1.1728543>.
- [28] J. Han, S. Tan, F. Guo, Subgrain rotation behavior in Sn_{3.0}Ag_{0.5}Cu–Sn₃₇Pb solder joints during thermal shock, *Journal of Electronic Materials*. 47 (2018) 124–132.
- [29] S. Tan, J. Han, F. Guo, Subgrain rotation at twin grain boundaries of a lead-free solder joint during thermal shock, *Journal of Materials Science: Material Electronics*. 27 (2016) 9642–9649.
- [30] J. Han, F. Guo, J.P. Liu, Recrystallization induced by subgrain rotation in Pb-free BGA solder joints under thermomechanical stress, *Journal of Alloys and Compounds*. 698 (2017) 706–713.
- [31] G.T. Galyon, L. Palmer, An integrated theory of whisker formation: The physical metallurgy of whisker formation and the role of internal stresses, *IEEE Transactions on Electronics Packaging Manufacturing*. 28 (2005) 17–30. <https://doi.org/10.1109/tepm.2005.847443>.
- [32] A. Chakraborty, P. Eisenlohr, A full-field crystal plasticity study on how texture and grain structure influences hydrostatic stress in thermally strained β -Sn films, *Journal of Applied Physics*. 124 (2018) 025302.
- [33] K.N. Tu, J.C.M. Li, Spontaneous whisker growth on lead-free solder finishes, *Materials Science and Engineering: A*. 409 (2005) 131–139. <https://doi.org/10.1016/j.msea.2005.06.074>.
- [34] K. Tu, Irreversible processes of spontaneous whisker growth in bimetallic Cu–Sn thin-film reactions, *Physical Review B*. 49 (1994) 2030.

- [35] P. Jagtap, A. Chakraborty, P. Eisenlohr, P. Kumar, Identification of whisker grain in Sn coatings by analyzing crystallographic micro-texture using electron back-scatter diffraction, *Acta Materialia*. 134 (2017) 346–359. <https://doi.org/10.1016/j.actamat.2017.05.063>.
- [36] E. Chason, N. Jadhav, W.L. Chan, L. Reinbold, K.S. Kumar, Whisker formation in Sn and Pb–Sn coatings: Role of intermetallic growth, stress evolution, and plastic deformation processes, *Applied Physics Letter*. 92 (2008) 171901.
- [37] M. Winning, G. Gottstein, L.S. Shvindlerman, On the mechanisms of grain boundary migration, *Acta Materialia*. 59 (2002) 353–363.
- [38] M. Winning, In-situ observations of coupled grain boundary motion, *Philosophical Magazine*. 87 (2007) 5017–5031. <https://doi.org/10.1080/14786430701601759>.
- [39] R.W. Balluffi, S.M. Allen, W.C. Carter, Motion of crystalline interfaces, in: *Kinetics of Materials*, John Wiley & Sons, Ltd, 2005: pp. 303–334. <https://doi.org/10.1002/0471749311.ch13>.
- [40] B.B. Rath, M. Winning, J.C.M. Li, Coupling between grain growth and grain rotation, *Applied Physics Letters*. 90 (2007) 161915. <https://doi.org/10.1063/1.2723195>.

5. NUCLEATION DUE TO LOCALIZED ROTATION AND YIELDING AND THE CONDITIONS FOR WHISKER GROWTH IN SN FILMS

5.1 Introduction

Sn coatings are widely employed on the Cu leads of electronic components in electronics to provide better solderability and prevent oxidation. However, Sn whiskers form spontaneously in coatings and may grow sufficiently long to bridge adjacent leads, increasing the risks of short circuits [1-4]. One reason for the formation of long whiskers lies in the fact that only 1 out of 10,000 grains grow as whiskers [5]. In other words, the stress-gradient driven diffusion will move a relaxed mass (atoms) from the entire film to a small amount of whisker sites, resulting in the growth of long whiskers. A key to mitigating the risks of whiskers rooted in the understanding of the selection rule of where whiskers nucleated and how in Sn films. Because whiskers are known to grow out from shallow surface grains [6, 7], the question becomes where the shallow grains nucleated in columnar-structured Sn films.

Many studies demonstrated that shallow grains likely nucleate in regions with locally high elastic strain energy density (ESED) [8-10], high geometrically necessary dislocation density (GNDs) [9], and high mismatch of out-of-plane coefficient of thermal expansion (CTE) [11], i.e., the process is sensitive to local stress states. Yet, Sn's anisotropic elasticity and thermal expansion make the local stress states highly dependent on the film texture and microstructure [12-13]. In polycrystalline Sn films, it is difficult to analyze local stress states in certain grains because of the influences of their surrounding grains. In order to obtain a simpler stress state in the grain of interest, an effort is to utilize β -Sn film with larger in-plane grain size (mm) relative to the film thickness (10-30 μm), allowing the tracing of each grain boundary (GB)'s relaxation responses including local crystallographic and microstructural changes. With such films, Chen et al. [11] reported different morphological and crystallographic changes along the entire length of different GBs, which can be distinguished by the number of local GB sliding and whisker formation. The observed microstructure variation gave examples of crystallography's profound effect on the local stress states and associated relaxation responses even in a non-polycrystalline structure. In particular, the formation of whiskers was linked with a high out-of-place mismatch of thermal expansion based on the assumption that all GBs were vertical because cross-sections of whiskers revealed the GB underneath the grain was vertical, as seen by previous studies [6-7, 14-16].

However, a follow-up study illustrated that GBs in large-grained Sn films could be curved prior to the nucleation of shallow grains [9]. Additionally, even in electrodeposited films where most grains are columnar, the geometry of the GBs would curve to maintain the continuity of the interfaces under external stresses, such as mechanical bending or thermomechanical stresses. Therefore, a gap existed in decoding the relationship between normal CTE mismatch and the possibility of nucleating whiskers taking into consideration of the GB geometry.

The challenge in understanding Sn whiskers is posed by not only the complexity of the stress localization, as introduced in the last paragraph, but also the entangled relaxation responses. The nucleation of Sn whiskers itself is a phenomenon resulting from a combination of deformation mechanisms, including creep [6, 17], local yielding [9], GB sliding [6, 11], and grain rotation [9, 18], as theorized by both experiments and simulations. Although several studies have established a model for nucleation of shallow grains entailing these mechanisms, the lack of orientation analysis at different cycles posed a challenge in categorizing each mechanism's contributions to the nucleation process, i.e., which mechanism led to what local changes. For example, whether the shallow grains nucleated first and later led to local morphological changes or vice versa remained to be an open question.

In this study, we approach the nucleation of whiskers through investigating (1) the factors that influence the stress localization (i.e., GB disorientation and GB geometry) and (2) the stress relaxation mechanisms that contribute to the formation of new shallow grains (i.e., GB sliding, local yielding, creep, and grain rotation) in large-grained pure Sn films. By comparing the microstructural and orientational changes at 0, 65, 120, 250, and 350 cycles, we found that grain rotation that led to the formation of shallow grains occurred later than creep, sliding, and yielding because the changes of misorientation measured from EBSD were identified only after the grains were locally deformed at the GBs. The subsurface microstructure of those locally deformed regions characterized by FIB immediately after the nucleation of shallow grains illustrated suggested that GBs could curve as a response to the local stress states. By considering this GB geometry (i.e., the inclination angle of the GB) in addition to the misorientation, we were able to accurately analyze the mismatch of CTE in-plane and out-of-plane between pairs of grains. By aligning this experimental analysis and plasticity simulations with the large-grained condition, we argue that the nucleation of shallow grains through localized grain rotation near the film surface is

a response to the locally high normal displacement due to the high mismatch of out-of-plane CTE between adjacent grains.

5.2 Experiments

5.2.1 Sample preparation

Polycrystalline Sn films were first electrodeposited on Cu substrates. Scratches on Cu substrates (99.99%, 0.0025-inch thickness, ultra-high conductivity, McMaster-Carr) were removed by electropolishing (current density 50 mA/cm²) in the pre-mixed solution with 700 ml phosphoric acid and 180 ml n-butanol for 20 minutes, as reported in [19]. A Sn film was then electrodeposited (current density 0.0133A/cm², voltage 30V) on a scratch-free Cu substrate in Sn electroplating electrolyte (SOLDERON, Dow Chemical) for 4 minutes. The average grain size of the polycrystalline Sn film was about 5 μm, and the average thickness was about 20 μm.

Large-grained Sn films were solidified from the electrodeposited Sn films. The deposited film was coated with a 5mm thick layer of flux (Kester TSF-6522) and placed on a hot plate (~510 K), slightly higher than the melting point of Sn (505K). The film was removed from the hot plate immediately after the deposited film melted and expanded outwards and placed on an Al block to cool down to room temperature. Since β-Sn crystal nuclei are difficult to nucleate during solidification, most of the crystal grains after solidification are grains with millimeter-long in-plane GBs. A detailed procedure was reported in Chapter 4.

5.2.2 Rapid thermal cycling

The samples moved back and forth between a hot chamber (set to 65°C) and a cold chamber (set to -25°C) every 10 minutes. The induced thermal strain in the films reached a maximum value during the short transition time between the two chambers, and gradually decreased during the holding time in each chamber. This cycling procedure differed from commercial thermal cycling, where the temperature increased or decreased at a constant rate, and therefore was referred to as “rapid” thermal cycling, similar to [9, 19-20].

5.2.3 Time-dependent characterization

Individual GBs were characterized with scanning electron microscopy (SEM, Quanta 650) and electron backscatter diffraction (EBSD, Quanta 650) at 0, 7, 35, 65, 120, 180, 250, and 350 cycles to quantify the evolution of local microstructure and orientation. SEM and EBSD performed before cycling (i.e., at 0 cycle) located the original GB geometry and positions. Only results demonstrated noticeable changes in either microstructure or orientation were shown in this paper, i.e., after 65, 120, 250, and 350 cycles. Cross-sections of regions exhibiting obvious morphological or crystallographic evolution were prepared by focused ion beam (FIB, Quanta 3D FEG). Thus, the subsurface GB geometry of selected areas was obtained.

5.2.4 CTE analysis along the GB

To investigate the effect of anisotropic thermal expansion on the local stress relaxation, CTE mismatches along the in-plane GB direction were calculated by rotating the CTE tensors from the sample frame to the crystal frames of the adjacent grains. The geometry used in the calculation was shown in Fig. 5.1. Since Sn is a body-centered tetragonal structure ($a/c = 1.833$), the GB direction needs to be transferred from the Cartesian coordinate to the crystal coordinates. The Z-axis is set to parallel to [001] direction, and the X-axis is set to parallel to [100] direction.

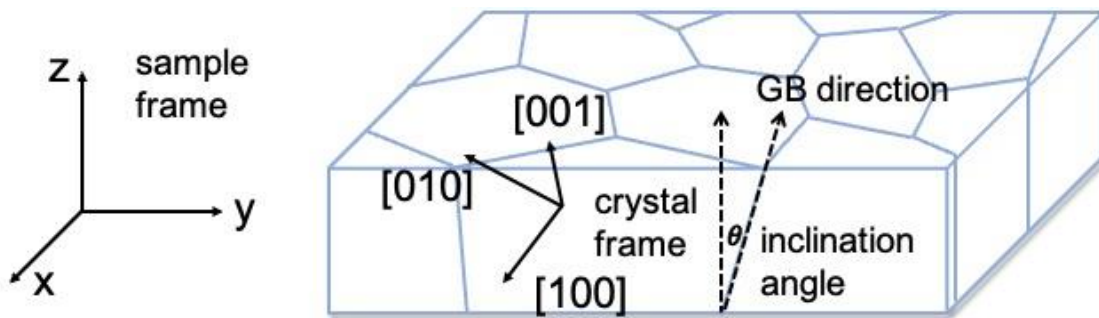


Figure 5.1. The geometry of the sample reference and crystal reference. θ is the inclination angle between the GB direction and normal direction.

The conversion of vectors (of the GB direction) from crystal coordinates (\vec{x}) to Cartesian coordinates (\vec{X}) can be defined by the conversion matrix A, as given in the following equation [21]:

$$\begin{bmatrix} X \\ Y \\ Z \end{bmatrix} = \begin{bmatrix} A_{11} & A_{12} & 0 \\ 0 & A_{22} & 0 \\ A_{31} & A_{32} & A_{33} \end{bmatrix} \cdot \begin{bmatrix} x \\ y \\ z \end{bmatrix} \quad (\text{Equ 5.1})$$

Therefore, the vectors in crystal coordinates can be converted from the Cartesian coordinates via the equation below:

$$x = M^{-1}X \quad (\text{Equ 5.2})$$

The components of the matrix A are listed below:

$$A_{11} = a \cdot \sin\beta$$

$$A_{12} = b \cdot \frac{\cos\gamma - \cos\beta \cdot \cos\alpha}{\sin\beta}$$

$$A_{22} = b \cdot \left(\sin^2\alpha - \frac{A_{12}^2}{b^2} \right)^{\frac{1}{2}}$$

$$A_{31} = a \cdot \cos\beta$$

$$A_{32} = b \cdot \cos\alpha$$

$$A_{33} = c$$

where a, b, c are the unit cell dimensions and α, β, γ are the angles in radians of the cell parameters. For β -Sn, $\alpha = \beta = \gamma = 90^\circ$, $a = b = 5.8314 \text{ \AA}$, $c = 3.1817 \text{ \AA}$.

With the Euler angles (ψ_1, Φ, ψ_2) and the rotation matrix detailed in Chapter 4.4, the vectors in sample frame can be converted to the crystal frame via the following equation:

$$g(\psi_1, \Phi, \psi_2) = g_3(\psi_2)g_2(\Phi)g_1(\psi_1) \quad (\text{Equ 5.3})$$

The CTE α_{hkl} along any radius vector of a unit sphere (where θ is the angle between the vector and the Z direction in unit cell) can then be calculated by the following equation [22]:

$$\alpha_{hkl} = \alpha_{11}\sin^2\theta + \alpha_{33}\cos^2\theta \quad (\text{Equ 5.4})$$

For β -Sn, the CTE tensor is shown below:

$$\alpha_{Sn} = \begin{bmatrix} \alpha_{11} & 0 & 0 \\ 0 & \alpha_{22} & 0 \\ 0 & 0 & \alpha_{33} \end{bmatrix}. \quad (\text{Equ 5.5})$$

Where $\alpha_{11} = \alpha_{22} = 16 \times 10^{-6} K^{-1}$, $\alpha_{33} = 32 \times 10^{-6} K^{-1}$ [12, 13]

5.3 Results and Discussion

5.3.1 Evolution of local microstructure

Microstructural changes were highly localized at GBs, and distinct types of deformation occurred at the same GB. Fig. 5.2. shows the evolution of the surface microstructure of one triple junction. The triple-junction structure was evidenced by the orientation map shown in Fig. 5.2(b). The red and blue lines on the orientation map represent a high-angle and a low-angle GB. Obvious local yielding at the high-angle GB between grain 1 and grain 2 was observed at 120 cycles, early in the cycling process, as shown in Fig. 5.2(d). Near those yielded areas, GB sliding, cracks, GB migration, and a nucleated whisker were then observed at 250 and 350 cycles, as detailed in Fig. 5.2(e-g). In contrast, little to no microstructural changes were captured at the low-angle GB.

Similar observations can be obtained in other monitored regions with slightly distinct relaxation responses. For example, Fig. 5.3 shows the morphological changes along another high-angle GB with the increased number of thermal cycles. The trace of a new GB emerged on the surface within the grain 4 at 120 cycles, suggesting a new grain may already nucleated, as seen in Fig. 5.3(b). During later cycles, GB sliding, subsidence, and local yielding were observed at high-angle and low-angle GBs, as detailed in Fig. 5.3(b-d). The GB segment between grains 1 and 3 slid first at 120 cycles, and then the segment between grains 3 and 4 slid at 250 cycles. At 350 cycles, a subsided region in the vicinity of the GB between grains 2 and 3 was observed.

In both cases, GB sliding was observed as the precursor of other plastic deformation such as local yielding and GB migration, agreeing with the results reported in Chapter 4. The three boundaries of the same grain (Grain 3) slid sequentially suggested that GB sliding was dependent on the misorientation across the different GBs, as previously pointed out in [9], which most likely resulting from the mismatch of the thermomechanical stresses along the GB direction due to the

anisotropic properties of the β -Sn. In contrast, the GB sliding during whisker growth is limited by GB diffusion [6].

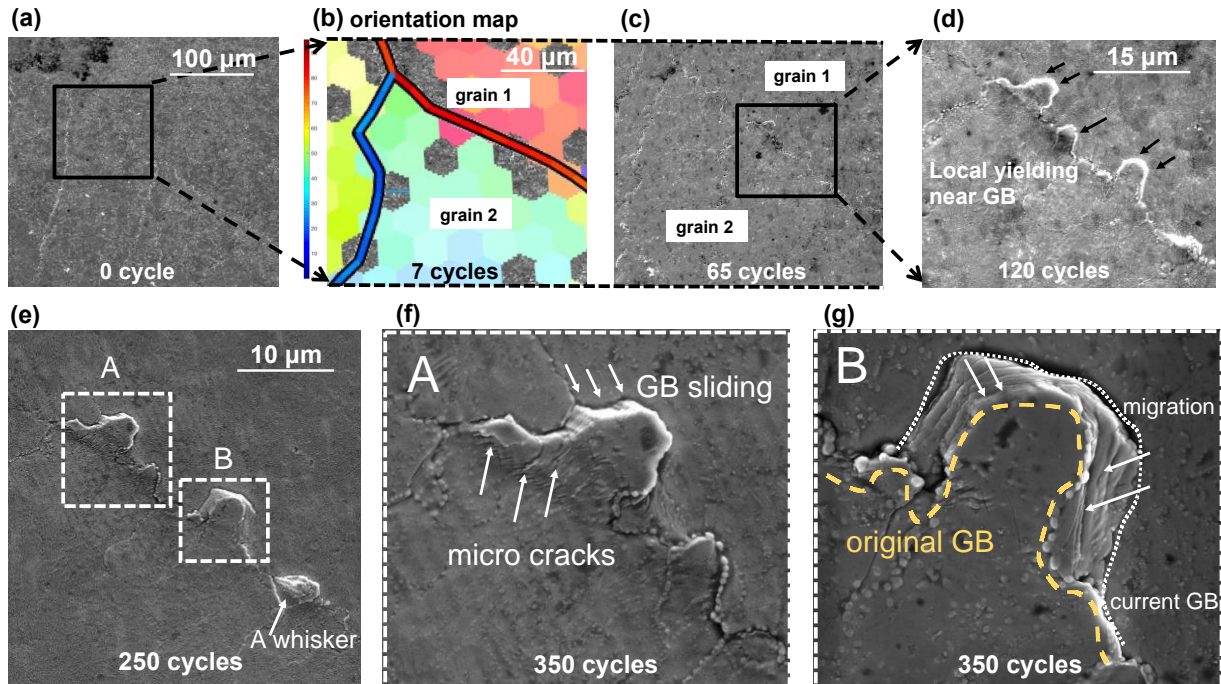


Figure 5.2. (a) Low-magnification SEM image of a selected region before cycling. (b) Orientation map of the area marked by the black square in (a) after 7 cycles. (c-e) SEM images of the monitored area at 65, 120, and 250 cycles. (f) and (g) are high-magnification images of area A and area B shown in (e) at 350 cycles.

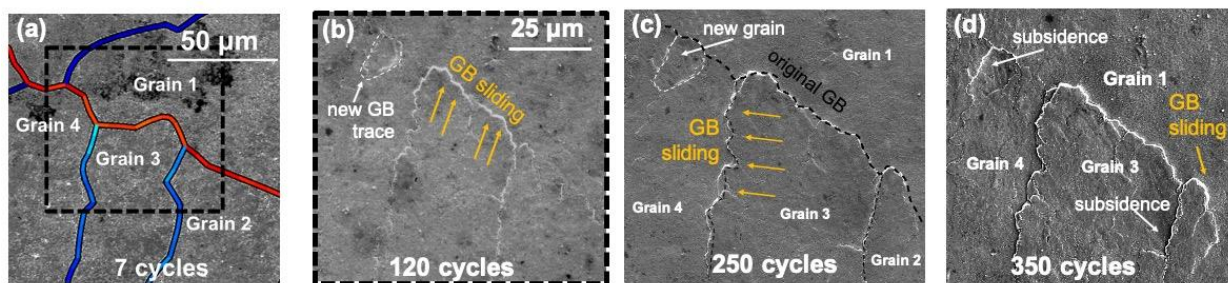


Figure 5.3. (a-d) SEM image of another monitored region after 7, 120, 250, and 350 cycles. New GB traces were observed between Grain 1 and Grain 4 in (b) at 120 cycles where a sinking grain later developed in (c-d). The three different GBs of the Grain 3 slid in sequence between 120 cycles and 350 cycles.

5.3.2 Evolution of local orientation

The changes of local crystallography of the deformed regions near the GBs were subtle and concentrated on the late stage of thermal cycling. Fig. 5.4 illustrates the evolution of the orientation by calculating the misorientation angles between four selected pairs of positions in regions analyzed in Fig. 5.2 and 5.3 at 0, 7, 120, 250, and 350 cycles. Misorientation angles larger than 2 degrees were only observed after 250 cycles, except for the pair of points 7 and 8, as indicated in Fig. 5.4 (c-d). Because multiple equivalent misorientation angle-axis pairs exist for a certain rotation operation and only one angle was selected in Fig. 5.4, pole figures of the four pairs of points are shown in Fig. 5.5 and Fig. 5.6 to clarify their rotation behavior. The blue points represent points 1, 3, 5, and 7, those away from the original GBs; the red points represent points 2, 4, 6, and 8, those closer to the GBs. Rotation, i.e., local orientational changes, were negligible at 120 cycles, as evidenced by the pole figures. In contrast, microstructural changes such as new GB traces or obvious local yielding were evident at 65 or 120 cycles, as previously shown in Fig. 5.2 and Fig. 5.3.

This localized rotation was seldom examined in Sn whiskers except for this work (as detailed in Chapter 3 and Chapter 4). However, studies of other materials such as Al [23] and iron [24] have reported that lattice rotation in the vicinity of the GBs. The extend of the rotation decreased with increased distance away from the deformed regions, i.e., GBs. The two studies proposed that the lattice rotation accommodated the plastic deformation. In our analysis, the fact that most orientational changes occurred after 120 cycles when the deformation was already obvious indicated that the lattice rotation was a response to the local yielding. This finding can explain why the angles measured from morphological rotation were different from the angles measured from crystallographic rotation, as discussed in Chapter 4. In other words, the microstructural changes and crystallographic changes prior to whisker formation are not simultaneously because sufficient “surface accretion” or sliding is the prerequisite of grain rotation near the GBs.

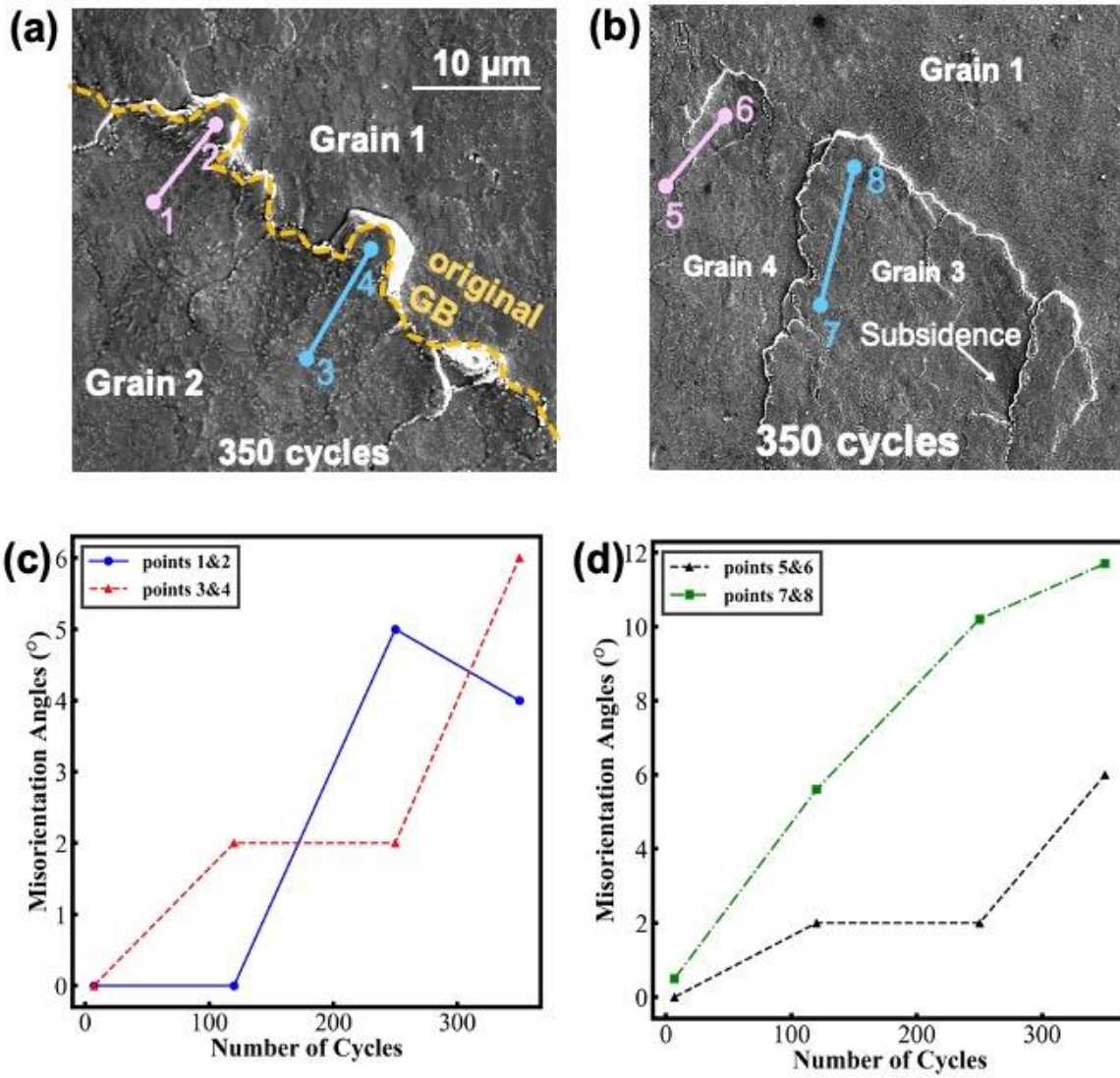
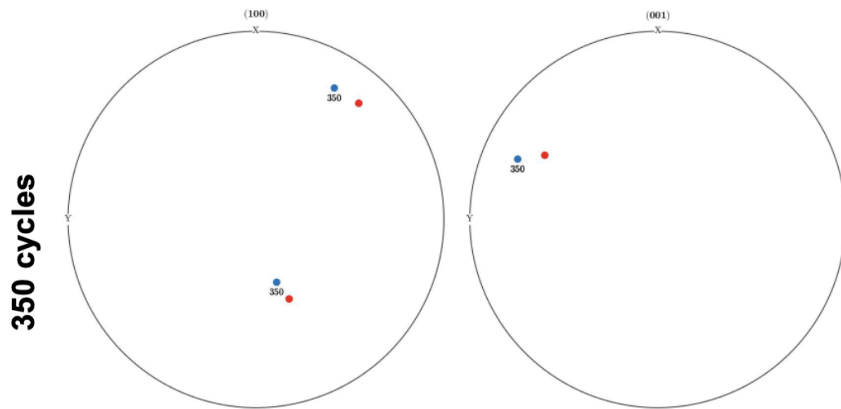
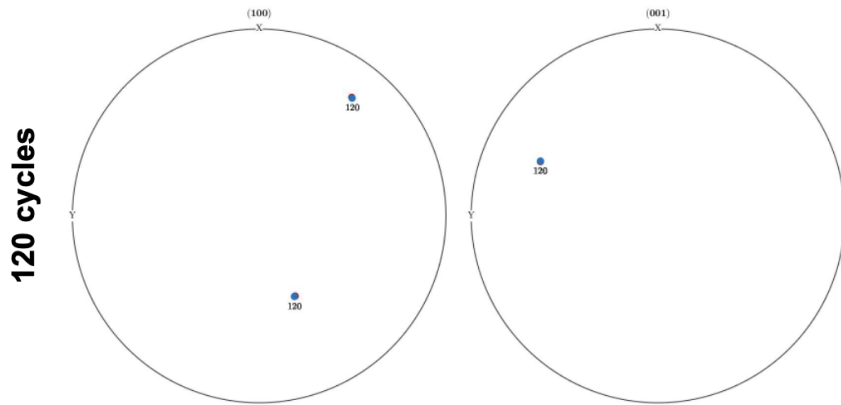


Figure 5.4. (a-b) SEM top-view of the region is shown in Fig. 2 and 3. (c-d) Misorientation angles between each pair of points in (a-b) with the increased number of thermal cycles.

(a) Points 1&2



(b) Points 3&4

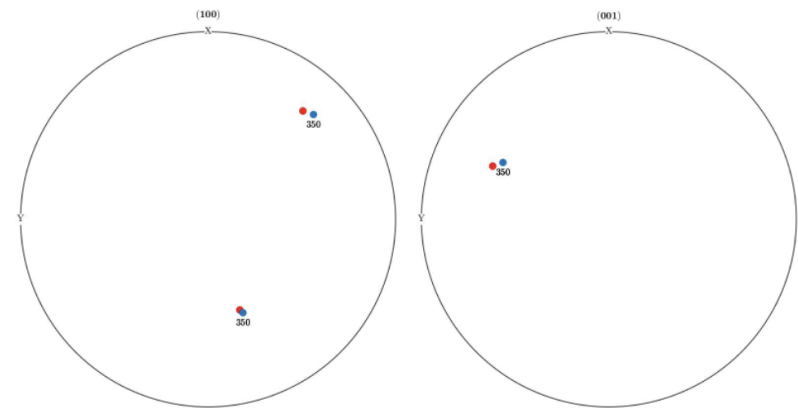
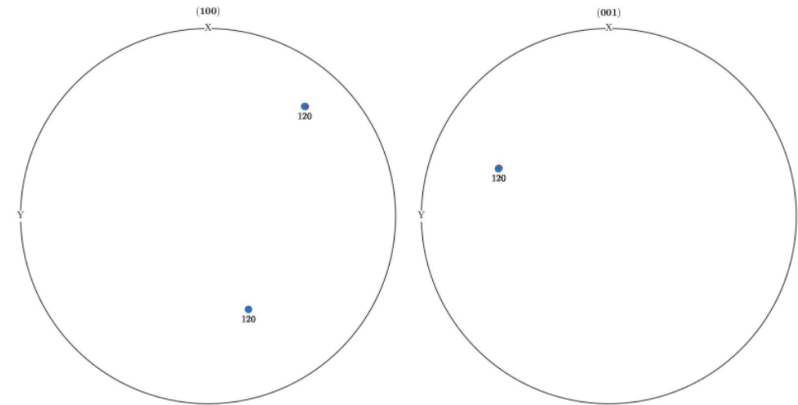
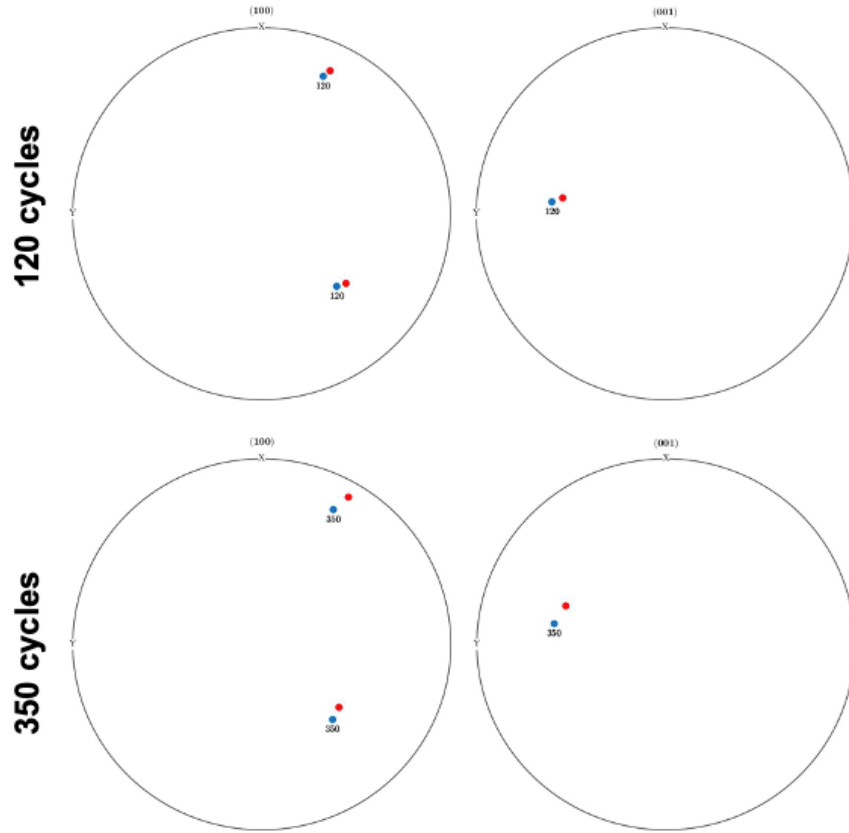


Figure 5.5. Pole figures of the pairs of points (1 and 2, 3 and 4) in Figure 7(a) at 120 and 350 cycles.

(a) Points 5&6



(b) Points 7&8

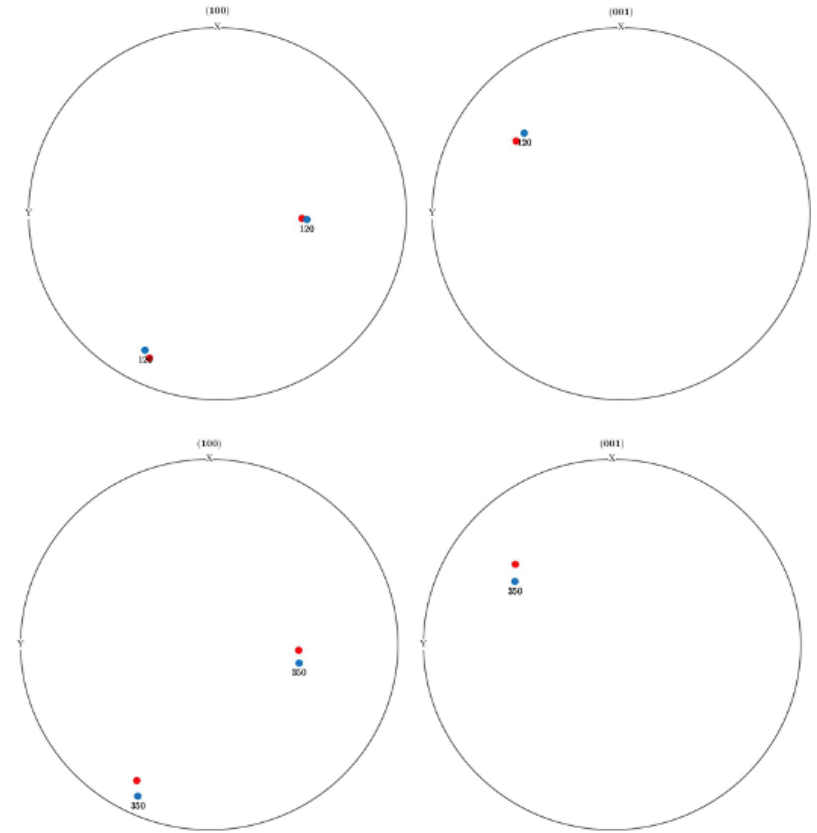


Figure 5.6. Pole figures of the pairs of points (5 and 6, 7 and 8) in Figure 8(a) at 120 and 350 cycle.

5.3.3 Grain geometry in rotated regions

Distinct grain geometries formed after thermal cycling, responding to local stress states. Cross-sections in the regions of interest were shown in Fig. 5.7 to relate post-cycling subsurface GB geometries to the local orientation and microstructure. Three types of grain geometries can be categorized, e.g., (1) inclined GB, (2) the formation of surface grains, and (3) the formation of sinking grains. The latter two were associated with the formation of new GBs near the original GBs, as indicated in Fig. 5.7(c), (e), and(f). The formed surface grains included a shallow surface grain and a deep surface grain.

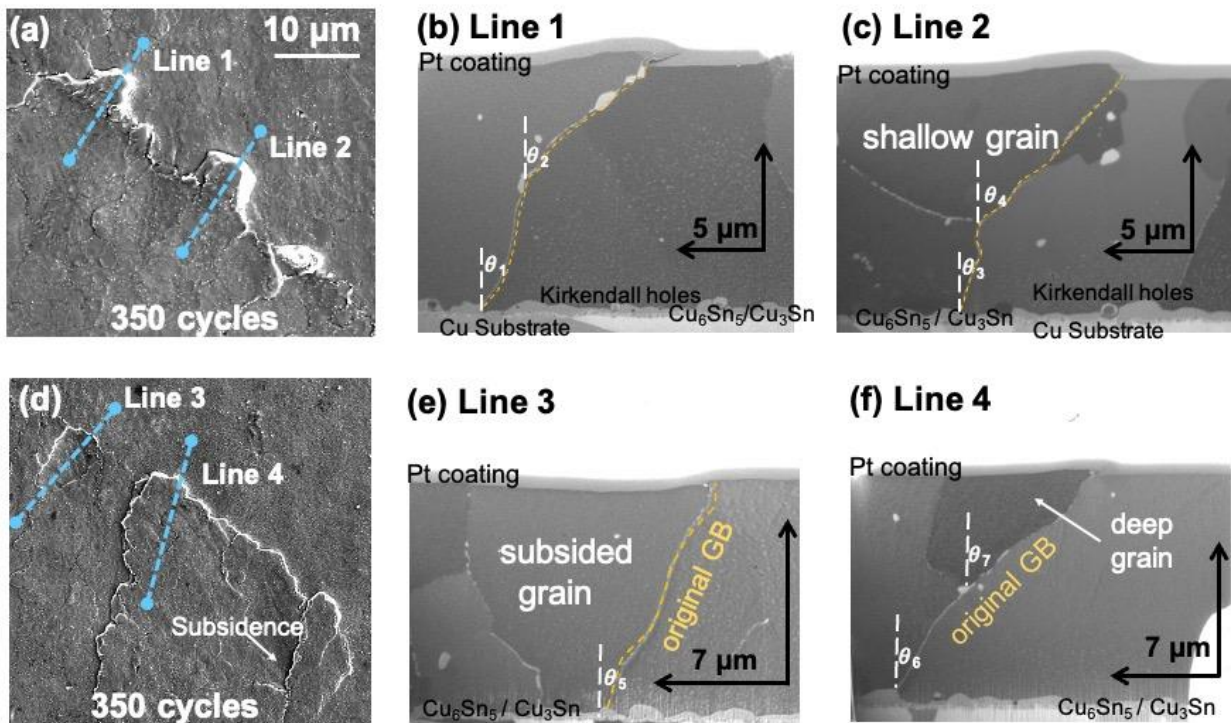


Figure 5.7. (a) SEM image of one monitored region at 350 cycles. (b) and (c) show the cross-sections at the positions marked by Line 1 and Line 2 in (a). (d) SEM top-view of another monitored region at 350 cycles. (e) and (f) show the cross-sections at the positions marked by Line 3 and Line 4 in (d).

The original GBs often curved, and the angles between the vertical direction and the GB direction of each segment were annotated in Fig. 5.7(c-d) and (e-f). The measured CTE mismatches are shown in Tab. 5.1. The values of CTE mismatch were higher along the GB

segments near the free surface comparing to those near the substrate. Therefore, shear stresses due to the CTE mismatch were higher near the surface of the film than that of the substrate.

Table 5.1. The mismatch of CTE along different GB segments shown in Fig. 5.7

	θ_1	θ_2	θ_3	θ_4	θ_5	θ_6	θ_7
Angles ($^\circ$)	14	35	12	33	18	21	35
CTE mismatch (10^{-6}K^{-1})	6	9.3	5	8.8	5.6	4.8	6.5

The relationship between the CTE mismatch and the nucleation of shallow grains has been investigated by Chen et al. [11], where the high out-of-plane CTE mismatch was associated with whisker formation and GB sliding. One limitation of the previous study lies in its assumption that all GBs in the films were vertical. The post-cycling cross-sections shown in Fig. 5.7. indicated that the assumption may not reflect the real GB conditions. Additionally, in similar large-grained Sn films, previous studies also reported the pre- and post-cycling cross sections and vertical GBs only accounted for a relatively small portion of the total GBs [9,11]. Considering the GB inclination, the formation of surface grains (either shallow or deep) seemed to associate with a large CTE mismatch along certain GB directions. High CTE mismatch along inclined GB direction may result in easier sliding or local yielding. Note that although no grain contrast has been observed along Line 1, as seen in Fig. 5.7, the EBSD results obtained in this region [Fig. 5.4(c) and Fig. 5.5(a)] indicated that a grain has formed. The lack of contrast may be an artifact resulting from the rotation in which the axis lies in-plane and parallel to the GB plane. Furthermore, the angles between GBs at the triple junction were close to 120° and the GBs near the substrate are more vertical than the GBs near the free surface. An extrapolation was that the formation of new surface grains pulled the original GB to a balancing position. However, whether the GBs were inclined before the thermal cycling remains to be another open question without the comparison of the local microstructure of the same location at the GB. For example, the possibility cannot be excluded that the GBs changed from vertical to oblique due to in-plane shear resulting from the in-plane CTE mismatch normal to the GB plane.

5.3.4 Crystal plasticity simulations

To analyze the localized rotation near the GB of the 2D bicrystal structure during thermal cycling, simulations employing crystal plasticity were performed with different orientations, as seen in Fig. 5.8. The plasticity model is detailed in the paper [18] as well as Chapter 4.4. The orientations assigned to the two grains are listed in Tab. 5.2. For each case, misorientation maps and pole figures before and after the deformation were plotted to visualize the rotation behavior. The simulated results agreed with experimental characterization in Fig. 5.5 and 5.6 where the misorientation angles across the GBs were small (usually less than 5°) but highly localized near the GBs.

Table 5.2. The Euler angles (Bunge) used the crystal plasticity simulation in Fig. 5.8.

	Case 1	Case 2	Case 3	Case 4
Left grain	$[40^\circ, 90^\circ, 10^\circ]$	$[57^\circ, 17^\circ, 64^\circ]$	$[10^\circ, 8^\circ, 12^\circ]$	$[50^\circ, 70^\circ, 100^\circ]$
Right grain	$[70^\circ, 20^\circ, 140^\circ]$	$[79^\circ, 97^\circ, 54^\circ]$	$[105^\circ, 78^\circ, 63^\circ]$	$[20^\circ, 45^\circ, 130^\circ]$

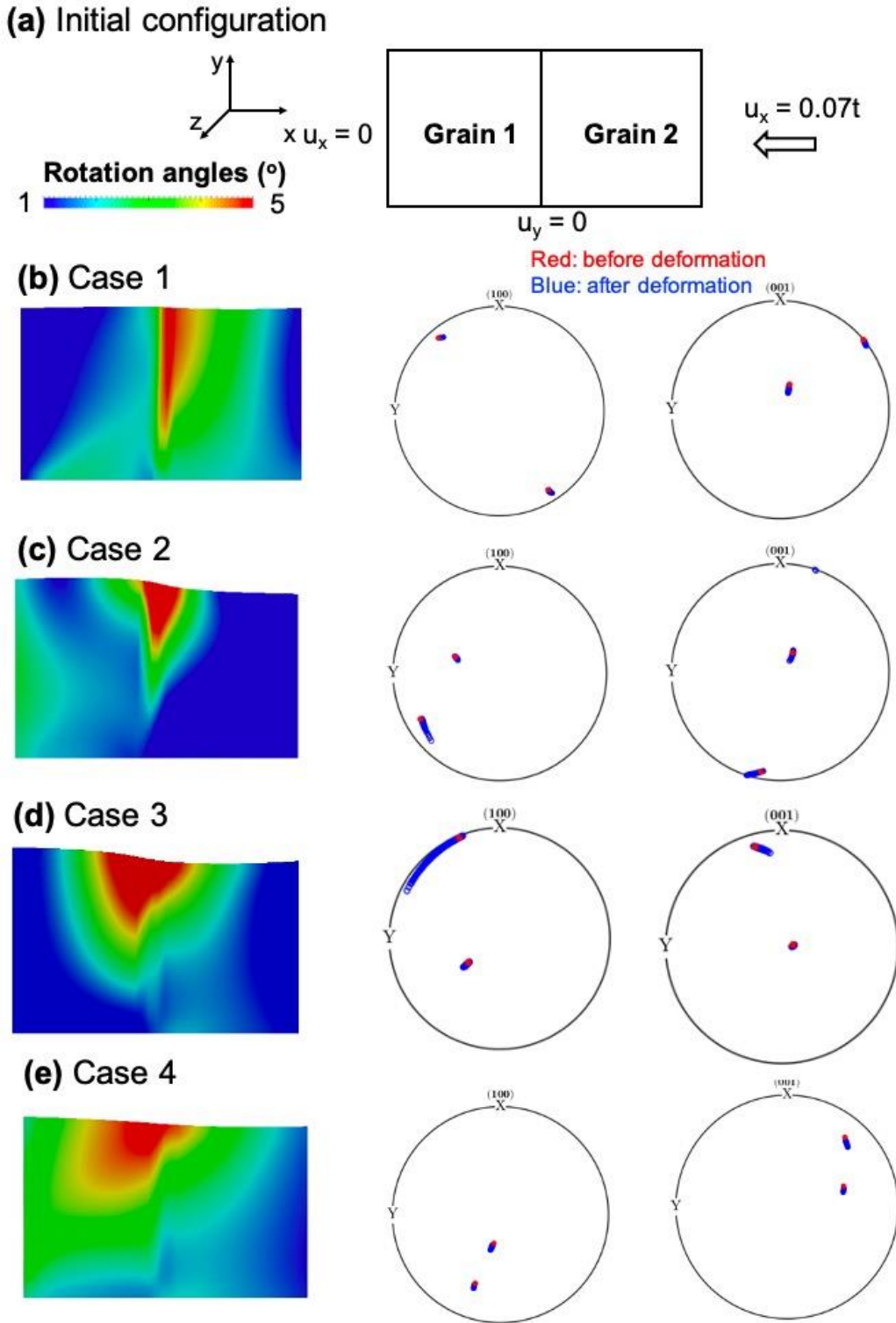


Figure 5.8. (a) The bicrystal geometry used by the crystal plasticity simulation. (b-e) Rotation maps and pole figures after deformation of four pairs of orientations listed in Tab. 5.2. Simulation credit: Xiaorong Cai. Reproduced with permission. Unpublished.

To further investigate the formation of the shallow surface grain and the relationships between the normal displacement, lattice rotation, and subgrain nucleation, the 3D structure of a simplified bicrystal structure was simulated using parameters measured from the experiments. The results are displayed in Fig. 5.9.

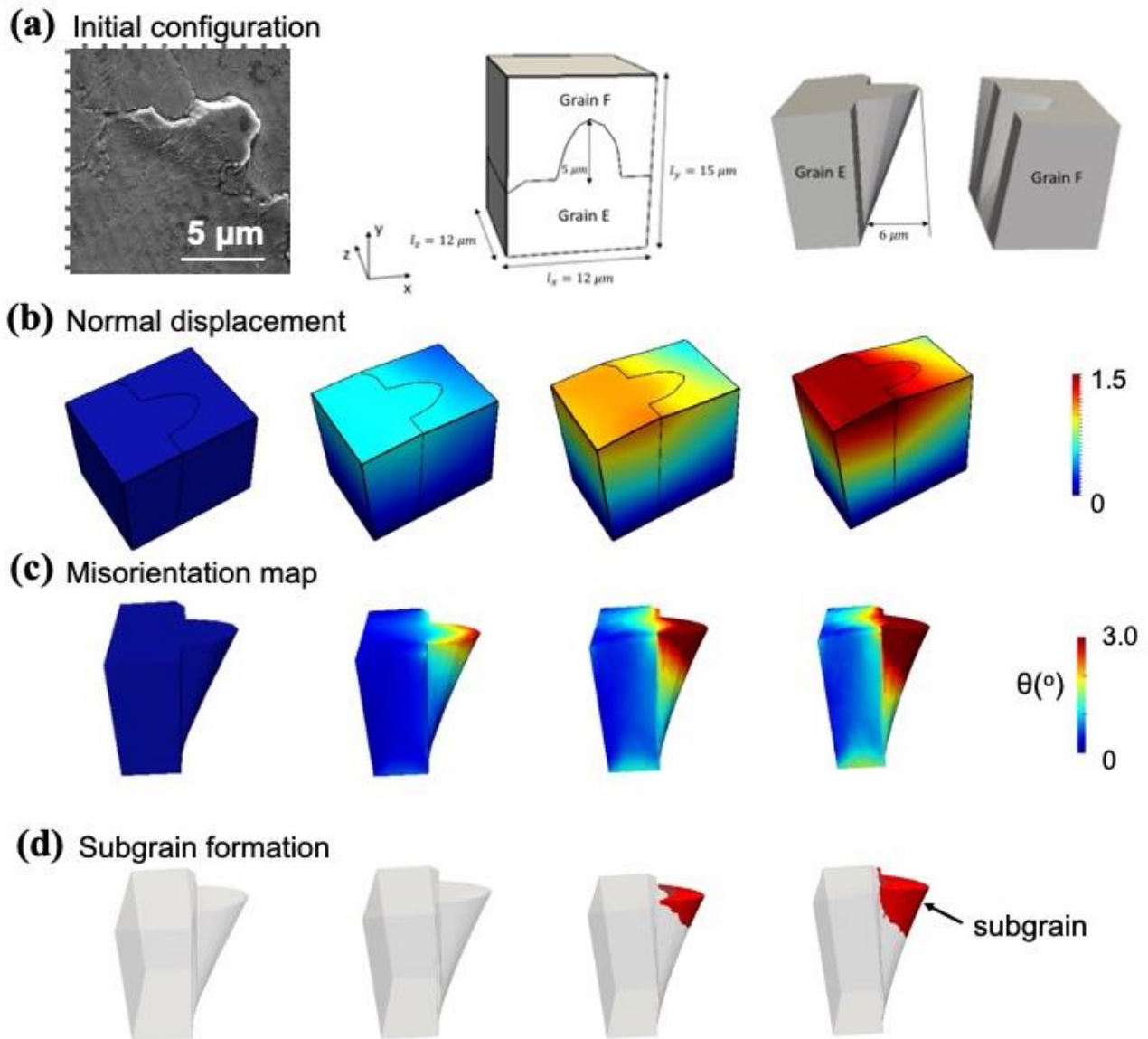


Figure 5.9. (a) The bicrystal geometry and orientation used by the 3D crystal plasticity simulation. (b) The evolution of normal displacement during deformation. (c) The misorientation map during deformation. (d) The nucleation of a subgrain near the free surface in the left grain. Simulation credit: Xiaorong Cai. Reproduced with permission. Unpublished.

A subgrain developed from the corner of the GB towards the center of the grain, in correspondence with the development of local misorientation. The recrystallization or the formation of subgrains due to rotation, though not commonly reported in whisker nucleation, were examined extensively in Sn-alloy solder joints [25-29]. In particular, the simulational results showed that lattice rotation occurred in regions with the highest normal displacement. Note that no GB sliding is allowed in this plasticity simulation because of the coherence at the GB. Yet, it is reasonable to extrapolate that, in reality, GB sliding must occur between Grain 1 and Grain 2 to accommodate the displacement (or local shape changes). If GB sliding is allowed, one can expect the local deformation due to combined effects of sliding and local yielding similar to the experimental characterization, as seen in Fig. 5.9(a).

We can now establish the correlation between local orientational changes and the subgrain formation based on both experimental and simulational results. The misorientation maps after deformation in Fig. 5.8 illustrated that the newly formed surface grains could be shallow or deep. Therefore, recrystallized grains cannot necessarily become whiskers. This finding can explain why whiskers only grow out from certain locations at one GB, even though a large extend of plastic deformation was observed along the entire GB, as shown in Fig. 5.2(e) and Fig. 5.4(a). A study also reported the formation of both deep surface grains and shallow surface grains in Sn films plastically deformed by indentation [30]. The shape of the subgrain is closely related to the shape of the dislocation walls formed during recrystallization [31]. Thus, future studies on slip behavior can reveal how specific dislocation motions lead to different shapes of the nucleated subgrains.

5.4 Conclusions

In summary, to answer the question of what the individual mechanism's are associated with nucleation of surface grains and their contributions, sequences, and interactions, incremental analysis of the evolution of local orientation and microstructure were measured, and multi-dimensional (2D and 3D) crystal plasticity simulations were employed performed. The following findings were summarized:

1. GB sliding and local yielding generally occurred earlier than grain rotation;
2. GB sliding and local yielding can result in normal displacement that required shape accommodations from grain rotation;
3. Grain rotation led to nucleation of shallow grains but not necessarily.

In addition, concerning why only some grains become whiskers, the grain microstructure of nucleated shallow grains was analyzed. We found that both shallow grains and deep grains can nucleate by subgrain formation. Nucleated grains need to meet the geometric requirement for whisker growth as known in the GB-sliding-limited whisker growth model. GB geometry prior to thermal cycles needs to be considered in future studies.

5.5 References

- [1] NASA. *Whisker Failures*. <https://nepp.nasa.gov/whisker/failures/index.htm>
- [2] Tu. (1994). Irreversible processes of spontaneous whisker growth in bimetallic Cu-Sn thin-film reactions. *Physical Review B: Condensed Matter*, 49(3), 2030-2034.
<https://doi.org/10.1103/physrevb.49.2030>
- [3] Lee, B.-Z., & Lee, D. N. (1998). Spontaneous growth mechanism of tin whiskers. *Acta Materialia*, 46(10), 3701-3714. [https://doi.org/10.1016/s1359-6454\(98\)00045-7](https://doi.org/10.1016/s1359-6454(98)00045-7)
- [4] Tu, K. N., & Li, J. C. M. (2005). Spontaneous whisker growth on lead-free solder finishes. *Materials Science and Engineering: A*, 409(1-2), 131-139.
<https://doi.org/10.1016/j.msea.2005.06.074>
- [5] Chen, W.-H. (2014). *Evaluation of local anisotropic elasticity and thermal expansion on whisker formation sites in beta-tin thin films*. Purdue University.
- [6] Sarobol, P., Blendell, J. E., & Handwerker, C. A. (2013). Whisker and hillock growth via coupled localized Coble creep, grain boundary sliding, and shear induced grain boundary migration. *Acta Materialia*, 61(6), 1991-2003. <https://doi.org/10.1016/j.actamat.2012.12.019>
- [7] Boettinger, W. J., Johnson, C. E., Bendersky, L. A., Moon, K.-W., Williams, M. E., & Stafford, G. R. (2005). Whisker and Hillock formation on Sn, Sn-Cu and Sn-Pb electrodeposits. *Acta Materialia*, 53(19), 5033-5050.
<https://doi.org/10.1016/j.actamat.2005.07.016>
- [8] Sarobol, P., Koppes, J. P., Chen, W. H., Su, P., Blendell, J. E., & Handwerker, C. A. (2013). Recrystallization as a nucleation mechanism for whiskers and hillocks on thermally cycled Sn-alloy solder films. *Materials Letters*, 99, 76-80.
<https://doi.org/10.1016/j.matlet.2013.02.066>
- [9] Chen, W.-H., Wang, C., Sarobol, P., Blendell, J., & Handwerker, C. (2020). Local variations in grain formation, grain boundary sliding, and whisker growth along grain boundaries in large-grain Sn films. *Scripta Materialia*, 187, 458-463.
<https://doi.org/10.1016/j.scriptamat.2020.06.033>

- [10] Hektor, J., Micha, J.-S., Hall, S. A., Iyengar, S., & Ristinmaa, M. (2019). Long term evolution of microstructure and stress around tin whiskers investigated using scanning Laue microdiffraction. *Acta Materialia*, 168, 210-221. <https://doi.org/10.1016/j.actamat.2019.02.021>
- [11] Chen, W.-H., Sarobol, P., Handwerker, C. A., & Blendell, J. E. (2016). Heterogeneous Stress Relaxation Processes at Grain Boundaries in High-Sn Solder Films: Effects of Sn Anisotropy and Grain Geometry During Thermal Cycling. *JOM*, 68(11), 2888-2899. <https://doi.org/10.1007/s11837-016-2070-3>
- [12] Bieler, T. R., Jiang, H., Lehman, L. P., Kirkpatrick, T., & Cotts, E. J. (2006). *Influence of Sn Grain Size and Orientation on the Thermomechanical Response and Reliability of Pb-free Solder Joints*. In. IEEE. <http://dx.doi.org/10.1109/ectc.2006.1645849>
- [13] Bieler, T. R., Hairong, J., Lehman, L. P., Kirkpatrick, T., Cotts, E. J., & Nandagopal, B. (2008). Influence of Sn Grain Size and Orientation on the Thermomechanical Response and Reliability of Pb-free Solder Joints. *IEEE Transactions on Components and Packaging Technologies*, 31(2), 370-381. <https://doi.org/10.1109/tcapt.2008.916835>
- [14] Jadhav, N., Buchovecky, E., Chason, E., & Bower, A. (2010). Real-time SEM/FIB studies of whisker growth and surface modification. *JOM*, 62(7), 30-37. <https://doi.org/10.1007/s11837-010-0105-8>
- [15] Sobiech, M. L. (2010). *Whisker formation on Sn thin films*. Universität Stuttgart.
- [16] Chason, E., Jadhav, N., Pei, F., Buchovecky, E., & Bower, A. (2013). Growth of whiskers from Sn surfaces: Driving forces and growth mechanisms. *Progress in Surface Science*, 88(2), 103-131. <https://doi.org/10.1016/j.progsurf.2013.02.002>
- [17] Pei, F., Buchovecky, E., Bower, A., & Chason, E. (2017). Stress evolution and whisker growth during thermal cycling of Sn films: A comparison of analytical modeling and experiments. *Acta Materialia*, 129, 462-473. <https://doi.org/10.1016/j.actamat.2017.03.005>
- [18] Cai, X., Handwerker, C. A., Blendell, J. E., & Koslowski, M. (2020). Shallow grain formation in Sn thin films. *Acta Materialia*, 192, 1-10. <https://doi.org/10.1016/j.actamat.2020.03.014>
- [19] Wang, Y. (2014). *Microstructure evolution and surface defect formation in tin films*. Purdue University.
- [20] Wang, Y., Blendell, J. E., & Handwerker, C. A. (2014). Evolution of tin whiskers and subsiding grains in thermal cycling. *Journal of Materials Science*, 49(3), 1099-1113. <https://doi.org/https://doi.org/10.1007/s10853-013-7788-5>
- [21] Xian, J. W., Zeng, G., Belyakov, S. A., Gu, Q., Nogita, K., & Gourlay, C. M. (2017). Anisotropic thermal expansion of Ni₃Sn₄, Ag₃Sn, Cu₃Sn, Cu₆Sn₅ and βSn. *Intermetallics*, 91, 50-64. <https://doi.org/10.1016/j.intermet.2017.08.002>

- [22] Newnham, R. E. (2005). *Properties of Materials*. Oxford University Press.
- [23] Zaefferer, S., Kuo, J.-C., Zhao, Z., Winning, M., & Raabe, D. (2003). On the influence of the grain boundary misorientation on the plastic deformation of aluminum bicrystals. *Acta Materialia*, 51(16), 4719-4735. [https://doi.org/10.1016/s1359-6454\(03\)00259-3](https://doi.org/10.1016/s1359-6454(03)00259-3)
- [24] Vetterick, G., Leff, A. C., Marshall, M., Baldwin, J. K., Misra, A., Hattar, K., & Taheri, M. L. (2018). Direct observation of a coincident dislocation- and grain boundary-mediated deformation in nanocrystalline iron. *Materials Science and Engineering: A*, 709, 339-348. <https://doi.org/10.1016/j.msea.2017.09.020>
- [25] Han, J., Guo, F., & Liu, J. P. (2017). Early stages of localized recrystallization in Pb-free BGA solder joints subjected to thermomechanical stress. *Journal of Alloys and Compounds*, 704, 574-584. <https://doi.org/10.1016/j.jallcom.2017.02.090>
- [26] Han, J., Guo, F., & Liu, J. P. (2017). Recrystallization induced by subgrain rotation in Pb-free BGA solder joints under thermomechanical stress. *Journal of Alloys and Compounds*, 698, 706-713. <https://doi.org/10.1016/j.jallcom.2016.12.281>
- [27] Han, J., Sun, J., Wen, T., & Guo, F. (2018). Analysis of continuous recrystallization (sub)grain rotation behavior in Pb-free solder bumps under a 0.1 $\mu\text{m/s}$ shear rate. *Journal of Materials Science: Materials in Electronics*, 29(13), 10992-10999. <https://doi.org/10.1007/s10854-018-9181-2>
- [28] Han, J., Tan, S., & Guo, F. (2018). Subgrain Rotation Behavior in Sn3.0Ag0.5Cu-Sn37Pb Solder Joints During Thermal Shock. *Journal of Electronic Materials*, 47(1), 124-132. <https://doi.org/10.1007/s11664-017-5864-3>
- [29] Tan, S., Han, J., & Guo, F. (2016). Subgrain rotation at twin grain boundaries of a lead-free solder joint during thermal shock. *Journal of Materials Science: Materials in Electronics*, 27(9), 9642-9649. <https://doi.org/10.1007/s10854-016-5022-3>
- [30] Chang, J., Kang, S. K., Lee, J.-H., Kim, K.-S., & Lee, H. M. (2015). Recrystallization as a Growth Mechanism for Whiskers on Plastically Deformed Sn Films. *Journal of Electronic Materials*, 44(10), 3486-3499. <https://doi.org/10.1007/s11664-015-3921-3>
- [31] Kumar, K. S., Reinbold, L., Bower, A. F., & Chason, E. (2008). Plastic deformation processes in Cu/Sn bimetallic films. *Journal of Materials Research*, 23(11), 2916-2934. <https://doi.org/10.1557/jmr.2008.0351>

6. THE TRANSITION FROM INFORMAL TO FORMAL ELECTRONICS RECYCLING IN GUIYU: A REVIEW OF THE GUIYU CIRCULAR ECONOMY INDUSTRIAL PARK

The following chapter is to be submitted to *Waste Management* as Wang, C., F, Zhao., Handwerker, C. (2021). The Transition from Informal to Formal Electronics Recycling in Guiyu: A Review of the Guiyu Circular Economy Industrial Park

6.1 Introduction

Guiyu is a town located in the eastern Guangdong Province of China, near the Lianjiang River, and 250 km away from Hong Kong, as seen in Fig. 6.1. It was known as one of the largest informal e-waste recycling sites in the world. Informal recycling refers to small-scale operations employing processes and practices that are low-technology and low-cost but highly polluting and often pose a significant risk to human health [1]. Within informal recycling, valuable metals such as gold, silver, lead, and copper can be recovered from e-waste without skilled labor, advanced technology, and heavy equipment cost. Guiyu has been involved in e-waste recycling for around forty years. Driven by the profit, e-waste generated worldwide was transported to Guiyu and recycled, informally, which became the dominant local business that peaked during the 1990s. The recycled materials are returned to the global market, but pollution and health issues are left behind. Researchers have studied extensively the environmental contamination associated with informal recycling in Guiyu, such as the pollution of heavy metal [2-6] and polybrominated diphenyl ethers (PBDEs) in the air [7], soil [8], and water [9]. Human health damages resulting from the severe pollution in Guiyu include workers' health problems [10], elevated blood lead levels of children [11, 12], a decrease in children's physical growth [13, 14], and damage to lung function [15].



Figure 6.1. Geographic location of (a) Guiyu town, Guangdong Province, China, and (b) Guiyu Circular Economy Industrial Park (GCEIP).

Driven by the pressing need for environmental protection and remediation, the state government, local government, and Guiyu residents, although with different interests, have been actively seeking political and technical solutions to transform the informal sectors, striking a balance between economic development and environment. One significant effort is the development of the Guiyu Circular Economic Industrial Park (GCEIP), a national-level circular economy initiative [16]. The circular economy refers to innovation under the constraints of sustainability, that is, the development of the new economy guided by the principles of Reduce, Reuse, and Recycle [17]. Specifically, for GCEIP, the goal is to transform the previous informal recycling business into a formal recycling business within a centralized site by offering high-tech facilities and supportive eco-infrastructure in processing and managing waste. Similar efforts have been made in other regions in China to build environmental-friendly recycling industries. For example, many formal recycling industrial parks similar to GCEIP have been constructed in urban cities such as Beijing, Tianjin, Qingdao, Hangzhou [1, 18]. Unlike GCEIP, those industrial parks were constructed as formal recycling projects in regions without a past history in informal recycling.

Globally, researchers have explored the possibility and evaluated the outcomes in regard to integrating formal and informal sectors. In research from Guibrunet [19], the case study of

municipal solid waste collection in Tepito, a Mexican neighborhood, illustrated that informal recycling could be integrated into formal collection service and even increase the system's sustainability. In Accra, a city with 20-year experience with formal solid waste management in Ghana, researchers and policymakers brought the formal sector and informal sector together by promoting strategic partnerships. Both collection coverage and recycling rates have significantly increased after two years of collaboration between informal providers and formal providers [20]. In the Southern Hemisphere, a case study demonstrated that the cooperation between the formal system and informal waste pickers in Londrina, Brazil, leads to a noticeable increase in the overall recycling system's productivity [21]. Like previous empirical studies, this research affirmed the importance of formulating a localized response in order to achieve a more sustainable economy, i.e., an informal collection system should not be ignored. Though studies on channeling informal recycling to formal recycling have emerged, the related empirical literature is still limited, especially in the field of e-waste recycling. Like Guiyu, many informal e-waste recycling sites in developing countries have struggled to adapt to changes where 50-80% of e-waste were recycled in informal sectors [22]. Underneath the struggles are complex economic, societal, technological, and political factors interconnected with the local context. GCEIP offers unique insights regarding a region's potential of transforming pre-existing informal sectors to formal sectors regarding e-waste recycling.

In this study, we attempt to provide a thorough background of informal recycling in Guiyu from the societal, economic, and historical perspectives and the overview of the transition to formal recycling made possible by the construction of the Guiyu Circular Economy Industrial Park (GCEIP). This study builds upon a series of official government documents about the policies, a field trip conducted in May 2017 examining the industrial structure, management, and assessment of GCEIP as well as follow-up communications, together with a literature review of journal papers and reports in Chinese and English featuring this informal-to-formal transition. The authors analyzed the historical, economic, societal, and technological perspectives in terms of the initiatives, barriers, and progress in transforming informal sectors. We report the policy design, project management, and technological innovations that enabled the successful implementation of GCEIP to obtain insights about the government and technologies' roles in this transition and the positive or negative interactions among authorities, individuals, and companies. Finally, the paper

summarizes a few key approaches from this case study for future research on transforming informal e-waste recycling.

6.2 Informal Recycling in Guiyu: An overview

6.2.1 Historical development of the recycling industry

Before the 1970s, the e-waste recycling business in China was managed by the nationally-owned China Co-op Group and State Commodities Bureau that constructed collection stations in urban and rural areas, thereby forming a waste collection network. Shortly after the reform and opening policy launched in the late 1970s, most local co-op stations gradually closed, providing opportunities for individuals to join the e-waste recycling sector. Many Guiyu people started to purchase and resell recyclable waste such as duck feathers, waste plastics, and waste metals from local and regional households. Those so-called "peddlers" make house calls with wagons and tricycles to collect household waste, bringing convenience to residents and often offering better prices [16, 23-24]. By the middle 1980s, Guiyu had become well known in Guangdong province because of the large number of residents involved in the recycling business.

6.2.2 Emergence of the e-waste recycling industry

Since the 1980s, the volume of e-waste exported for recycling from developed countries to developing countries gradually increased. Guiyu was one of the regions in developing countries that recycled 50% - 80% of the global e-waste [25-26]. Apart from its low-cost labor and loose environmental regulations, geographical and economic factors also played essential roles in the formation of the informal e-waste recycling industry in Guiyu. For example, in the early years, transboundary e-waste made up the majority of the feedstock in informal recycling, most of which was transported from Hong Kong and Vietnam [27]. Imported e-waste often contains higher gold content and can be purchased at lower prices than domestic e-waste purchased from peddlers; additionally, e-waste from developed countries has not undergone many repairs before disposal, so more functional components can be sold at higher prices. The considerable difference in profits drove backyard workshops to seek illegally imported waste electrical and electronic equipment (WEEE). Guiyu quickly became one of the largest e-waste recycling sites in the world, and there is no telling how much e-waste was recycled in Guiyu during the peak time. In particular, Hong

Kong allowed e-waste imports even after the ban of imported e-waste in mainland China, leaving room for illegal disposal and transboundary transfer. Guiyu, near the coast and only 250 kilometers away from Hong Kong (straight-line distance), remained the preferred site for dumping e-waste for a long time.

6.2.3 Environmental pollution and societal consequences

Since the 1990s, the typical streetscape in Guiyu was e-waste, and the remnants from the informal recycling occupied the roads outside small buildings where people lived upstairs and used the first floors as recycling workshops. During recycling, e-waste was first manually dismantled to sort out the plastic housings from the printed circuit boards (PCBs). Workers then “baked” PCBs on coal stoves until the polymers softened and removed the integrated circuits and electronic components such as capacitors and resistors with pliers. Gold was recovered via acid leaching of collected electronic components, and copper was recovered by burning the bare boards. The waste acid was poured into rivers and streams, and the rest of the residue was burned in the open air. This leaching process polluted local water, soil, and air, damaging health of local communities [28].

Informal e-waste recycling also caused enormous societal consequences. For example, studies pointed out two conflicts in social relationships, i.e., the conflict between wealthy and poor locals and the tension between migrant workers and locals [29]. For example, unlike those who made fortunes from e-waste recycling, locals who had not been involved in informal recycling remained poor. The poor suffered from economic disparities as well as serious health effects caused by pollution. For instance, poor locals could no longer plant rice because of soil contamination, which initially accounted for most income. Additionally, because there was no potable water in Guiyu, people had to purchase drinking water from locations farther away. The demand was so large that a unique business grew up, i.e., transporting water via trucks from other towns to Guiyu. Wealthy locals chose to purchase water for drinking or cooking, while poor locals had no choice but to drink contaminated water or bear the higher cost-of-living. According to Greenpeace [29], an undergraduate student from Guiyu wrote, “you can tell whether a person is poor or rich by looking at their teeth. Poor residents have black teeth because they drink the local water.”

The tension between locals and migrant workers emerged when tens of thousands of migrant laborers from less developed Chinese provinces gathered in Guiyu starting in the 1990s. From years of operating uncontrolled recycling of e-waste, local people realized the severe impact of the poor working conditions and severe environmental degradation on their health. As a result, many local people who initially profited from illegal e-waste recycling left Guiyu and the e-waste recycling business. Most of the locals who stayed opened their workshops as managers and were not directly involved in the operations, employing migrant to work as frontline workers for recycling e-waste, without appropriate technology and personal protection. In 2005, those workers only made \$2 per day. As mentioned above, the tap water in Guiyu was trucked in from the neighboring towns at an almost triple the price of local water; therefore, only one-third of migrant workers chose to have tap water at their residences [30]. While migrant workers complained about the wages and the working environment, the locals demonized migrant workers, accusing them of street crimes and deteriorated public safety [29].

6.3 Planning of GCEIP

6.3.1 Initiatives

Prior to the initiation of GCEIP, the Guiyu government made multiple efforts to regulate its uncontrolled recycling business, but unfortunately failed. For instance, Guiyu authorities tried to eradicate the informal sectors many times after the ban of e-waste imports in 2000 when the Basel Convention was ratified in China, but informal recycling repeatedly rebounded. Because informal recycling requires minimal skilled labor and equipment, those backyard workshops could easily move the business somewhere else: if not in towns, then in rural villages; if not during daytime, then at midnight. Previous studies on informal recycling also revealed this challenge in wiping out informal recycling [1]. The government simply did not have enough resources to enforce environmental regulations when facing thousands of adaptive, mobile, and scattered backyard workshops.

In 2005, Guiyu was selected as one of the regions to construct a national-level pilot circular economy industrial park (i.e., GCEIP) in order to improve the sustainability of the local recycling industry [31]. The goal of GCEIP is to include all the processing in the park and offer centralized treatment for hazardous waste while making illegal any recycling activities outside the park.

However, GCEIP was not constructed until seven years later, i.e., in 2012. Table 6.1 lists the timeline of the milestones leading to the construction of GCEIP by 2014.

Table 6.1. Timeline of the development of GCEIP regarding policies, major projects, and investment prior to the construction of GCEIP.

Year	Milestones
2004	Domestic WEEE Dismantling Center was approved by Guangdong Provincial Environmental Protection Bureau
2004	Guiyu demonstration project for dismantling WEEE was approved by the State Ministry of the Information Industry
2005	Guiyu was nominated as a national pilot circular economy zone by the National Development and Reform Commission
2009	The construction of the Domestic Waste Hardware Dismantling Center was completed
2010	Chaoyang District Government approved Guiyu Electronic Marketplace
2010	GCEIP development plan initiated with the provincial and municipal efforts
2012	China State Council approved GCEIP
2012	Guiyu government issued a standard based on environmental impact assessment to certify existing family workshops in informal recycling
2012	The contract signing ceremony between GCEIP and TCL Deqing Environmental Protection and Development Ltd on the collaboration of dismantling factory for electric appliances
2013	The Guangdong Provincial Environmental Protection Bureau approved the comprehensive Regulation of Guiyu WEEE Pollution Scheme
2013	GCEIP construction initiated

6.3.2 Barriers

The barriers to initiating the implementation of GCEIP originated from economic and societal conflicts.

Firstly, economic resistance originated from the decrease in profit and the increase of investment in transforming informal to formal recycling businesses. Guiyu has been recycling e-waste for nearly forty years, and local development relies heavily on informal sectors. In 2007, the value of e-waste and plastics recycling, dismantling, and processing in Guiyu reached nearly 1.56 billion Chinese yuan, accounting for more than 90% of the town's total industrial output [32]. Informal recycling became the primary source of income for locals. In other words, other industries were relatively weak, and Guiyu thereby was highly dependent on informal recycling. Eliminating

informal recycling meant cutting off the income of most families. The economic resistance also applied to Guiyu authorities. The local government was left shouldering the responsibilities of restoring the environment without sufficient financial resources: only a tiny amount of the income generated from informal recycling was taxed. For example, in 2007, the entire recycling industry's output value in Guiyu reached 1.56 billion yuan, whereas the tax revenue was only 16 million yuan and accounted for over 90% of the total tax revenue of the local government [32]. It reflected a hidden drawback of informal recycling: with most unlicensed and unregistered backyard workshops, local governments cannot collect enough money via taxes to initiate environmental protection projects or activities.

Secondly, there was resistance deeply rooted in the social realities of Guiyu. On the one hand, most locals doubted their ability to start any other type of business after having been participating in e-waste recycling since childhood. On the other hand, a major challenge was that those who produced the harmful consequences were not those who suffered from them, as previously mentioned. Furthermore, some residents believed that informal recycling had already ruined the environment, and the local government would ruin the economy by banning those backyard workshops and replacing them with the GCEIP, leading to a double loss. A key feature of the policy design of GCEIP was addressing these two concerns directly.

6.3.3 Policy design of GCEIP

In the 1980s, consumer electronics had yet to reach many households in developing countries, while developed countries moved heavily polluting industries (including solid waste treatment) overseas. It was in this social context that the Basel Convention was initiated in 1992 to advocate for the prohibition of illegal export of toxic e-waste from developed countries to developing countries [33]. The legal issues involved in transboundary e-waste recycling are multifaceted, including intellectual property protection, commercial secrets, foreign trade, and economic development. From the perspective of public management, the government bears the primary responsibility because recycling and processing of e-waste influence the social and economic relations of society [34]. Though the Chinese government ratified Basel Convention in 2000, illegal e-waste was continuously transferred to Guiyu from Shenzhen port when the ban was not being enforced, and from farther ports such as Dalian and Guangxi when Shenzhen port was under strict inspection. To stop illegal imports, China executed more regulations with detailed

restrictions on WEEE imports, i.e., "Technical Policies for Controlling Pollution of WEEE" (effective in 2006) and "Measurement for the Administration of Prevention and Treatment of Pollution by Electronic Information Products" (effective in 2007). However, as of 2009, 70% of e-waste received by China was still illegal [35].

Prior to initiating national-level projects such as GCEIP, the foremost task for the Chinese government was to establish a series of more comprehensive and effective policies regulating the import of transboundary e-waste and the construction of recycling facilities aimed at a circular economy. Previous studies examined the importance of a practical legal framework for financial support in reshaping the recycling industry [1] and promoting the circular economy [36]. Table 6.2 summarized the political efforts after 2011 that laid the groundwork for the construction of GCEIP. WEEE management policies before 2011 have been described in various studies [32, 37]. Note that only nation-wide policies and regulations are summarized in Tab. 6.2, many of which greatly influenced the informal recycling industry in Guiyu. For example, the China WEEE issued in 2011 has a special provision for family workshops in the informal recycling sector: it prohibits organizations or individuals that have not obtained the qualification for the disposal of WEEE to enter the recycling industry. Another example is the funding system (i.e., subsidies) for recycling and processing WEEE established in the Measures for the Collection, Use, and Management of Funds for the Disposal of WEEE. This fund system allows the companies in the formal recycling industry to operate with subsidies because their costs of equipment and management are high. It is with this funding system that large companies were brought into GCEIP, such as the TCL Deqing Environmental Protection and Development Co., Ltd.

Table 6.2. An overview of e-waste and circular economy-related policies in China after 2009. (Compiled from various sources)

Time	Legislation and Regulations	Key Components
2011 Effective; 2019 Revised	Regulation on the Administration of the Recovery and Disposal of Waste Electrical and Electronic Products (China WEEE)	With the approval of the provincial government, a centralized disposal field for waste electrical and electronic products can be set up.
2012 May	Measures for the Collection, Use, and Management of Funds for the Disposal of Waste Electrical and Electronic Products	The producers of electrical and electronic products and the consignee or agent of imported electrical and electronic products are taxed. The taxes collected are passed on to recycling plants as a fixed subsidy based on the number of dismantled appliances.
2013 May	Administrative Measures for the Circulation of the Used Electrical and Electronic Products	Introduce "used electrical and electronic products." Strengthen the circulation of used electrical and electronic products; promote the comprehensive utilization of resources; registration is required with detailed information such as original vouchers and sellers for used electrical and electronic products.
2015 February	Disposal Catalogue of Waste Electrical and Electronic Products (2014 Edition)	The range of products covered was extended to 14 products, namely: refrigerators, air conditioners, washing machines, electric water heaters, gas water heaters, printers, copiers, fax machines, televisions, monitors, computers, mobile communication handsets, telephones. (Amended in 2016 March.)
2016 July	Measures for the Administration of the Restricted Use of the Hazardous Substances Contained in Electrical and Electronic Products	Introduction of "Electrical and electronic products" and "Pollution caused by electrical and electronic products"; Restrictions on the use of the hazardous substances contained in electrical and electronic products. Development of "Catalogue for the Standard Compliance Administration of the Restricted Use of the Hazardous Substances Contained in Electrical and Electronic Products"
2017 January	Implementation Plan for the Extended Producer Responsibility (China EPR)	Introduction of the main body, objects, and mode of implementation for the EPR; promote the eco-friendly design and encourage the use of renewable resources; set up recycling standards;
2017 July	Implementation Plan for Prohibiting the Entry of Foreign Garbage and Advancing the Reform of the Solid Waste Import Administration System	A total ban on the entry of "foreign waste." Starting from January 2018, China stopped importing twenty-four types of foreign garbage. By the end of 2019, the import of solid waste that domestic resources can replace will be phased out.

Table 6.2 continued

2018 April	Import Waste Management Catalogue	Sixteen types of solid waste such as scrap metal, waste ships, scrap car parts were removed from "The Catalogue of Solid Waste Restricting Imports Used as Raw Materials" and transferred to "The Catalogue of Prohibited Imports of Solid Waste." (Implemented since December 31, 2018)
2008 effective; 2018 amended	Circular Economy Promotion Law of the People's Republic of China (2018 amendment)	For products such as electrical and electronic equipment that may cause environmental pollution during dismantling and disposal, the use of toxic and hazardous substances are prohibited during manufacturing; improving the resource utilization efficiency concerning reducing, reusing, and recycling activities in production, circulation, and consumption; encouraging and supporting the research and education of science and technology related to a circular economy.

6.4 Implementation of GCEIP

6.4.1 Projects and timeline

Table 6.3. The functions and capacities of major plants and projects constructed in GCEIP after 2014. (Source: compiled from various sources)

Projects	Year	Functions	Capacities
TCL Appliances Dismantling Factories	2014	Recycling computers and appliances; Only complete televisions, refrigerators, washing machines, and air conditioners are accepted; invested by TCL Deqing Environmental Protection and Development Co., Ltd.	50,000 tons/year
Physical Separation Facilities	2014	Recycling of WPCBs via physical separation with hydraulic shakers. Burning and acid leaching are excluded.	60,000 tons/year
Sewage Treatment Plant	2015	Household wastewater treatment in Guiyu town	30,000 tons/year
Disassembly Facilities	2016	Phase I: the manual dismantling of wasted printed circuit boards (WPCBs); Phase II & III: manual dismantling with tools such as pliers and hammers; manual sorting of plastics, cables, wires, aluminum, etc.	
Pyrometallurgy Facilities	2016	Pyrometallurgical treatment of WPCBs (bare boards), invested and managed by Shantou Recycling Resources Technology Co., Ltd, an enterprise of the state-owned company, China Energy Conservation and Environmental Protection Group (CECEP). By 2017, its annual capacity increased to 20,000 tons from 10,000 tons.	20,000 tons/year
Hydrometallurgy Facilities	2016	Hydrometallurgical treatment of integrated circuits (ICs) to recover precious metals. The patent belongs to the University of Guangdong Technology. Waste acids solutions were processed via the Mechanical vapor recompression (MVR) technique with inorganic salts as end products.	5,000 tons/year
Waste Transfer Stations	2017	Two out-park transfer stations at Xianma and Guiyu counties with twenty-six waste collection locations.	N/A
Hazardous Waste Transfer Stations	2017	In-park Hazardous Waste Transfer	160,000 tons/year
Waste Plastic Cleaning Plants		Seven plants for cleaning waste plastics before sorting, located among the disassembly buildings	N/A
Industrial Wastewater Treatment Plant		GCEIP wastewater treatment	6000 tons/day
Guiyu Electronics Trade Market		The upgraded platform consolidated markets among Guiyu and neighboring regions for transactions of waste electronic components and metals.	N/A
Loading Lot		Loading and unloading of e-waste, functional components, and recycled products. The sources, categories, and the weight of incoming e-waste need to be registered before acceptance. Imported e-waste is prohibited.	N/A

Driven by the urgent need for environmental protection and supported by more detailed and more strict laws and regulations within the legislative framework, the construction of GCEIP has been advanced throughout the years by national, provincial, and municipal governments. Table 6.3 lists the major projects completed and corresponding functions and capacities inside GCEIP and the projects aimed to mitigate the environmental pollution outside GCEIP. The programs or plants all bear the purpose of advancing and centralizing waste management in the e-waste recycling industry.

6.4.2 Companies in residence

The objective of GCEIP is to transform the local informal sectors into formal sectors by providing pollution-control and waste-management facilities within a centralized site. Except for those workshops that only sort e-waste, the remaining small-scale workshops were reorganized into 49 large-scale companies focusing on recycling PCBs or plastics, all of which have operated in GCEIP from 2016 onward with a two-year tax exemption period. Details of the reconstruction of those 49 companies are explained in a later section. Additionally, the Guiyu government also invites enterprises in the formal recycling sector to reside in GCEIP to increase the recycling capacity in order to achieve economies of scale and to boost profitability. Meanwhile, those companies can bring jobs for people previously working in the informal sectors and stimulate local economic growth. In 2012, six ministries and commissions of the Chinese government, including the State Administration of Taxation, jointly issued the Administrative Measures on the Collection and Use of Waste Electrical and Electronic Products Processing Funds. Televisions, refrigerators, washing machines, air conditioners, and computers were included in the first batch of WEEEs that received subsidies. Encouraged by this policy and the supportive eco-facilities constructed in GCEIP, TCL Corporation (a leading multinational electronics enterprise) and a local company in Guiyu, Deqing Shantou WEEE Dismantling and Recycling Ltd, co-founded TCL Deqing Environmental Protection and Development Co., Ltd. The joint venture invested 50 million Chinese yuan in building appliance dismantling factories with a total construction area of 0.024 km². The first phase of the project has been certified and began operating and receiving state subsidies at the end of 2013 with an annual capacity of 30,000 tons, equivalent to 1.2 million sets of electrical appliances. Due to the expansion of business, the original project's scale could not meet its operational needs. In 2016, the company officially launched the preparatory work to add

a 95,000-ton annual capacity with the follow-up investment of 30 million Chinese yuan. After the expansion, the total capacity reached 145,000 tons per year.

6.4.3 Source control of e-waste

The foremost task of GCEIP is to exclude illegal transboundary e-waste that had penetrated in Guiyu through many routes. To ensure the incoming e-waste feedstocks were obtained from licensed sources, GCEIP issued site access cards to each company in residence and trucks carrying e-waste must present the cards to enter the parking lot where the loading, unloading, and trading occur. Incoming e-waste is registered with detailed information required on the e-waste sources and weights to ensure no imported e-waste is mixed into the load. GCEIP allows three types of trading. Firstly, private recycling companies can purchase domestic e-waste from the sellers inside their previous networks. After undergoing registration in the loading lot, e-waste will be assigned directly to affiliated companies. It is a win-win condition which, for GCEIP, guarantees a stable e-waste network with personal connections and, for private companies, offers supplementary sources. Alternatively, upstream collectors will send e-waste to GCEIP. In this scenario, for each batch of e-waste, the private companies can bid, and whichever company with the highest bid will claim the ownership. Lastly, TCL Deqing Environmental Protection and Development Co., Ltd relies on appliances collected via its network, mostly managed through the nationwide trade-in program. This trading framework eliminates competition for the feedstocks between the private companies and high-tech recycling companies but ensures the government's inspection of in-park transactions.

6.4.4 Recycling technologies and waste treatment

Fig. 6.2 illustrates the overall recycling scheme of GCEIP. After passing the inspection and trading stages in GCEIP, e-waste feedstock is dismantled and categorized as (1) functional units (including cables, bare wires, or large-size electric units), (2) waste plastics, (3) waste PCBs, and (4) other types of wastes. For the first category, those functional units directly enter the end-products trading markets. For the second category, recycled plastic particles can be obtained after cleaning, sorting, and cutting waste plastics. For waste PCBs, a refined manual dismantling process was performed, as seen in Fig. 6.3. After this refined manual dismantling, components were further

separated into three different groups, i.e., microelectronic components, bare PCBs, and ICs. GCEIP carries out three recycling routes for different components in waste PCBs. These treatments replaced the rudimentary recycling technologies used in Guiyu prior to the construction of GCEIP, including hydrometallurgy to recover gold from ICs (replacing open-air aqua regia acid baths), pyrometallurgy to recover Cu from bare PCBs (replacing open-air burning of PCBs), and physical separation with hydraulic shakers as a supplementary method to recover fine metal powders. Note that for microelectronic components such as capacitors and resistors, dismantled units were first tested before recycling treatments: if tested functional, units will be traded in secondary markets; if not functional, units were dispatched to pyrometallurgy plant. Technical details of the pre-processing (dismantling), the individual treatment, and pollution control measures are explained in the following section.

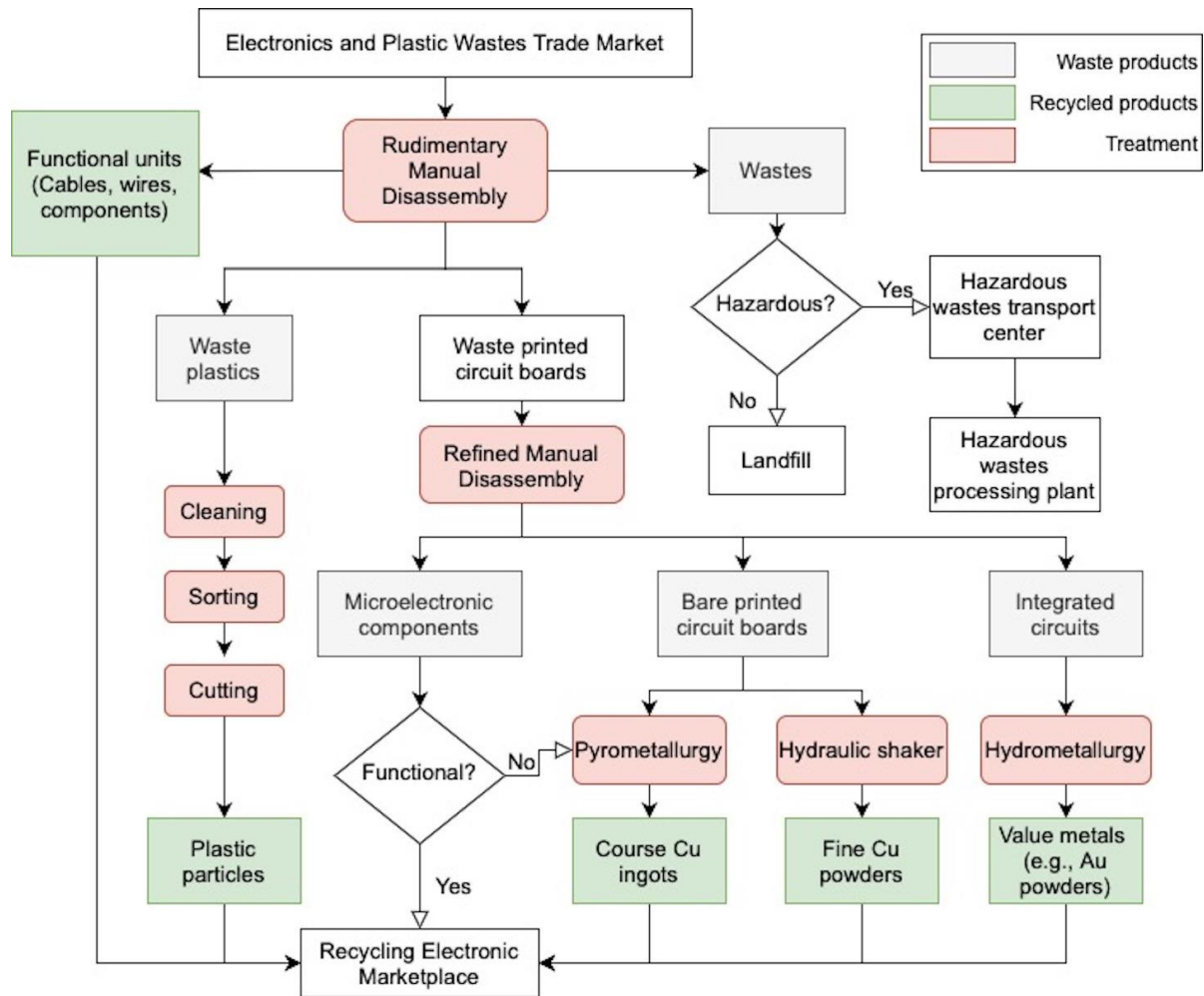


Figure 6.2. An overview of the mixed technologies employed in pre-processing and treatments in Guiyu Circular Economy Industrial Park.

6.4.4.1 Dismantling

Manual dismantling yields a higher percentage of recyclable materials than shredding, but with higher labor costs. In the informal sector, manual dismantling often uses primitive and hazardous processes [38]. Recycling businesses in Guiyu explored “low-technology” innovations to reach the goals of increased recycling fraction, pollution control, and safer working conditions while keeping the labor costs low. For instance, on the one hand, dismantling companies in GCEIP have adopted the technology in the electrical maintenance industry and use hot air guns to partially soften the circuit board to extract electronic components; on the other hand, Disassembled components were carefully separated and sorted by functions, each of which will be tested for functionality, and a large portion of them can be resold or reused [39], as shown in Fig. 6.3. These solutions to recycling e-waste gained popularity in Guiyu many years ago and are probably the most noticeable differences that singled out Guiyu from other recycling locations [40]: the value of reuse and refurbishment reaches 80% of the total revenue of the recycling industry. GCEIP allows this recycling pattern to continue, i.e., the high degree of separation of components still constitutes an essential and salient characteristic of the local recycling industry a salient characteristic of recycling businesses in developing countries [41].

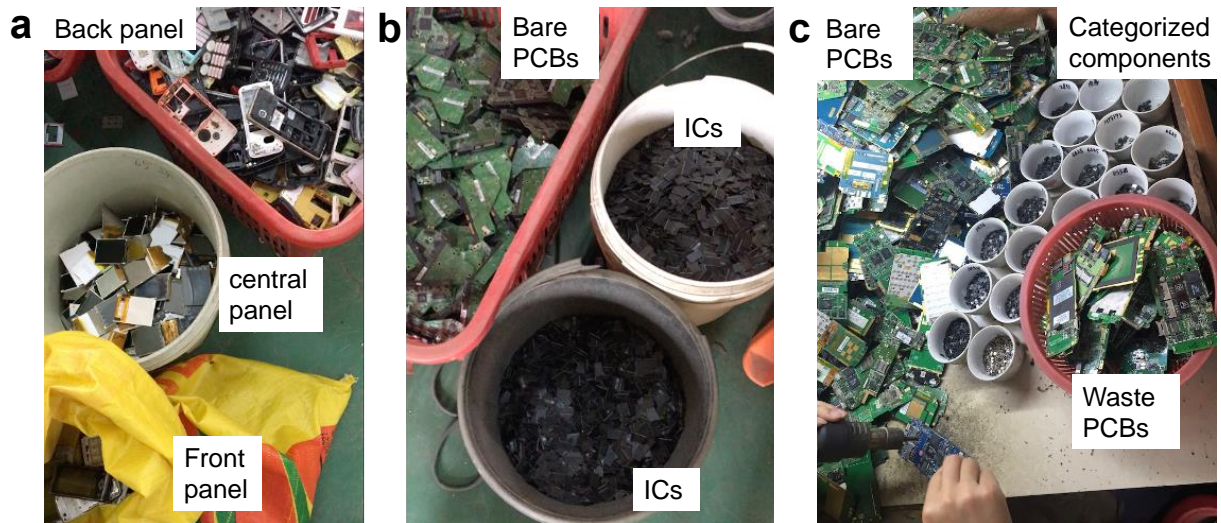


Figure 6.3. The end products of a cellphone dismantling procedure carried out in GCEIP. (a) dismantling the housing and large-size electronic components; (b) dismantling integrated circuits and PCBs; (c) dismantling and sorting different types of small electronic components such as cameras and memories. Photo credits: Congying Wang.

6.4.4.2 Hydrometallurgy: Gold recovery

Hydrometallurgy separates metals, primarily gold, by dissolving metals or plastics in different inorganic or organic solvents to producing relatively pure metal products. The environmental concern of hydrometallurgy is the large amount waste acid, acid mist, and waste residues generated in the process [42]. GCEIP collaborated with the Guangdong University of Technology and designed a patented hydrometallurgy process to extract gold from ICs with modules to collect and filter the acid mists and waste acid, as shown in Fig. 4. The filtering of waste acid is achieved by mechanical vapor compression (MVP). The upgraded hydrometallurgy plants have five processing lines for gold recovery with an annual capacity of 5,000 tons and include a storage infrastructure of acids to appropriately store acids when no recovery operations were executed, as seen in Fig. 6.4(d).

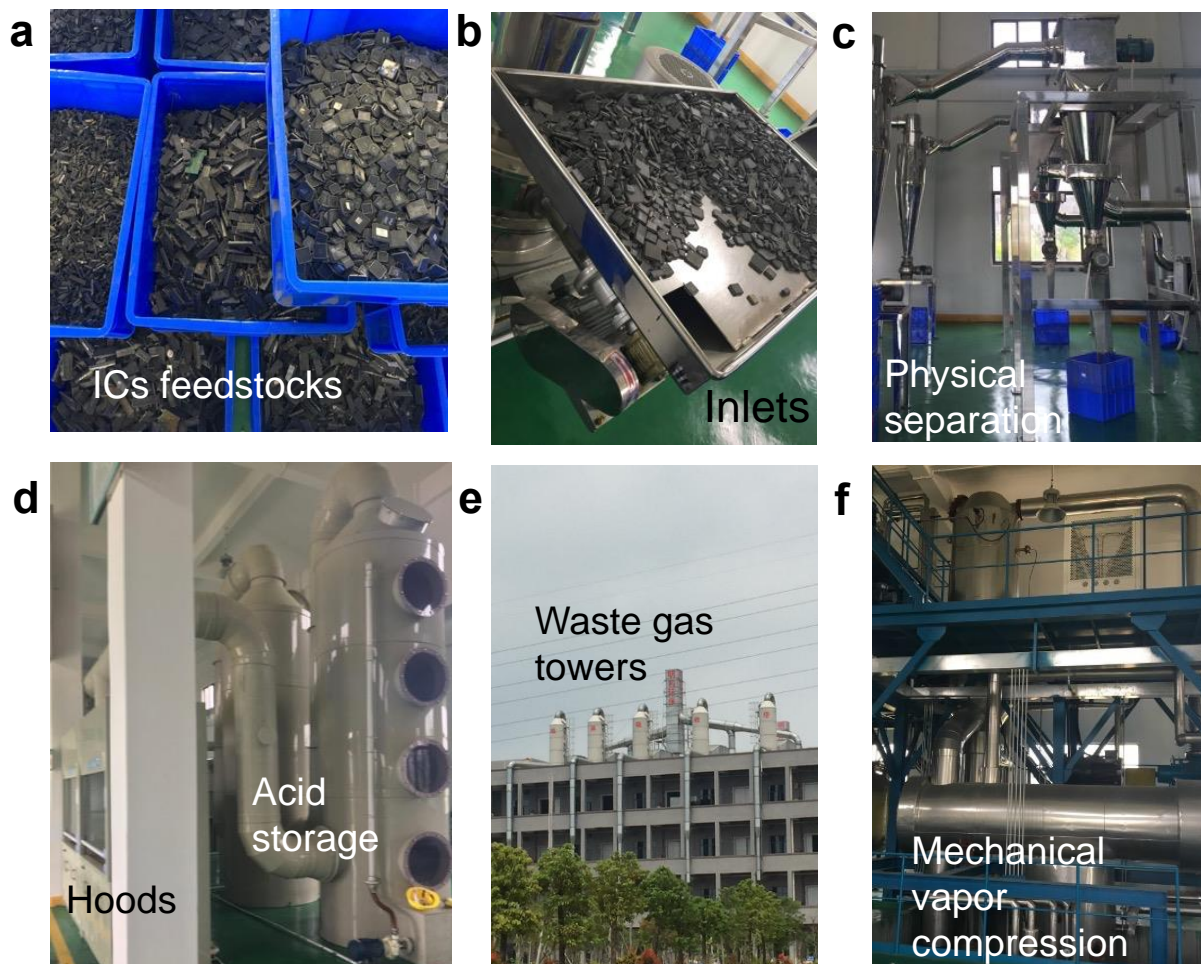


Figure 6.4. The recycling and treatment processes for gold recovery. (a) The stocks of dismantled and sorted integrated circuits (ICs). (b) The inlet of ICs. (c) Physical separation equipment. (d) Hydrometallurgy facilities and (e) waste gas tower on the roof of one of the plants. (f) Waste solution processing by mechanical vapor compression (MVP) equipment. Photo credits: Congying Wang.

6.4.4.3 Pyrometallurgy: Cu recovery

Pyrometallurgy recovers non-ferrous metals (Cu) from bare PCBs by carbonizing non-metallic materials at high temperatures, which requires low operating costs but offers a large processing capacity and high recovery rate. Nevertheless, two challenges existed: the substantial expense incurred by the equipment and the treatment of exhaust gas to remove pollutants such as dioxin and polybrominated diphenyl ethers [43]. Because the local government cannot provide GCEIP with either the costs or technology, GCEIP collaborated with Energy Conservation and

Environmental Protection Group (CECEP), a state-owned and high-tech enterprise, to form the CECEP Shantou Recycling Resources Technology Co., Ltd, and invested the pyrometallurgy plants in GCEIP. The company developed a new pyrometallurgy technique with a controlled temperature between 1200°C and 1250°C so that the generation of various dioxin precursors is suppressed [44]. Concerning the exhaust gas treatment, the gas generated in the bath smelting is cooled down in quenching towers, and the dust in the cooled gas is collected in bag filters. After dust collection, the flue gas enters the alkaline adsorption towers, where acid gas is recovered, and bromine is further extracted. After dioxins and heavy metals are captured by activated carbon, the gas is released via a chimney. The pollutants-free solid residue can be used in road construction. The pyrometallurgy plants in GCEIP were the first in China that employed bath smelting in recovering copper from waste PCBs and have operated since 2016 with an annual capacity of 10,000 tons. In March 2017, the capacity were expanded to 20,000 tons per year.

6.4.4.4 Physical separation

Physical separation (with hydraulic shaker) is based on different densities and can effectively avoid the toxic gases and dust generated in the crushing and sorting processes. Maoteng Shantou Recycling Resources Technology Ltd invested the physical separation plants in GCEIP (60,000 tons per year). These hydraulic shakers operate at low costs but generate a massive amount of wastewater. Technical specifications of pollution control for processing WEEE (issued in 2010 by the Ministry of Environmental Protection) requires any recycling facilities equipped with hydraulic shakers to process and reclaim the wastewater. Apart from the reclaimed water, the separation facilities were designed to cost 8559 tons of tap water annually.

6.5 Contextualized Analysis: The Transformation of Informal Recycling to Formal Recycling in Guiyu

6.5.1 Changes in the local recycling industry

Fig. 6.5 illustrates the recycling industry's overall architecture in Guiyu after the construction of GCEIP. GCEIP maintained, to a large extent, the original structure of the local informal recycling sectors. Therefore, Guiyu kept the unique advantages of its local recycling industry developed throughout several decades, i.e., broad collection networks, vast end markets,

reuse value, and the abilities of recovering distinct materials from e-waste, including plastics and various metals. In addition, GCEIP avoided severe unemployment from the banned informal sectors by integrating Guiyu's existing recycling industry. What GCEIP brings to the local society are (1) external resources such as technologies and investment, (2) strict source monitoring of the incoming e-waste, and (3) technology-enriched pollution management. With initial financial support from state and provincial governments, GCEIP has grown to hold 80 enterprises and about 3,500 employees with an annual output value of 1.035 billion yuan, 1.75 billion yuan, 1.465 billion yuan in 2016, 2017, and 2018 according to Ministry of Ecology and Environment of the People's Republic of China [45]. The local government's tax income has increased to 30 million Chinese Yuan per year from GCEIP [46]. The government's increased income will lower the economic barriers to initiate programs to restore the environment and fund advanced recycling technologies.

When evaluating GCEIP, it is necessary to consider the changes in recycling capacity at the local and national scale, i.e., whether GCEIP's capacity is significant. Before the establishment of GCEIP, the recycling industry in Guiyu digested 1.5 million tons of e-waste per year, the majority of which were imported; at present, GCEIP's annual capacity is approximately 1.08 million tons of domestic e-waste [45], reaching more than 70% of the capacity of previous informal sectors. At the national level, however, the limited, outdated, and inconsistent data make the analysis difficult. For instance, domestically generated e-waste in China was estimated to be 7 million tons in 2016 [47], 4-5 million tons [48], or 15 million tons in 2020 [49-50]. Based on the maximum estimated number, GCEIP's current capacity accounts for approximately 7% of the total amount of domestic WEEE. However, this is still an underestimated ratio because only a relatively small portion of generated WEEE was collected for recycling. Though we are not able to find the accurate number for China, it was estimated that merely 20% of WEEE was collected and recycled globally [51]. Therefore, the actual contribution of GCEIP to the nation's entire recycling industry will only be higher. We advocate for systematic studies about this gray area, i.e., the total number of generated e-waste and the collected percentage, which will greatly advance the understanding of e-waste recycling for the research community.

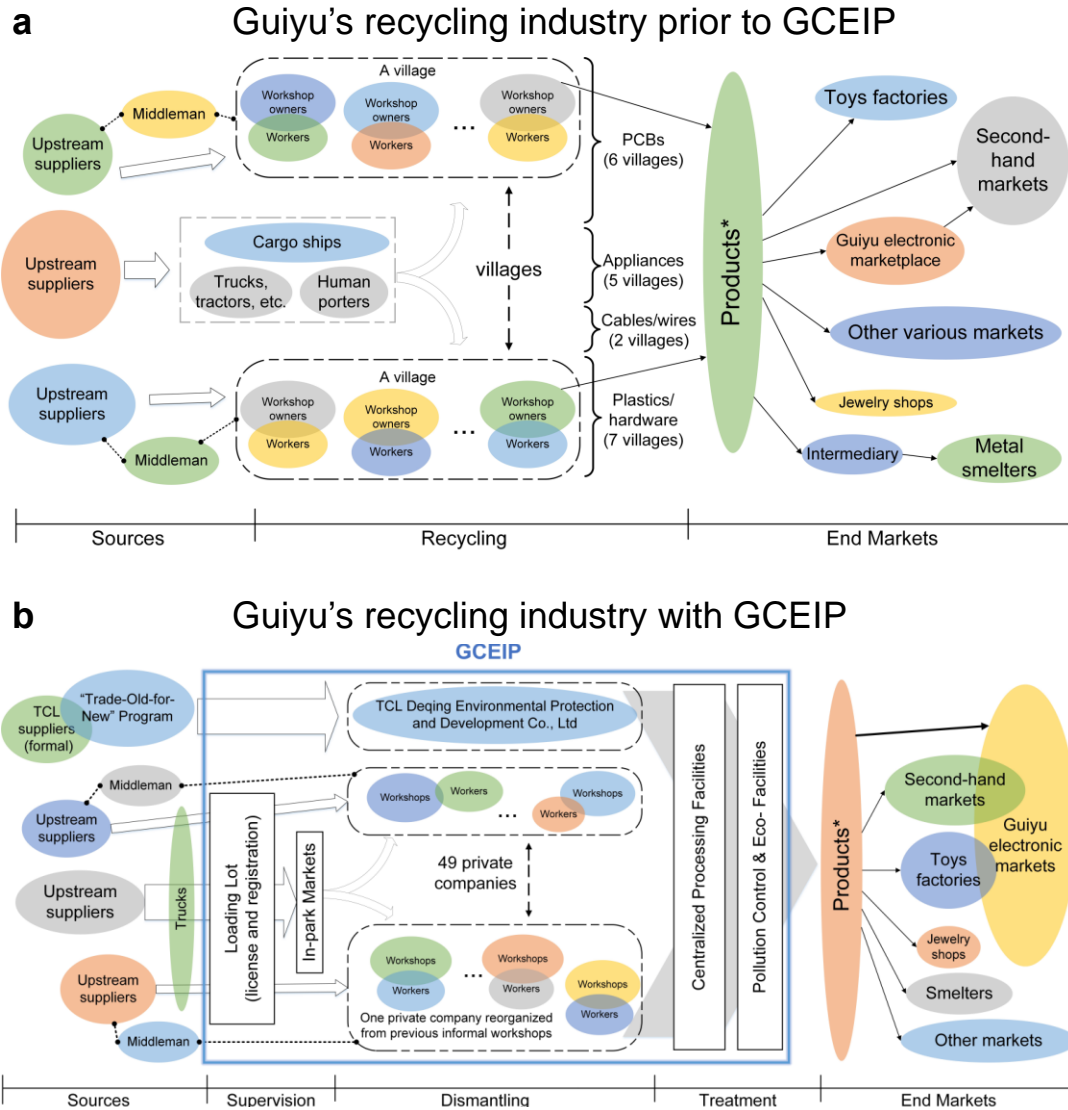


Figure 6.5. The recycling scheme of (a) informal sectors in Guiyu before the construction of GCEIP, and (b) integrated informal sectors and formal sectors in Guiyu after GCEIP

6.5.2 Synergy of the solution

Positioning GCEIP into the overall framework, four themes can be summarized based on Guiyu's solution to transform and regulate previously uncontrolled e-waste recycling activities. The themes included (1) the construction of facilities dedicated to recycling and waste treatment in GCEIP, (2) the collaboration between GCEIP and large companies or research institutions, (3) the reconstruction of backyard workshops, and (4) the establishment of the end markets. The

details of the last two themes are summarized below. (The first two themes have been extensively discussed in the previous sections).

6.5.2.1 Reconstruction of backyard workshops

When the GCEIP development plan was initiated in 2012, more than 21 townships (out of 27 in total at Guiyu), 300 private enterprises, 60,000 people, and 5,000 unlicensed backyard workshops were in the informal recycling business, which digested 1,550,000 tons of WEEE and waste plastics per year. It was impossible to construct an industrial park capable of absorbing the entire informal sector. Therefore, the local government established a standard of environmental impact assessment and allowed one year for all workshops to meet the criteria. According to the standard, uncontrolled acid leaching and board burning were strictly prohibited; additionally, each workshop was required to (1) solidify the ground to prevent soil pollution from wastewater; (2) install a gas collecting hood to filter exhaust gas; (3) provide workers with protective masks and gloves. In 2013, about 3000 workshops were temporarily certificated with environmental permits, business licenses, and tax registration. The rest of the 2000 workshops were forced to shut down. A year later, 727 workshops that failed to pass the assessment were again required to close, of which 441 workshops were licensed in 2013, and 286 were unlicensed workshops that restarted operation illegally. By the time GCEIP finished the first-stage construction, 2700 temporarily approved workshops had remained, most of which were small-scale, which must reorganize to large-scale companies to receive permissions from GCEIP. In the end, 1243 workshops of PCB recycling formed 29 companies, and 218 workshops of plastic recycling formed 20 companies, all of which have operated in GCEIP since 2016. (Note that for plastic recycling, 1172 workshops that only focus on sorting stayed outside GCEIP). After a year of operation in GCEIP, those 49 companies were further reconstructed to 80 companies.

During the reconstruction, both national-level regulations and local-level administration played critical roles. For the former, policy development such as the Regulation on the Administration of the Recovery and Disposal of WEEE (China WEEE in 2011) provided legal bases for Guiyu authorities to close informal recycling workshops that failed to obtain the qualification. For the latter, the local government stepped out of this reorganization process considering that local culture that people tend to do business with acquaintances. Therefore, those workshops had autonomy in making decisions such as what company they attempted to set up,

how many workshops should be included, and who should take the management responsibility. Three primary forms of reorganization occurred, i.e., the combination of recycling workshops by geological locations such as villages, by social relations such as relatives and friends, or by recycling products such as gold or copper.

6.5.2.2 End Markets of Recycled Products

Historically, a variety of end markets flourished in Guiyu, driven by other industries' demand for secondary materials and the rural markets' demand for second-hand electronic and electrical equipment. This tradition of focusing on the reuse of dismantled electronics is not uncommon in developing countries. Additionally, the second-hand markets for electronic components boomed as a result of the "fine dismantling" process rooted in the local recycling industry's culture, i.e., e-waste is manually dismantled and classified to the level of transistors and resistors as shown in Fig. 6.3(e). Components with reuse values are sorted, tested, and sold on the local market. For example, toy factories in neighboring towns often purchase second-hand but functional motors to produce toy cars. However, the reuse practice mentioned above lacks proper inspection, which may cause: (1) hardware quality problems regarding product functions and product life; (2) patent risks due to the authorization of components and supporting software; and (3) information security concerning the reuse of storage components (Greenpeace, 2019). From a circular economy perspective, the recycling and reuse of resources should follow the principle from high-value to low-value. On the basis of not destroying the original parts, reuse is in line with the principle of a circular economy. However, in view of the above concerns about hardware, software, and information security, this industry still needs to be regulated and managed.

In regard to trading, a common question is "who owns the recycled products?" especially for value metals such as gold. Indeed, though the local government established an electronic trading market to provide a licensed platform for trading recycled products, the end markets still heavily rely on the "old" social connections or supply chains built by previously informal family workshops. Private businesses in GCEIP can determine which end markets or agents the recycled products will enter, after paying off the fee of operating recycling facilities. If those businesses fail to find an appropriate buyer, GCEIP can purchase, collect, sell, and distribute those recycled or recovered products.

6.5.3 Comparisons between GCEIP and similar efforts

GCEIP is one representative case study of transforming informal recycling to formal recycling, but not the only one. Positioning the construction of GCEIP in the complete picture of the global efforts to promote recycling and mitigate pollution, this section compares GCEIP with similar projects both within and outside China.

6.5.3.1 National level

On the national level, the Chinese government has initiated similar programs to shape e-waste recycling under the framework of the circular economy. Generally speaking, those programs can be classified into two categories: one type of recycling project adapt state-of-the-art recycling facilities and technologies such as the recycling plants in Qingdao; the other projects absorb the existing industry and rely on technologies that tailored for local realities. GCEIP belongs to the latter. One may argue that Guiyu could construct brand-new formal recycling plants, considering many other high-tech industrial facilities have been built recently in China [37]. However, the lack of e-waste sources emerges as the main challenge confronted by those recycling plants. For example, one of the formal recycling factories in Tianjin, China, has faced a shortage of incoming e-waste after finishing the construction [51-54]. Similarly, Hangzhou Dadi recycling industrial park only reached 4% of its maximum capacity (284 out of 7000 tons) as of 2006 [53]. This issue is deeply rooted in the lack of a formal WEEE collection system in China. Second-hand markets, distribution stations in rural areas, and individual recyclers were the three leading players in collecting WEEE in China [1]. Traditionally, except for the first route, the rest of the WEEE was collected by individual peddlers and recycled with little to zero technology and protection by unlicensed workshops or individuals. Without a systematic collection network under the local government's supervision, the amount of feedstock collected by formal sectors is insufficient for the recycling industry to scale up and reach a profitable scale. On the other hand, even taking advantage of the original collection network in Guiyu, GCEIP still faces shortage issues due to the ban of transboundary e-waste, on which Guiyu's recycling business heavily relied in the past. To address this challenge, those private recycling enterprises (transformed from previous backyard workshops) have set up more than 1,000 purchase stations and dispatched more than 3,000 personnel to those stations across China.

6.5.3.2 Global level

Though regional governments can ban all informal recycling to mitigate the damage, the proper treatment of e-waste remains to be a challenge on the global scale due to the mobility of WEEE, i.e., banning may not be the most desirable solution. For instance, China's stricter regulations and censorship on transboundary e-waste, alternative e-waste dumping sites in other developing countries emerged, such as Thailand and Malaysia [55]; it is evident that reshaping informal e-recycling has been, is, and will be a third-world problem for many years to come.

Researchers also seek for solutions to bridge and combine the value of manual dismantling (usually in developing countries) and that of waste management (usually in developed countries), such as the best-of-two-world model [56]. The best-of-two-world model proposed a local-scale dismantling procedure (usually in developing countries) and global-scale high-tech treatment (usually in developed countries). Though GCEIP seems to echo the best-of-two-world philosophy within a local scale, scaling up this practice to a global scale will result in additional challenges, especially ethical problems. On the one hand, the two cases both advocate for using manual dismantling at the pre-processing stage and employing technically advanced facilities at the end-processing stage. On the other hand, GCEIP's approach included filtering out illegal transboundary e-waste and establishing a domestic recycling network. Even if the best-of-two-world model and the experiences of GCEIP can be applied to other regions, it remains to be a critical ethic question that whether this solution should be used to address the worldwide e-waste problem or not. The collaboration between developed countries and developing countries may turn out to justify unfair shares of rights and responsibilities, i.e., who pays for who; who generates, uses, and discard electronics; who offers treatment, and where the waste goes—the question of "sustainability for who" should be repeatedly revisited and answered. The challenges faced by similar developing countries in e-waste recycling should be addressed from two perspectives: How can local governments effectively prohibit the import of e-waste? How can pollution control be integrated into the local informal sectors and gradually drive the industry towards formal sectors?

6.5.4 Limitations

Guangdong province, Shantou city, Chaoyang district, and Guiyu town have jointly invested 1.53 billion Chinese yuan in building GCEIP. However, the comprehensive

environmental remediation plan issued by the provincial and municipal government, the maintenance of current facilities, and the construction of subsequent projects still need a considerable amount of investment. The local government needs to repay the previous loan principal and interest of 400 million yuan, plus the fees for GCEIP's daily operations. GCEIP still heavily relies on the state government's budget fund, e.g., its expenditure budget for 2020 is 145 million yuan [46]. Because the financial foundation of the Guiyu government has long been weak without sufficient taxes, the fundraising needs are still urgent and remain the most significant barriers. Moreover, the local government lacks technical personnel for pollution control and for responding to emergencies. Simultaneously, the skills of the employees in Guiyu's current recycling industry cannot support the development of new technologies, which restricts the transformation and upgrading of the "transformed" formal recycling industry.

After five years of implementing GCEIP, the number of literature and reports regarding the changes in Guiyu is still limited. A study by Schulz and Lora-Wainwright [57] claimed that the local elite manipulated the progress to today under the so-called name of "circular economy." While many of the observed conflicts held valid, such as the uneven distribution of power and wealth, it is critical to examine the situation through a historical lens, as demonstrated in this study. The socially and financially disadvantaged groups (e.g., local poor, migrant workers) have existed long before GCEIP. Indeed, the effort of transforming the informal activities should and could further improve, but the damages resulted from four decades of unregulated informal recycling should not be attributed to GCEIP. It is vital not to underestimate the struggles the developing countries have faced when examining recycling activities from outside.

6.6 Conclusion

Guiyu was the largest e-waste dismantling and distributing center in the country and even in the world, and it is also one of the most recognized victims of the pollution caused by e-waste processing. In the late 1980s, Guiyu started a profitable informal dismantling business, and the scale has gradually expanded since then. At the same time, foreign e-waste entered Guiyu in large quantities through the transfer points of Shenzhen, Guangzhou, and Hong Kong. By the 1990s, 80% of the families in Guiyu participated in this industry. As of March 2012, there were 5169 dismantling units in the town with more than 100,000 employees. The GCEIP has shifted the

informal, heavily polluted recycling business to a "technology-hybrid" industry in the past decade. During this transition, three themes are critical:

Legislation: Policies and legislation are of great significance in driving the informal recycling sector to abandon illegal recycling techniques and transboundary e-waste. In Guiyu's case, the initiation and implementation of GCEIP are closely related to the progress of environmental legislation by the Chinese government. For instance, Regulation on the Administration of the Recovery and Disposal of WEEE (China WEEE in 2011) prohibits the recycling or dispose of e-waste by businesses and individuals that have not obtained the qualification, which targeted at those backyard workshops in Guiyu; Measures for the Collection, Use, and Management of Funds for the Disposal of WEEE stipulated that the state establishes a WEEE product disposal fund to subsidize the processing costs of WEEE products.

Localization: Although GCEIP drastically reformed local informal sectors, the recycling industry in Guiyu keeps forward its societal and cultural context. On the other side, GCEIP may face enormous resistance if the recycling industry's histories and traditions were not respected. The intrinsic driving force for a circular economy relies on the regional innovation led by the government and enterprises, such as the manual dismantling techniques with heating to prevent from burning the PCBs. Enterprises in the GCEIP are self-organized and market-oriented. GCEIP expands the existing e-waste source network, thereby avoiding the pitfall resulted from a shortage of raw materials for recycling. To summarize, stakeholders and decision-makers always need to consider locating and maintaining the unique advantages rooted in local communities.

Collaboration: Technology and informal recycling are not mutually exclusive. GCEIP manifests a collective effort of national-owned companies, private companies, "used-to-be" informal recycling businesses, research institutes, and thousands of workers. The government should be the agent connecting all the sectors. The characters played by the government include but are not limited to providing subsidies to motivate environmental-friendly companies to join the recycling industry, promoting novel technologies or patents from research institutions to applications, and establishing effective communications between each sector.

On a global scale, however, the question becomes complicated. If the global concern of e-waste inevitably turns into a local problem, especially in developing countries, the solution must also be local. Guiyu's lesson offers precious experiences to deal with e-waste in other regions where tailor-made solutions and multi-year efforts must be made. Particular advantages of

informal sectors root in the historical, societal, and economic factors in the local context. It is critical to locate, direct, and incorporate those advantages when developing a sustainable e-waste recycling industry. Formal recycling and informal recycling are not mutually exclusive, and the alignment between the two sectors can be achieved with a contextualized understanding of the local recycling industry.

6.7 References

- [1] Chi, X., Streicher-Porte, M., Wang, M. Y., & Reuter, M. A. (2011). Informal electronic waste recycling: A sector review with special focus on China. *Waste Management*, 31(4), 731–742. <https://doi.org/10.1016/j.wasman.2010.11.006>
- [2] Guo, Y., Huang, C., Zhang, H., & Dong, Q. (2009). Heavy Metal Contamination from Electronic Waste Recycling at Guiyu, Southeastern China. *Journal of Environmental Quality*, 38(4), 1617–1626. <https://doi.org/10.2134/jeq2008.0398>
- [3] Leung, A. O. W., Duzgoren-Aydin, N. S., Cheung, K. C., & Wong, M. H. (2008). Heavy Metals Concentrations of Surface Dust from e-Waste Recycling and Its Human Health Implications in Southeast China. *Environmental Science & Technology*, 42(7), 2674–2680. <https://doi.org/10.1021/es071873x>
- [4] Lin, X., Xu, X., Zeng, X., Xu, L., Zeng, Z., & Huo, X. (2017). Decreased vaccine antibody titers following exposure to multiple metals and metalloids in e-waste-exposed preschool children. *Environmental Pollution*, 220, 354–363. <https://doi.org/10.1016/j.envpol.2016.09.071>
- [5] Quan, S. X., Yan, B., Lei, C., Yang, F., Li, N., Xiao, X. M., & Fu, J. M. (2014). Distribution of heavy metal pollution in sediments from an acid leaching site of e-waste. *Science of The Total Environment*, 499, 349–355. <https://doi.org/10.1016/j.scitotenv.2014.08.084>
- [6] Song, Q., & Li, J. (2014). Environmental effects of heavy metals derived from the e-waste recycling activities in China: A systematic review. *Waste Management*, 34(12), 2587–2594. <https://doi.org/10.1016/j.wasman.2014.08.012>
- [7] Deng, W., Zheng, J., Bi, X., Fu, J., & Wong, M. (2007). Distribution of PBDEs in air particles from an electronic waste recycling site compared with Guangzhou and Hong Kong, South China. *Environment International*, 33(8), 1063–1069. <https://doi.org/10.1016/j.envint.2007.06.007>
- [8] Leung, A. O. W., Luksemburg, W. J., Wong, A. S., & Wong, M. H. (2007). Spatial Distribution of Polybrominated Diphenyl Ethers and Polychlorinated Dibenzo-p-dioxins and Dibenzofurans in Soil and Combusted Residue at Guiyu, an Electronic Waste Recycling Site in Southeast China. *Environmental Science & Technology*, 41(8), 2730–2737. <https://doi.org/10.1021/es0625935>

- [9] Luo, Q., Cai, Z. W., & Wong, M. H. (2007). Polybrominated diphenyl ethers in fish and sediment from river polluted by electronic waste. *Science of The Total Environment*, 383(1–3), 115–127. <https://doi.org/10.1016/j.scitotenv.2007.05.009>
- [10] Bi, X., Thomas, G. O., Jones, K. C., Qu, W., Sheng, G., Martin, F. L., & Fu, J. (2007). Exposure of Electronics Dismantling Workers to Polybrominated Diphenyl Ethers, Polychlorinated Biphenyls, and Organochlorine Pesticides in South China. *Environmental Science & Technology*, 41(16), 5647–5653. <https://doi.org/10.1021/es070346a>
- [11] Huo, X., Peng, L., Xu, X., Zheng, L., Qiu, B., Qi, Z., Zhang, B., Han, D., & Piao, Z. (2007). Elevated Blood Lead Levels of Children in Guiyu, an Electronic Waste Recycling Town in China. *Environmental Health Perspectives*, 115(7), 1113–1117. <https://doi.org/10.1289/ehp.9697>
- [12] Zhang, B., Huo, X., Xu, L., Cheng, Z., Cong, X., Lu, X., & Xu, X. (2017). Elevated lead levels from e-waste exposure are linked to decreased olfactory memory in children. *Environmental Pollution*, 231, 1112–1121. <https://doi.org/10.1016/j.envpol.2017.07.015>
- [13] Xu, X., Liu, J., Huang, C., Lu, F., Chiung, Y. M., & Huo, X. (2015). Association of polycyclic aromatic hydrocarbons (PAHs) and lead co-exposure with child physical growth and development in an e-waste recycling town. *Chemosphere*, 139, 295–302. <https://doi.org/10.1016/j.chemosphere.2015.05.080>
- [14] Yang, H., Huo, X., Yekeen, T. A., Zheng, Q., Zheng, M., & Xu, X. (2012). Effects of lead and cadmium exposure from electronic waste on child physical growth. *Environmental Science and Pollution Research*, 20(7), 4441–4447. <https://doi.org/10.1007/s11356-012-1366-2>
- [15] Zeng, X., Xu, X., Boezen, H. M., Vonk, J. M., Wu, W., & Huo, X. (2017). Decreased lung function with mediation of blood parameters linked to e-waste lead and cadmium exposure in preschool children. *Environmental Pollution*, 230, 838–848. <https://doi.org/10.1016/j.envpol.2017.07.014>
- [16] Zhang, L. (2009). From Guiyu to a nationwide policy: e-waste management in China. *Environmental Politics*, 18(6), 981–987. <https://doi.org/10.1080/09644010903345736>
- [17] Murray, A., Skene, K., & Haynes, K. (2015). The Circular Economy: An Interdisciplinary Exploration of the Concept and Application in a Global Context. *Journal of Business Ethics*, 140(3), 369–380. <https://doi.org/10.1007/s10551-015-2693-2>
- [18] Shinkuma, T., & Nguyen Thi Minh Huong. (2009). The flow of E-waste material in the Asian region and a reconsideration of international trade policies on E-waste. *Environmental Impact Assessment Review*, 29(1), 25–31. <https://doi.org/10.1016/j.eiar.2008.04.004>

- [19] Guibrunet, L. (2019). What is “informal” in informal waste management? Insights from the case of waste collection in the Tepito neighbourhood, Mexico City. *Waste Management*, 86, 13–22. <https://doi.org/10.1016/j.wasman.2019.01.021>
- [20] Oduro-Appiah, K., Afful, A., Kotey, V. N., & De Vries, N. (2019). Working with the Informal Service Chain as a Locally Appropriate Strategy for Sustainable Modernization of Municipal Solid Waste Management Systems in Lower-Middle Income Cities: Lessons from Accra, Ghana. *Resources*, 8(1), 12. <https://doi.org/10.3390/resources8010012>
- [21] Miranda, I. T. P., Fidelis, R., de Souza Fidelis, D. A., Pilatti, L. A., & Picinin, C. T. (2020). The Integration of Recycling Cooperatives in the Formal Management of Municipal Solid Waste as a Strategy for the Circular Economy—The Case of Londrina, Brazil. *Sustainability*, 12(24), 10513. <https://doi.org/10.3390/su122410513>
- [22] United Nations Environment Programme. (2006). *Vital Waste Graphics 2* (2nd ed.). United Nations.
- [23] Tong, X., Tao, D., & Lifset, R. (2018). Varieties of business models for post-consumer recycling in China. *Journal of Cleaner Production*, 170, 665–673. <https://doi.org/10.1016/j.jclepro.2017.09.032>
- [24] Zhang, S., Ding, Y., Liu, B., Pan, D., Chang, C. C., & Volinsky, A. A. (2015). Challenges in legislation, recycling system and technical system of waste electrical and electronic equipment in China. *Waste Management*, 45, 361–373. <https://doi.org/10.1016/j.wasman.2015.05.015>
- [25] Wang, Z., Zhang, B., & Guan, D. (2016). Take responsibility for electronic-waste disposal. *Nature*, 536(7614), 23–25. <https://doi.org/10.1038/536023a>
- [26] Wong, M., Wu, S., Deng, W., Yu, X., Luo, Q., Leung, A., Wong, C., Luksemburg, W., & Wong, A. (2007). Export of toxic chemicals – A review of the case of uncontrolled electronic-waste recycling. *Environmental Pollution*, 149(2), 131–140. <https://doi.org/10.1016/j.envpol.2007.01.044>
- [27] Wang, K., Qian, J., & Liu, L. (2020). Understanding Environmental Pollutions of Informal E-Waste Clustering in Global South via Multi-Scalar Regulatory Frameworks: A Case Study of Guiyu Town, China. *International Journal of Environmental Research and Public Health*, 17(8), 2802. <https://doi.org/10.3390/ijerph17082802>
- [28] Sepúlveda, A., Schluep, M., Renaud, F. G., Streicher, M., Kuehr, R., Hagelüken, C., & Gerecke, A. C. (2010). A review of the environmental fate and effects of hazardous substances released from electrical and electronic equipments during recycling: Examples from China and India. *Environmental Impact Assessment Review*, 30(1), 28–41. <https://doi.org/10.1016/j.eiar.2009.04.001>

- [29] Greenpeace & Department of Anthropology at Sun Yat-sen University. (2007, November). 汕头贵屿电子垃圾拆解业的人类学调查报告.
https://www.greenpeace.org.cn/china/Global/china/_planet-2/report/2007/11/guiyu-report.pdf
- [30] Gao, W., & Liu, Y. (2007). Guiyu is still hardly to get rid of an awkward predicament. Investigation Research.
<https://www.ixueshu.com/document/22a17b58bd7ca83f2f35cdacc067a7a7318947a18e7f9386.html>
- [31] Zhou, L., & Xu, Z. (2012). Response to Waste Electrical and Electronic Equipments in China: Legislation, recycling system, and advanced integrated process. Environmental Science & Technology, 46(9), 4713–4724. <https://doi.org/10.1021/es203771m>
- [32] Zhang, L. (2009b). Guiyu, when it can achieve the real Industrial transition? Resource Recycling. <https://d.wanfangdata.com.cn/periodical/ysjszsyly200905006>
- [33] Secretariat of the Basel Convention. (2018, May). Basel convention on the control of transboundary movements of hazardous wastes and their disposal.
http://wiki.ban.org/images/8/84/UNEP-CHW-IMPL-CONVTEXT_-_English.pdf
- [34] Li, Y. (2010, December). E-waste recycling of on the Guiyu case study. University of Lanzhou. <http://d.wanfangdata.com.cn/thesis/Y1703836>
- [35] Wong, N. (2018). Electronic Waste Governance under “One Country, Two Systems”: Hong Kong and Mainland China. International Journal of Environmental Research and Public Health, 15(11), 2347. <https://doi.org/10.3390/ijerph15112347>
- [36] Hu, Y., & Poustie, M. (2018). Urban mining demonstration bases in China: A new approach to the reclamation of resources. Waste Management, 79, 689–699.
<https://doi.org/10.1016/j.wasman.2018.08.032>
- [37] Yu, L., He, W., Li, G., Huang, J., & Zhu, H. (2014). The development of WEEE management and effects of the fund policy for subsidizing WEEE treating in China. Waste Management, 34(9), 1705–1714. <https://doi.org/10.1016/j.wasman.2014.05.012>
- [38] Gmünder, S. (2007, October). Recycling-from waste to resource: Assessment of optimal manual dismantling depth of a desktop PC in china based on eco-efficiency calculations. Swiss Federal Institute of Technology (ETH) and Swiss Federal Laboratories for Materials Testing and Research (EMPA).
<http://citeseerx.ist.psu.edu/viewdoc/download?doi=10.1.1.474.2854&rep=rep1&type=pdf>
- [39] Tong, L., Hai, R., Xie, T., & Sun, Y. (2005). Study on the programming of guangdong Guiyu waste machinery and electronic products disassembly and using demonstration district. China Resources Comprehensive Utilization, 24(6), 4–8.
<https://doi.org/10.3969/j.issn.1672-724X.2005.04.004>

- [40] Kirby, P. W. (2019). Materialities meet the mangle: Electronic waste scavenging in Japan and China. *Geoforum*, 102, 48–56. <https://doi.org/10.1016/j.geoforum.2019.03.011>
- [41] Lines, K., Garside, B., Sinha, S., & Fedorenko, I. (2016, March). Clean and inclusive? Recycling e-waste in China and India. International Institute for Environment and Development. <https://greene.gov.in/wp-content/uploads/2018/01/IIED-Recycling-E-waste-in-China-and-India.pdf>
- [42] Tuncuk, A., Stazi, V., Akcil, A., Yazici, E., & Deveci, H. (2012). Aqueous metal recovery techniques from e-scrap: Hydrometallurgy in recycling. *Minerals Engineering*, 25(1), 28–37. <https://doi.org/10.1016/j.mineng.2011.09.019>
- [43] Huang, K., Guo, J., & Xu, Z. (2009). Recycling of waste printed circuit boards: A review of current technologies and treatment status in China. *Journal of Hazardous Materials*, 164(2–3), 399–408. <https://doi.org/10.1016/j.jhazmat.2008.08.051>
- [44] Lei, Z., Liu, F.-, & Zhang, P.-. (16 C.E.). 顶吹炉处理废旧印刷电路板的生产实践. *Nonferrous Metals (Extractive Metallurgy)*, 22, 20–22. <https://doi.org/10.3969/j.issn.1007-7545.2016.12.006>
- [45] Ministry of Ecology and Environment of the People’s Republic of China. (2019, August 28). 疏堵结合 “电子垃圾之都”转型跨越—广东汕头市贵屿镇“散乱污”综合整治实践. https://www.mee.gov.cn/xxgk2018/xxgk/xxgk15/201908/t20190828_730337.html
- [46] Management Committee of Guiyu Circular Economy Industrial Park. (2020). Departmental budget of the administrative committee of Guiyu circular economy industrial park. <http://www.gdcy.gov.cn/attachment/0/9/9240/1770384.pdf>
- [47] Balde, C. P., Forti, V., Gray, V., Kuehr, R., & Stegmann, P. (2017). The global e-waste monitor 2017: Quantities, flows and resources [E-book]. United Nations University, International Telecommunication Union, and International Solid Waste Association. <https://www.itu.int/en/ITU-D/Climate-Change/Documents/GEM%202017/Global-E-waste%20Monitor%202017%20.pdf>
- [48] Oliveira, C. R. D., Bernardes, A. M., & Gerbase, A. E. (2012). Collection and recycling of electronic scrap: A worldwide overview and comparison with the Brazilian situation. *Waste Management*, 32(8), 1592–1610. <https://doi.org/10.1016/j.wasman.2012.04.003>
- [49] Greenpeace & China Association of Electronics for Technology Development. (2019, March). The potentiality of the circular economy of waste electronic products in China. <https://www.greenpeace.org.cn/the-potentiality-of-the-circular-economy-of-waste-electronic-products-in-china-report/>
- [50] Zeng, X., Duan, H., Wang, F., & Li, J. (2017). Examining environmental management of e-waste: China’s experience and lessons. *Renewable and Sustainable Energy Reviews*, 72, 1076–1082. <https://doi.org/10.1016/j.rser.2016.10.015>

- [51] World Economic Forum. (2019, January). A new circular vision for electronics: Time for a global reboot. http://www3.weforum.org/docs/WEF_A_New_Circular_Vision_for_Electronics.pdf
- [51] Tong, X., Lifset, R., & Lindhqvist, T. (2004). Extended Producer Responsibility in China: Where Is “Best Practice”? *Journal of Industrial Ecology*, 8(4), 6–9. <https://doi.org/10.1162/1088198043630423>
- [52] Hicks, C., Dietmar, R., & Eugster, M. (2005). The recycling and disposal of electrical and electronic waste in China—legislative and market responses. *Environmental Impact Assessment Review*, 25(5), 459–471. <https://doi.org/10.1016/j.eiar.2005.04.007>
- [53] Kojima, M., Yoshida, A., & Sasaki, S. (2009). Difficulties in applying extended producer responsibility policies in developing countries: case studies in e-waste recycling in China and Thailand. *Journal of Material Cycles and Waste Management*, 11(3), 263–269. <https://doi.org/10.1007/s10163-009-0240-x>
- [54] Cao, J., Lu, B., Chen, Y., Zhang, X., Zhai, G., Zhou, G., Jiang, B., & Schnoor, J. L. (2016). Extended producer responsibility system in China improves e-waste recycling: Government policies, enterprise, and public awareness. *Renewable and Sustainable Energy Reviews*, 62, 882–894. <https://doi.org/10.1016/j.rser.2016.04.078>
- [55] Sasaki, S. (2020). The effects on Thailand of China’s import restrictions on waste: measures and challenges related to the international recycling of waste plastic and e-waste. *Journal of Material Cycles and Waste Management*, 23(1), 77–83. <https://doi.org/10.1007/s10163-020-01113-3>
- [56] Wang, F., Huisman, J., Meskers, C. E., Schluep, M., Stevels, A., & Hagelüken, C. (2012). The Best-of-2-Worlds philosophy: Developing local dismantling and global infrastructure network for sustainable e-waste treatment in emerging economies. *Waste Management*, 32(11), 2134–2146. <https://doi.org/10.1016/j.wasman.2012.03.029>
- [57] Schulz, Y., & Lora-Wainwright, A. (2019). In the Name of Circularity: Environmental Improvement and Business Slowdown in a Chinese Recycling Hub. *Worldwide Waste: Journal of Interdisciplinary Studies*, 2(1), 1–13. <https://doi.org/10.5334/wwwj.28>

7. MOTIVATING STUDENTS BY CONTEXTUALIZING SUSTAINABILITY IN INTERDISCIPLINARY GRADUATE PROGRAM OR K-12 CLASSROOM

The following chapter, with journal permissions, significantly reuses the material originally published in Wang, C., Clarkson, C. M., Andler, J., Korey, M., Frost, K. D., Reeves, M. S., Handwerker, C. A. (2020). Lessons Learned from the NSF IGERT Program: Cultivating Student Motivation in the Interdisciplinary and International Contexts. *2020 ASEE Virtual Annual Conference & Exposition Proceedings*. (doi:10.18260/1-2-34912) and Wang, C., Dandridge, T., Cardella, M. E., Handwerker, C. A. (2019). Work In Progress: Integrating Sustainability Engineering Education and Design into the K-12 Classroom: A Case Study in Electronics Recycling for Middle-School Youth. *2019 ASEE Annual Conference & Exposition Proceedings*. (doi:10.18260/1-2-32227).

7.1 Introduction to sustainability education and challenges

The emerging call for future engineers with global-citizen mindsets, inside the field of sustainability, asks for a re-evaluation of current educational experiences provided in higher education [1]. Sustainability is traditionally covered by civil engineering [2], environmental engineering [3], and chemical engineering [4] and is now extended to a broader discipline, e.g., software engineering [5]. Scholars have identified the three pillars of sustainability as environmental, economic, and societal, making it a multidisciplinary subject [3]. Apart from international learning experiences, interdisciplinary curricular development in higher education has attracted many educators' attention and was reported to be suitable for topics that require inputs from both STEM and non-STEM fields, such as sustainability [6]. Many universities have also integrated sustainability content into current engineering education to cultivate students who can deal with the societal and economic perspectives associated with technology advancement [7,8]. Apart from the challenges of sustainability education include the misconception resulted from the ignorance of societal and economic effects [9, 10], insufficient resources and training for educators, and lack of motivations for students to participate in sustainability-related activities also hindered sustainability education [11].

7.2 Case study 1: Cultivating student motivation in Interdisciplinary Graduate Education and Research Traineeship (IGERT) on Sustainable Electronics

In light of this emphasis on integrating sustainability in STEM education and addressing above-mentioned challenges, the Interdisciplinary Graduate Education and Research Traineeship (IGERT) program was developed by the National Science Foundation as a traineeship that prepares graduate students to enter the workforce by focusing on collaborative, interdisciplinary training. A multi-year traineeship was established at Purdue and Tuskegee Universities and is focused on sustainable electronics. Graduate student trainees conduct research in fields relevant to electronics and sustainability and take four classes in addition to participating in annual workshops, domestic industry trips and an international trip to India. Of the three cohorts sponsored by the program, the final IGERT cohort went beyond the original programming of the curricula. For instance, when their final class was canceled due to a professor's sabbatical, the class proposed a student-led seminar class in which the curriculum was designed to fill in the student-reported knowledge gaps from the cohort. This research will focus on the experiences of the third, final cohort from the IGERT which exhibited a high level of self-motivation throughout their tenure.

7.2.1 Overview of the NSF IGERT program in sustainable electronics

This section provides an overview of the last cohort's experience in the IGERT program in sustainable electronics.

7.2.1.1 Class structure

The IGERT trainees were located at two different universities, separated by 670 miles. The trainees are required to take four classes that focus on sustainable electronics. The students in each university assembled in a classroom with at least one faculty member and the class was conducted through WebEx. The first two classes, Design for Global Sustainability I and II (DGS-I or DGS-II), served as the foundation for learning; topics included sustainability, general processing and manufacturing knowledge of electronics, and policies and regulations for waste management. The third class on life cycle assessment (LCA) focused on understanding the environmental and economic implications of products by monitoring all inputs and outputs of a system. The final class focused on applying the knowledge of the previous classes to a research topic of interest. This class looked different depending on the cohort as cohort 3 created their own class. Since the

third cohort's experiences are the subject of the present paper, this topic will be discussed in depth in the subsequent section in Examples of Student-Driven Programming.

7.2.1.2 Domestic workshops

Early in the first semester of classes, the students and faculty from Purdue and Tuskegee Universities visited three companies in Indianapolis. The goal was to understand the electronics supply chain and the role of sustainability in each of the companies and to give the members of the cohort an opportunity to meet and form deeper relationships than in distance collaborations during the class. This field trip was important for the IGERT cohort as (1) it was the first physical exposure to electronics manufacturing, recycling, and business strategy for most trainees, and (2) the students were able to interact with peers in an informal setting.

7.2.1.3 International workshops

The summer after the first year of the program was spent visiting different companies and organizations in India to learn more about electronics manufacturing, policy, and recycling. The students met with chief officers, owners, directors, workers, and students from various businesses, colleges, and non-governmental organizations near New Delhi, Jaipur, and Udaipur. For each visit, two students were assigned to lead the discussions and to provide the detailed information and context of the subject of matter to the group prior to the visit. The students learned how electronic materials are made, how electronic elements are mined and recycled, what it takes to build a successful business, how organizations give back to the community and much more related topics. To gain an appreciation and deeper understanding of what was learned or experienced throughout the day, the students would discuss and record critical incident assessments (CIA) as a group [12]. These assessments consisted of a structured discussion on a specific event that had some memorable or lasting impact where we thought valuable lessons could be learned or interesting insights could be shared.

7.2.1.4 Examples of student-driven programming

1. Self-organized seminar course. Design for Global Sustainability III (DGS-III) was a student-led seminar course expanding on prior knowledge concerning electronic sustainability. In this seminar, students taught each other about sustainable

electronics topics relevant to their research and passions. Students developed the syllabus, prepared presentations and homework, and invited external speakers to derive maximal value from the course. For example, classes were composed of targeted group discussions, innovative sustainability seminars related to members' theses, and interacting with Congress where the class participated in lobbying with a member of congress. The opportunity for students to propose, design, and implement their own seminar course presented itself when the final structured class became logistically impossible for a portion of the distance learning students.

2. Mentoring the LOREX students. IGERT trainees advised approximately thirty students from different geographic regions participating in international research internships through the Limnology and Oceanography Research Exchange (LOREX) program at Umea University, Sweden. These internships are hosted at six different locations with the purpose of providing training in international research for graduate students. IGERT trainees advised these students on the concept and execution of a CIA to enhance cultural learning during their international experience. The CIA was subsequently adapted by the LOREX students into a blog post describing various incidents throughout their research experience abroad.
3. Puerto Rico workshop. Additionally, as the final workshop for the IGERT program, the same cohort of students planned a second field trip on their own to study resilience in the electronics supply chain in Puerto Rico after Hurricane Maria. The students designed a two-week pre-trip seminar course and were responsible for developing the syllabus, identifying learning objectives, locating the contacts, preparing learning materials for peers, building a trip itinerary, and leading the discussions on-site. The third cohort also invited all IGERT alumni to participate in the workshop in Puerto Rico.

7.2.2 Research questions

Considering the international and interdisciplinary setting for the IGERT program, it is natural to assume the self-driven activities were related to this setting. However, few studies with similar learning settings reported how student motivation changed. With limited literature on

interdisciplinary or international programs that affect student motivation, the teaching practices that led the third IGERT cohort to be self-motivated are valuable to identify. Therefore, this paper is guided by two questions: "What kind of motivation were exhibited and changed throughout the IGERT program?" and "If changed, what projects or educational experiences triggered it?"

7.2.3 Conceptual framework

7.2.3.1 Self-determination Theory

What learning motivation is and how it may be stimulated has been a long-established research topic in learning theories over the past century developed with both cognitive theories and behavioral theories. Concluding from a series of experiments of trial and error on cats, [13] discovered that positive reinforcement, i.e., rewards, were much more effective in motivating cats to emit a desirable behavior than punishment. This is the view of motivation from the early behaviorism. Later on, the goal setting theories emerged and established a primary relationship between conscious goals and motivations, i.e., people who are more likely to achieve those goals developed higher levels of motivation [14, 15]. Also, building upon the law of effect theory [13], [16], in his operant conditioning theory, regarded motivation as a result of a series of (positive) responses one received on his specific behavior. It is obvious that the early stage of the development of motivation theories is closely related to psychology, particular to behaviorism. On the other hand, though the "autonomy" was reported as a critical factor in motivation back in 1960s [17], it had not attracted enough attention until the self-determination theory (SDT) occurred for the purpose of explaining intrinsic motivations and extrinsic motivations [18], which holds true for the expectancy theory [19] as well. On the one hand, self-determination theory later gained the public attention and has been supported by experimental studies over 30 years. For example, [20] proposed a hierarchical model of intrinsic motivation based on the SDT where a person can possess multiple levels of motivations depending on the external environment. On the other hand, the real-life applications and teaching practices has been scarce compared to the Theoretical studies behind SDT. To summarize, self-determination theory is well-developed, is closely related to some of the previous theories, and should still benefit from the inputs from practical studies. Therefore, the SDT has been selected as the main theory which contribute to the main skeleton of this Theoretical framework.

For self-determination theories, three elements will be included which are autonomy, the feeling one's behavior is self-determined and fosters intrinsic motivation; competency, the social-contextual events - i.e. feedback and rewards - that contribute to feeling qualified or skilled; and relatedness, the sense of security and connection in interpersonal settings.

7.2.3.2 Expectancy-Value Model

Expectancy-value model is another well-developed branch of motivation theories. As mentioned earlier, [19] brought up expectancy as a motivation driver. The expectancy theory detoured from the positive reinforcement (i.e., the reward) theory [13] because the expectancy theory claimed that it is individual's prediction or evaluation on how likely he can get the desired reward that matters instead of the reward itself. There is also, to some extent, a connection existing between the achievement theory and the expectancy theory. As for the value factor, Bruner, in his work *The Process of Education* emphasized the importance of the value of the knowledge taught: Bruner instructed that the best way to stimulate interests is to make knowledge usable, which is the role of the structure of curricula plays [21].

Perhaps the most detailed explanation for the expectancy-value model is provided by [22], which focused on both children's learning and adults' beliefs from a developmental perspective of view. These papers discussed the theoretical explanations upon which people make decisions (or get motivated) based on their expectancy and how useful they see the knowledge will be in their future lives as a member of the society. The expectancy-value theory has been generally supported by current studies. For example, a study examining the acquisition of the spatial skills found that the interviews who considered spatial skills to be of great importance in various engineering practices or who were curious about their competence in those skills, demonstrated better performance and stronger intrinsic motivations. In recent years, an extension theory, expectancy-value-cost model, has been developed in [23] where the predicted or expected efforts (i.e., the cost) needed to achieve the goal also impact individuals' motivation, but in a negative direction.

Because the "expectancy" factor resembles the "competence" in the self-determination theory and the "cost" is oftentimes categorized into the "value" factor, only the "value" factor is incorporated into our theoretical framework. In summary, four factors in motivation theory have been selected, i.e., value, relatedness, competence, and autonomy, as the reference for guiding the research question.

7.2.4 Methodology

There were 11 graduate students in the third cohort in IGERT who majored in materials engineering, anthropology, math, and environmental and ecological engineering at Purdue University or Tuskegee University when the traineeship started in 2016. A Qualtrics survey was developed to collect students' opinions and feedback about the IGERT program in the context of student motivation through autonomy, competence, relatedness, and values. Survey questions consisted of matrix questions, Likert scale questions, ranking questions, and open-ended response questions which can be found in the supplemental information. The survey was distributed to the 9 students who were enrolled at the end of the program (cohort 3) and one student from cohort 1 who chose to participate in the Puerto Rico workshop. The authors received 9 responses (response rate 90%). Demographic variables such as gender and age were excluded from the survey.

7.2.5 Internalization of student motivation

Students were asked about why they participated in three representative projects (India workshop, DGS-III, and the Puerto Rico workshop), arranged chronologically, during the program: was it because of their own interests, or the expectations from the faculty and peers? The options provided cover two major categories in motivation theory, i.e., intrinsic motivation (internal interests) and extrinsic motivation (external expectations). The results illustrated in Fig. 7.1 reveals that the majority of the students were motivated by both intrinsic and extrinsic factors. Notably, the importance of the expectations from the faculty, an extrinsic factor in student motivation, showed a declining trend, indicating trainees being able to internalize extrinsic motivations at a later stage of the program. On the other side, the importance of the expectations from the peers, another extrinsic factor, increased for the seminar class and Puerto Rico workshop compared to the India workshop. A successful multi-year program may consider offering ample opportunities for students to internalize extrinsic motivation.

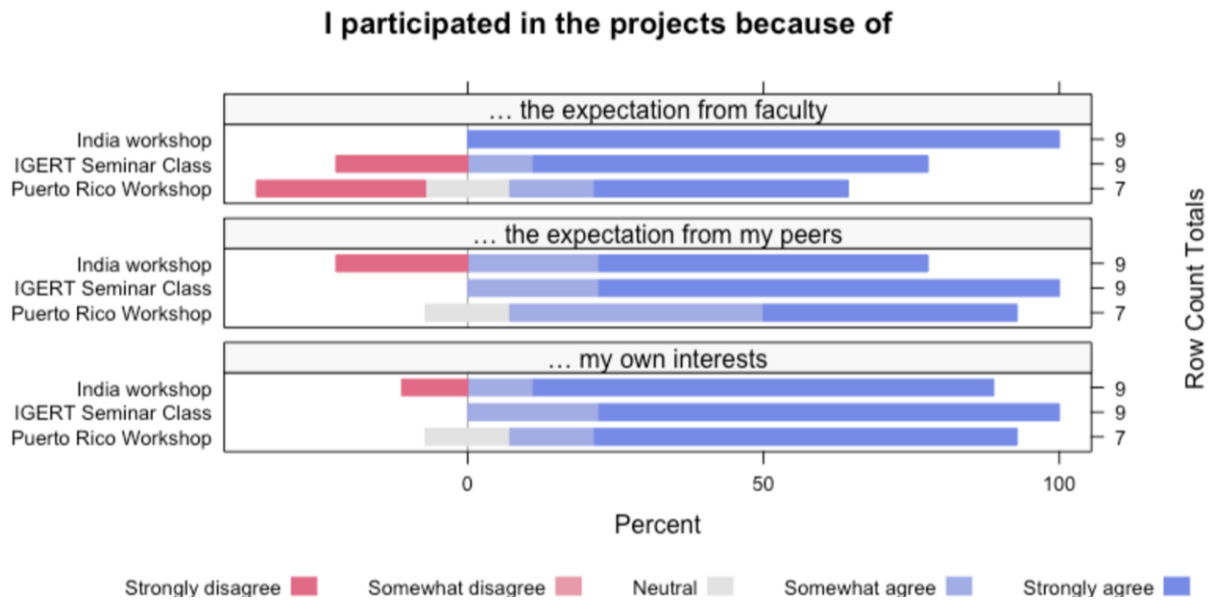
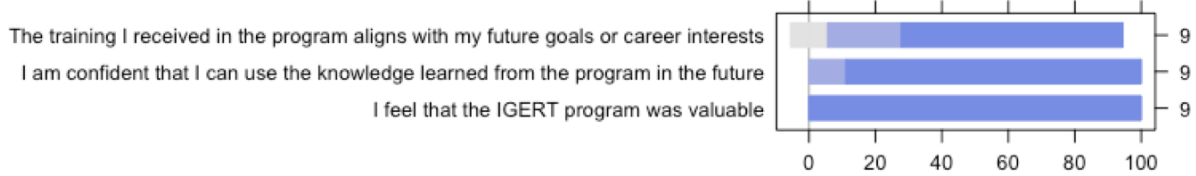


Figure 7.1. Overview of the changes in students' motivation for major self-organized projects throughout the IGERT program.

As shown in Fig. 7.2(a), all students responded they strongly agreed with the statement that the IGERT program was valuable; all students agreed that they could use the knowledge they learned in the program in the future; all students agreed that the training provided by the IGERT program aligned with their career goals and interests. Overall, the participants were able to see the value of the IGERT program from different perspectives.

To avoid ambiguity, three core values designed to be delivered by the IGERT program were explicitly described in the survey. Survey responses indicated a trend that students were more likely to agree with them after the program, as shown in Fig. 7.2(b), which also suggests a successful teaching outcome of the IGERT program.

(a) Students' perceptions of the value of the IGERT program



(b) How strongly you believed in the following statements before and after the IGERT program?

- #1 Sustainability is essential for present and future individuals and should be systematically embedded into all disciplines
- #2 Interdisciplinary collaboration is essential to solving the complex, intersectional challenges associated with sustainability
- #3 International collaboration is essential to breaking barriers and creating more sustainable practices globally

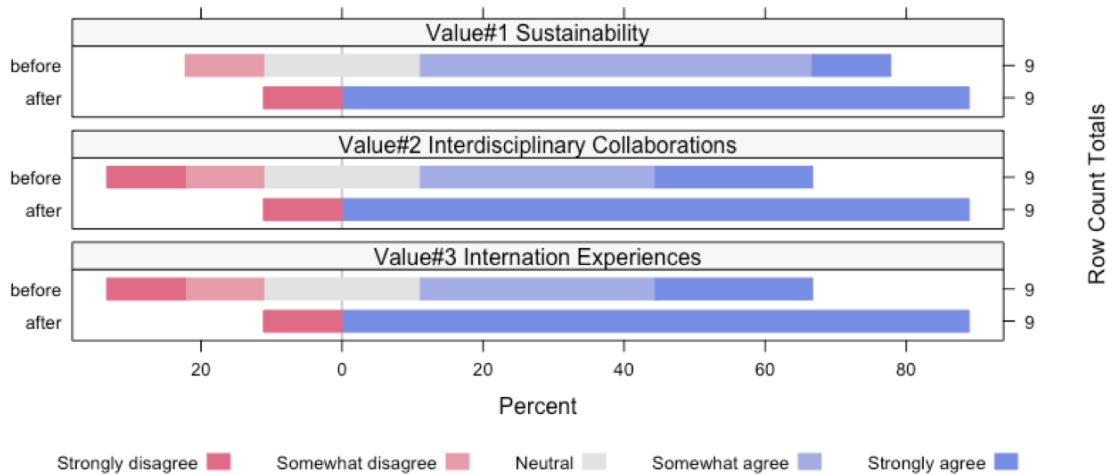


Figure 7.2. (a) The values of IGERT in sustainable electronics were well-perceived by the participants. (b) Students understood the three core values of IGERT in sustainable electronics deeper throughout the program.

The majority of respondents believed that they shared a common vision and set of values with their primary advisor, and that their advisor shared a common vision with other faculty in the program (see Fig. 7.3). Considering the sheer number of different disciplines from engineering, economic, and societal sectors involved in the program and the non-traditional format of its structure, it is fair to claim that the IGERT in sustainable electronics program offered a cohesive and positive learning environment.

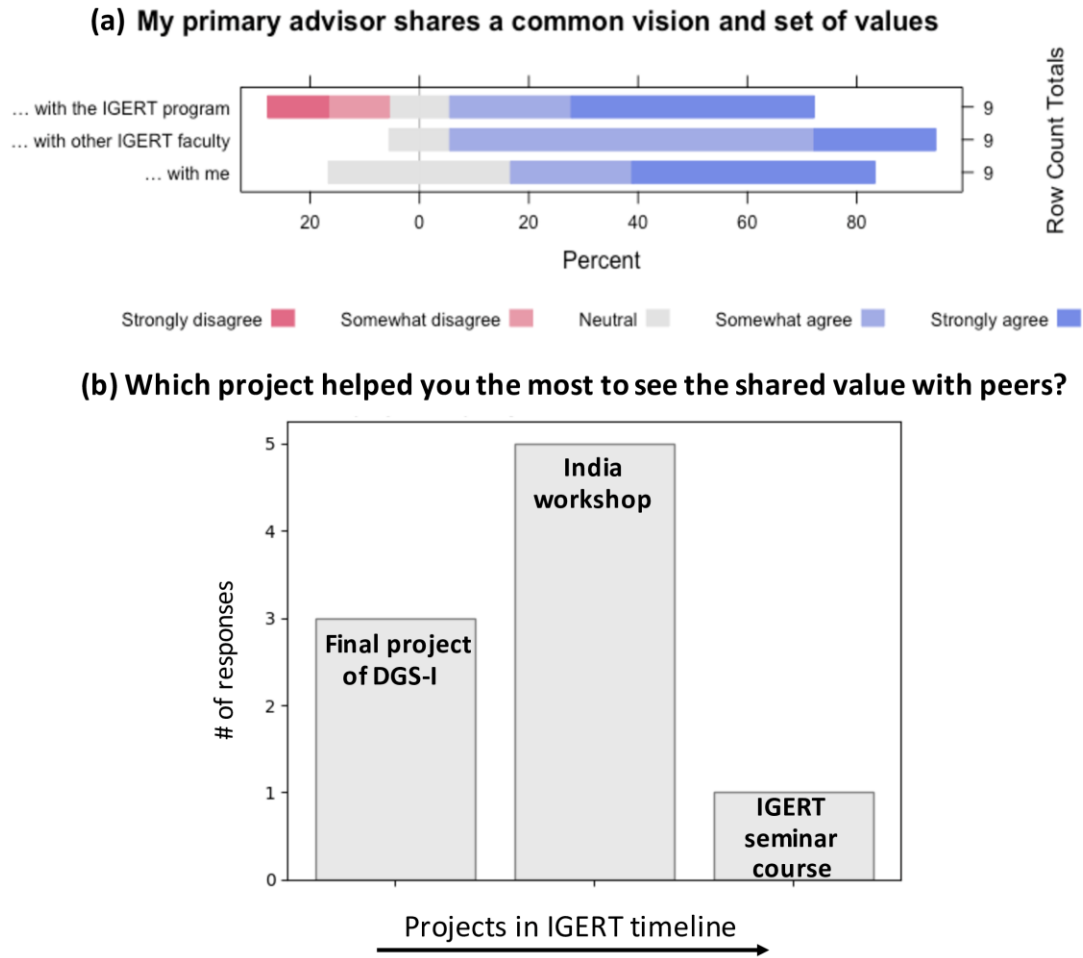


Figure 7.3. (a) Values that between students and faculty and between faculty and program are in great alignment, creating a benign environment to grow relatedness within the program. (b) The majority of the students started to see the shared value among the cohort after the international learning experience in India or the collaborative projects required in an interdisciplinary course.

As previously shown in Fig. 7.2(b), the trainees' value evolved with the program. It is, therefore, of interest to investigate what projects made students start to realize a set of shared values with their peers and how this transition occurred. As shown in Fig. 7.3(b), the majority of the participants identified the India workshop as the turning point. Three students responded that they started to see the shared values, earlier than the India workshop, during the collaborative project of DGS-I, upon finishing the first semester.

Comparing the competence factor of student motivation in an early learning experience, the India workshop, and a final experience, the Puerto Rico workshop, the responses in Fig. 7.4 exhibited a strong trend of increasing competence in participating in group activities over their

tenure in the IGERT program. For the three activities surveyed, most students reported that they felt confident or qualified to participate in group discussions, lead group discussions, and schedule and plan meetings during the Puerto Rico trip. Whereas for the India trip, the positive responses in each question were notably lower.

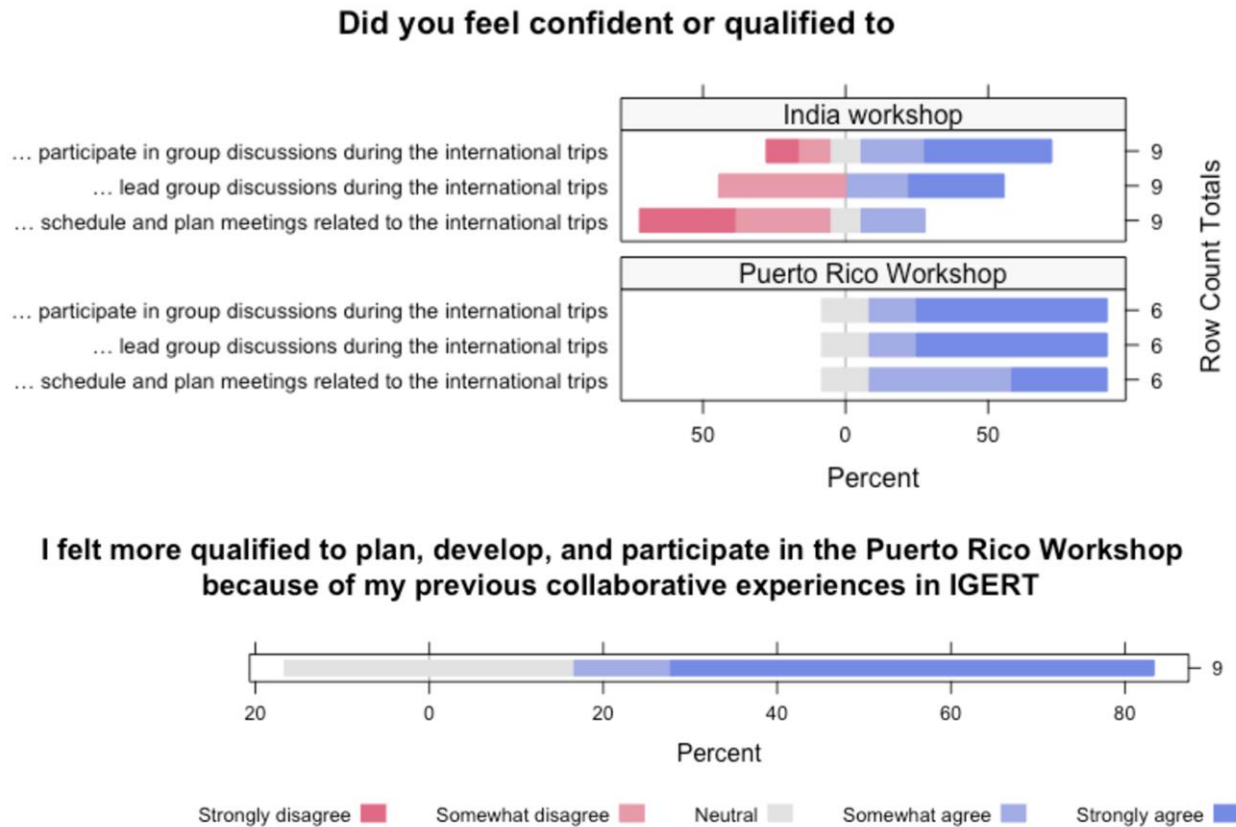


Figure 7.4. Near the end of the IGERT program, students were more confident and qualified to participate in various activities including the planning and preparation of optional projects beyond the original programming. Students reported a higher level of confidence in dealing with projects at a later stage due to previous collaborative experiences.

Most students agreed that they felt more qualified to participate in, develop, and plan the Puerto Rico workshop due to previous learning experiences in the IGERT program, (see Fig. 7.4). The India workshop is classified as one of these educational experiences which promoted future growth.

The results demonstrated that the IGERT trainees and faculty possessed a common set of values that not only existed when launching the program, but also were reinforced by the program.

Those values, originally being intrinsic motivation, later echoed with internalized extrinsic motivation [18]. A relevant question is when and how the internalization of external values and the conceptualization of shared values took place in current teaching practices. The results shown in Fig. 7.4 shed light on two potential answers: collaborative, problem-based learning (the final project of DGS-I) and intercultural experiences (India workshop).

The purpose of the India trip was to gain an understanding and appreciation of all the stakeholders in the global electronics supply chain. Meeting with people from NGOs, businesses, and other organizations gave the IGERT cohort a thorough understanding of the work necessary to build electronic products, uphold policies, or manage international businesses. Not only was discussing business logistics with upper management and observing the labor of employees educational from an academic perspective, but the meetings also allowed for an appreciation of the influence of corporate social responsibility (CSR) on the community. An equally important aspect of the trip were the discussions, both extemporaneous and those generated by the CIA forms. The perspectives introduced in these discussions were not always similar, and it was valuable to have an educated and constructive conversation about shared experiences. By the conclusion of the trip, the IGERT cohort was able to gain an understanding of employee-employer relationships, effective corporate models, and the impact of policies and education on the environment. These lessons directly relate to our understanding of electronics sustainability – socially, economically, and environmentally.

The India workshop, as shown in Fig. 7.4(b), helped the majority of the last cohort realize the shared value with the group. Some earlier studies on international experiences that had a positive influence on student motivation may provide insights on what IGERT's India workshop did correctly. Arzberger et al. [24] provided an all-round analysis of PRIME (Pacific Rim Experience for Undergraduates), a four-year international, research-oriented, and sustainable program. The goal was to train undergraduate students as global professionals and equip students with global citizen mindsets through collaboration between research institutes and industries across cultures and disciplines. One key feature of the PRIME program is that students are required to initiate the discussion on potential research topics they are interested in with mentors. In another study, Layer and Gwaltney [25] reported an international capstone program in which students were bestowed with a sense of difference-making when they completed the assigned projects, as those projects originated from actual industrial or societal needs. The study considered many cultural

aspects, such as cultural awareness, as both inputs and outcomes. Meanwhile, the post-project survey demonstrated a substantial increase in students' understanding of attributes that are indirectly related to intercultural differences such as global awareness and emotional experience. Particularly, the motivation attribute (i.e., students' motivation to learn) was significantly enhanced in this learning experience.

The emphasis on group discussion, global citizen mindsets, and cultural awareness in these two studies resembles the purpose of the IGERT India trip. As earlier introduced in the background section, the students were required to discuss and record critical incident assessments (CIAs) as a group on a daily basis to gain a deeper understanding of incidents taking into consideration cultural differences and emotional responses [26-27]. More importantly, the IGERT India trip aimed to prepare the students with toolboxes for navigating cultural differences. Though no students identified this preparation work (pre-meetings and presentations) as the turning point, it is an essential step in laying the groundwork for effective learning. The planning of the trip in which few students participated, was carefully handled by the faculty so that students would visit companies or organizations in India that were similar to the previous visits in the U.S.A. Building the connections between clustered experiences ensured the quality of this intercultural learning experience, which reflected Dewey's classical philosophy on experience and education [28]. By the end of this trip, the last cohort had insightful discussions on almost every aspect of the trip including similarity in corporation models, differences in culture, and inspiring businesses with a dedication to the community in relation to economic, environmental, or social sustainability. Several responses from IGERT trainees on the India trip collected by our survey are quoted below:

"The IGERT India Trip on a whole was certainly a defining moment of my educational experience, ... the numerous opportunities to meet with stakeholders first-hand, and to see various aspects of the electronics supply chain in person, were invaluable in bringing the concepts we had studied into concrete terms and highlighting the urgency and importance of working toward sustainable practices."

"I don't think I saw how any of the knowledge we had been taught in class really applied until we went on the India trip. Everything we saw on our domestic trips while providing insight, was kind of what I expected it to be... This trip made me realize the bigger picture and the severity of the challenges faced in..."

"For instance, visiting Heritage [in a previous domestic field trip] was really inspiring to me because... This (same) idea was seen multiple times in India where it is much easier due to lower regulations to use..."

Shared value, or relatedness, is likely to be conceptualized with intercultural communication of scientific outcomes that were cultivated via sequential training on cultural awareness and stakeholder perspectives taking place throughout the entire program. Student-initiated discussions or reflections through the adapted methods of CIA provided a supervised and secure space for this communication to occur.

7.2.6 Contextualization of sustainability education via problem-based learning (PBL)

The DSG-I project marked the first collaborative experience for the IGERT trainees in a professional setting. The final project of DGS-I was named "Project X," meaning the students were free to choose any subject-matter, as long as the subject was under the electronics umbrella, for this collaborative assignment. The goal of the semester-long team research project is to apply the sustainability concepts learned in the classroom or self-study to a specific class of electronic products. Students were required to analyze the product "X" in terms of societal, environmental, and industrial/economic sectors, and the opportunities for greater value recovery. Naturally, students considered real-life questions such as how it was designed by the engineers, how it was sold by retailers, and how it was used by the customers and the real-life challenges caused by any of those questions.

Perhaps because the majority of current interdisciplinary programs and project/problem-based learning cases aim to bring real-world challenges into the classroom, an overlapped region clearly exists between the two research fields [29-33]. For example, Kuo et al. [30] proposed the concept of Interdisciplinary Project-Based Learning (IPBL): Motivated Strategies for Learning Questionnaire which was used to evaluate the participant's perception of learning motivation via three subscales: self-efficacy, the joyfulness of learning, and valuing the significance of learning on future career development. Within the time frame of 18 weeks, guided by design thinking, the IPBL approach was reported to have significant impacts on student's learning motivation. Bischof et al. [33] argued that project-based learning employed in mathematics courses would be especially useful to engineering students because it is crucial to have engineering students understand how mathematics can help them with their future studies and professional careers. The selected problems all included at least one section needed to be solved with mathematics knowledge that was slightly beyond their current abilities. Confronted with those challenging problems, students realized the gaps between their understanding of engineering mathematics and the knowledge

required to solve real-life problems with industry (for example, joint research with BMW). This realization, in turn, motivated students to devote time and energy to learn mathematics. Note that this program carefully re-designed the curriculum of engineering mathematics so that its contents were of students' interests and could be directly applied to their future studies.

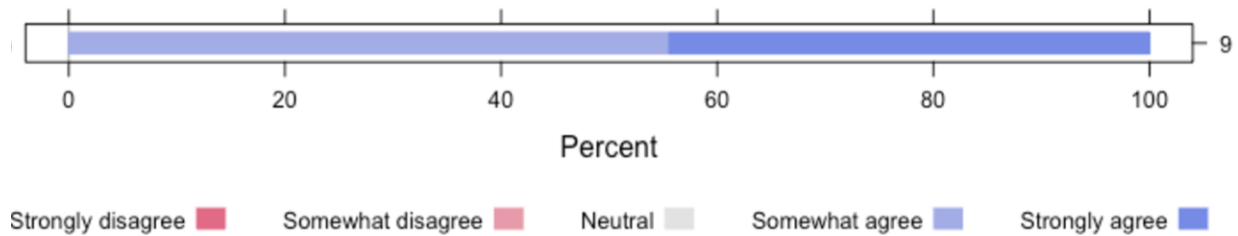
One of the written responses from IGERT participants, when asked what aspect was most valuable, also provides evidence to Bischof's conclusion [33]:

"The work I conduct within my program department (Mathematics) is highly specialized and very technical in nature, and it can be very easy to lose sight of practical applications... The IGERT program provided a much-needed opportunity to expand my research perspective and helped to open my mind to a number of different interdisciplinary research collaborations that broadened the scope of my research and thinking in general."

For an interdisciplinary curriculum, apart from educational institutes, other collaborators include government agencies, industries, and nonprofit organizations. Under the framework of project-based learning, the program not only introduced real-world issues to students, but also sought opportunities to transfer students' solutions into applications, which in turn, would help students see the value of the projects and see the shared value among peers, and ultimately motivate students by building the value system and group relatedness within the program.

In the India workshop, students were more involved in passive learning experiences (participation in the group discussion) compared with active ones (planning of the activities). To investigate the role autonomy played throughout the program, students were asked if they felt they had control over the IGERT program. These data are shown in Fig. 7.5(a). Autonomy as a salient feature in the IGERT program is evidenced by the overwhelmingly positive feedback. Most students picked "upon finishing the second-year courses" as the time when they felt autonomy in the IGERT program. The students reported the IGERT self-designed seminar course (DGS-III) as the most helpful project to develop their sense of autonomy. These data are consistent with a growing sense of autonomy regarding the planning of shared experiences, also shown in Fig. 7.6(a).

**(a) Although I was a student in the IGERT program,
I feel like I was part of designing it**



(b) If so, which project helped you feel comfortable to do so?

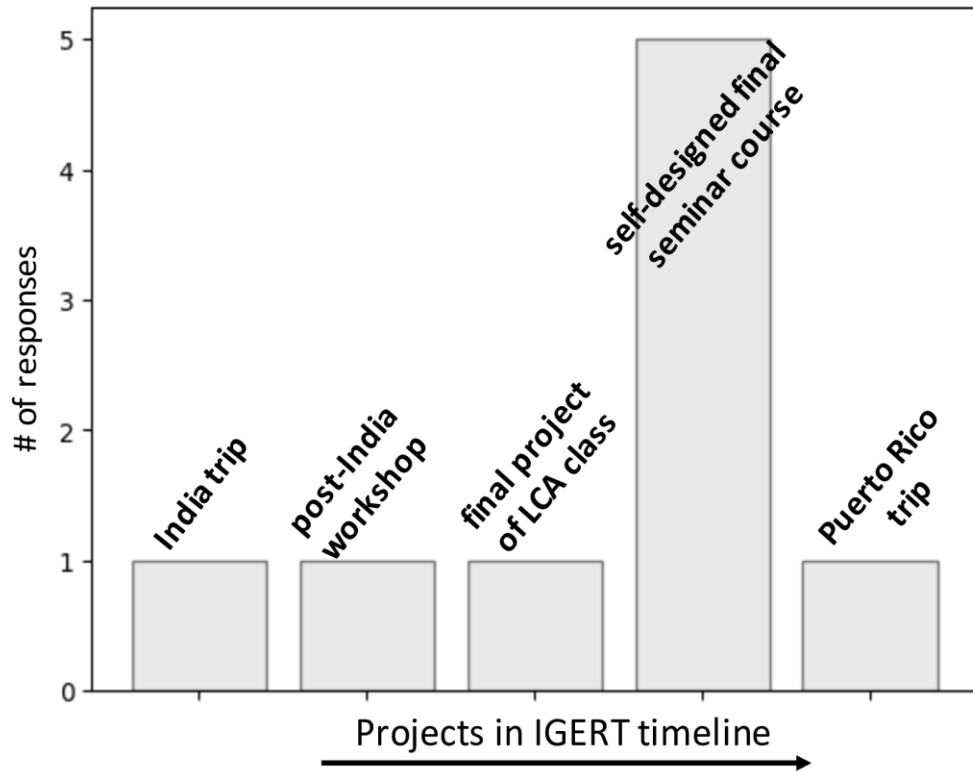


Figure 7.5. (a) All students believed that they were involved in the design of the IGERT program. (b-c) A large portion of the students identified the self-designed seminar course as the starting point.

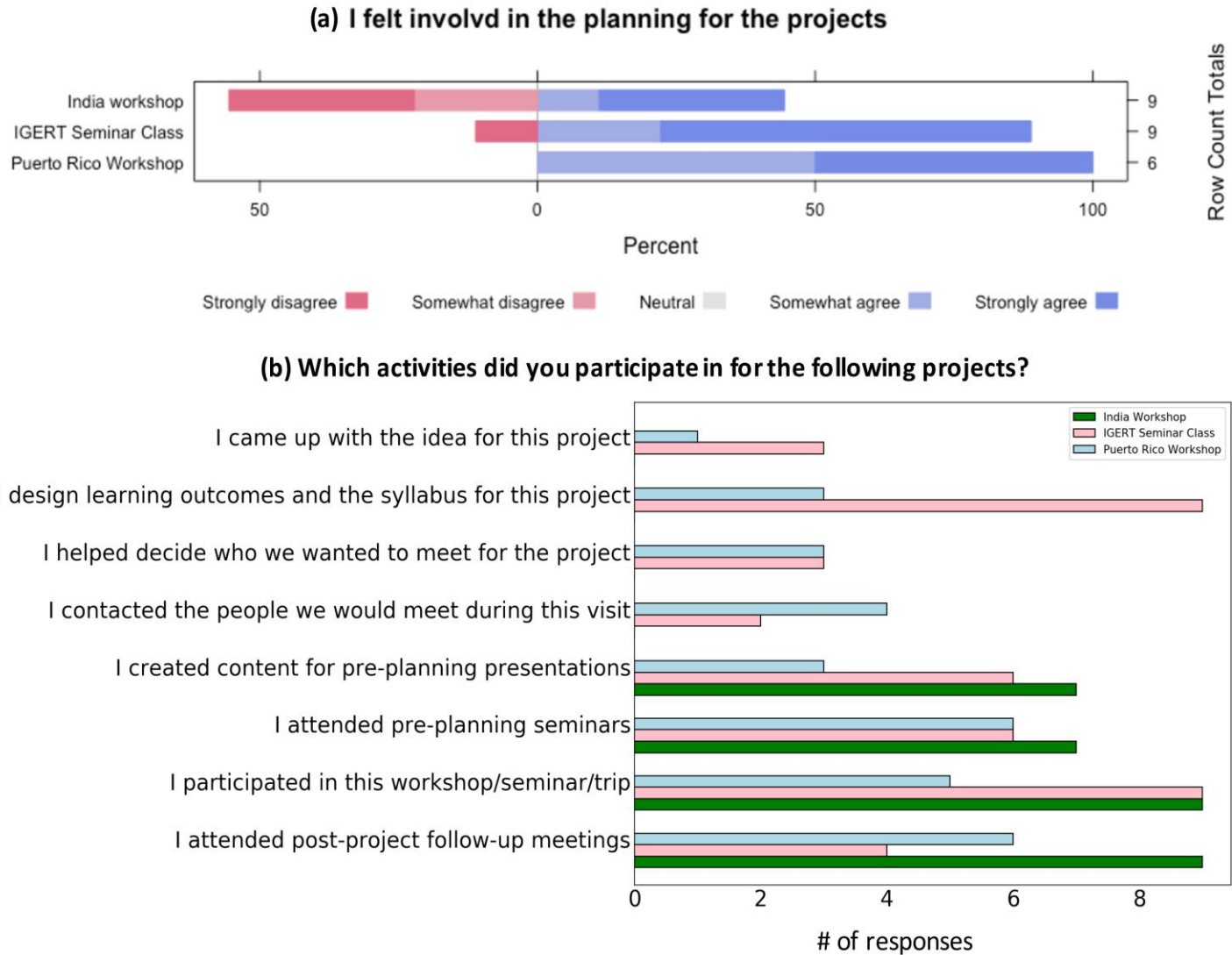


Figure 7.6. (a) Students were more involved in later learning experiences than earlier ones. (b) Students actively participated in the preparation and planning of the self-organized seminar course and self-organized Puerto Rico field trip.

To tie the students' feeling of autonomy to specific projects, students were asked to select their participation in activities related to the IGERT programming. Students reported more autonomy with developing and logistically planning their learning objectives over the duration of the IGERT program, as shown in Fig. 7.6(b). For example, of the students who participated, some students felt involved in the India workshop planning, most students felt involved in the seminar class planning, and all students who participated felt involved in the Puerto Rico workshop planning. A slow, but steadily increasing exposure to autonomous behaviors may help facilitate motivation regarding new behaviors and experiences. A steadily increasing exposure first introduces students to a working knowledge of the subject. After a basic understanding is developed, allowing creative adaptation of the main goals of the project can help students redefine these goals in their own terms. This creative adaptation is the autonomy necessary for motivation – having a clear concept for how to proceed. The IGERT program helped to facilitate autonomous feelings and behavior in the students by having them create and refine their learning objectives after having a working understanding of where this experience ties into the goals of the program.

7.2.7 Integration of societal and cultural sectors

The aspects of the IGERT program that students found most valuable are ranked in Fig. 7.7. Weighted scores were summed up for each aspect on the right hand side based on the criteria that ranking #1 to #6 were assigned with values from 6 to 1. We found that students most valued intercultural workshops and peers. When ranking components of the IGERT program against each other, over half of the students reported intercultural workshops as either number one or two and one-third of students reported peers and either number one or number two. Note that the option of intercultural workshops, in the context of this survey, includes both the trips to India and Puerto Rico. Courses, domestic field trips, and faculty mentorship were ranked after the previous three. Bi-annual workshops at Purdue University and Research Experience for Teachers (RET) were ranked the lowest within the last cohort. One reason for RET being the least favorable factor may be the limited number of students who participated in the program.

Select and rank which aspects of the IGERT program were highly valuable

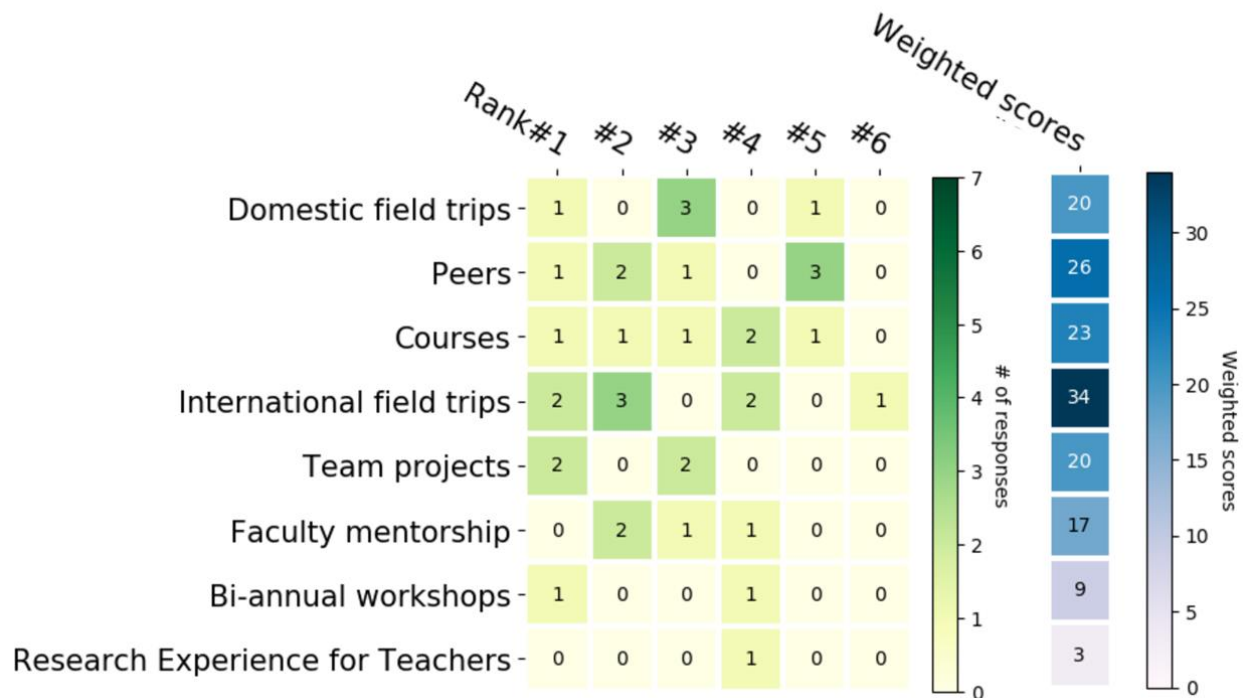


Figure 7.7. International filed trips were highlighted by the rating on the most valuable aspects of the IGERT in sustainable electronics program that were perceived by the students.

Internalization is the reconstruction of external operations from internal minds [34], which occurs through the interactions between learners and their social and cultural context. Effective teaching in school, which is primarily a social environment, is impossible without the realization that individuals are inseparable from their sociocultural setting [35]. This importance of the social context in the IGERT program can be partially shown in Fig. 7.7; International trips, peers, and courses were ranked as the three most valuable aspects of the IGERT program. An international trip than can contextualize the cultural materials of the subject and a learning community that encourages collaboration on projects rooted in real-life challenges are critical yet may be easily overlooked compared with other factors such as the faculty mentorship. In fact, when backing the choice to the question "which project helped you see the shared value the most?" a student wrote the following statement:

"Actively teaching my research and topic of interest to peers and making my own connections to the shared IGERT values, especially where obligation from professors was not an influential factor in developing my discussion topic (I could choose whatever I wanted to share and teach my peers)."

The quote pointed out that a social environment without external influence (obligation from professors) grants autonomy described in the self-determination theory [18]. This principle can also be traced back to the educational philosophy "Democracy and Education" established by Dewey a century ago, that the education is between the self-realizing pupils and their external social context in which no presupposed fixed end exists [36].

An initiative taken by the IGERT program is allowing the last cohort to self-design the final course, which was specifically organized to create a symbiotic teaching/learning environment between the IGERT trainees. Instead of a traditional lecture-style class, this class was developed to enhance learning and discussion by having each class taught by one of the trainees in a facilitating environment. The trainees presented lectures, discussion topics, and/or other interactive material directly related their main thesis work to the rest of the cohort, and clearly presented how the material learned in the previous courses were able to enhance their research. These in-depth, relevant topics helped the trainees expand on their knowledge formulated in the three previous courses. With the entire last cohort having agreed that they were part of the designing force of the IGERT programming [see Fig. 7.5(a)], this self-organized course was deemed as the turning point when the feeling of autonomy became dominant in more than half of the students [see Fig. 7.5(b)]. This course's profound influence can also be decoded from Fig. 7.6(a) in which the number of the students who felt involved in the planning of this course was twice that of the earlier India workshop. Digging deeper into what specific tasks were taken by the students in Fig. 7.6(b), it reveals that nine students were involved in the design of the learning outcomes and syllabus for the seminar course. Indeed, a deeper understanding and appreciation of learning outcomes exposes students to the "whole game" instead of scattered pieces of knowledge within the individual disciplines [37, 38]. This may be especially true for interdisciplinary (or multidisciplinary) curricular development as the knowledge roots in mixed backgrounds and fields.

However, promoting student autonomy does not mean eliminating faculty mentorship. Koch et al. [39] concluded that a differentiated support system or agency from the faculty side can substantially help fulfill students' psychological needs and academic performance. When providing the reasoning for the ranking of valuable factors, one IGERT trainee's responses pointed out what types of support from faculty were most effective:

"There is a difference between faculty in general and [the PI], who was emotionally encouraging, financially supportive, and willing to take initiative contacting the correct individuals to facilitate many of our group ideas. So although "support from faculty" is listed as moderately important, I would rate "support from [the PI]" as extremely important."

This student's reflection demonstrates that specific types of support can be immensely valuable during the learning process. In fact, while planning and organizational responsibilities fell increasingly on students, students still received faculty mentorship throughout their planning process in an instructional capacity as well as emotional. When asked whether the group's initiative came from situational happenstance, the student responded:

"I believe we were able to effectively execute the Puerto Rico workshop because [the PI] believed we would put in the effort needed to make it happen..."

In addition to other factors listed by the student, the PI's emotional support or belief in their success was one of the reasons that the student felt the cohort could take initiative beyond the scope of the original programming. Therefore, promoting autonomy needs the combined efforts from both the faculty and students. For the former, the defining element in an educative mentorship is the effort to promote self-realizing personalities, a wider sociocultural context, and an interactive learning experience. If applicable, instructors may consider, to some extent, allowing students to participate in the design of the learning outcomes, if not completely.

7.2.8 Conclusions

The NSF IGERT in sustainable electronics nurtured value, relatedness, competence, and autonomy in the final cohort which aligns with the self-motivated activities or initiatives taken by the participants. Students experienced the internalization of external values, during which the guided international learning experience in India and the self-organized seminar course are of great importance for developing relatedness (shared value) and student autonomy within the learning community. The last cohort rated the international trips as the most valuable aspect of the IGERT program, which included the India workshop organized by the faculty early in the program and the

Puerto Rico organized by the students a year later. Students exhibited a higher level of competence, autonomy, and relatedness during the latter trip, implying the successful learning experiences designed and delivered by the IGERT program.

Lessons learned based on our teaching experiences can be concluded as the following: Project- or problem-based learning theory can be easily adapted into interdisciplinary curricula to introduce authentic contexts, which is beneficial to student motivation for the students can better grasp the value of the knowledge taught. Intercultural communication promotes group cohesiveness if a learning community is involved. An effective way to achieve an authentic intercultural learning experience is international workshops with coherent training on cultural awareness and student-led reflective discussions.

7.3 Case study 2: Revealing hidden societal factors in sustainability education in a K-12 classroom for underrepresented middle-school youth

7.3.1 Purpose of study

To address those challenges, previous studies reported that a community-oriented approach with more constructive but less technological activities can not only enhance students' knowledge of sustainability [10] but also trigger students' interests in sustainability [40]. Therefore, K-12 classroom becomes a favorable place to implement practices of integrating sustainability with the purpose of increasing precollege children's awareness and motivations and preventing misconceptions with a constructively designed curriculum. A real-life implementation of curriculum integration of sustainability in the K-12 setting plays a key role in validating and evaluating the feasibility of this approach. In this study, a module of sustainability was designed for 12 one-hour sessions over 3 months with a focus on the recycling of electronics and was implemented in an industrial-oriented class. We use instructor reflections to provide preliminary insights for addressing difficulties associated with sustainability education, i.e., whether middle school youth can relate the societal and economic aspects to the sustainability concept.

The purpose of the study is to reformulate a college-level curriculum on global sustainability project into a module that would be suitable for middle school students. The lessons focus on electronics waste (e-waste) that falls under the category of sustainability. The goal of the module is to increase students' awareness of living a sustainable lifestyle and become familiar

with the enduring concepts of the three pillars of sustainability, i.e., environment, economy, and society. The research team includes graduate students and faculty from the departments of environmental engineering, materials engineering, and engineering education, reflecting the multidisciplinary nature of sustainability education.

7.3.2 Project design

We design the sustainability module for an industry-orientated course at a public middle school in a Midwestern city. The students in this class are enrolled in 7th and 8th grade. It requires an understanding of the students' preference and responses on various learning topics to bridge the gap between the college and K-12 classroom. A graduate student with an interdisciplinary traineeship on global sustainability served as the primary instructor for the course, with the support of the host teacher. The schedule for the visiting instructor is: (1) in week 1-2, the instructor observes the class and accepts training on K-12 education; (2) during week 3-6, the instructor assists the host teacher during the course and develop a lesson plan; (3) in week 7-9, the instructor teaches the designed module and collects reflections from the students; (4) Post-project, the instructor evaluates and reflects on students' participation and outcomes.

The focus of this industry-orientated course is to introduce middle school students the engineering design concepts with hands-on projects such as creating a bridge using straws and making wooden car models. Each student will learn to use tools such as the Autodesk software and the mechanical cutting machine. Each week students will be introduced to a new project by the instructor and divided into teams where they will collaborate to design real world products.

1. Session 1: Name it! In this activity, the class was divided into two different groups, A and B. Each group would be asked to name an electronic device within five seconds (every group member may answer) and the instructor would record each item under the group list (A and B) in PowerPoint. For example, the instructor would type "laptops" under list A if group A mentioned it. The game stopped whenever one of the groups failed to name an electronic device within five seconds and the other group won. The purpose of this activity was to help students recognize how many electronics were used and electronic wastes were produced in daily lives.

2. Session 2: Disassembling a hard drive. Students were set to teams with a capacity of two and each team was provided with a hard drive repair kit along with a wasted hard drive. Each team disassembled their hard-drive and inventoried components into organizing containers. The purpose of this activity was for students to familiarize themselves with the components inside a hard-drive and to understand the challenges in hard drive recycling industry.
3. Session 3: Electronics junk drawer. Each student was required to make a two-page PowerPoint slideshow. On the first page, students would take two photographs of an e-waste “junk drawer” (actual drawer, closet shelf, bin or any other container/location where they keep electronic devices that were no longer in use) at their home. On the second page, students were required to discuss with people they live with about the following two questions and write down the answers: (1) Why do you/your family keep e-wastes at home rather than recycling them? (2) Do you care more about the e-wastes recycling after this course and who else do you think should know about it? The purpose of this activity was to extend what students learned in this lesson into real-life applications. Students would realize how close we are related to electronics and think about the difficulties in collecting e-waste from households to recycling companies.

7.3.3 Preliminary findings

7.3.3.1 Student motivation

During the first session, students were very responsive to the “Name it” activity. The instructor set up a 15-minute time block, but students were unwilling to stop when the time was up and insisted on listing more everyday electronics. A 20-minute lecture was also given to familiarize students with the ideas of recycling and the concepts of electronic wastes and the associated toxicity. During the lecture, students gradually lost interests, especially in classes with over twenty students. During the second session, most students showed significant interests and curious about disassembling hard drives, asking a considerable amount of questions even before the class started. The instructor showed an already-disassembled hard drive and elaborated the technical functions and the materials used in each unit and a step-by-step guide on disassembling. After the

class, most students correctly differentiated various components such as printed circuit boards and silicon discs. Some students successfully related the material source to the components. Several students asked for permission to disassemble another hard drive after finishing the first one. Few asked to keep the printed circuit boards because they were interested in the structure, or because they realized PCBs contain valuable metals such as gold and silver.

7.3.3.2 Societal and economic awareness

During the third session, twenty-three out of one-hundred students submitted the PowerPoint slides for the “junk drawer” project. The majority of the students (16 out of 23) answered that they care more about electronic wastes after this course. The answers to the question “do you care more about the e-wastes recycling after this course?” included “toxic materials,” “damage to the environment,” and “recycling can help the planet.” The answers to the question “who else do you think should know about e-waste?” included “everyone,” “the adults,” “more people,” “the mayor,” “the waste recyclers” (because of the profits), and “should not be shared.” The answers to the question “Why do you/your family keep e-wastes at home rather than recycling them?” included “to sell them for money,” “to fix them in the future,” “as backups when other electronics broke down,” “we don’t know what to do with them,” “we know valuable materials are in them,” and “old electronics are memories.” Two students reflected that though they knew recycling is critical for the sustainability of the electronic industry, they would still keep e-wastes at home because of the recycling fee for electronics. Responses from students concerning e-wastes related the environment (toxicity, environmental protection, etc.) with the societal aspects (human emotions, social roles, individual responsibilities, etc.) and economic aspects (valuable materials, recycling fee, recycling profits, etc.) towards sustainability.

7.3.4 Conclusions

This study demonstrated that granting precollege children access to a sustainable design curriculum in the K-12 classroom can introduce the societal and economic aspects of sustainability to middle-school youth. In addition, the less-technological and society-oriented content in this educational module increased precollege students’ interests in sustainability associated activities, triggering students’ motivations for more entries into the future engineering pathway.

For future study, one challenge of integrating sustainability into engineering education is the lack of resources and training for educators [11]. As K-12 courses often touch on lower-order concepts in engineering education compared to higher education, the required resources are less demanding. Current college educational resources on sustainability have vast potentials to transplant in the K-12 curriculum. For instance, we reshaped the junk drawer project from a graduate-level course and triggered positive responses from the students. The strategies include avoiding jargons in the sustainability research and simplifying technical content but keeping the frameworks either in economic or societal aspects.

7.4 References

- [1] Wan Alwi, S. R., Manan, Z. A., Klemeš, J. J., & Huisingh, D. (2014). Sustainability engineering for the future. *Journal of Cleaner Production*, 71, 1-10. <https://doi.org/10.1016/j.jclepro.2014.03.013>
- [2] Siller, T. J. (2001). Sustainability and Critical Thinking in Civil Engineering Curriculum. *Journal of Professional Issues in Engineering Education and Practice*, 127(3), 104-108. [https://doi.org/10.1061/\(asce\)1052-3928\(2001\)127:3\(104\)](https://doi.org/10.1061/(asce)1052-3928(2001)127:3(104))
- [3] Mihelcic, J. R., Phillips, L. D., & Watkins, D. W. (2006). Integrating a Global Perspective into Education and Research: Engineering International Sustainable Development. *Environmental Engineering Science*, 23(3), 426-438. <https://doi.org/10.1089/ees.2006.23.426>
- [4] García-Serna, J., Pérez-Barrigón, L., & Cocero, M. J. (2007). New trends for design towards sustainability in chemical engineering: Green engineering. *Chemical Engineering Journal*, 133(1-3), 7-30. <https://doi.org/10.1016/j.cej.2007.02.028>
- [5] Penzenstadler, B., Bauer, V., Calero, C., & Franch, X. (2012). *Sustainability in software engineering: a systematic literature review*. In. IET. <http://dx.doi.org/10.1049/ic.2012.0004>
- [6] Verner, I. M., & Ahlgren, D. J. (2002). Fire-Fighting Robot Contest: Interdisciplinary Design Curricula in College and High School. *Journal of Engineering Education*, 91(3), 355-359. <https://doi.org/10.1002/j.2168-9830.2002.tb00715.x>
- [7] Davidson, C. I., Matthews, H. S., Hendrickson, C. T., Bridges, M. W., Allenby, B. R., Crittenden, J. C., Chen, Y., Williams, E., Allen, D. T., Murphy, C. F., & Austin, S. (2007). Adding sustainability to the engineer's toolbox: a challenge for engineering educators. *Environ Sci Technol*, 41(14), 4847-4850. <https://doi.org/10.1021/es072578f>
- [8] Murphy, C. F., Allen, D., Allenby, B., Crittenden, J., Davidson, C. I., Hendrickson, C., & Matthews, H. S. (2009). Sustainability in engineering education and research at U.S. universities. *Environ Science & Technology*, 43(15), 5558-5564. <https://doi.org/10.1021/es900170m>

- [9] Guerra, A. (2017). Integration of sustainability in engineering education. *International Journal of Sustainability in Higher Education*, 18(3), 436-454. <https://doi.org/10.1108/ijshe-02-2016-0022>
- [10] Segalàs, J., Ferrer-Balas, D., & Mulder, K. F. (2010). What do engineering students learn in sustainability courses? The effect of the pedagogical approach. *Journal of Cleaner Production*, 18(3), 275-284. <https://doi.org/10.1016/j.jclepro.2009.09.012>
- [11] Biswas, W. K. (2012). The importance of industrial ecology in engineering education for sustainable development. *International Journal of Sustainability in Higher Education*, 13(2), 119-132. <https://doi.org/10.1108/14676371211211818>
- [12] Korey, M., Clarkson, C., Frost, K., Andler, J., Wang, C., Reeves, M., & Handwerker, C. (2020). *Critical Incident Assessment as a Tool to Reflect on Students' Emotional Responses During International Experiences*. In. ASEE Conferences. <http://dx.doi.org/10.18260/1-2--34355>
- [13] Thorndike, E. L. (1927). The Law of Effect. *The American Journal of Psychology*, 39(1/4), 212. <https://doi.org/10.2307/1415413>
- [14] Murray, H. A. (1964). Explorations in Personality, 1963. *Journal of Projective Techniques and Personality Assessment*, 28(2), 172-172. <https://doi.org/10.1080/0091651x.1964.10120115>
- [15] MACE, C. A. (1948). Nature of Incentives. *Nature*, 162(4119), 557-558. <https://doi.org/10.1038/162557a0>
- [16] Skinner, B. F. (1963). Operant behavior. *American Psychologist*, 18(8), 503-515. <https://doi.org/10.1037/h0045185>
- [17] Adams, J. S. (1963). Towards an understanding of inequity. *The Journal of Abnormal and Social Psychology*, 67(5), 422-436. <https://doi.org/10.1037/h0040968>
- [18] Ryan, R. M., & Deci, E. L. (2000). Self-determination theory and the facilitation of intrinsic motivation, social development, and well-being. *American Psychologist*, 55(1), 68-78. <https://doi.org/10.1037/0003-066x.55.1.68>
- [19] Vroom, V. H. (1994). *Work and Motivation*. Jossey-Bass.
- [20] Vallerand, R. J. (1997). Toward A Hierarchical Model of Intrinsic and Extrinsic Motivation. In *Advances in Experimental Social Psychology: Advances in Experimental Social Psychology Volume 29* (pp. 271-360). Elsevier. [https://doi.org/10.1016/s0065-2601\(08\)60019-2](https://doi.org/10.1016/s0065-2601(08)60019-2)
- [21] Bruner, J. S. (1977). *The Process of Education*. Harvard University Press.
- [22] Eccles, J. S., & Wigfield, A. (2002). Motivational beliefs, values, and goals. *Annual Review of Psychology*, 53, 109-132. <https://doi.org/10.1146/annurev.psych.53.100901.135153>

- [23] Barron, K. E., & Hulleman, C. S. (2015). Expectancy-Value-Cost Model of Motivation. In *International Encyclopedia of the Social & Behavioral Sciences* (pp. 503-509). Elsevier. <https://doi.org/10.1016/b978-0-08-097086-8.26099-6>
- [24] Arzberger, P., Wienhausen, G., Abramson, D. A., Galvin, J., Date, S., Lin, F-P., Nan, K., & Shimojo, S. (2010). Prime: An integrated and sustainable undergraduate international research program. *Advances in Engineering Education*, 2(2), 1 - 34.
- [25] Layer, J., & Gwaltney, C. (2009). *International Capstone Design Projects: Evaluating Student Learning and Motivation Associated With International Humanitarian Projects*. In. ASEE Conferences. <http://dx.doi.org/10.18260/1-2--5067>
- [26] Edvardsson, B., & Roos, I. (2001). Critical incident techniques. *International Journal of Service Industry Management*, 12(3), 251-268. <https://doi.org/10.1108/eum0000000005520>
- [27] Flanagan, J. C. (1954). The critical incident technique. *Psychol Bull*, 51(4), 327-358. <https://doi.org/10.1037/h0061470>
- [28] Dewey, J. (1997). *Experience And Education*. Free Press.
- [29] Kitts, C., & Quinn, N. (2004). An interdisciplinary field robotics program for undergraduate computer science and engineering education. *Journal on Educational Resources in Computing*, 4(2), 3. <https://doi.org/10.1145/1071620.1071623>
- [30] Kuo, H.-C., Tseng, Y.-C., & Yang, Y.-T. C. (2019). Promoting college student's learning motivation and creativity through a STEM interdisciplinary PBL human-computer interaction system design and development course. *Thinking Skills and Creativity*, 31, 1-10. <https://doi.org/10.1016/j.tsc.2018.09.001>
- [31] DeLozier, S. J., & Rhodes, M. G. (2017). Flipped Classrooms: a Review of Key Ideas and Recommendations for Practice. *Educational Psychology Review*, 29(1), 141-151. <https://doi.org/10.1007/s10648-015-9356-9>
- [32] Bishop, J., & Verleger, M. (2013). *The Flipped Classroom: A Survey of the Research*. In. ASEE Conferences. <http://dx.doi.org/10.18260/1-2--22585>
- [33] Bischof, G., Bratschitsch, E., Casey, A., & Rubesa, D. (2007). *Facilitating Engineering Mathematics Education by Multidisciplinary Projects*. In. ASEE Conferences. <http://dx.doi.org/10.18260/1-2--2027>
- [34] Vygotsky, L. S. (1980). *Mind in Society: The Development of Higher Psychological Processes*. Harvard University Press.
- [35] Hausfather, S. J. (1996). Vygotsky and Schooling: Creating a Social Context for Learning. *Action in Teacher Education*, 18(2), 1-10. <https://doi.org/10.1080/01626620.1996.10462828>
- [36] Dewey, J. (1923). *Democracy and Education: An Introduction to the Philosophy of Education*. Macmillan.

- [37] Perkins, D. N. (2010). *Making Learning Whole*. John Wiley & Sons.
- [38] Hansen, E. J. (2012). *Idea-Based Learning*. Stylus Publishing, LLC.
- [39] Koch, F. D., Dirsch-Weigand, A., Awolin, M., Pinkelman, R. J., & Hampe, M. J. (2017). Motivating first-year university students by interdisciplinary study projects. *European Journal of Engineering Education*, 42(1), 17-31.
<https://doi.org/10.1080/03043797.2016.1193126>
- [40] Boks, C., & Diehl, J. C. (2006). Integration of sustainability in regular courses: experiences in industrial design engineering. *Journal of Cleaner Production*, 14(9-11), 932-939.
<https://doi.org/10.1016/j.jclepro.2005.11.038>

8. CONCLUSIONS

For Sn whisker, previous literature focused on the growth models or mechanisms due to local or global stresses and theorized the relationship between whisker growth and film microstructure, i.e., whiskers can only grow from grains with oblique GBs. Yet, existing theories or models lacked explanations to questions of why, when, and how those grains formed, given the columnar-structured grains in electrodeposited Sn films. The exact mechanism of how stresses accumulate, localize, and relax to nucleate shallow surface grains remains unclear. In this work, Chapters 2-5 are dedicated to answering this research question.

Chapter 2 analyzed the whisker density in polycrystalline Sn films under heating-only or cooling-only cycling conditions, using room temperature as the standard. The results illustrated that whisker formation was highly sensitive to local stresses and quickly reached a saturation point within the first 100 cycles during thermal cycling. Therefore, it provided the motivation of the following chapters (Chapters 3-5) to (1) focus on the early stage of thermal cycling and (2) to utilize large-grained Sn films to simplify the local stress states that lead to the nucleation of whisker grains.

Chapter 3 examined two pre-selected GBs with regard to orientations and microstructure before and after 500 cycles. The results provided direct evidence that whiskers grew from newly nucleated surface grains in a large-grain Sn-alloy film. Chapter 2 answered when shallow grains formed, i.e., grains nucleating to respond to the accumulated stresses. However, the study failed to answer what mechanisms contributed to the nucleation process and how due to the lack of time-dependent characterization. This limitation became the motivation of the rest of the whisker study.

Chapter 4 measured the evolution of morphological, crystallographic, and curvature changes near grain boundaries as a function of the number of thermal cycles for large-grain Sn films on Cu substrates. Different combinations of processes occurred at different GBs, with GB sliding and near-GB rotation occurring at fewer thermal cycles than other phenomena. The analysis of slip behavior together with the crystal plasticity simulation suggested that dislocations moved along known slip planes in Sn and were involved in the formation of new GBs, thereby nucleating surface grains. This work answered the question of what mechanisms contribute to whisker nucleation: dislocations were generated and rearranged to accommodate this localized grain rotation at GBs. One limitation was that many deformation mechanisms are not separable in

experiments. Each mechanism's role should be further investigated, perhaps by combining experiments and plasticity simulation for specific orientational relationships where the further isolation of critical factors is possible.

Chapter 5 answered the last part of the research question, i.e., how surface grains nucleated and whether those nucleated grains can later grow out as whiskers or not. The results showed that localized rotation near grain boundaries led to shallow grain nucleation. Those nucleated grains could later grow as whiskers when meeting the geometric requirements for growth. The stress relaxation mechanisms leading to the local yielding were found different from the ones leading to the grain rotation because the local orientation and microstructure changed asynchronously. Sufficient displacement along grain boundaries due to mismatch of CTEs leads to grain rotation and subgrain nucleation.

Concluding the work on Sn whiskers, this dissertation proposes a nucleation model of shallow grains based on the understanding of local microstructure, crystallography, slip behavior, creep, and anisotropic properties in certain regions in Sn films, the experimental observations cannot conclude a generalized mechanism cannot be completed due to the limitation of experimental observations. For example, it is impossible to analyze and summary a direct relationship of the local orientation and the nucleation of shallow grains because not all GB misorientations exist in one sample. Experiments and simulations on a larger scale or additional GB misorientations may be considered for future study.

For the work on e-waste recycling, recent literature in e-waste recycling has investigated the formal and informal sectors and theorized the merge of the two sectors. However, few studies provide an empirical evaluation of each procedure of the informal sector and the implications in the reformation of e-waste recycling. This study fills this gap by investigating the political, technological, and economic solutions that reformulated the local recycling industry in Guiyu, a well-known e-waste recycling town. Chapter 6 illustrated that centralizing waste treatment in high-tech facilities while maintaining the advantage of manual dismantling is critical. The construction of those facilities resulted from the collaboration among local government, companies, and research institutes through subsidies, investment, and patents. Screening transboundary e-wastes and maintaining original networks of sources and markets contribute to a stable and manageable recycling business. The lessons learned could be applied to broader regions with similar contexts.

For this reason, the results of this work have valuable implications for areas sharing similar contexts with Guiyu, particularly for developing countries.

Lastly, concerning sustainability education, Chapter 7 utilized two case studies to demonstrate how authentic contexts and global perspectives on sustainable electronics reduced the misconceptions, established shared value, and motivated students to make sustainable choices, either in higher education or the K-12 sector.

In summary, this study contributes to sustainable electronics from multiple stages of electronics' life cycles by (1) understanding the reliability of the Pb-free coatings, i.e., Sn whiskers, when temperature changes, (2) giving examples of the transition from informal recycling to formal recycling of e-waste during the end-of-life treatment, and (3) contextualizing sustainable electronics for STEM education in higher education and K-12 education.

PUBLICATIONS

1. Chen, W., Wang, C., Sarobol, P., Blendell, J., Handwerker, C. A. (2020). Local Variations in Grain Formation, Grain Boundary Sliding, and Whisker Growth along Grain Boundaries in Large-Grain Sn Films. *Scripta Materialia*, 187, 458-463.
2. Wang, C., Clarkson, C. M., Andler, J., Korey, M., Frost, K. D., Reeves, M. S., Handwerker, C. A. (2020). Lessons Learned from the NSF IGERT Program: Cultivating Student Motivation in the Interdisciplinary and International Contexts. 2020 ASEE Virtual Annual Conference & Exposition Proceedings.
3. Korey, M., Clarkson, C. M., Frost, K. D., Andler, J., Wang, C., Reeves, M. S., Handwerker, C. A. (2020). Critical Incident Assessment as a Tool to Reflect on Students' Emotional Responses during International Experiences. 2020 ASEE Virtual Annual Conference & Exposition Proceedings.
4. Wang, C., Dandridge, T., Cardella, M. E., Handwerker, C. A. (2019). Work In Progress: Integrating Sustainability Engineering Education and Design into the K-12 Classroom: A Case Study in Electronics Recycling for Middle-School Youth. 2019 ASEE Annual Conference & Exposition Proceedings.
5. Clarkson, C., Molaei, F., Morris, M., Wang, C., & Robinson, L. (2018). Lessons Learned from DMMM3. *JOM*, 70(12), 2790-2795.